Institute of Chemistry
Postgraduate Program in Chemistry

Doctoral Thesis

Bond Ellipticity Alternation: An Accurate Descriptor of the Nonlinear Optical Properties of pi-Conjugated Chromophores

Author: Thiago Oliveira Lopes

Advisor: Dr. Heibbe C. B. de Oliveira

BRASÍLIA,

May 14, 2018

University of Brasília

Doctoral Thesis

Bond Ellipticity Alternation: An Accurate Descriptor of the Nonlinear Optical Properties of pi-Conjugated Chromophores

---

Author:
Thiago Oliveira Lopes

Advisor:
Dr. Heibbe C. B. de Oliveira

A thesis submitted in fulfillment
of the requirements for the
degree of Doctor of Philosophy.

LEEDMol
Institute of Chemistry

BRASÍLIA,
May 14, 2018

Folha de Aprovação

Comunicamos a aprovação da Defesa de Tese do (a) aluno (a) **Thiago Oliveira Lopes**, matrícula nº **14/0115471**, intitulada "***Bond Ellipticity Alternation: An Accurate Descriptor of the Nonlinear Optical Properties of pi-Conjugated Chromophores***"**,** apresentada no (a) Auditório Lauro Morhy do Instituto de Química (IQ) da Universidade de Brasília (UnB) em 14 de maio de 2018.

Prof. Dr. Heibbe Cristhian Benedito de Oliveira
Presidente de Banca (IQ/UnB)

Prof. Dr. Clodoaldo Valverde
Membro Titular (UEG)

Prof. Dr. Ricardo Gargano
Membro Titular (IF/UnB)

Prof.ª Dra. Elaine Rose Maia
Membro Titular (IQ/UnB)

Prof. Dr. Rafael Oliveira Rocha
Membro Suplente (IQ/UnB)

Em 14 de maio de 2018.

I dedicated this work to...

My beloved wife, Graziele S. P. Lopes, a loving and very patient person, who has always been at my side, even in the worst moments.
My parents, Francisco E. L. da Silveira and Cleuza A. de Oliveira, who has always supported me along this extremely long journey.

" I do not fear computers.
I fear the lack of them."

Isaac Asimov

Acknowledgements

Firstly, I have to give a special thanks to my beloved family:

- to my dear wife Graziele S. Pereira Lopes, who always stood by me, got in my back in the best and worst moments, and I know how difficult it was to put up with;
- to my parents, Francisco E. Lopes da Silveira and Cleuza A. de Oliveira, who have always been by my side, giving me support, in this long journey;
- to my godmother, Maria das Graças Lopes, who contributed a lot to my intellectual formation, besides my personality;
- to my brothers, Lucas M. Lopes and Iracema J. Lopes, and my sisters-in-law, Olívia P. Pereira and Eliane S. Pereira;
- to my in-laws, Maria José S. Pereira and Luís Gonzaga Pereira;
- and to the two newest members of my family, my beloved nephews, Maria Clara P. Juventino and Marcos Antônio P. da Silva.

I can not forget to thank my lab colleagues and all those who have been through LEEDMol for a coffee and have a good laugh at the time of relaxation:

- to Sandro Brito, Mateus Barbosa, Ueslei Vasconcelos, Ana Grabriela Oliveira, Fernanda Santos, Nayara Coutinho and Arsênio Vasconcelos;
- and to our faithful companion a Black N' Decker coffee machine, model CM300;

To all the former LMSC companions and the IQ-UnB colleagues, somehow, all were important in my formation.

To the co-authors of my article, professor Jean-Luc Brédas and professor Chad Risko, whose help was fundamental to the execution of this work:

Especially to Daniel F. S. Machado, who at the time of those years became a great friend and an important collaborator; and to who provided the execution of this work of doctorate, my mentor and friend, Heibbe C. B. De Oliveira;

To CAPES, for the financial support, during my doctoral program.

And last but not least, I thank myself for my patience and perseverance, waiting for the brightest days ahead.

UNIVERSITY OF BRASÍLIA

Abstract

Postgraduate Program in Chemistry
Institute of Chemistry

Doctor of Philosophy

Bond Ellipticity Alternation:
An Accurate Descriptor of the Nonlinear Optical Properties of pi-Conjugated Chromophores

by Thiago Oliveira Lopes

Structure-property parameters display a pivotal role in the design of new π- conjugated molecules and polymeric materials for nonlinear optical (NLO) applications. Some established parameters such as bond-length alternation (BLA) and π-bond order alternation (BOA) have proven its usefulness to be well correlated with NLO quantities BLA corresponds to a measure of the molecular geometric structure while the BOA corresponds to molecular electronic effects. Nevertheless, these parameters are reported to be well correlated with NLO properties only when the molecular geometry is optimized in the environment of interest. Computing BLA and BOA in complex environments (electric field, solvent, etc.) poses a challenge on whether NLO quantities such as (hyper)polarizabilities, correlates or not with such parameters. We propose an alternative parameter, coined here as bond ellipticity alternation (BEA) to assess its ability to well correlate with NLO quantities obtained via electronic structure calculations in a prototype polymeric chromophore streptocyanine of 5 and 9 carbon atoms length. New BEA parameter is a simple yet robust to assess the NLO characteristic of organic chromophores and illustrates its effectiveness in the case of streptocyanines. BEA is based on the symmetry of the electron density, a physical observation that can be determined from experimental X-ray electron densities or from quantum-chemical calculations. Critical points are obtained from the Quantum Theory of Atoms in Molecules (QTAIM) framework, in which the molecular properties are partitioned into the contributions of its constituent atoms, hence both geometric and electronic effects are attainable in a single bonding descriptor: bond ellipticity at

the critical points of electron density. To assess the role of BEA on NLO quantities an external electric field was applied along the molecular axis, optimizing the molecular geometry as well as constraining the molecular geometry to the C_{2v} point group. Through comparisons to the well-established bond-length alternation and π-bond order alternation parameters, we demonstrate the generality of BEA to foreshadow NLO characteristics and underline that, in the case of large electric fields. BEA is a more reliable descriptor and basis set independently Hence, this study introduces BEA as a prominent descriptor of organic chromophores of interest for NLO applications.

UNIVERSIDADE DE BRASÍLIA

Resumo

Programa de Pós-Graduação em Química
Instututo de Química

Doutor

Alternância de Elipticidade de Ligação: Um Novo Descritor de Propriedades Não-Lineares de Cromofóros pi-Conjugados

por Thiago Oliveira Lopes

Parâmetros de propriedades relacionadas a estrutura molecular exibem um papel fundamental no *design* de novas moléculas π-conjugadas e materiais poliméricos para aplicações Ópticas Não-Lineares (do inglês *Nonlinear Optics* - NLO). Alguns parâmetros bem estabelecidos, como a Alternância de Comprimento de Ligação (do inglês *Bond Length Alternation* - BLA) e a Alternância de Ordem de Ligação π (do inglês *Bond Order Alternation* - BOA), provaram sua utilidade na correlação de quantidades NLO. O BLA corresponde a uma medida da geometria da estrutura molecular, enquanto o BOA corresponde aos efeitos eletrônicos moleculares. No entanto, esses parâmetros são relatados como bem correlacionados com as propriedades NLO, somente quando a geometria molecular é otimizada no ambiente de interesse. A quantificação de BLA e BOA em ambientes complexos (campo elétrico, solvente, etc.) apresenta um desafio sobre se as quantidades NLO, (hiper-)polarizabilidades, por exemplo, se correlacionam ou não com tais parâmetros. Propomos um parâmetro alternativo, nomeado aqui como Alternância de Elipticidade de Ligação (do inglês *Bond Ellipticity Alternation* - BEA) para avaliar sua capacidade de correlacionar bem com quantidades de NLO, obtidas através de cálculos de estrutura eletrônica, em protótipos de cromóforos poliméricos de estreptocianina, com comprimento de 5 e 9 átomos de carbono. O novo parâmetro BEA é um parâmetro simples, mas mesmo assim robusto, e avalia as características ópticas não-lineares de cromóforos orgânicos, ilustrando, aqui, sua eficácia no caso das estreptocianinas. O BEA é baseado na simetria da densidade eletrônica, um fator físico observável que pode ser determinado a partir de densidades eletrônicas de raios-X experimentais ou a partir de cálculos quânticos. Os pontos críticos foram

obtidos a partir de cálculos baseados em Teoria Quântica de Átomos em Moléculas (do inglês *Quantum Theory of Atoms in Molecules* - QTAIM), na qual as propriedades moleculares são divididas em contribuições dos átomos que as constituem, portanto efeitos geométricos e eletrônicos são atingíveis em um único descritor do ligação: elipticidade de ligação nos pontos críticos da densidade eletrônica. Para avaliar o papel do BEA nas qualidades ópticas não-lineares, um campo elétrico externo foi aplicado ao longo do eixo molecular, otimizando a geometria molecular em um grupo de cálculos e limitando a geometria molecular ao grupo pontual C_{2v}, em outro grupo de cálculos. Por meio de comparações com os parâmetros já estabelecidos, BLA e BOA, demonstramos a generalidade de BEA para prever características ópticas não-lineares e reiteramos que, no caso de campos elétricos fortes, BEA é um descritor mais confiável e independente de conjunto de funções de base. Assim, este estudo introduz o BEA como um descritor proeminente para cromóforos orgânicos de interesse para aplicações NLO.

Contents

List of Figures

List of Tables

List of Abbreviations

AIM	**A**toms **i**n **M**olecules
BCP	**B**ond **C**ritical **P**oint
BCP-L	The **l**eftmost **B**ond **C**ritical **P**oint in streptocyanine main chain
BCP-R	The **r**ightmost **B**ond **C**ritical **P**oint in streptocyanine main chain
BEA	**B**ond **E**llipticity **A**lternation
BEDA	**B**ond **E**lectron **D**ensity **A**lternation
BELA	**B**ond **L**aplacian of **E**lectron Density **A**lternation
BLA	**B**ond **L**ength **A**lternation
BO	**B**orn-**O**ppenheimer Aproximation
BOA	**B**ond **O**rder **A**lternation
BP	**B**ond **P**ath
CP	**C**ritical **P**oint
CCP	**C**age **C**ritical **P**oint
CCSD	**C**oupled **C**luster **S**ingle-**D**oble
CPKS	**C**oupled **P**ertubated **K**ohn-**S**ham
DFT	**D**ensity **F**unctional **T**heory
GTF	**G**aussian **T**ype **F**unctions
HF	**H**artree-**F**ock
HFR	**H**artree-**F**ock-**R**oothan
LEEDMol	**L**aboratório de **E**strutura **E**letrônica e **D**inâmica **Mol**ecular
KS	**K**ohn-**S**ham
NLO	**N**on**l**inear **O**ptics
NACP	**N**uclear **A**ttractor **C**ritical **P**oint
RCP	**R**ing **C**ritical **P**oint
RMSD	**R**oot **M**ean **S**quare **D**eviation
SCF	**S**elf **C**onstant **F**ield
QTAIM	**Q**uantum **T**heory of **A**toms in **M**olecules
TD	**T**ime-**D**ependent
UnB	**Un**iversidade de **B**rasília
XC	E**x**change-**C**orrelation

Chapter 1

Introduction

Since the 1800s, when the synthetic dyes are discovered, to the present days, scientist seeks to understand the relationship between molecular geometry, electronic structure and optical properties.[3] In order to get a deep understanding, it is natural to seek for a unified descriptor that correlates these properties and in the last decades, several studies focused on the search and understanding of this descriptor.

With the advent of the realm of Nonlinear Optics (NLO) and its applications in the photonics industry,[4,5] great attention was paid to the donor-acceptor polyenes (Figure 1.1), because of a high charge-transfer that its hyperconjugated structure posses, which causes high NLO response at different shows of magnitude.[6,7]

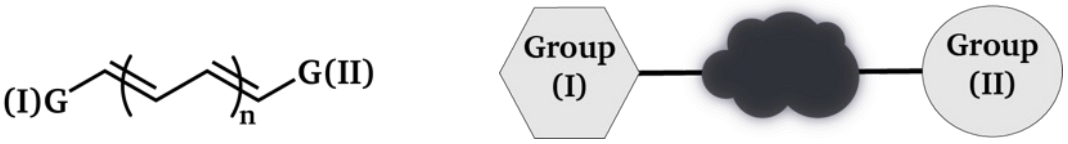

Figure 1.1: A generic donor-acceptor polyene moiety (left) and a schematic representation of a push/pull π-extended electronic cloud (right) with two groups attached to it, G(I) and G(II), possibly with electron-donating / withdrawing character.

Based on the hyperconjugated chain, most of the descriptors focuses on the alternation of bond properties between single and double bonds. Marder and co-workers, for instance, unified two important parameters, i.e. the Bond Length Alternation (BLA) and Bond Order Alternation (BOA) patterns,[3,8] to rationalize the NLO response and guide the synthesis of new materials.

BLA, one of the simplest descriptors, focuses basically on the distance between two atoms, and is strongly correlated with electronic[9] and photonic properties.[10] However the correlation was suggested to breakdown when molecular structures are simulated

in a solvent medium.[11] This issue was recently addressed by highlighting the limitations of BLA when considering molecular geometries far from equilibrium, i.e., BLA is a suitable structure-property parameter only in unperturbed scenarios.[12]

When the molecular structure is studied in complex environments (e.g. implicit and explicit solvents, electric fields, etc.), BOA, on the other hand, endows a suitable parameter to predict changes in NLO properties. The concept of bond order is a fundamental chemical concept that is associated with the intuitive sense of covalent chemical bonds and structure-property relationships of molecules. Several orbital-based population schems such as Mulliken,[13] Wiberg,[14] and Mayer[15] have been proposed to estimate BOA parameters. Mulliken bond order may be understood as a measure of the population overlap between two atoms, although it is strongly basis-set dependent.[16] Wiberg bond order is based on the squared density matrix and has been useful when the atomic orbital basis forms an orthonormal set such as semi-empirical methods. Mayer bond order is an extension of the Wiberg definition in *ab initio* molecular orbital theories.[16] Orbital-based population analysis methods are generally founded on the arbitrary partitioning of the density matrix and intimately associated with basis set orthonormalization.[17] When diffuse orbitals are demanded, these methods are expected to be inadequate.

Our objective is to find a robust yet simple bond descriptor that overcomes these problems. In particular, we find in Atoms in Molecules (AIM) theory a good bond descriptor that correlates exceptionally well with NLO properties, regardless the basis set employed. For this purpose, we explore the applicability of the quantum theory of atoms in molecules (QTAIM) approach. QTAIM relies on a fundamental physical observable, i.e. on the electron density.[18] Based on the density gradient zero-flux condition, which makes the real space to be partitioned into non-overlapping atomic domains or atomic basins (Figure 1.2). QTAIM properties are computed from the topological analysis, provided that the electron density is known either from experimental (e.g. X-ray diffraction) measurements or from theoretical calculations, whether taken from wavefunction approximations or on Density Functional Theory (DFT).[19]

In particular, one of the QTAIM quantities,the ellipticity of the electron density has been employed to characterize electrocyclic reactions owing to its ability to capture the changes in the anisotropy of the electron density at the bond critical point (BCP)[20] and to clarify the nature of intermolecular interactions.[21,22] The bond ellipticity (ε) is defined in terms of the cylindricity of the electron density at the BCP, accounting for its principal curvatures (eigenvalues of the Hessian matrix, λ_1, λ_2 and λ_3, such that λ_1 and λ_2 are the negative eigenvalues). The negative eigenvalues of the electron density Hessian at the BCP degenerate when the axis associated with its respective curvatures

are symmetrically equivalent, as in the case of a single CarbonCarbon (CC) bond in ethane, $\lambda_1 = \lambda_2$ and $\varepsilon = 0$. The ellipticity, $\varepsilon = \lambda_1 / \lambda_2 - 1$, provides a quantitative generalization of the concept of σ and π bond character, i.e. ε measures the extent to which the electron density is preferentially distributed in a particular plane containing the bond axis.[23] As pointed out by Scherer and coworkers, positive values of indicating some π character in a bond,[12] showing evidence of hyperconjugative interactions. Modifications in the CC bond pattern of unsaturated carbon chains resulting from external effects, say electric fields for instance, are associated with hyperconjugative delocalization, though they remain quantitatively difficult being experimentally measured.

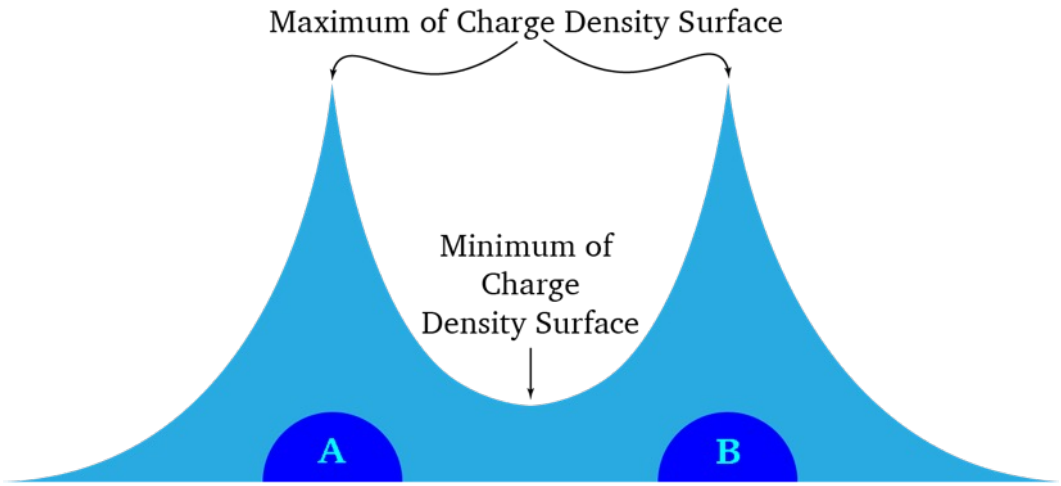

Figure 1.2: A zero flux surface (in a bi-Dimensional representation) between two attractors (A and B), on which the charge density is a minimum perpendicular to the surface

As pointed out in the work of Gieseking et al. (Reference 12), geometric and electronic changes are of utter importance when correlating BLA or BOA with NLO properties when electric fields are present. The QTAIM approach, hence, serves as an interesting method to analyze the electronic effects of π-bonds delocalization in unsaturated carbon chains since $\rho(r)$ is the only demanding quantity to define the topological analysis. Scherer and coworkers showed that ε provides an experimentally observable criterion to assess the extent of delocalization in the tight agreement between experiment and theory. Here we propose a general bond descriptor based on the ellipticity at the BCP as a useful structure-property parameter to predict trends for the electric dipole moment, linear polarizability, and first and second order hyperpolarizabilities of polymeric materials aiming at NLO applications.

Thus, we introduce here a general bond descriptor based on the ellipticity at the BCP as a structure-property parameter able to predict the evolution with an electric field of the electric dipole moment, linear polarizability, and second and third-order polarizabilities. We refer to this parameter as the bond ellipticity alternation (BEA); it is defined in Figure 1.3, along with the conventional NLO descriptors BLA and BOA. We find that the bond ellipticities along the molecular backbone when large electric field are applied describes the chemically intuitive distribution of charge especially when a diffuse basis set is employed to a much better extent than the bond orders.

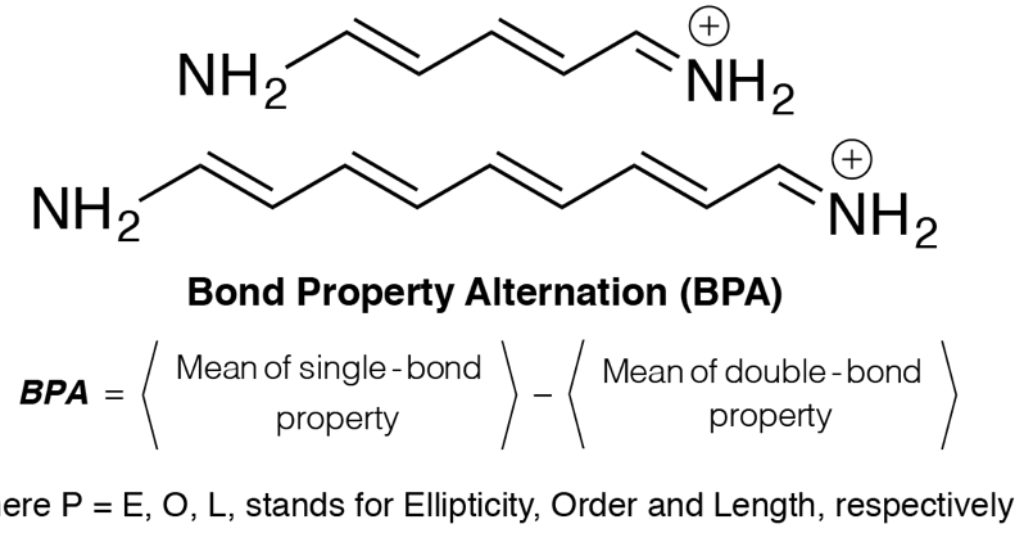

Figure 1.3: Chemical structures of the five-carbon (5C) and nine-carbon (9C) streptocyanines and definition of the bond alternation parameters.[1]

In order to validate the new BEA parameter and to compare it with the parameters BLA and BOA already established in the literature, we chose the same molecules used in the work of Gieseking et al. (Reference 12), Figure 1.3, as well as the same electric field influence parameters. As for the levels of theory used in this work, was also based on Reference 12, but with some changes, the DFT hybrid functional ωB97XD using four different basis set, two Dunning type and two Pople type, each with or without the addition of diffuse functions. This choice was made with the intention of validating the independence of the quality of the BEA parameter in relation to the basis set, something already known in the literature, as an achilles heel of some definitions of Bond Order.[16,17]

In the following chapters, we will first develop the theoretical foundations underlying the work performed during the Ph.D. period in a succinct way. Then, we turn to the methodology, i.e., the theoretical calculations used to compute the novel BEA

parameter. Finally, the performance of BEA is computed with well-established BOA, leaving BLA results to the Appendix section. The details of QTAIM descriptors other than ϵ can be found in Appendix A. The published paper resulting from this thesis is presented in Appendix B, and the home-made codes built in Python used to catalogue the results is presented in Appendix C.

Chapter 2

Theoretical Foundations

2.1 Electronic Structure Approximations in Quantum Chemistry

Quantum chemistry is an application of quantum mechanics to problems of chemistry. Having this fact in mind, it is necessary to understand that up to chemical problem spans from a simple approximation of a proton to a molecular fragment or the behavior of a drug in the active site of an enzyme. It is therefore incoherent to suppose that a single method of theoretical calculation could solve all the problems in chemistry, and it is more logical to say that among the various methods of calculations in theoretical chemistry, each one has its specificity and range of applicability.[24]

Among the methods of theoretical calculations, the most popular are Semi-empirical methods, Hartree-Fock and post-Hartree-Fock, as well as the Density Functional Theory (DFT) methods.[24,25] In this thesis, only the latter two will be further discussed, since they were the underlying methods applied to solve the electronic structure of the targeted chromophore.

2.1.1 The Molecular Problem

This section will be devoted to a brief description of the methods used to obtain approximate results of the electronic properties of molecular systems in general. Considering a generic molecular system formed by M nuclei and N electrons that can be represented by a coordinate system called molecular coordinates (Figure 2.1).[26]

The indices A and B refer to the nuclei, whereas i and j refer to the electrons; the distance between the nuclei A and B is $R_{AB} = |\boldsymbol{R}_A - \boldsymbol{R}_B|$; the distance between the electron i and the nucleus A is $r_{iA} = |\boldsymbol{r}_i - \boldsymbol{R}_A|$ and the distance between the electrons i and j is $r_{ij} = |\boldsymbol{r}_i - \boldsymbol{r}_j|$.

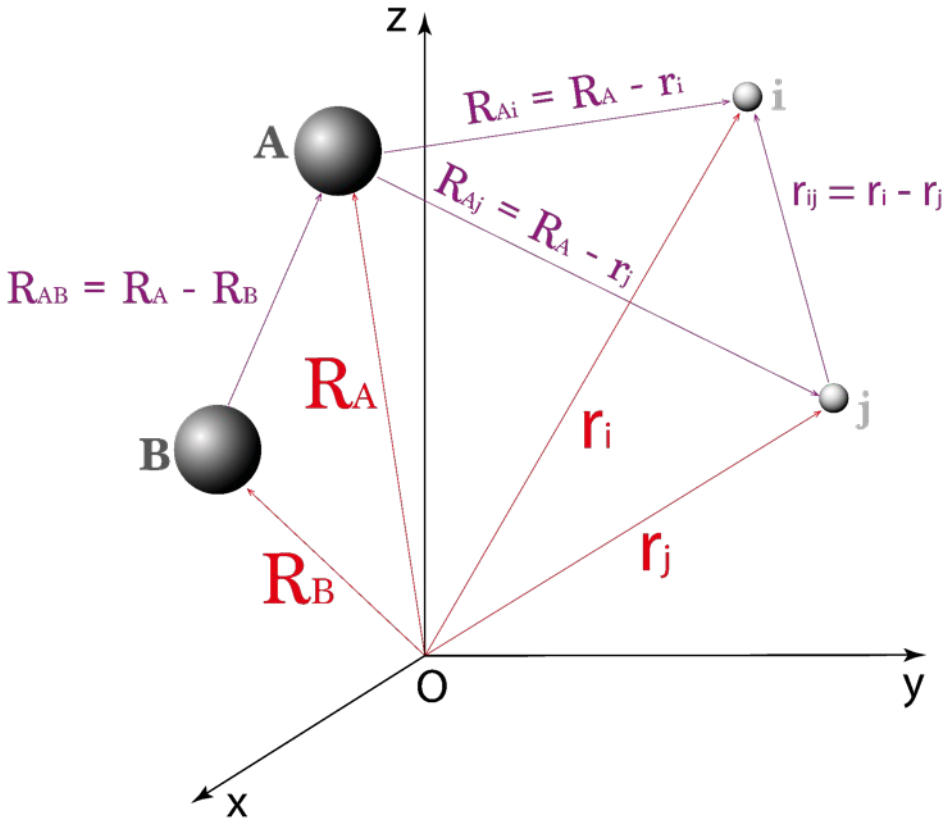

Figure 2.1: Representation of the molecular coordinate system for a generic collection of electrons and nuclei.

To calculate any properties of generic molecular system it is necessary to solve the Schrödinger's equation, given by:

$$\hat{H}\Psi = E\Psi, \tag{2.1}$$

where $\hat{H}$ is the Hamiltonian operator and E is the total energy of the molecular system.

The time-independent nonrelativistic molecular Hamiltonian for this molecular system, in atomic units ($\hbar = m_e = e = k = 1$) is given by:[27]

$$\hat{H} = -\frac{1}{2}\sum_{i=1}^{N}\nabla_i^2 - \sum_{A=1}^{M}\frac{1}{2M_A}\nabla^2 + A - \sum_{A=1}^{M}\sum_{i=1}^{N}\frac{Z_A}{r_{iA}} + \sum_{A=1}^{M-1}\sum_{B>A}^{M}\frac{Z_A Z_B}{R_{AB}} + \sum_{i=1}^{N-1}\sum_{j>i}^{N}\frac{1}{r_{ij}}. \tag{2.2}$$

The terms of molecular Hamiltonian are, respectively: electronic kinetic energy operator, nuclear kinetic energy operator, coulomb interaction potential between the

nuclei and the electrons, coulomb interaction potential between the nuclei and electrons. This equation can be written in a more compact way, as follows:[2]

$$\hat{H} = \hat{T}_e(\boldsymbol{r}) + \hat{T}_N(\boldsymbol{R}) + \hat{V}_{eN}(\boldsymbol{r},\boldsymbol{R}) + \hat{V}_{NN}(\boldsymbol{R}) + \hat{V}_{ee}(\boldsymbol{r}). \tag{2.3}$$

In the Schrödinger's equation (Equation 2.1), $\Psi(\boldsymbol{r},\boldsymbol{R})$ represents the complete wavefunction, which describes the properties of the molecular system as a whole. The Schrödinger's equation only have exactly analytical solutions for some ideal systems like the particle in the box, harmonic oscillator, rigid rotator and also the hydrogen atom. More complex systems than the ones mentioned above can be solved by theoretical approximation, which will be briefly presented in the following subsections.

2.1.2 Born-Oppenheimer Approximation

Expliciting the hamiltonian operator, the Equation 2.2, in the Schrödinger equation for any system, Equation 2.1, we have:

$$\left[-\frac{1}{2}\sum_{i=1}^{N}\nabla^2 - \sum_{A=1}^{M}\frac{1}{2M_A}\nabla^2 - \sum_{A=1}^{M}\sum_{i=1}^{N}\frac{Z_A}{r_{iA}} + \sum_{A=1}^{M-1}\sum_{B>A}^{M}\frac{Z_A Z_B}{R_{AB}} + \sum_{i=1}^{N-1}\sum_{j>i}^{N}\frac{1}{r_{ij}}\right]\Psi(\boldsymbol{r},\boldsymbol{R}) = E\Psi(\boldsymbol{r},\boldsymbol{R}). \tag{2.4}$$

This equation is impossible to be solved, however, the key for this problem resides in the Born-Oppenheimer Approximation (BO). M. Born and J. R. Oppenheimer developed a quantitative model based on the fact that the nuclei are much more massive than electrons ($m_p/m_e \approx 1840$). Therefore the electrons move much faster than the nuclei, and as a good estimate, it is considered that electrons can adapt itself to the "slow" nuclear movement. The BO is applied considering the adiabatic theorem, which states that if a perturbation applied to the system is sufficiently slow so that the system adapts to its new condition, and its eigenstate is maintained. So if the molecule moves slowly it can be considered that the electrons move in a field of fixed nuclei (thus, the nuclear motion does not involve different electronic states).

Using the adiabatic approximation, the second term of Equation 2.2 (which measures the kinetic energy of the nuclei) is much smaller than the ones terms and can be neglected and the fourth term of the hamiltonian (which measures the internuclear repulsion) can be considered a constant. This constant will not affect the eigenfunctions of the Schrödinger's equation, and it will only shift its eigenvalues and the terms that were not canceled in Equation 2.2, giving rise to the so-called electronic Hamiltonian

($\hat{H}_{ele}$) given by:

$$\hat{H}_{ele} = -\frac{1}{2}\sum_{i=1}^{N}\nabla_i^2 - \sum_{A=1}^{M}\sum_{i=1}^{N}\frac{Z_A}{r_{iA}} + \sum_{i=1}^{N-1}\sum_{j>i}^{N}\frac{1}{r_{ij}}. \tag{2.5}$$

This operator is used in Schrödinger's equation for the description of electronic properties subject to a potential of fixed nuclei,

$$\hat{H}_{ele}\psi(\boldsymbol{r}_i, \boldsymbol{R}_A) = E_{ele}\psi(\boldsymbol{r}_i, \boldsymbol{R}_A), \tag{2.6}$$

which the electronic wavefunction (ψ) describes the electrons movement and depends explicitly on the electronic coordinates $\boldsymbol{r_i}$ and parametrically of the nuclear coordinates $\boldsymbol{R_A}$. In other words, the electronic energy is calculated for each nuclear configuration and then, for each nuclear configuration one must add the constant term referring to nuclear repulsion,

$$E_{tot} = \sum_{A=1}^{M-1}\sum_{B>A}^{M}\frac{Z_A Z_B}{R_{AB}} + E_{ele}. \tag{2.7}$$

In order to solve the electronic problem it is necessary to solve the Equation 2.6. However, in any calculation of quantum chemistry, the molecular geometry must be optimized so that the properties of interest are correctly obtained. This sets up another problem to be overcome: the nuclear problem can be solved under the same BO hypothesis as we did for the electronic problem. For this reason, because of the relative speed difference between nuclei and electrons, it is fair to consider that nuclei feel only an average potential due to the electrons and therefore, the hamiltonian is simplified:

$$\hat{H}_N = -\sum_{A=1}^{M}\frac{1}{2M_A}\nabla_A^2 + \left\langle -\frac{1}{2}\sum_{i=1}^{N}\nabla_i^2 - \sum_{A=1}^{M}\sum_{i=1}^{N}\frac{Z_A}{r_{iA}} + \sum_{i=1}^{N-1}\sum_{j>i}^{N}\frac{1}{r_{ij}}\right\rangle + \sum_{A=1}^{M-1}\sum_{B>A}^{M}\frac{Z_A Z_B}{R_{AB}}, \tag{2.8a}$$

$$\hat{H}_N = -\sum_{A=1}^{M}\frac{1}{2M_A}\nabla_A^2 + E_{ele}(\boldsymbol{R_A}) + \sum_{A=1}^{M-1}\sum_{B>A}^{M}\frac{Z_A Z_B}{R_{AB}}, \tag{2.8b}$$

$$\hat{H}_N = -\sum_{A=1}^{M}\frac{1}{2M_A}\nabla_A^2 + E_{tot}(\boldsymbol{R_A}). \tag{2.8c}$$

The total energy, $E_{tot}(\boldsymbol{R_A})$, forms the potential energy surface for the nuclei move, obtained by solving the electronic problem. The solutions of the nuclear Schrödinger's equation describe the vibrations, rotations, translations and geometry of the molecule.

The total energy in the Born-Oppenheimer approximation includes electronic, vibrational, rotational and translational energy. The wave function used in the BO is derived from the adiabatic expansion:

$$\Psi(\boldsymbol{r}_i, \boldsymbol{R}_A) = \psi(\boldsymbol{r}_i, \boldsymbol{R}_A)\phi(\boldsymbol{R}_A). \tag{2.9}$$

2.1.3 Hartree-Fock Formalism

The operator of Equation 2.5, its eigenvalues and eigenfunctions, Equation 2.7, do not considering relativistic effects, no spin-orbit coupling, it only takes into account the fermionic indistinguishability of the electrons.[27]

This indistinguishability must be taken into account in the electronic structure calculations, i.e., it is necessary to specify the electronic spin coordinates, introducing a ortogonal complete set of two functions $\alpha(\omega)$ and $\beta(\omega)$, corresponding, respectively, to the spin up and spin down states, which depends of a non-specific variable, ω.

With this new spin coordinate the electron which depends of three spatial coordinates, is now function of four coordinates, such as:

$$x = x(\boldsymbol{r}, \omega). \tag{2.10}$$

The electronic wavefunction can be written like a spatial orbital product $\phi(r)$ and its spin functions, forming two spin-orbitals:

$$X(x) = \begin{cases} \phi(\boldsymbol{r})\alpha(\omega) \\ \phi(\boldsymbol{r})\beta(\omega) \end{cases}. \tag{2.11}$$

According to the Equation 2.11, for each spatial orbital, we can associate two spin-orbitals. Resorting to the postulates of quantic mechanics, the wavefunction which describes N-electronic systems must be antisymmetric when exchanging coordinate x of any two electrons:

$$\phi\left(\boldsymbol{x}_1, \boldsymbol{x}_2, \ldots, \boldsymbol{x}_i, \ldots, \boldsymbol{x}_j, \ldots, \boldsymbol{x}_N\right) = -\phi\left(\boldsymbol{x}_1, \boldsymbol{x}_2, \ldots, \boldsymbol{x}_j, \ldots, \boldsymbol{x}_i, \ldots, \boldsymbol{x}_N\right). \tag{2.12}$$

As an example of the antisymmetric principle, consider the fundamental state of an atom of two electrons, $1s^2$ state. This electronic state can be described by two wavefunctions:

$$\psi_{1,2} = 1s(1)\alpha(1)1s(2)\beta(2), \tag{2.13a}$$

$$\psi_{2,1} = 1s(2)\alpha(2)1s(1)\beta(1), \tag{2.13b}$$

where the numbers in parenthesis indicates electron 1 and electron 2.

Two possibles combinations are usually considered:

$$\psi_A = \frac{1}{\sqrt{2}}\left(1s(1)\alpha(1)1s(2)\beta(2) - 1s(2)\alpha(2)1s(1)\beta(1)\right), \tag{2.14a}$$

$$\psi_B = \frac{1}{\sqrt{2}}\left(1s(2)\alpha(2)1s(1)\beta(1) - 1s(1)\alpha(1)1s(2)\beta(2)\right), \tag{2.14b}$$

respectively, the symmetric and antisymmetric combination. The factor $(2)^{-1/2}$ arises from the normalization of the total wavefunction.

The Pauli Exclusion Principle assert that any two electrons can not have the same set of four quantum numbers. If this Principle is violated, that means the eigenstate is the same, and only the antisymmetric wavefunction cancels. Therefore, in order for the Pauli exclusion principle to be satisfied, the electronic wave function must be antisymmetric.[28]

The antisymmetric wavefunction also can be written in terms of a matrix determinant:

$$\psi_A(1,2) = \frac{1}{\sqrt{2}}\begin{vmatrix} 1s(1)\alpha(1) & 1s(2)\alpha(2) \\ 1s(1)\beta(1) & 1s(2)\beta(2) \end{vmatrix} \tag{2.15}$$

Using determinants to describe the electronic wave function becomes convenient, since both the Pauli exclusion principle (if two electrons occupy the same spin-orbital we will have two equal columns, making the determinant null) and antisymmetry (changing the coordinates of two electrons is equivalent to changing two lines, which changes the signal of the determinant) are satisfied in this way.

The Equation 2.15 can be generalized for any N-electron system:[29]

$$\phi_A(\boldsymbol{x}) = \frac{1}{\sqrt{N!}}\begin{bmatrix} \chi_1(x_1) & \dots & \chi_1(x_N) \\ \vdots & \ddots & \vdots \\ \chi_N(x_1) & \dots & \chi_N(x_N) \end{bmatrix}. \tag{2.16}$$

Wavefunction writing as a one determinant is known as a Slater's determinant.

Equation 2.16 can also be represented, in a simplified way as:

$$\phi(\boldsymbol{x}) = |\chi_1\chi_2\dots\chi_N\rangle \tag{2.17}$$

To solve the Schrödinger electronic equation (Equation 2.6) to molecular systems is still mathematically impractical, due to the repulsive term between the electrons in the electronic Hamiltonian (Equation 2.5). An alternative to find the (approximate)

wavefunction of the polyelectronic system is to use the Hartree-Fock approximation. Douglas R. Hartree and Vladimir Fock proposed a seminal method for calculating the electronic structure of atomic and molecular systems. They used a formalism in which the interaction potential of the electrons is represented by a mean potential and the electronic wave function is approximated by a Slater determinant. With this treatment the Schrödinger equation for a system of N electrons can be transformed into N equations considering only one electron.

The Hartee-Fock formalism is based in the Variational Principle, according to which the best form of the electronic wavefunction ψ is the one corresponding to the lowest possible energy when the spin-orbital functions $\chi(x)$ are changed, i.e, find the wavefunction $\chi(x)$ which minimize the expected value of $\langle\phi|\hat{H}_{ele}|\phi\rangle$.

According to the variational theorem, the expected value of the energy is an upper limit for the exact state energy, that is,

$$\langle\phi|\hat{H}_{ele}|\phi\rangle \geq E_{exact}. \tag{2.18}$$

The electronic hamiltonian (Equation 2.5) can be separated as the contribution of one and two electrons:[2]

$$\hat{H}_{ele} = \sum_{i=1}^{N}\hat{h}(i) + \sum_{i=1}^{N}\sum_{j>i}^{N}\hat{g}(i,j), \tag{2.19}$$

with:

$$\hat{h}(i) = -\frac{1}{2}\sum_{i=1}^{N}\nabla_i^2 - \sum_{A=1}^{M}\frac{Z_A}{r_{Ai}}, \tag{2.20a}$$

$$\hat{g}(i,j) = \frac{1}{r_{ij}}. \tag{2.20b}$$

Defining the energy functional for the ground state ($\in_0[\chi_i]$), we get:

$$\in_0[\chi_i] = \langle\phi|\hat{H}_e|\phi\rangle, \tag{2.21}$$

This functional must be minimized to the constraint to that the molecular spin-orbitals are kept orthonormalized, that is:

$$\langle\chi_i|\chi_j\rangle = \delta_{ij}, \tag{2.22}$$

The expected value for the energy in the ground state $\in_0$ is given by:

$$\in_0 [\chi_i] = \sum_{i=1}^{N} \langle \chi_i | \hat{h} | \chi_i \rangle + \frac{1}{2} \sum_{i=1}^{N} \sum_{j=1}^{N} \big(\langle \chi_i \chi_j | \chi_i \chi_j \rangle - \langle \chi_i \chi_j | \chi_j \chi_i \rangle \big). \tag{2.23}$$

In order to minimize this functional it is possible to use Lagrange's indeterminate multipliers method. This method consists of minimizing another functional $L[\chi_i]$ which minimize the functional $\in_0$, subjected to the constraint in Equation 2.22. Defining the functional:

$$L[\chi_i] = \in_0 [\chi_i] - \sum_{i=1}^{N} \sum_{j=1}^{N} \lambda_{ij} \big(\langle \chi_i | \chi_j \rangle - \delta_{ij} \big), \tag{2.24}$$

where the coefficient λ_{ij} are the indeterminate multipliers of Lagrange.

By varying infinitesimally the spin-orbital functions, we obtain:

$$\delta L[\chi_i] = \delta \in_0 [\chi_i] - \sum_{i=1}^{N} \sum_{j=1}^{N} \lambda_{ij} \delta \langle \chi_i | \chi_j \rangle, \tag{2.25}$$

and expliciting the new functional fot the ground state, we obtain:

$$\begin{aligned} \delta L[\chi_i] = & \sum_{i=1}^{N} \sum_{j=1}^{N} \langle \delta \chi_i | \hat{h} | \chi_j \rangle + \sum_{i=1}^{N} \sum_{j=1}^{N} \langle \delta \chi_i \chi_j | \chi_i \chi_j \rangle + \sum_{i=1}^{N} \sum_{j=1}^{N} \langle \delta \chi_i \chi_j | \chi_j \chi_i \rangle + \\ & + \sum_{i=1}^{N} \sum_{j=1}^{N} \lambda_{ij} \langle \delta \chi_i | \chi_j \rangle + \textit{complex conjugate} \end{aligned}, \tag{2.26}$$

Introducing the Coulomb ($\hat{J}_j$) and Exchange ($\hat{K}_j$) operators, defined as:

$$\hat{J}_j(\boldsymbol{x}_1) \chi_i(\boldsymbol{x}_1) = \left[\int \chi_j^*(\boldsymbol{x}_2) \frac{1}{r_{12}} \chi_j(\boldsymbol{x}_2) d\boldsymbol{x}_2 \right] \chi_i(\boldsymbol{x}_1), \tag{2.27a}$$

$$\hat{K}_j(\boldsymbol{x}_1) \chi_i(\boldsymbol{x}_1) = \left[\int \chi_j^*(\boldsymbol{x}_2) \frac{1}{r_{12}} \chi_i(\boldsymbol{x}_2) d\boldsymbol{x}_2 \right] \chi_j(\boldsymbol{x}_1), \tag{2.27b}$$

the Equation 2.26 can be re-written as:

$$\begin{aligned} \delta L[\chi_i] = \sum_{i=1}^{N} \int \delta \chi_i^*((\boldsymbol{x})_1) \Big\{ & \hat{h}(\boldsymbol{x}_1 \chi_i(\boldsymbol{x}_1)) + \sum_{i=1}^{N} \big[\hat{J}_j(\boldsymbol{x}_1 - \hat{K}_j(\boldsymbol{x}_1) \big] \chi_i(\boldsymbol{x}_1) + \\ & - \sum_{j=1}^{N} \lambda_{ij} \chi_i(\boldsymbol{x}_1) \Big\} d\boldsymbol{x}_1 + \textit{complex conjugate}, \end{aligned} \tag{2.28}$$

The Coulomb operator represents the coulombic repulsion arising from all other $N-1$ electrons, distributed as a probability density. The exchange operator takes into account the spin correlation, that is, the same spin electrons tend to be avoided, which reduces the global coulombian potential between them.[27]

For the functional $L[\chi_i]$ to be a minimum, we must impose the condition that $\delta L[\chi_i] = 0$ in Equation 2.28 and considering that the variation $\delta\chi_i^*$ is arbitrary, we have:

$$\left\{\hat{h}(\boldsymbol{x}_1) + \sum_{j=1}^{N}\left[\hat{J}_j(\boldsymbol{x}_1) - \hat{K}_j(\boldsymbol{x}_1)\right]\right\}\chi_i(\boldsymbol{x}_1) = \sum_{j=1}^{N}\lambda_{ij}\chi_i(\boldsymbol{x}_1), \tag{2.29}$$

with a similar expression for the conjugate complex. The term in brackets in Equation 2.29 is called the Fock operator:

$$\hat{f}(\boldsymbol{x}_1) = \hat{h}(\boldsymbol{x}_1) + \sum_{j=1}^{N}\left[\hat{J}_j(\boldsymbol{x}_1) - \hat{K}_j(\boldsymbol{x}_1)\right]. \tag{2.30}$$

Thus we can write the Hartree-Fock equation succinctly, as:

$$\hat{f}(\boldsymbol{x}_1)\chi_i(\boldsymbol{x}_1) = \sum_{j=1}^{N}\lambda_{ij}\chi_i(\boldsymbol{x}_1). \tag{2.31}$$

Through a unitary transformation, Equation 2.31 can be converted into a canonical eigenvalue equation, since the Fock operator is invariant under any unitary transformation. Therefore, we can write:

$$\hat{f}(\boldsymbol{x}_1)\chi_i(\boldsymbol{x}_1) = \in_i \chi_i(\boldsymbol{x}_1), \tag{2.32}$$

in which the Lagrange multipliers were replaced by $\in_i$ to indicate that it represents the energy. Equation 2.32 is called the canonical Hartree-Fock equation.

Although Equation 2.31 must be solved to obtain the spin-orbit functions $\chi_i(x_1)$, the Coulomb operator equation (Equation 2.27a) shows that it is necessary to know all the other occupied spin-orbital functions in order to assemble the operators $\hat{J}_j$ and $\hat{K}_j$, and thus obtain $\chi_i(x_1)$.

To overcome this such a cumbersome problem, one can make an ansatz about the initial form of all the spin-orbital wavefunctions of an electron $\chi_i(x_1)$, use them in the definitions of Coulomb operators and exchange, and solve the canonical Hartree-Fock equations. The calculation is repeated until the energies and the new spin-orbit functions remain unchanged.

This method is known as Hartree-Fock Self-Consistent Field method (HF-SCF) and

has as a difficulty that the numerical solution of the Hartree-Fock equations, which are computationally expensive, so that exact solutions to Equation 2.32 are obtained only for atoms and molecules with few electrons. The main problem of the Hartree-Fock method is that it uses only a single Slater determinant and treats the electron-electron interaction in an average way, not taking into account the correlated movement of the electrons, which leaves aside a small fraction of the total energy of the system. It is defined that this small fraction of the total energy of the system (correlation energy) as being the difference between the exact non-relativistic energy and the Hartree-Fock energy:[29]

$$E_{corr} = E_{exact} - E_{HF}. \tag{2.33}$$

Because of the importance of systematically determining the Correlation Energy, several methods that consider this effect are implemented in the calculations, and are termed post-Hartree-Fock methods.

Subsequently, in 1951, the landmark work of Clemens C. J. Roothaan made an extremely important contribution that made it possible to apply this method to more complex systems. Roothaan proposed the use of N-known functions, called base functions, to expand as a linear combination the spatial part of each function of an electron (spin-orbital) such as:

$$\chi_i = \sum_{i}^{N} c_{i\nu}\theta_i(\boldsymbol{r}), \tag{2.34}$$

where $\theta_i(r)$ are known basis functions and $c_{i\nu}$ are the expansion coefficients to be determined.

This reduced the problem of solving Hartree-Fock coupled integral-differential equations to a linear algebra problem. This method is known as the Hartree-Fock-Roothaan (HFR) method.

The main problem is to choose the best set of basis functions to be used in the expansion proposed by Roothaan. Hydrogen-like and Slater functions were applied, but the ones that brought better results and computational feasibility were the Gaussian Type Functions (GTF) proposed in 1950 by Boys, enabling the calculations of the integrals involved in the HFR method and capable to describe the systems well chemicals.

2.1.4 DFT Methods

The Density Functional Theory was formulated by P. Hohenberg and W. Kohn based on the electronic density and not the wavefunction as in the Hartree-Fock method. This theory describes a system of interacting electrons under an external potential in

terms of electron density ($\rho(\boldsymbol{r})$). DFT has proven to be extremely useful as it is an alternative to treat the electronic correlation problem and it has a low computational cost compared to the methods based on the Hartree-Fock approach.[28,30,31]

In 1964, P. Hohenberg and W. Kohn proved that the exact state energy of a molecule is uniquely determined by the electron density:

$$E[\rho] = E_{classic}[\rho] + E_{XC}[\rho], \tag{2.35a}$$

$$E[\rho] = \langle\psi|\hat{T} + \hat{U}|\psi\rangle + \langle\psi|\hat{V}|\psi\rangle, \tag{2.35b}$$

$$E[\rho] = F[\rho] + \langle\psi|\hat{V}|\psi\rangle, \tag{2.35c}$$

where $E_{classic}[\rho] = F[\rho]$ is a universal functional valid for any coulombic system which consists of the sum of the kinetic energy of the electrons with the electron-core interactions and the classical electron-electron potential, $E_{XC}[\rho] = \langle\psi|\hat{V}|\psi\rangle$ is the Exchange-Correlation (XC) energy which takes into account non-classical interelectronic effects due to spin and corrections to classical kinetic energy.

Thus, we can assert that by finding the form of the electronic density $\rho(\boldsymbol{r})$, the ground state electronic properties can be obtained on the basis of the Kohn-Shan equations, which are discussed in the next sub-subsection.

2.1.4.1 Kohn-Sham Equations

Considering that the Coulombic interactions are long-range interactions, we can separate the classical terms from of the quantum terms,[32–34]

$$F[\rho] = \frac{1}{2}\int\int \frac{\rho(\boldsymbol{r})\rho(\boldsymbol{r}')}{|\boldsymbol{r}-\boldsymbol{r}'|} d\boldsymbol{r}\, d\boldsymbol{r}' + G[\rho], \tag{2.36}$$

such that:

$$E[\rho] = \int v(\boldsymbol{r})\rho(\boldsymbol{r}) d\boldsymbol{r} + \frac{1}{2}\int\int \frac{\rho(\boldsymbol{r})\rho(\boldsymbol{r}')}{|\boldsymbol{r}-\boldsymbol{r}'|} d\boldsymbol{r}\, d\boldsymbol{r}' + G[\rho]. \tag{2.37}$$

In this equations $G[\rho]$ is a universal functional.

In 1965, Kohn and Sham presented a strategy for calculating the electronic structure of many-body systems using the functional density $E[\rho]$. The proposed strategy consisted in replacing the original problem of several interacting bodies with a fictitious alternative problem with independent particles. Thus, the functional $G[\rho]$ can be written as:

$$G[\rho] \equiv T_0[\rho] + E_{XC}[\rho], \tag{2.38}$$

where $T_0[\rho]$ is the kinetic energy of a non-interacting electron system with density $\rho(\boldsymbol{r})$ and $E_{XC}[\rho]$ is the exchange-correlation energy of a system with electronic density $\rho(\boldsymbol{r})$. The exact functional form of $E_{XC}[\rho]$ is not simple, and it configures one of the problems that the DFT faces.

According to the variational theorem, applying a variation in the functional $E[\rho]$, with the constraint that the total electronic charge is constant we have:

$$\int \rho(\boldsymbol{r})d\boldsymbol{r} = N \Rightarrow \int \rho(\boldsymbol{r})d\boldsymbol{r} - N = 0. \tag{2.39}$$

Imposing the extreme condition in the Equation 2.39:

$$\delta\left(E[\rho] - \mu\left[\int \rho(\boldsymbol{r})d\boldsymbol{r} - N\right]\right) = 0, \tag{2.40}$$

so we obtain:

$$\int \delta\rho(\boldsymbol{r})\left\{\frac{\delta T_0}{\delta\rho} + v(\boldsymbol{r}) + \int \frac{\rho(\boldsymbol{r}')}{|\boldsymbol{r}-\boldsymbol{r}'|}d\boldsymbol{r}' + v_{XC}[\rho] - \mu\right\}d\boldsymbol{r} = 0, \tag{2.41}$$

here μ is a Lagrange multiplier that represents the chemical potential of the system and v_{XC} is the exchange-correlation potential, given by:

$$v_{XC}[\rho] = \frac{\delta E_{XC}}{\delta\rho}. \tag{2.42}$$

The kinetic energy functional can be written as:

$$T_0[\rho] = -\frac{1}{2}\sum_i \int \psi_i^* \nabla^2 \psi_i d\boldsymbol{r}, \tag{2.43}$$

and since the electron density can be expressed as a contribution of each electron present in the molecular system (auxiliary charge density),

$$\rho(r) = \sum_{i=1}^{N} |\psi_i(\boldsymbol{r})|^2, \tag{2.44}$$

and applying in the Schrödinger equation, we find the complementary Kohn-Sham (KS) equation, given by:

$$\hat{h}^{KS}\phi(\boldsymbol{r}) = \left(-\frac{1}{2}\nabla^2 + v^{KS}[\rho]\right)\psi_i(\boldsymbol{r}) = \in_i \psi_i(\boldsymbol{r}), \tag{2.45}$$

where $\in_i$ are the eigenvalues of the Kohn-Sham hamiltonian and $v^{KS}[\rho](\boldsymbol{r})$ is the Kohn-Sham potential, gived by:

$$v^{KS}[\rho](\boldsymbol{r}) = v(\boldsymbol{r}) + \int \frac{\rho(\boldsymbol{r}')}{|\boldsymbol{r}-\boldsymbol{r}'|} d\boldsymbol{r}' + v_{XC}[\rho]. \tag{2.46}$$

Using Equations 2.41, 2.44 and 2.45 the total energy of the system can be obtained as a function of the sum of the eigenvalues of the Kohn-Sham Hamiltonian:

$$\sum_{i=1}^{N} = T_0[\rho] + \int v(\boldsymbol{r})\rho(\boldsymbol{r})d\boldsymbol{r} + \int\int \frac{\rho(\boldsymbol{r})\rho(\boldsymbol{r}')}{|\boldsymbol{r}-\boldsymbol{r}'|} d\boldsymbol{r}\, d\boldsymbol{r}' + \int v_{XC}[\rho(\boldsymbol{r})]\rho(\boldsymbol{r}).d\boldsymbol{r} \tag{2.47}$$

When compared with the energy functional in Equation 2.36, we obtain:

$$E[\rho] = \sum_{i=1}^{N} \in_i - \int\int \frac{\rho(\boldsymbol{r})\rho(\boldsymbol{r}')}{|\boldsymbol{r}-\boldsymbol{r}'|} d\boldsymbol{r}\, d\boldsymbol{r}' + \int \rho(\boldsymbol{r}) \in_{XC} [\rho] - v_{XC}[\rho] d\boldsymbol{r}, \tag{2.48}$$

which is the total energy in function of the eigenvalues $\in_i$.

The $v_{XC}[\rho]$ plays a fundamental role within the DFT, since it represents the energy related to the electronic correlation and the possibilities of the electrons to occupy distinct quantum states, that is, a potential that carries information about the electron-electron interactions and the interaction of the electron with itself. This term has no analytical expression which leads to an error for the DFT, because in this case, it is necessary to use approximations in the calculation of electronic structure.

2.2 Nonlinear Optical Properties

The electronic density can be used to determine all the individual properties of a molecule, obviously disregarding the possible effect of surroundings, we can extrapolate to the property of the study material.[35]

One of these properties is the dipole moment, which magnitude indicates the difference in distribution of positive and negative charges throughout the molecule. The permanent dipole moment (μ_0) follows from the partial charges on the atoms of the molecule arising from differences in electronegativity or other bonding characteristics, Figure 2.2a and 2.2b. Since non-polar systems can acquire a dipole moment (just as polar molecules can have their dipole moment aligned to the field) when subjected to an external electric field, their electronic densities tend to be distorted as a function of this field, this dipole moment is called the induced dipole moment (μ^*) and is temporary, disappearing as soon as the disturbing field is removed.[2]

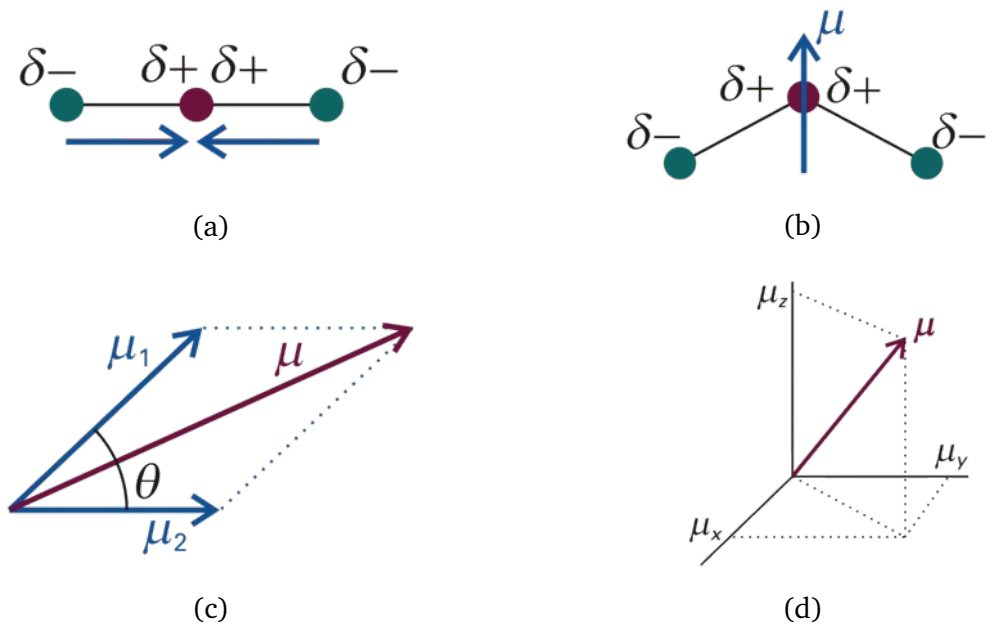

Figure 2.2: Representation of (a) Non-polar molecule; (b) molecule with a permanent dipole moment; (c) Vector addition of two dipole moments; (d) Vector components of a 3-D dipole moment in the laboratory framework.[2]

For a linear molecule (Figure 2.2a and 2.2b) it is easy to find the dipole moment, being the result of the partial charges of the atoms of the molecule, but for complex systems, the total dipole moment will be the result of the dipoles in the three directions, Figure 2.2d.

When we observe the dipole moment, submitted to an electric field, we notice a certain proportionality of the induction in relation to the intensity of the field, this proportionality constant is called linear electrical polarizability (α). The higher the polarization, the greater will be the induced dipole moment for a given applied field:[2]

$$\mu^* = \mu + \alpha F. \tag{2.49}$$

Nonetheless, in the case of extremely intense fields, polarization tends to depart from linearity, depending on the strength of the applied field, and on increasing order of magnitude known, such as the first (β) and second (γ) hyperpolarizabilities, and so on. All the polarizabilities are tensors associated to the field and dipole moment vectors:[36,37]

$$\mu^* = \mu + \alpha F + \beta F^2 + \gamma F^3 \ldots \tag{2.50}$$

From a theoretical point of view, these nonlinear optical quantities can be calculated by differentiating the electronic energy with respect to the applied field. According the Hellman-Feynman theorem, the dipole moment, linear polarizability, and hyperpolarizabilities can be expressed as a Taylor expansions for field-dependent energy in a static case:[27,38,39]

$$\begin{aligned} E(F) =& E_0 + \sum_i \frac{\partial E}{\partial F} F_i + \frac{1}{2} \sum_{i,j} \frac{\partial^2 E}{\partial F_i \partial F_j} F_i F_j + \frac{1}{6} \sum_{i,j,k} \frac{\partial^3 E}{\partial F_i \partial F_j \partial F_k} F_i F_j F_k \\ &+ \frac{1}{24} \sum_{i,j,k,l} \frac{\partial^4 E}{\partial F_i \partial F_j \partial F_k \partial F_l} F_i F_j F_k F_l + \dots \end{aligned} \tag{2.51}$$

Simplifying:[40]

$$E(F) = E_0 + \sum_i \mu_i F_i + \frac{1}{2} \sum_{i,j} \alpha_{ij} F_i F_j + \frac{1}{6} \sum_{i,j,k} \beta_{ijk} F_i F_j F_k + \frac{1}{24} \sum_{i,j,k,l} \gamma_{ijkl} F_i F_j F_k F_l + \dots \tag{2.52}$$

Hence, all these field-dependent electrical properties can be obtained by differentiating the energy with respect to the Field in which they were submitted. There are several methods to obtain these derivatives, both analytically and numerically. In this work we used an analytical method to obtain these terms.

2.2.1 Computational NLO Calculations

The electrical properties of a molecule can be calculated from derivatives (analytical or numerical) of the energy in relation to the applied field. The expressions for the components of these electrical properties can be obtained directly from Equation 2.52, and are given by:[27,38,39]

$$\mu_i = -\left(\frac{\partial E}{\partial F_i}\right)_{F=0}, \tag{2.53a}$$

$$\alpha_{ij} = \left(\frac{\partial \mu_i}{\partial F_j}\right)_{F=0} = \left(\frac{\partial^2 E}{\partial F_i \partial F_j}\right)_{F=0}, \tag{2.53b}$$

$$\beta_{ijk} = \left(\frac{\partial^2 \mu_i}{\partial F_j \partial F_k}\right)_{F=0} = \left(\frac{\partial^3 E}{\partial F_i \partial F_j \partial F_k}\right)_{F=0}, \tag{2.53c}$$

$$\gamma_{ijkl} = \left(\frac{\partial^3 \mu_i}{\partial F_j \partial F_k \partial F_l}\right)_{F=0} = \left(\frac{\partial^4 E}{\partial F_i \partial F_j \partial F_k \partial F_l}\right)_{F=0}. \tag{2.53d}$$

2.3 Quantum Theory of Atoms in Molecules

Until the early twentieth century, the current chemical theory asserted that molecules are a set of atoms (at least two) connected by a network of chemical bonds. Only after the advent of the Quantum Mechanics and Quantum Electrodynamics, by Richard Feynman and Julian Schwinger, this understanding was changed. A molecule can be seen as a set of subatomic particles bound by forces, hitherto unknown. In the midst of this new scenario, Richard Bader, noting that topology of the distribution of electronic charge in real space, produces a unique partitioning, a set of limited spatial regions, realized that the shape and properties of these limited spatial regions resembled the atoms and functional groups of empirical chemistry. So Bader formulated a theory that used the whole operational idea of molecule of the old chemistry but preventing it from the moorings of empiricity, using all the predictive power of quantum mechanics, there arose the Quantum Theory of Atoms in Molecules (QTAIM).[41]

In these section, will be presented in a summary form to QTAIM, focusing on the relevant points that led to the execution of this thesis and in the formulation of the parameter Bond Elliptical Alternation (BEA).

2.3.1 The Electron Density

In Richard Bader's time, when one thought of theoretical chemistry, two concepts came to mind: Pauling's concept that if the distance of two interacting atoms is smaller than its atomic rays, these atoms would be chemically bonded;[42] and that of the quantum chemistry that any and all information, coming from a chemical environment can be obtained through the wavefunction, when one applies the correct mathematical operator.[43] In an attempt to unify these two concepts, Bader proposed that any information of a chemical system can be obtained through electronic density[44].

Electron density, although chemically very intuitive, has always been considered a controversial physicochemical parameter due to the lack of a clear analytical expression that could describe it and that can be used in the interpretation of the concentration of charge at specific molecular sites. Some researchers have presented some proposals for the analytical interpretation of the electronic density, for example, based on the concepts of Hirshfeld:[44]

$$I = f\rho_A(\boldsymbol{r})ln\left(\frac{\rho_A(\boldsymbol{r})}{\rho_A(\boldsymbol{r})^0}\right)dr + f\rho_B(\boldsymbol{r})ln\left(\frac{\rho_B(\boldsymbol{r})}{\rho_B(\boldsymbol{r})^0}\right)d\boldsymbol{r}, \tag{2.54}$$

in which A and B are two atoms, I is amount of electronic charge lost in A-B atomic overlap, $\rho_A(\boldsymbol{r})$ and $\rho_B(\boldsymbol{r})$ are the electric density of atoms A and B, and, finally, $\rho_A(\boldsymbol{r})^0$ and $\rho_B(\boldsymbol{r})^0$ are the electric density of the free atoms.

In order to correlate electronic density with the wavefunction, Bader took the electron density as a quantum-mechanical quantity, in which numerical calculations are performed to obtain properties, and the electron density gradient vector is responsible for determining the molecular topology.[44,45] Considering the atoms as open-shell systems and restricting boundary conditions on the molecular surface, we have that the charge density flux is zero at any point on this surface:[18]

$$\boldsymbol{n}(\boldsymbol{r}) \cdot \nabla\rho(\boldsymbol{r}) = 0, \tag{2.55}$$

thus, the gradient lines ending in distinct nuclei do not intersect, and here the zero flux surface is defined.[46]

From a sequence of $\nabla\rho(\boldsymbol{r})$ is that all the trajectories of the electronic density are obtained, showing positive or negative slopes towards the nuclei positions in the space, i.e., the attractors.[47] Since the gradient is a function of its attractors, these are properly the nuclei of the molecular system.[48] Ignoring the non-nuclear attractors, the set of these trajectories defines an atomic basin, called an open-shell system, which in a chemical interpretation is called atom.[44] The sum of this atomic basins defines the shape of the molecule and form the electron density, Figure 2.3

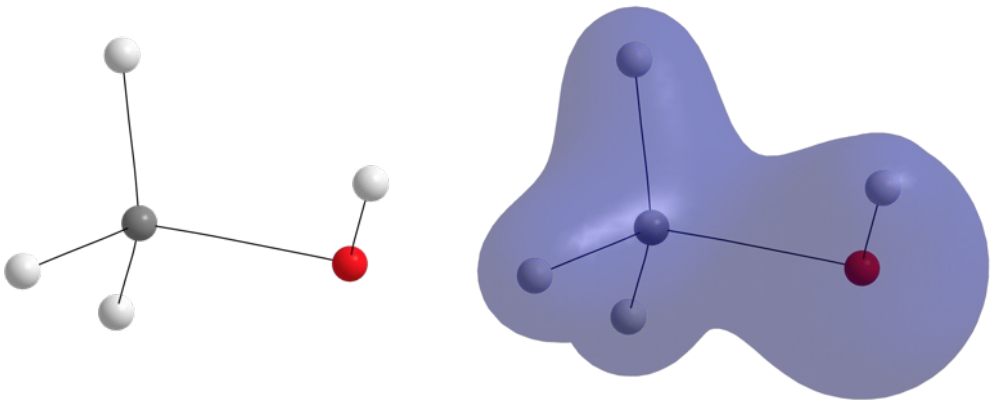

Figure 2.3: Molecular Representation of the Methanol molecule (left) and its qualitative electron density (right).

Looking at the electron density in a two-dimensional way, Figure 2.4a, note that an accumulation of electron density closer to the attractor in the plane of the contour lines, which can be better visualized on a relief map, Figure 2.4b. Note that on the plane containing the carbon-oxygen attractors, it is show that there is a maximum in

the electron density on the attractors and become more diffuse as one moves away from these centres of attraction. The electron density increases close to the atomic nuclei due to electrostatic interaction, and the presence of this maximum on the attractors and presence of local maxima at the positions of the nuclei is the general and also the dominant topological property of $\rho(\boldsymbol{r})$.[18]

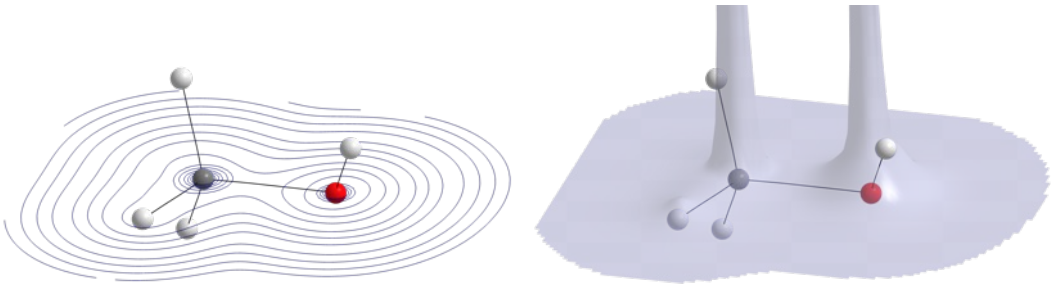

(a) Contour Lines of $\rho(\boldsymbol{r})$ (b) Relief Map of $\rho(\boldsymbol{r})$

Figure 2.4: Contour Lines (a) and Relief Map (b) of Qualitative Electron Density of Methanol in the Plane of Oxygen-Carbon Bond.

2.3.1.1 The Critical Points and the Bond Path

In mathematics, a critical point, also called a stationary point, is a point in the domain of a function where the first derivative vanishes (points in which a fictitious tangent line would have no inclination) or is not defined, Figure 2.5.

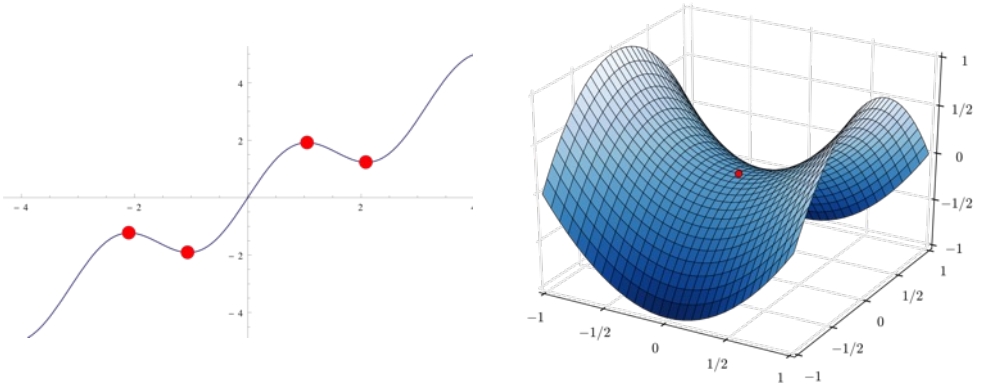

Figure 2.5: Mathematical definition of critical point in a curve (left) and in a surface (right). The red points are the critical points, a point where the first derivate is zero.

The critical points will always be points of maximum or minimum. When it is a three-dimensional function, this point is maximum, minimum or saddle point (a point in space that is maximum and minimum depending on the directionality). To reveal

the true nature of a critical point it is necessary to observe its second derivative, so one can disclose whether a point is a minimum or a maximum.[43]

Starting from this mathematical assumption and considering the topology of $\rho(\boldsymbol{r})$ as the mathematical surface, we will have points without inclination in that surface, there appears the Critical Points (CP) of QTAIM. Remember that in mathematics, the gradient of electronic density ($\nabla\rho(\boldsymbol{r})$, our first derivative) does not reveal the true nature of this critical point, for this it is necessary to calculate the Laplacian of Electronic Density ($\nabla^2\rho(\boldsymbol{r})$, our second derivative).[18,47]

2.3.1.1.1 Types of Critical Points

Then, as we look at the second derivative of $\rho(\boldsymbol{r})$, we see that there are nine spatial derivatives that can be arranged in a matrix called the Hessian matrix:[18]

$$A(r_c) = \begin{pmatrix} \frac{\partial^2\rho}{\partial x^2} & \frac{\partial^2\rho}{\partial x\partial y} & \frac{\partial^2\rho}{\partial x\partial z} \\ \frac{\partial^2\rho}{\partial y\partial z} & \frac{\partial^2\rho}{\partial y^2} & \frac{\partial^2\rho}{\partial y\partial z} \\ \frac{\partial^2\rho}{\partial z\partial x} & \frac{\partial^2\rho}{\partial z\partial y} & \frac{\partial^2\rho}{\partial z^2} \end{pmatrix}, \tag{2.56}$$

when evaluated at the critical point r_c, the matrix is readily diagonilized:

$$\Lambda = \begin{pmatrix} \frac{\partial^2\rho}{\partial x^2} & 0 & 0 \\ 0 & \frac{\partial^2\rho}{\partial y^2} & 0 \\ 0 & 0 & \frac{\partial^2\rho}{\partial z^2} \end{pmatrix}. \tag{2.57}$$

The sum of the three eigenvalues of the main diagonal of the hessian matrix (λ_1, λ_2, λ_3) is the $\nabla^2\rho(\boldsymbol{r})$:

$$\nabla^2\rho(\boldsymbol{r}) = \lambda_1 + \lambda_2 + \lambda_3 = \frac{\partial^2\rho}{\partial x^2} + \frac{\partial^2\rho}{\partial y^2} + \frac{\partial^2\rho}{\partial z^2}. \tag{2.58}$$

Through this second derivative, we can see that there are 4 different types (Figure 2.6) of CP that can be found in a molecule: the Nuclear Attractor Critical Bond (NACP), a point on the $\rho(\boldsymbol{r})$ is maximum with relations to all directions, and is the atomic nucleus itself; the Bond Critical Point (BCP) is a point where $\rho(\boldsymbol{r})$ is a minimum with respect to the maximum density path which connecting two NACPs and at the same time is maximum in the other directions, i.e. a saddle point in the $\rho(\boldsymbol{r})$; the Ring Critical Point (RCP) is another saddle point of $\rho(\boldsymbol{r})$, but unlike BCPs there is

only one direction in which it can be minimal, being maximum in the other two; and finally the Cage Critical Point (CCP) a real minimal point in the $\rho(\boldsymbol{r})$ surface.[18,48]

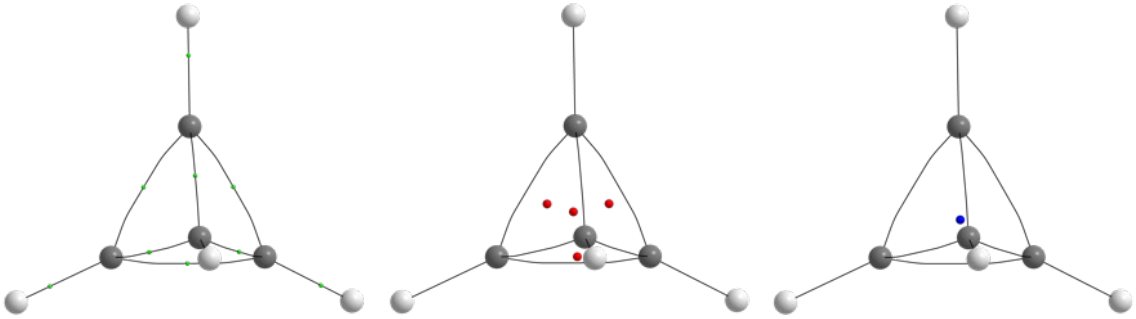

(a) BCPs (b) RCPs (c) CCP

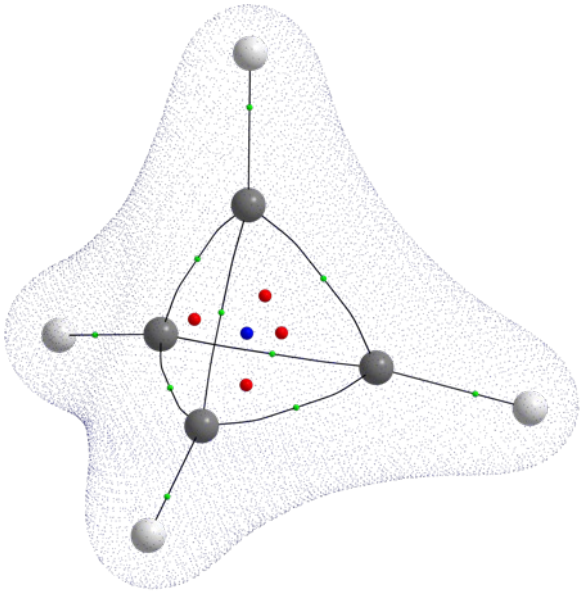

(d) BCPs, RCPs and CCP of a Tetrahedrane

Figure 2.6: Qualitative (a) Bond Critical Points, (b) Ring Critical Point, (c) Cage Critical Points, and (d) the 3 Types of Critical Points of $\rho(r)$ for the Tetrahedrane molecule.

Each critical point can be classified according to its rank and signature, (ω, σ), see Table 2.1. The rank represents the number of non-null eigenvalues of the main diagonal of the Hessian matrix. The signature denotes local curvatures of the CP with respect to the x, y, and z directions.[48]

There is an application of the differential topology called as the Poincaré-Hopf rule in QTAIM:[48]

$$NACPs - BCPs - RCPs - CCPs = 1, \tag{2.59}$$

Table 2.1: The Classification of the Critical Points with the Respective Signatures.

Type of Critical Point	λ_1	λ_2	λ_3	**Signature** (ω, σ)
NACP	−	−	−	$(3,-3)$
BCP	−	−	+	$(3,-1)$
RCP	−	+	+	$(3,+1)$
CCP	+	+	+	$(3,+3)$

the violation of this equality indicates that some critical point has not been found, and a new search for this critical point(s) is needed. Ultimately, it may be an indicative that the geometry is note properly defined.

2.3.1.1.2 The Bond Path

The presence of a zero flux surface between two bonded atoms is accompanied by another fundamental topological feature: there is a line of local maximum $\rho \boldsymbol{r}$ between two NACPs, Figure 2.7, these lines are called the Bond Path (BP).

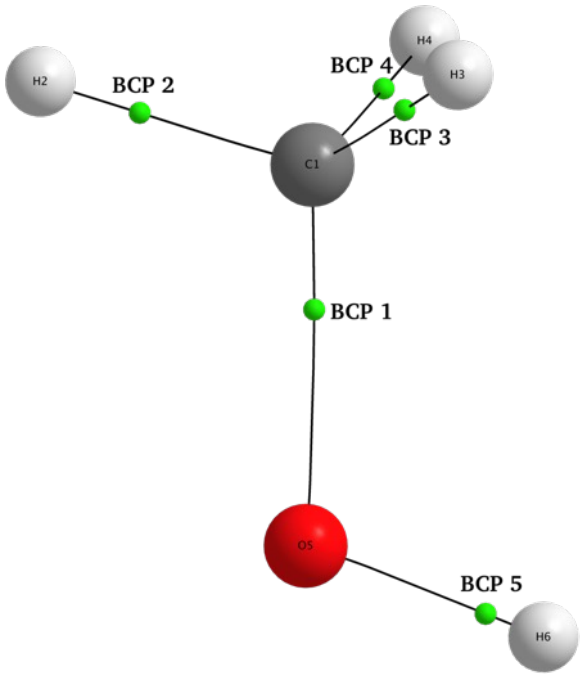

Figure 2.7: Qualitative Bond Critical Points and Bond Path in a Methanol Molecule.

There is a BP for every interaction between two NACPs, which nature unravels if they are chemical bonds, van der Waals interactions or even Hydrogen Bonds. The point at which the BP is a minimum is called BCP, which coincides with the bridge where BP intersects the zero flow surface between two bound atoms.[48]

2.3.1.2 Electron Density and Atomic / Molecular Shape Relationship

The atomic basins are $\nabla\rho(\boldsymbol{r})$ lines, Figure 2.8, that leave the NACPs and go to the limit of the atomic domain. At infinity, a free atom exhibits a spherical atomic basin, because the electron density distribution radially with equal probability. When there is an atomic approximation, these basins are deformed, generating a new topology.[48,49]

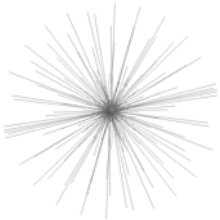

(a) The C Atomic Basin

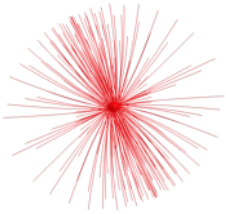

(b) The O Atomic Basin

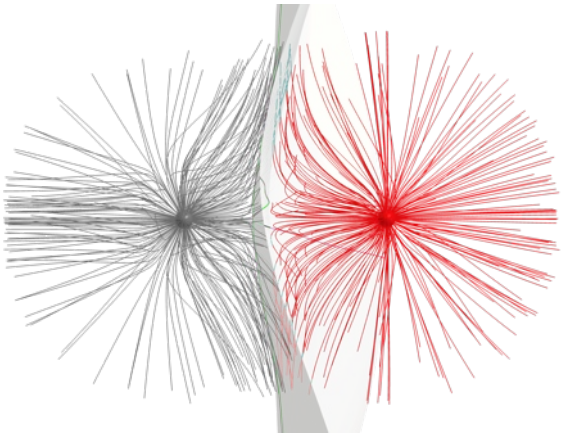

(c) C-o Bond on a Methanol

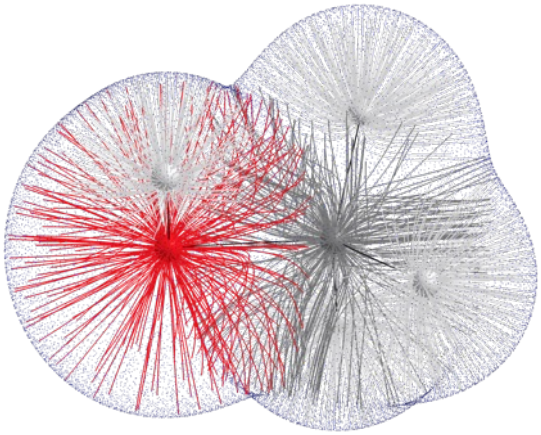

(d) The Overlay of Atomic Basin and the $\rho(\boldsymbol{r})$

Figure 2.8: Qualitative Atomic Basin for the Isolated Carbon atom (a), the Isolated Oxygen atom (b), Delimitating Interatomic Surface of the Carbon and Oxygen Basin (c), and the overlay of atomic basins and the $\rho(\boldsymbol{r})$ of a methanol molecule.

In a molecule, the sum of this atomic basins form the molecular topology of $\rho(\boldsymbol{r})$, and this surface coincides which the molecular shape. Note that the propagation limits of $\nabla\rho(\boldsymbol{r})$ lines from two NACPs is the BCP between both.

2.3.2 The Laplacian of Electron Density

Another valuable QTAIM property commonly used is the Laplacian of the Electronic Density. Following the discussion in Sub-subsection 2.3.1.2, the isolated atom has a spherical symmetry, but when a chemical bond is formed, the spherical symmetry breaks down. The Laplacian of $\rho(\boldsymbol{r})$ has the ability to recoup the Lewis / Pauling picture of the shell model in the electronic distribution for isolated atoms.

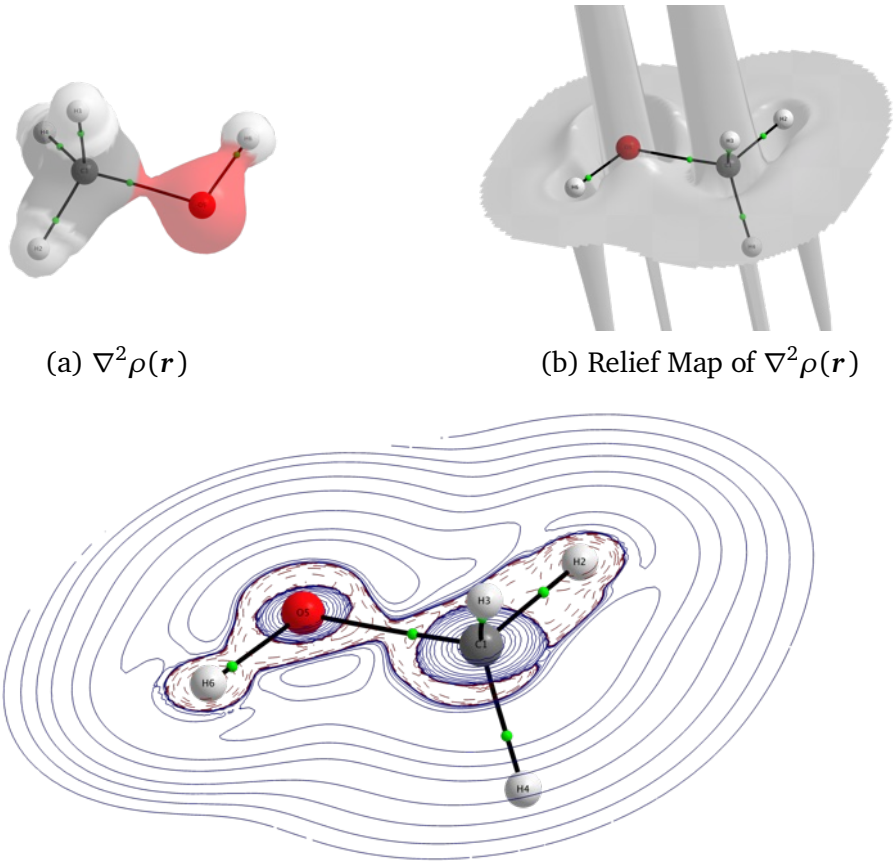

(a) $\nabla^2\rho(\boldsymbol{r})$

(b) Relief Map of $\nabla^2\rho(\boldsymbol{r})$

(c) Contour Lines of $\nabla^2\rho(\boldsymbol{r})$

Figure 2.9: Laplacian of Electron Density (a), Relief Map (b), and Contour Lines (c) of the Laplacian of Electron Density on plane containing the Oxygen-Carbon atoms of Methanol.

Since Laplacian is essentially a second derivative (see Equation 2.58), its sign indicates regions of local charge concentration or depletion with respect to immediate neighborhoods. Based on this fact, it can be summarized that if $\nabla^2\rho(\boldsymbol{r}) > 0$, the density is locally diminished and expanded with respect to the mean distribution (indicating an electron acceptor region) and if $\nabla^2\rho(\boldsymbol{r}) < 0$, the density is locally augmented and compressed with respect to the distribution (indicating an electron donating region).

2.3.2.0.1 Bonds in QTAIM

Within QTAIM terminology, each Bond Path can be classified as SHARED-SHELL (found between covalently bound atoms) or CLOSED-SHELL (corresponding to ionic bonds or intermolecular forces). The $\nabla^2\rho(\boldsymbol{r})$ in the BCP can be used to classify an interaction as of shared-shell or closed-shell nature:

- if $\nabla^2\rho(\boldsymbol{r}) < 0$, then the corresponding link can be classified as shared-shell (covalent bond);
- if $\nabla^2\rho(\boldsymbol{r}) > 0$, then the corresponding link can be classified as closed-shell (ionic bond).

2.3.3 The Bond Ellipticity

Now we turn our attention to the most important QTAIM descriptor for this work, the Bond Ellipticity. The Ellipticity, simply put, measures the anisotropy of electron distribution (directional distribution), in a plane perpendicular to the bond path and passing through the BCP, at which the $\rho(\boldsymbol{r})$ accumulates along a chemical bond, Figure 2.10.[48]

This anisotropy refers to the charge distribution of the atomic orbitals that form the bond. In a single bond there is only the formation of a σ-type molecular orbital (Figures 2.12a and 2.13a), either with the frontal approximation of two *s*-orbitals (spherical topology, Figure 2.11), or with the frontal approximation of two *p* orbitals (dumbell topology, Figure 2.11). The resulting topology (molecular orbital) will be cylindrical along the bond path, and especially, the contour lines in the BCP, parallel to the bond path, will result in a circumference.[26,48]

In a double bond there is a formation of σ- and one π-bond (Figures 2.12b and 2.13b). The σ-bond is the same of single bond, but the π-bond results from the parallel aproximation of two *p* atomic orbitais, i.e., the overlap topology has an ellipsoid shape and of greater volume than the σ-bond. When densities of the σ-bond is added to the π-bond, the result is still an ellipsoid whose contour lines in the BCP form an ellipse.[26,48] Triple bonds, in turn, are made of σ- and two π-bonds (Figures 2.12c and 2.13c). The second π-bond is perpendicular to the first π-bond, i.e, are two ellipsoids in perpendicular positions, so the sum of densities will result in a cylindrical symmetry. Therefore, the contour lines in BCP will be circular.[26,48]

With these concepts in mind, Richard Bader formulated the definition of Bond Ellipticity in QTAIM, Figure 2.14, as being the ratio between the two eigenvalues of

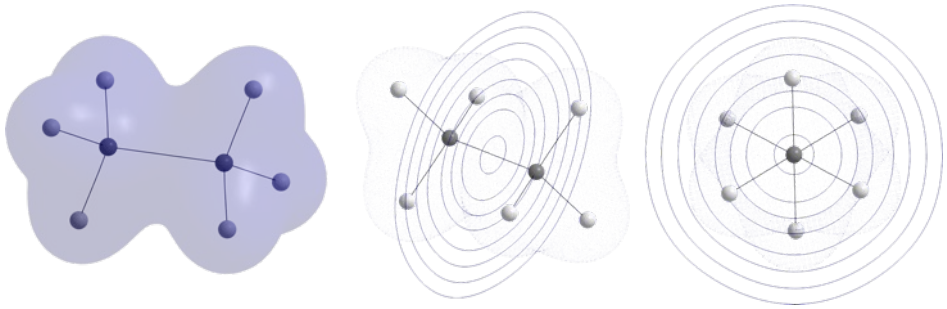

(a) $\rho(\boldsymbol{r})$ of Ethane

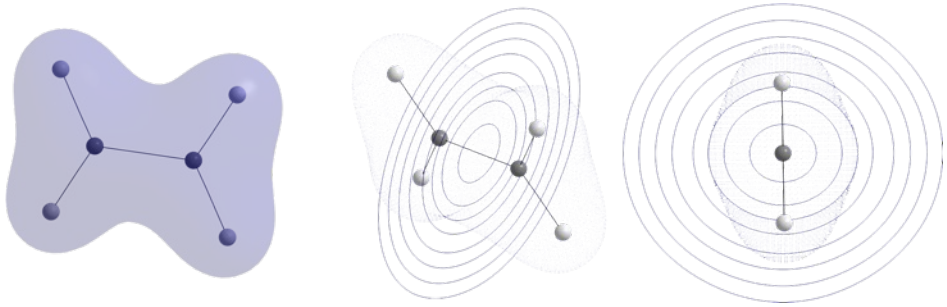

(b) $\rho(\boldsymbol{r})$ of Ethene

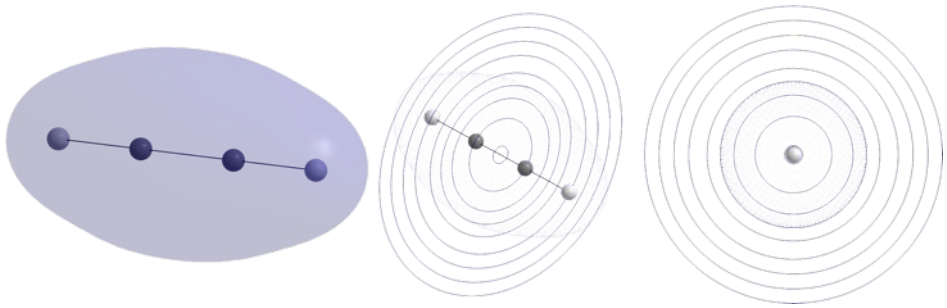

(c) $\rho(\boldsymbol{r})$ of Ethine

Figure 2.10: Qualitative tridimensional surface, isometric projection and front view contour lines of $\rho(\boldsymbol{r})$, along the CC bond path for (a) ethane, (b) ethene, and (c) ethine hydrocarbons.

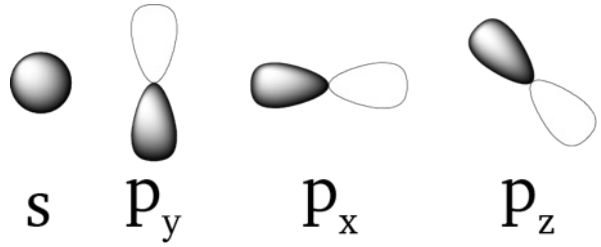

Figure 2.11: Pictoric representation of s and p atomic orbitals.

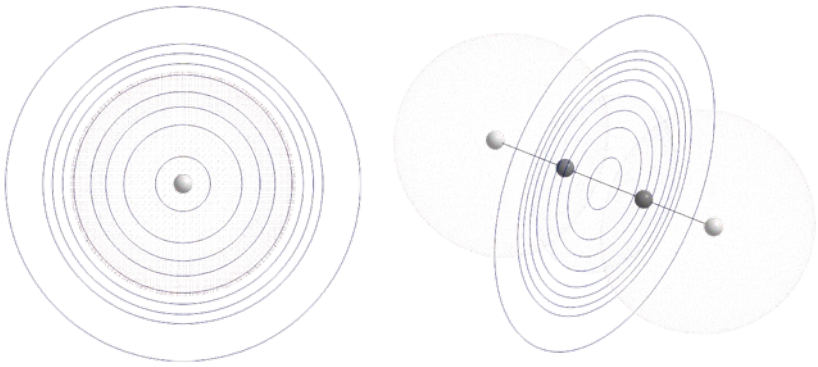

(a) σ-Bond

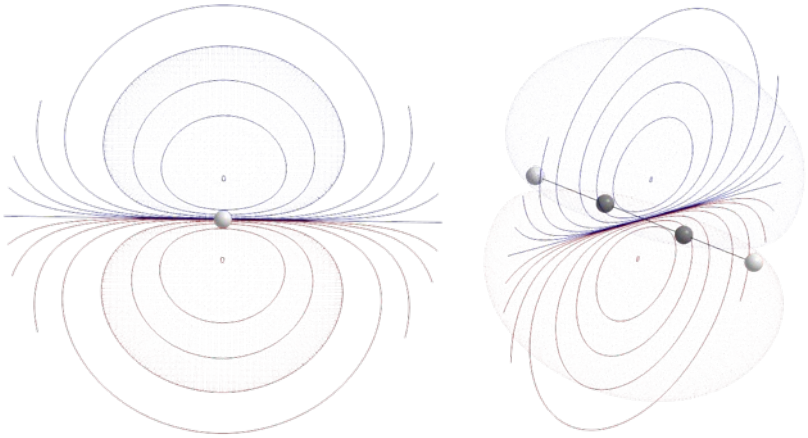

(b) π_1-Bond

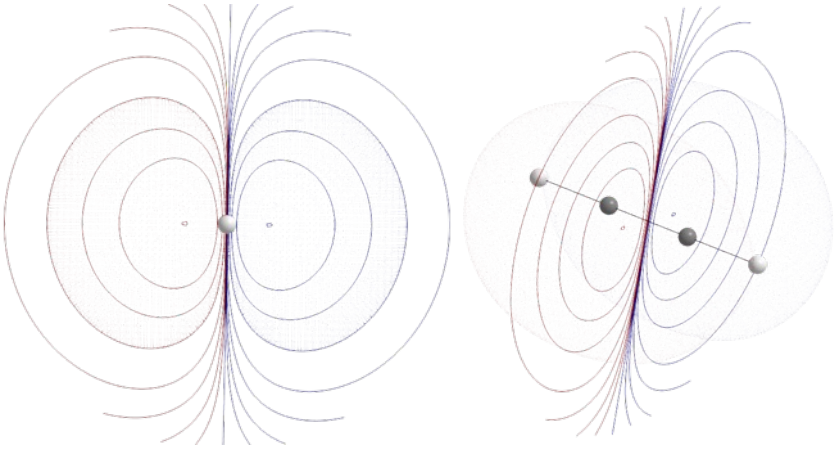

(c) π_2-Bond

Figure 2.12: Qualitative representation of the molecular orbitals involved in the CC triple bond for hydrocarbon ethine: (a) σ-bond, (b) π_1-bond, and (c) π_2-bond.

the diagonalized Hessian Matrix (Equation 2.57) wich participates of $\rho(\boldsymbol{r})$ Contour Lines in BCP, parallel to bond path.

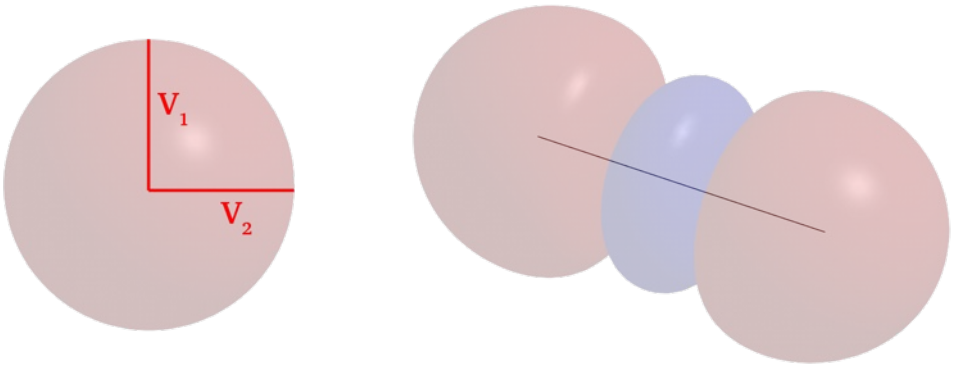

(a) Single CC-Bond

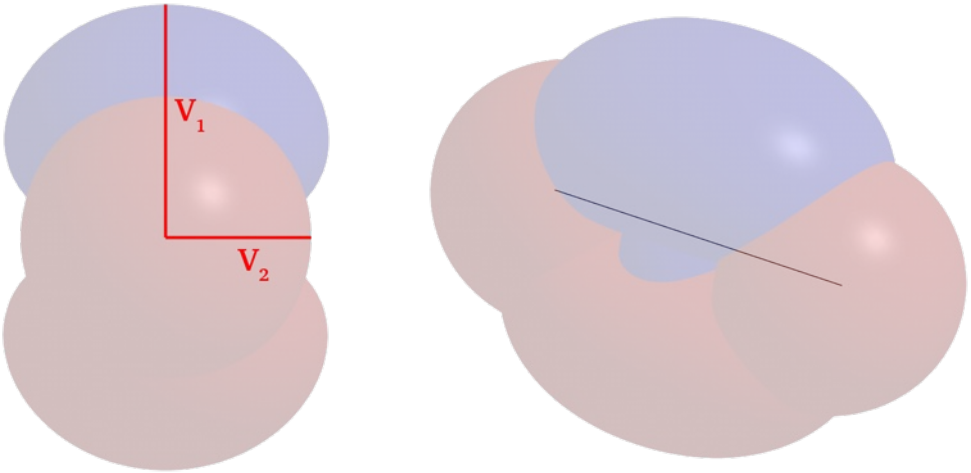

(b) Double CC-Bond

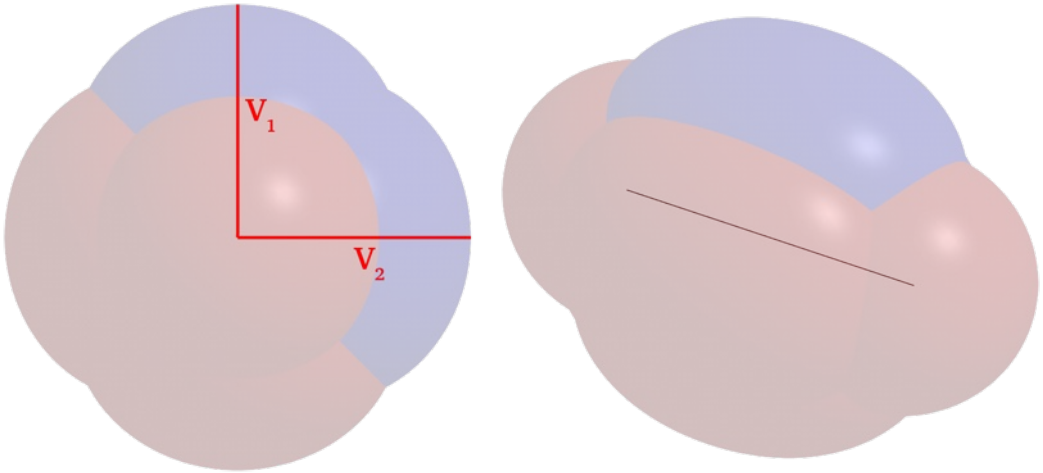

(c) Triple CC-Bond

Figure 2.13: Qualitative representation of (a) single, (b) double, and (c) triple bond according to the Molecular Orbital Theory (TOM).

Mathematically, ε is defined as:

$$\varepsilon = \frac{\lambda_1}{\lambda_2} - 1. \tag{2.60}$$

If $\lambda_1 = \lambda_2$, so $\varepsilon = 0$ and the chemical bond is cylidrically simetrical and has simple ou triple character, if $\lambda_1 \neq \lambda_2$, so $\varepsilon \neq 0$ and the chemical bond has a double character.

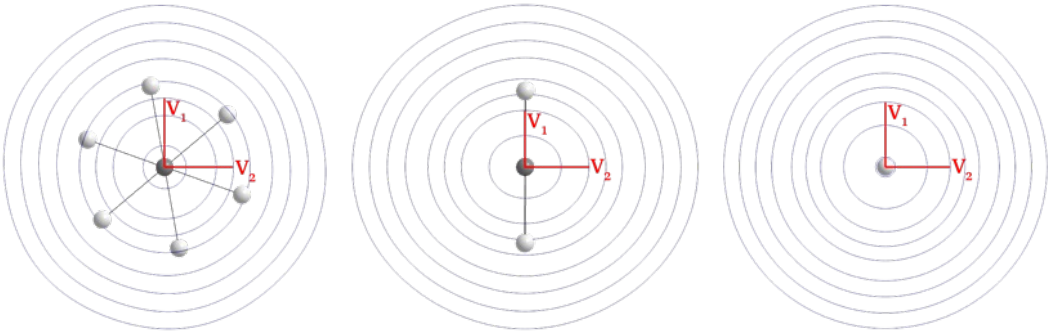

(a) $\lambda_1 = \lambda_2$ and $\varepsilon = 0$ (b) $\lambda_1 \neq \lambda_2$ and $\varepsilon \neq 0$ (c) $\lambda_1 = \lambda_2$ and $\varepsilon = 0$

Figure 2.14: Qualitative contour lines of $\rho(\boldsymbol{r})$ in the plane that contains the bond critical point (BCP) along the CC bond for ethane (a), ethene (b) and ethine (c) along the eigenvectors V_1 and V_2 (the major axes) of the Hessian matrix $\nabla^2\rho$, whose eigenvalues, λ_1 and λ_2 , respectively, are used to calculate the ellipticity at the BCP. The CC single bond in ethane and ethine is cylindrically symmetric resulting in $\varepsilon = 0$, while for the CC double bond in ethene, the ε value is positive.

Even though single and triple bonds present similar values of ε at the BCP, we focus here only in the case of single-double conjugated organic polymers, Hence, the usefulness of ε in providing a novel clear-cut NLO descriptor is held, because there is a clear numerical difference of this quantity between single and double bonds.

Chapter 3

Methodology

Based on the work of Gieseking et al. (Reference 12), we have evaluated the BEA's performance as a descriptor of electronic and NLO properties of two representative NLO chromophores, the 5- and 9-carbon streptocyanines (Figure 3.1).

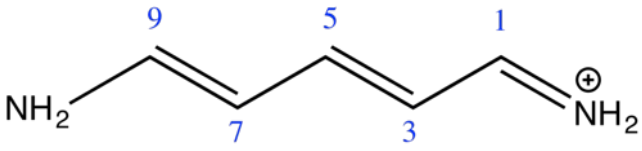

(a) 5C-Strepetocyanine

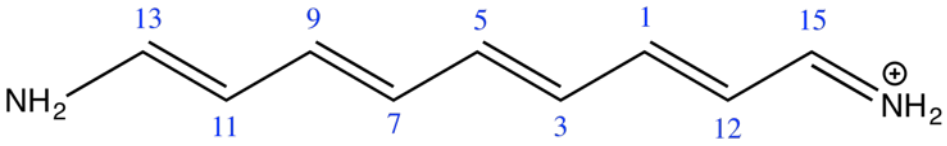

(b) 9C-Strepetocyanine

Figure 3.1: Chemical Structures of the Five-Carbon Streptocyanine (a) and the Nine-Carbon Streptocyanine (b), with the numbering of the relevant atoms.

To represent the electronic and geometric contributions of the presence of an electric field, the system was divided into three series of calculations (Figure 3.2):[1,12]

- **In Series 1:** an electric field is applied along the longitudinal axis, and the molecular geometry is fully optimized for each value of the electric field. This series accounts for both electronic and geometrical effects on the streptocyanine NLO properties;
- **In Series 2:** an electric field is applied along the longitudinal direction as in Series 1, but the molecular structure is constrained to the C2v point group. In this instance, only the electronic contributions to the NLO properties are considered;

- **In Series 3:** based on the geometries obtained in Series 1, single-point calculations are performed in the absence of any external electric field. Here, only the geometric contributions are accounted for.

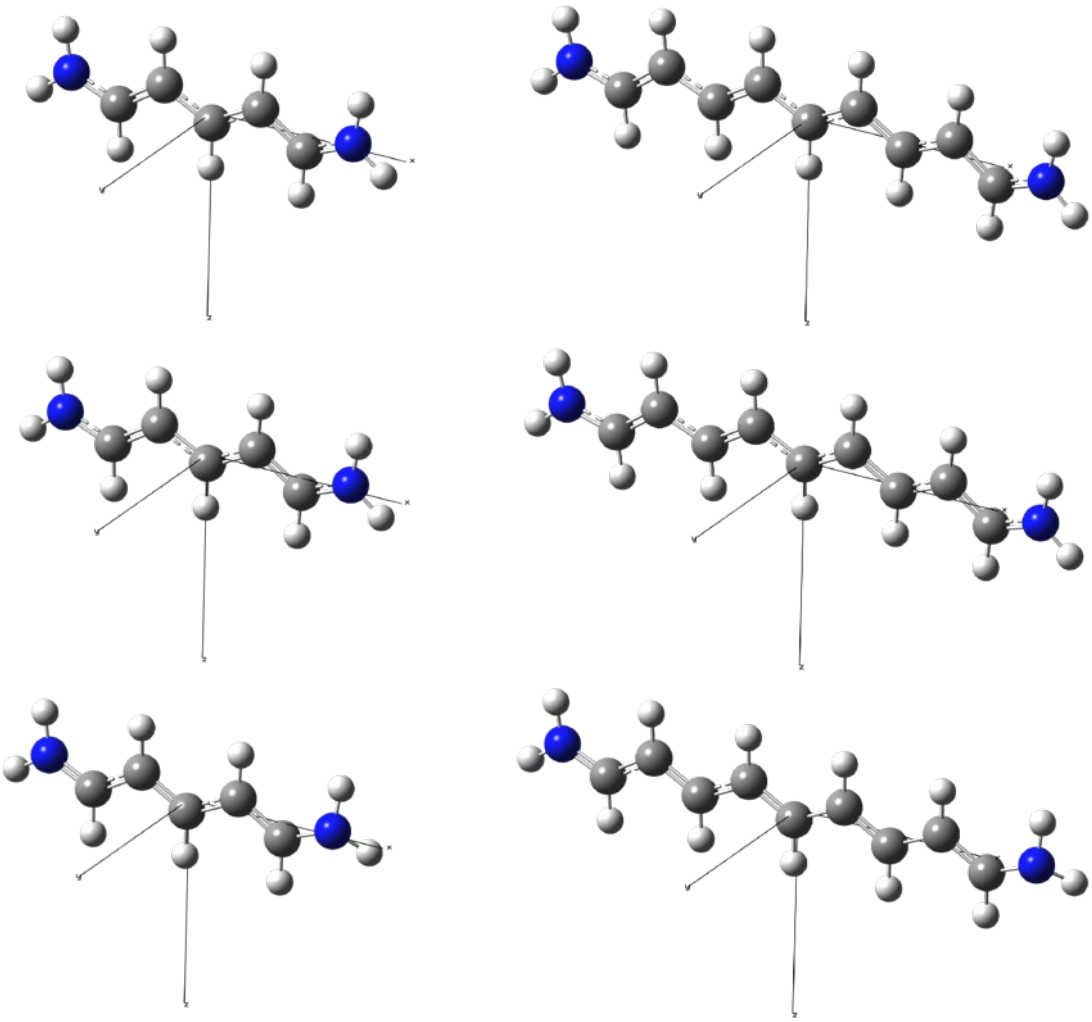

(a) 5C-streptocyanine (b) 9C-streptocyanine

Figure 3.2: Geometries of (a) 5-carbon and (b) 9-carbon streptocyanines in the C_{2v} point group (upper panel), relaxed in the presence of a minimal (middle panels), and maximum electric field (bottom panels).

All DFT calculations were performed using the long-range corrected hybrid functional ωB97XD, and to assess the impact of different basis set, we devised four levels of calculation: cc-pVDZ **(Level 1)**, aug-cc-pVDZ **(Level 2)**, 6-31G(d,p) **(Level 3)** and 6-31++G(d,p) **(Level 4)** using the "Gaussian 09 Revision-D02" software package.[34] These basis sets were selected to assess both Dunning (**Levels 1** and **2**) and Pople type (**Levels 3** and **4**) with and without diffuse functions, to check how different

basis functions affects the BEA parameters. For the 5-carbon streptocyanines the applied electric fields ranged from -7.5 to $+7.5 \times 10^7 V.cm^{-1}$ (similar to Reference 12) whereas for the 9-carbon streptocyanines the electric fields ranged here from -4.5 to $+4.5 \times 10^7 V.cm^{-1}$.

The NLO properties were computed by means of coupled perturbated Kohn-Sham (CPKS) method,[50] and since all calculations were performed with the molecular axis coinciding with the x-Cartesian axis, all ONL properties were evaluated using only the x-axis components (μ_x, α_{xx}, β_{xxx} and γ_{xxxx}).

The bond ellipticity at the critical point was computed using the "AIMALL" software package.[51] Two QTAIM properties other than ε were also considered within the framework of the bond property alternation (BPA) definitions as shown in Figure 1.3, the electron density ($\rho(r)$) and the Laplacian of electron density ($\nabla^2\rho(r)$), but their correlation with NLO characteristics are not as good as BEA (see Appendices A), so we opt to focus our discussion only for BEA and only demonstrate some results of these properties, leaving the largest volume of results for the Appendices A.1 and A.2.

Different bond order definitions were considered to compare BOA with BEA performance: Mulliken[13] (BOA Mulliken), Wiberg[14] (BOA Wiberg) and Mayer[15] (BOA Mayer). These bond order definitions were calculated using the Multiwfn software package.[52]

All alternating parameters were calculated with Figure 1.3 in mind, with double and single bonds being considered according to Table 3.1, and all codes used to process the results were home-made using Python 3.6[53] and are available in Appendix C. The graphics were plotted using the Gnuplot package[54].

Table 3.1: The bonds considered as simple and double in the alternating properties calculations.

Streptocyanine 5C			
Simple Bond	**Atoms involved**	**Double Bond**	**Atoms involved**
1	C1 - C3	1	C3 - C5
2	C5 - C7	2	C7 - C9
Streptocyanine 9C			
Simple Bond	**Atoms involved**	**Double Bond**	**Atoms involved**
1	C15 - C12	1	C12 - C1
2	C1 - C3	2	C3 - C5
3	C5 - C7	3	C7 - C9
4	C9 - C11	3	C11 - C13

The results in Reference 12, highlighted that an electronic parameter is preferable over a geometric when the molecular structure is driven away from equilibrium in the specific environment. It is important to bear in mind that, since BEA originates from the electronic density, it adapts to the environment where the chromophore is embedded, even when the molecular geometry is fixed (Series 3); on the other hand, bond order definitions consider the local atomic orbital coefficients between the two atoms involved in the chemical bonds. As a consequence, the environmental effects are treated explicitly in BEA and only implicitly in BOA.[1]

Chapter 4

Results and Discussions

4.1 Electronic Density and Geometric Analysis

We will begin our discussion with the evaluation of the geometric and electronic effects due to the application of an electric field on a molecule and in this analysis, only the Level 4 is considered (ωB97XD/6-31++G(d,p)). This choice will be justified when we show, in Section 4.5, that it presents better overall results. In our three series (see Chapter 3), only Series 2, does not take into account the geometric effect when an electric field is applied along the molecular axis, since it has the geometry restricted to a point group with bilateral symmetry (C_{2v}). In Series 1 and 3, geometry was optimized in the presence of an electric field range, with no constraints imposed. Obviously, the larger the electric field, the greater the distortion with respect to the geometry without any disturbing electric field.

In Figures 4.1 and 4.2 we have the overlays of the optimized structures with geometric constraint (C_{2v}), without the presence of electric field and in the presence of electric field. It is observed that the optimized structure without restriction and without the presence of electric field show similar geometry (9C-streptocyanine), with a Root Mean Square Deviation (RMSD) of 0.01 Å, or identical (5C-streptocyanine) with $RMSD = 0.00$ Å, which strengthens the hypothesis that to observe only the electronic contribution of the electric field application, it is enough to apply the field in the restricted geometry in C_{2v}.

For the geometric overlay between the unrestricted molecules with and without applying electric field ($7.5\times10^{7} V\cdot cm^{-1}$ for 5C-streptocyanine and $4.5\times10^{7} V\cdot cm^{-1}$ for 9C-streptocyanine), a significant change in geometry can be noticed, with $RMSD = 0.13$ Å (5C-streptocyanine) and 0.21 Å (9C-streptocyanine). This is expected, since the electric field is very large, and it is in fine tune with our second hypothesis that to consider only the geometric response to the electric field application would require re-optimization in an electric field, thus generating a molecular distortion, followed

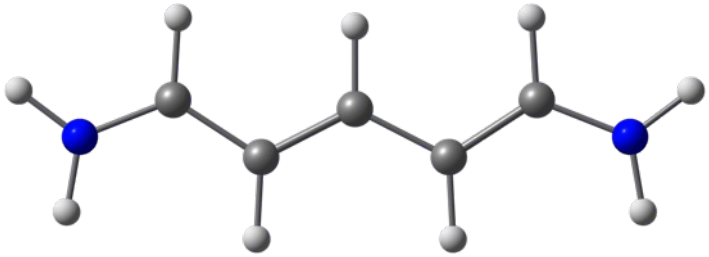

(a) $RMSD = 0.00$Å

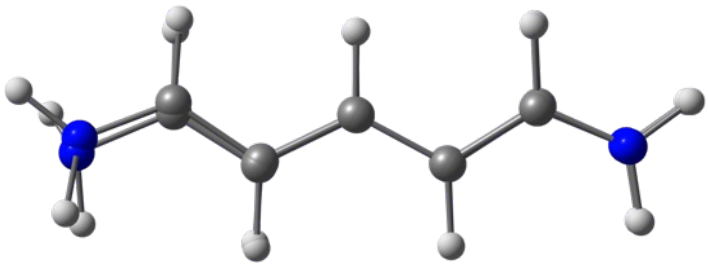

(b) $RMSD = 0.13$Å

Figure 4.1: Superimposed geometries of 5-C streptocyanines for (a) relaxed without electric field vs. rigid C_{2v} geometry, and (b) relaxed without electric field vs relaxed in the presence of electric field ($+7.5. \times 10^7 V \cdot cm^{-1}$). The wingspan (N-N distance) of C_{2v} structure is above 7.26 Å, which results in a relation wingspan / RMSD of 1.79%. Calculations preformed at ωB97XD/6-31++G(d,p) level of theory.

by a pure energy calculation (single-point type) without the application of this field. It is also observed that the real geometric distortion is higher in 9C-streptocyanine (Figure 4.2) than in 5C-streptocyanine (Figure 4.1), even when the applied electric field is significantly larger in the smaller chain streptocyanine. In fact, this was expected, since 9C streptocyanine has a larger molecular structure, and when the displacement is observed in relation to the molecular backbone (N-N wingspan), it is perceived that the displacement is very similar.

For a purely electronic analysis it is necessary to verify the effect that the electric field causes on the electronic properties of the molecule, and to do so we can identify the displacement of the electronic density in a rigid structure, after the application of the electric field. In Tables 4.1 and 4.2, it is presented by the displacement of the spatial positions of the Bond Critical Points of the 5C- and 9C-streptocyanine ends (involving the terminal carbons and the nitrogen bonded to it). For better appreciation of these effects in Figure 4.3, it shows the overlap of the Contour Lines (in the molecular plane) of the Electron Density of the two Streptocyanines with and without applying electric field ($+7.5. \times 10^7 V \cdot cm^{-1}$ for 5-C and $+4.5. \times 10^7 V \cdot cm^{-1}$ for that of

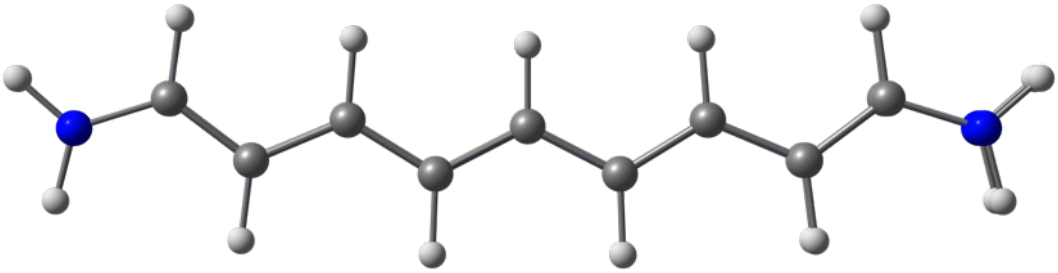

(a) $RMSD = 0.01$Å

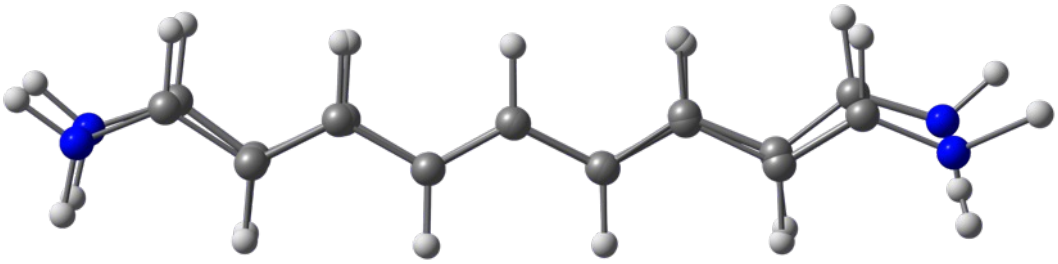

(b) $RMSD = 0.21$Å

Figure 4.2: Superimposed geometries of 9-C streptocyanines for (a) relaxed without electric field vs. rigid C_{2v} geometry, and (b) relaxed without electric field vs relxaed in the presence of eletric field ($+4.5. \times 10^7 V \cdot cm^{-1}$. The wingspan (N-N distance) of C_{2v} structure is above 12.17 Å, which results in a relation wingspan / RMSD of 1.73%. Calculations preformed at ωB97XD/6-31++G(d,p) level of theory.

9-C streptocyanines).

Table 4.1: Distance between the Atoms Involved in Terminal C-N bonds and their respective BCP of Series 2 5C-streptocyanine without and with $7.5 \times 10^7 V \cdot cm^{-1}$ Electric Field Applied. Calculations preformed at ωB97XD/6-31++G(d,p) level of theory.

$F = 0V \cdot cm^{-1} = 0$		
Critical Point	**Distance of Carbon Atom**	**Distance of Nitrogen Atom**
BCP-L (C9 - N14)	0.8469Å (33.84%)	1.6554Å (66.16%)
BCP-R (C1 - N11)	0.8469Å (33.84%)	1.6554Å (66.16%)
$F = +7.5 \times 10^7 V \cdot cm^{-1}$		
Critical Point	**Distance of Carbon Atom**	**Distance of Nitrogen Atom**
BCP-L (C9 - N14)	0.8542Å (34.18%)	1.6448Å (65.82%)
BCP-R (C1 - N11)	0.8362Å (33.42%)	1.6661Å (66.58%)

The electric field was applied from left-to-right along the molecular axis (see Figure 4.3), and the Bond Critical Point of the leftmost Carbon-Nitrogen bond was labeled

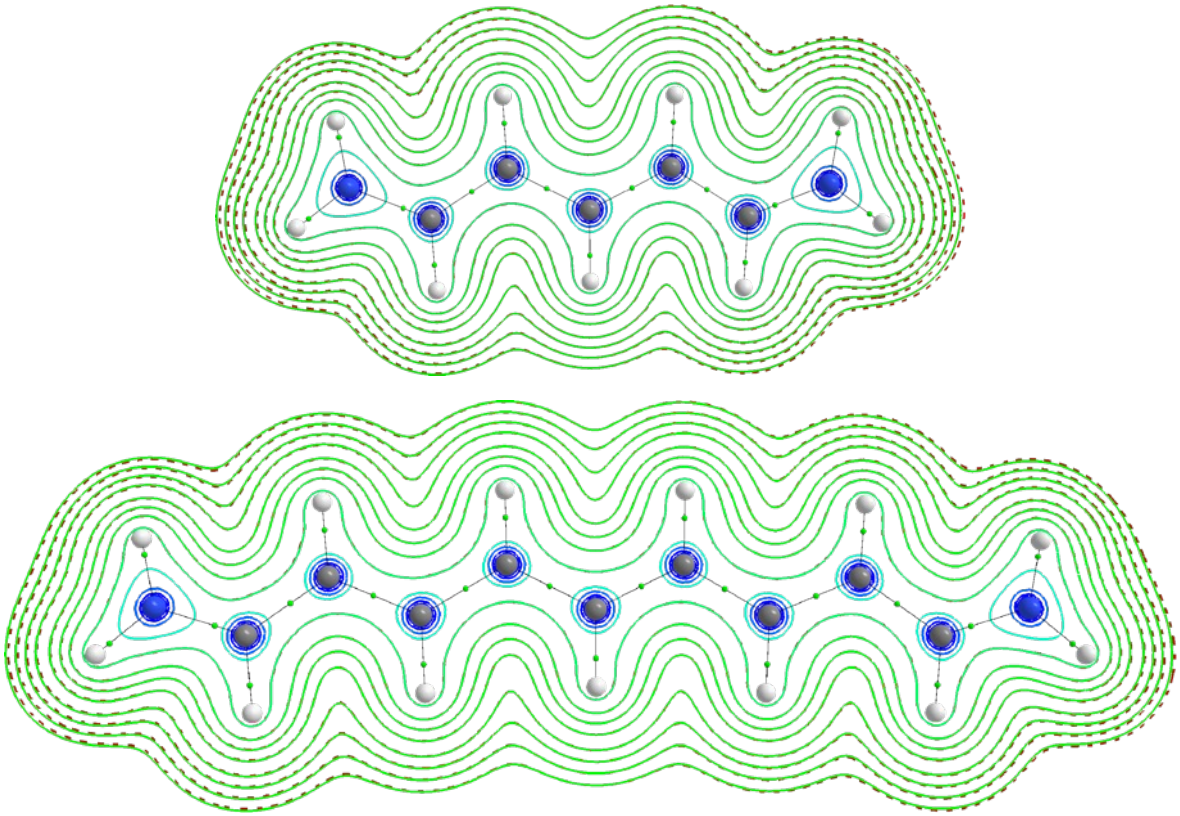

Figure 4.3: Overlay of Electron Density Contour Lines molecular plane for Streptocyanine 5C (top) and 9C (bottom) from optimized relaxed geometries without electric field (solid green lines) and in the presence of an external electric field (dashed red lines) of magnitude $+7.\times10^{7}V\cdot cm^{-1}$ (5C) and $+4.5.\times10^{7}V\cdot cm^{-1}$ (9C) oriented along the molecular axis. Calculations preformed at ωB97XD/6-31++G(d,p) level of theory.

Table 4.2: Distance between the Atoms Involved in Terminal C-N bonds and their respective BCP of Series 2 9C-streptocyanine without and with $4.5\times10^{7}V\cdot cm^{-1}$ Electric Field Applied. Calculations preformed at ωB97XD/6-31++G(d,p) level of theory.

$F = 0V\cdot cm^{-1}$		
Critical Point	**Distance of Carbon Atom**	**Distance of Nitrogen Atom**
BCP-L (C13 - N22)	1.6641Å (66.07%)	0.8547Å (33.93%)
BCP-R (C15 - N19)	1.6641Å (66.07%)	0.8547Å (33.93%)
$F = +4.5\times10^{7}V\cdot cm^{-1}$		
Critical Point	**Distance of Carbon Atom**	**Distance of Nitrogen Atom**
BCP-L (C13 - N22)	1.6570Å (65.79%)	0.8618Å (34.21%)
BCP-R (C15 - N19)	1.6741Å (66.47%)	0.8446Å (33.53%)

here (with the intention of making a rapid association) as BCP-L while the rightmost Carbon-Nitrogen bond as BCP-R. The electron density displacement is in favor of the electric field, and looking at Figure 4.3 it is observed that dashed contour lines (from the calculation with electric field) are shifted from left-to-right compared to the solid lines (from the calculation without the electric field), while atoms remain in the same position (since the geometry is restricted).

There is a noteworthy pattern in the displacement of the Bond Critical Points themselves, Tables 4.1 and 4.2. Just like the as electric density, the critical points shift in favor of the electric field. Although there is a displacement of the electronic properties when a strong electric field is applied, this displacement is more subtle, compared to the geometric distortion that occurred in the unrestricted optimized geometry (Series 1 and 2). While there was a displacement of about 1.0% in the BCPs of the two streptocyanines, we observed a geometric variation of about 1.7% if we consider only the molecular backbone.

4.2 Bond Order Dependence with Basis Functions

In order to analyze the dependence, already known in the literature (References 16 and 17), of the Bond Order definitions with respect to the basis set functions, we now discuss only two level of theory cited in Chapter 3. The levels chosen were those containing the Pople type basis set: a level without diffuse functions (Level 3 - ω/6-31G(d,p)) and one with diffuse functions (Level 4 - ω/6-31++G(d,p)), the other two levels, with Dunning type basis set (with and without diffuse functions), presented similar results to the two Pople types and were removed to Appendices A.6, A.5 and A.7. The results presented here are for the 9C-streptocyaine, since it is the most polarizable of the two studied molecules, the same results for the 5C-streptocyanine are found in the Appendices A.6, A.5 and A.7.

It is important to point out that in the attempt to create a general formation law for these NLO quantities that encompasses all the computational conditions - when the domain is only electronic (Series 2), only geometric (Series 3) or both (Series 1) - it is necessary to find a descriptor that is more closely associated to these conditions. Therefore, the focus here will be the search for a descriptor that describes, as nearly as possible, the three series simultaneously.

In Figures 4.4, 4.5, 4.6 and 4.7 it are presented the relation of the Bond Order Alternation according to the definitions of Mulliken, Wiberg and Mayer with the NLO quantities at the two chosen calculation levels. The field applied comprises a symmetrical range of 33 equally-spaced points, between the maximum field ($+7.5\times10^{7}V\cdot cm^{-1}$

for the 5C- and $+4.5 \times 10^7 V \cdot cm^{-1}$ for the 9C-streptocyanines) and the minimum field ($-7.5 \times 10^7 V \cdot cm^{-1}$ and $-4.5 \times 10^7 V \cdot cm^{-1}$), passing through the null field. When the field is null the streptocyanines are in the so-called cyanine limit (hyperconjugation of the Carbon-chain), whereas in the case of larger electric field, the molecule approaches to the polyenic limit (well-defined alternation of π-bonds).

Regarding Linear Polarizability along the molecular axis (α_{xx}), Figure 4.5, we have the same conclusion as for μ_x, an erratic pattern observed in Mulliken's Bond Order, and expected pattern for the Bond Orders of Wiberg and Mayer, with subtle changes in the curves pattern. These can be easily associated with changes in NLO values at different levels of theory, once the 9C-streptocyanine has a relatively high polarizability, due to its hyperconjugated chain. However, observing in a more critical way, it is possible to notice that the BOA Mayer, without the presence of diffuse functions is the one that shows more similarity between the three series.

Figure 4.6 depicts the NLO quantity that presented the worst correlation among the three series, the First Hyperpolarisability component along the molecular axis (β_{xxx}). Although BOA Mulliken's elusive behavior was again noted, none of the Bond Orders were able to simultaneously predict the β_{xxx} behavior for the three molecular conditions (Series 1, 2 and 3), which will be discussed in due course.

Similarly, for the second hyperpolarizability along the molecular axis (γ_{xxxx}), Figure 4.7, the same behavior is also found in relation to the presence of diffuse functions, while BOA Mulliken becomes erratic, the other two Bonds Orders deteriorate noticeably, but maintains, to a certain extent, the expected pattern within the cyanine and polyenic limits. However, here again it appears that the BOA Mayer, without the presence of diffuse functions, presents very good values among the three series, allied with the fact that its worsening in the presence of diffuse functions does not contaminate the analysis.

Henceforth, we opted to discuss more deeply the performance of BOA Mayer with respect to our new NLO descriptor, while results for the other Bond Orders are restricted to Appendix A.

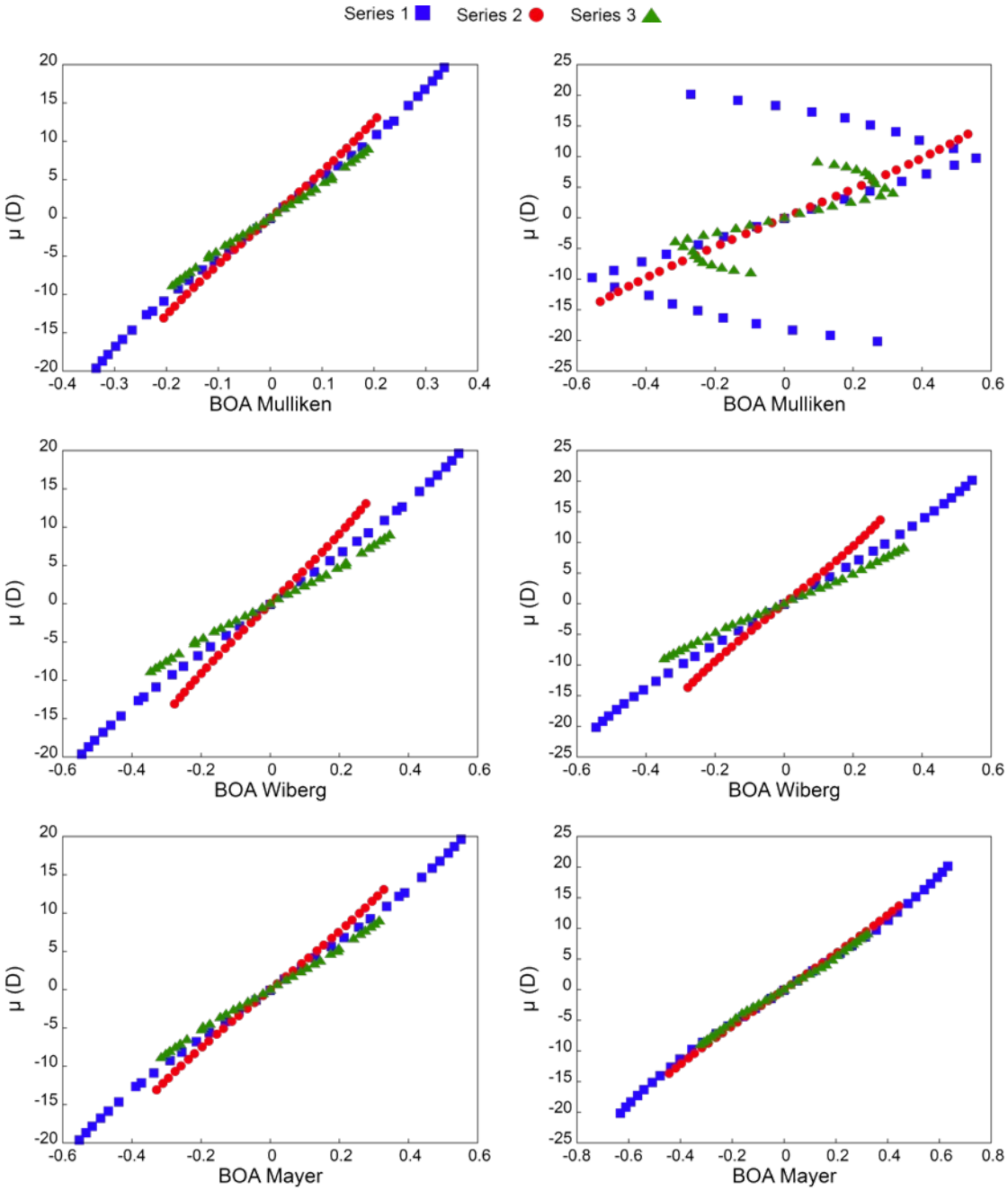

(a) ωB97XD/6-31G(d,p) (b) ωB97XD/6-31++G(d,p)

Figure 4.4: Correlation of μ_x with BOA Mulliken (top), Wiberg (middle) and Mayer (bottom) for 9-Carbons Streptocyanine in series 1, 2, and 3 for 2 level of theory, Level 3 (a) and Level 4 (b).

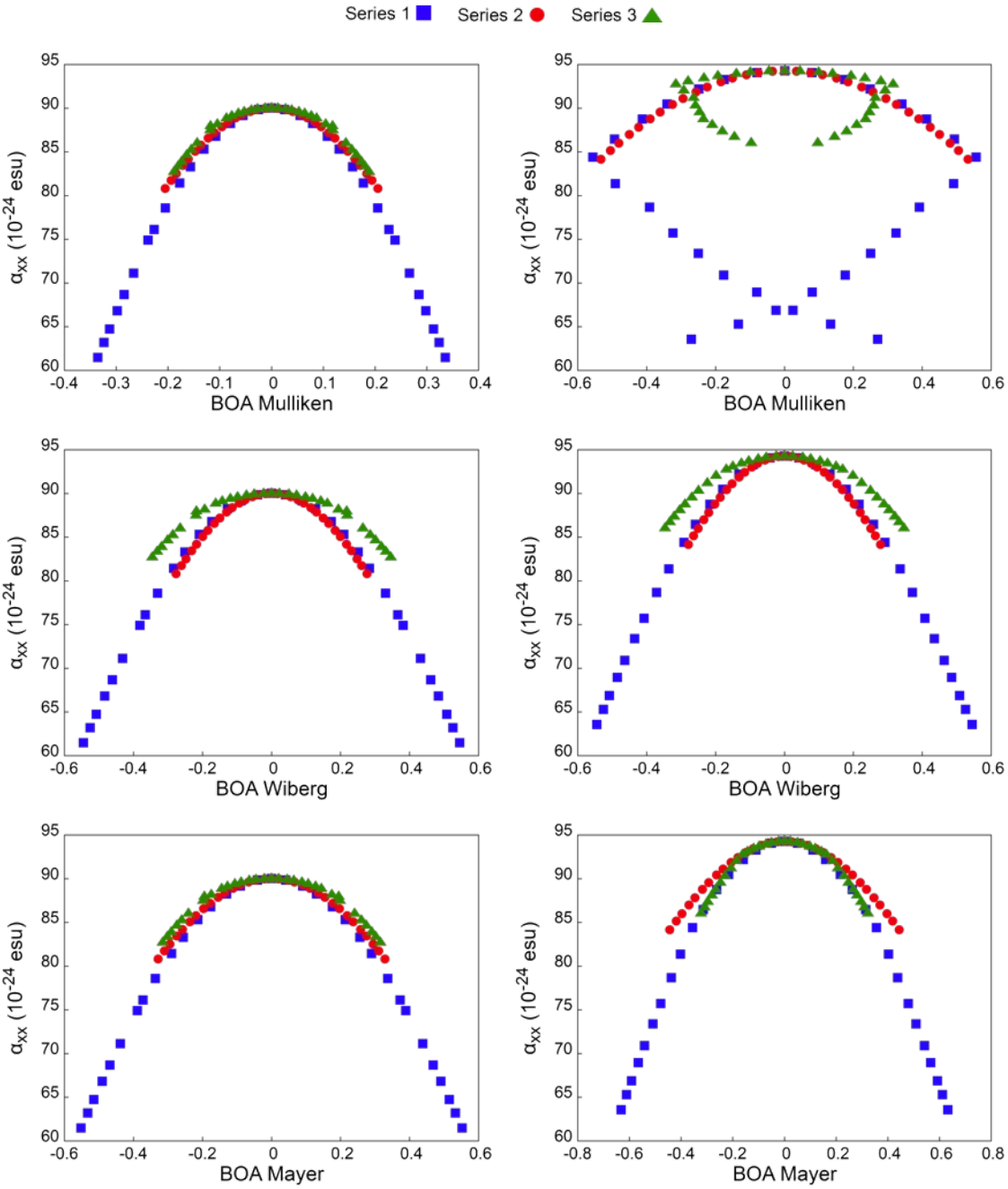

(a) ωB97XD/6-31G(d,p) (b) ωB97XD/6-31++G(d,p)

Figure 4.5: Correlation of α_{xx} with BOA Mulliken (top), Wiberg (middle) and Mayer (bottom) for 9-Carbons Streptocyanine in series 1, 2, and 3 for 2 level of theory, Level 3 (a) and Level 4 (b).

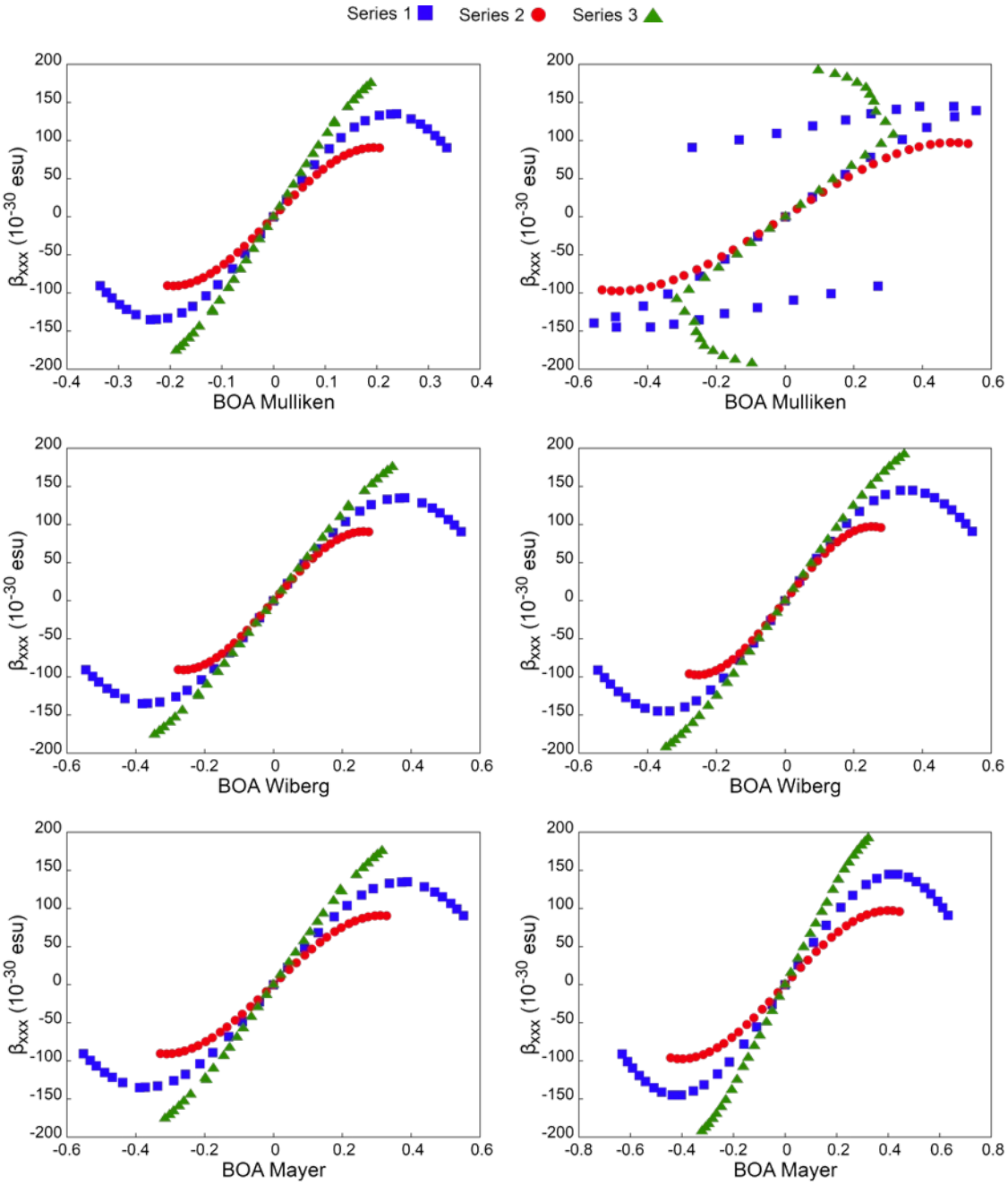

(a) ωB97XD/6-31G(d,p) (b) ωB97XD/6-31++G(d,p)

Figure 4.6: Correlation of β_{xxx} with BOA Mulliken (top), Wiberg (middle) and Mayer (bottom) for 9-Carbons Streptocyanine in series 1, 2, and 3 for 2 level of theory, Level 3 (a) and Level 4 (b).

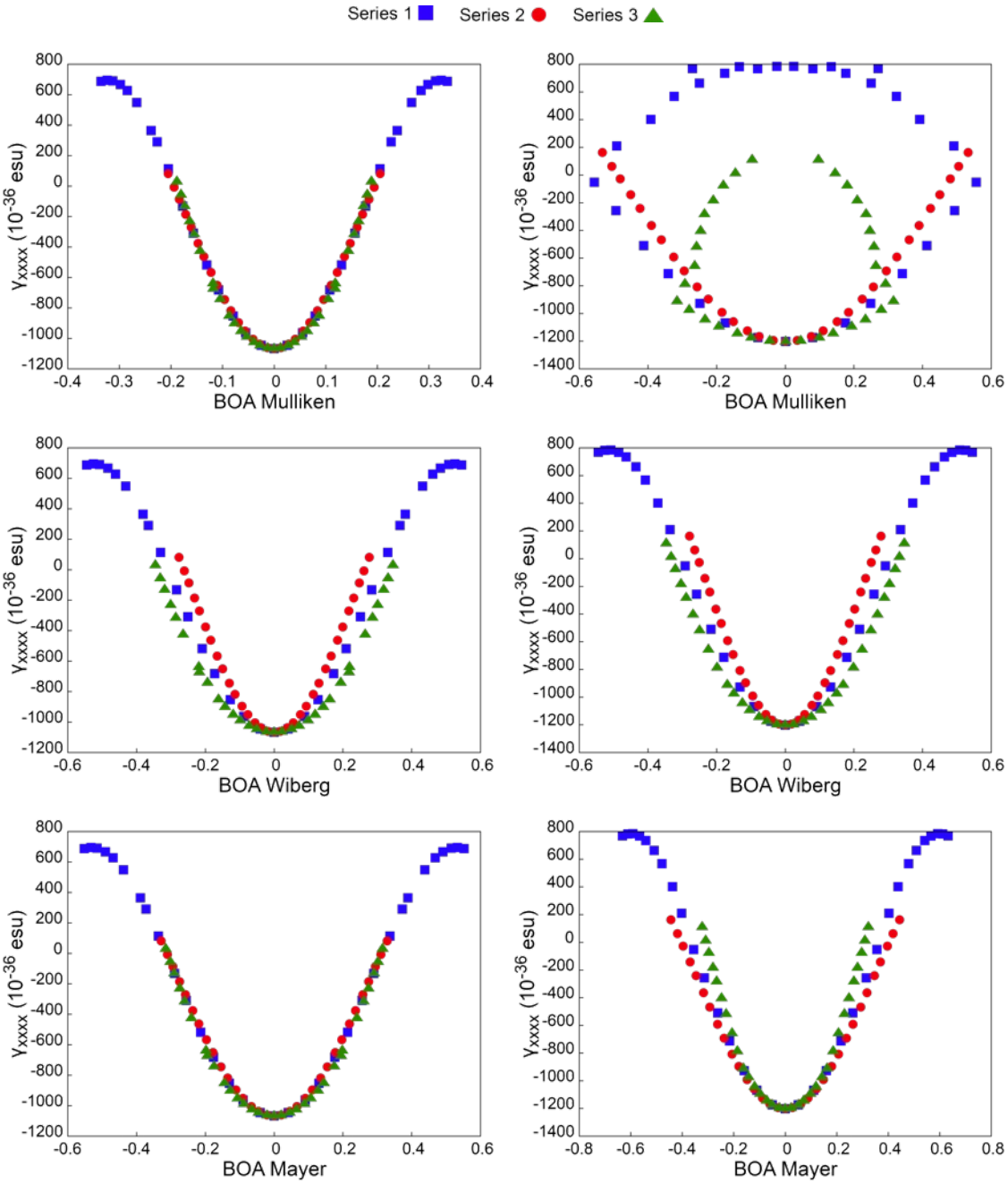

(a) ωB97XD/6-31G(d,p) (b) ωB97XD/6-31++G(d,p)

Figure 4.7: Correlation of γ_{xxxx} with BOA Mulliken (top), Wiberg (middle) and Mayer (bottom) for 9-Carbons Streptocyanine in series 1, 2, and 3 for 2 level of theory, Level 3 (a) and Level 4 (b).

4.3 Mayer Bonder Order Alternation (BOA) in opposition to Bond Length Alternation (BLA)

When searching for works with bond alternation parameters to describe NLO quantities, there is no doubt that two dominate the scenario, they are the BLA[8,9,55–57] and the BOA[3,58–60]. However, these two parameters are not flawless, especially when it comes to the description of NLO properties. We have already discussed in Section 4.2 that the BOA presents some limitations regarding the level of theory chosen to simulate a chemical environment and when it is investigated more deeply, it is perceived that authors already will iterate on the limitations of the BLA, when they are treated of systems in non-equilibrium[10,12]. Therefore, in order to do justice, by choosing the best classical descriptor, a comparison between these two descriptors is necessary.

Here again we chose in the comparison for the 9C-streptocyanine, the results for the 5C- are analogous and are listed in Appendix A.4, A.6, A.5 and A.7. The analysis of the behavior of BLA and BOA in relation to the NLO quantity can be observed in Figures 4.8, 4.9, 4.10, and 4.11. It is notable that for μ_x, α_{xx}, β_{xxx} and γ_{xxxx}, the BLA loses in performance. The BLA cannot describe series 2 in any scenario. This is already expected, since in series 2, the molecules are with the geometry restricted to a point group C_{2v}, that is, there is no geometric contribution of the electric field range application in the series 2 and the BLA is a purely geometric parameter.

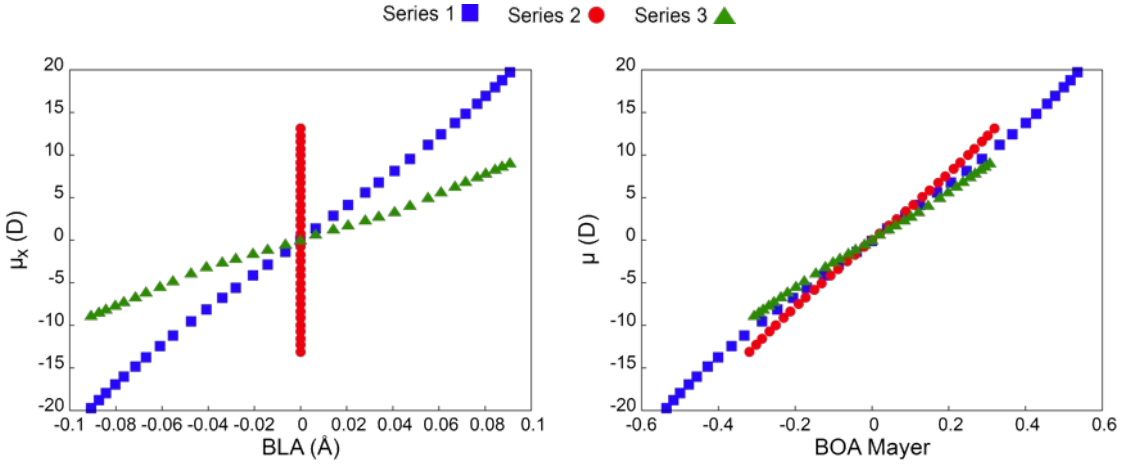

Figure 4.8: Correlation of μ_x with BLA (left) and BOA Mayer (right) for 9-Carbons Streptocyanine in series 1, 2, and 3, as obtained at the ωB97XD/cc-pVDZ level of theory.

At a first sight, it can be concluded that in series 2, the streptocyanines do not depart from the cyanine limit, since the BLA stays at 0 for the entire range of the

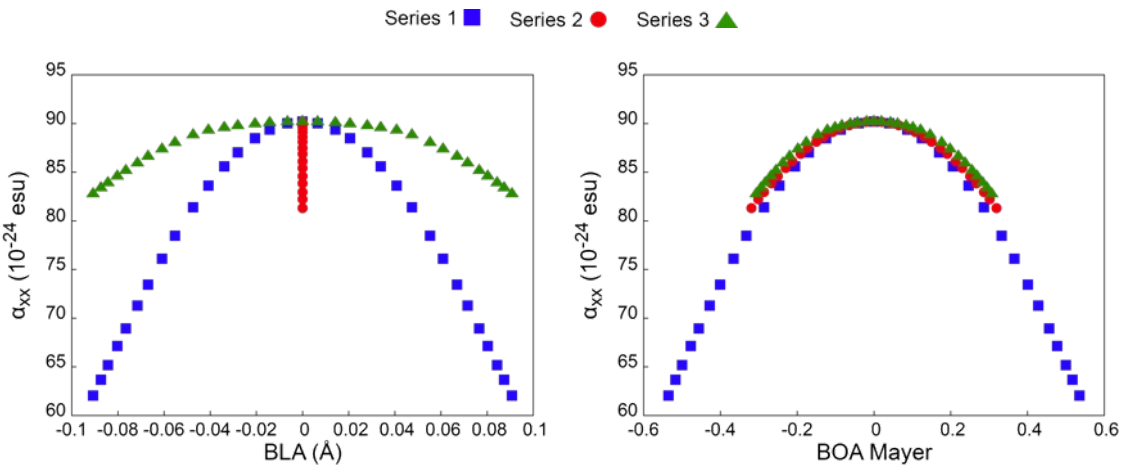

Figure 4.9: Correlation of α_{xx} with BLA (left) and BOA Mayer (right) for 9-Carbons Streptocyanine in series 1, 2, and 3, as obtained at the ωB97XD/cc-pVDZ level of theory.

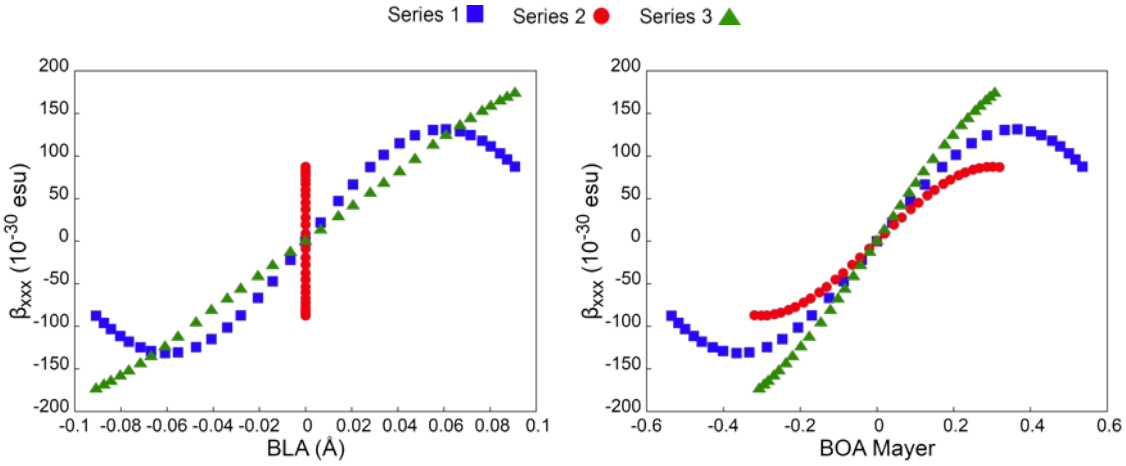

Figure 4.10: Correlation of β_{xxx} with BLA (left) and BOA Mayer (right) for 9-Carbons Streptocyanine in series 1, 2, and 3, as obtained at the ωB97XD/cc-pVDZ level of theory.

applied electric field application. Indeed, a deeper look reveals that BLA is not the correct parameter for assessing this type of molecular situation.[12] The geometries were optimized in a point group with bilateral symmetry and with inversion axis, the sizes of the CC bonds are identical to their complementary ones, which cancels out any parameter of purely geometric alternation.

Obviously the series 2 has departed from the cyanine limit with the application of the field, since this can be seen in the other alternation parameters. We therefore, refrain from discussing further the BLA results because of it inaccuracy in predicting

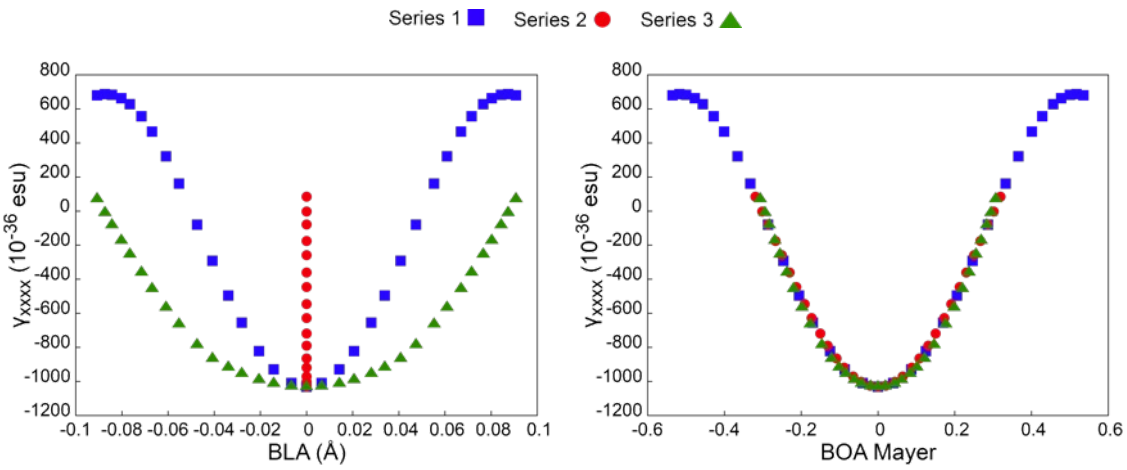

Figure 4.11: Correlation of γ_{xxxx} with BLA (left) and BOA Mayer (right) for 9-Carbons Streptocyanine in series 1, 2, and 3, as obtained at the ωB97XD/cc-pVDZ level of theory.

any NLO quantity in complex environments, and it is listed only in the Appendix A.4. For the next Section (Section 4.4), it will be analyzed which of the QTAIM properties should be carried forward for a final comparison with the BOA.

4.4 The QTAIM Alternation Parameters

As described in Section 2.3, each QTAIM descriptor has a specific physical meaning, in the attempt to find the QTAIM descriptor that best correlates in the three series with the NLO quantity, three descriptors were pre-selected: Electronic Density at the Bond Critical Point, Laplacian of the Electronic Density at the Bond Critical Point and the Bond Ellipticity. In order to remove non-relevant results for the Appendices, only one of these three descriptors will continue in the discussion of this work, so this section will serve to select this optimal descriptor. Since QTAIM properties do not undergo behavioral changes with the addition of diffuse functions to their calculation levels (see Appendices A.3, A.1 and A.2 and Subsection 4.4.1), it does not make sense to proliferate these sections with redundant results, so the Level chosen for this comparison is Level 4 ($6-31++G(d,p)$).

Aiming at using these QTAIM properties to define a reference parameter, as done with BOA and BLA, we define the same pattern, already consolidated, of Alternating properties in the bonds (see Chapter 3).[9–12,58,61] Thus appears the Bond Electron Density Alternation (BEDA), Bond Laplacian of Electron Density Alternation (BELA) and Bond Ellipticity Alternation (BEA), the three parameters that directly associate

the charge density in the BCP, accumulation or decrease of charge in the BCP and the σ- or π-character of the bond, respectively. In Figures 4.12, 4.13, 4.14 and 4.15, the relationship of these new QTAIM-based Bond Alternation parameters between the μ_x, the α_{xx}, the β_{xxx} and the γ_{xxxx}.

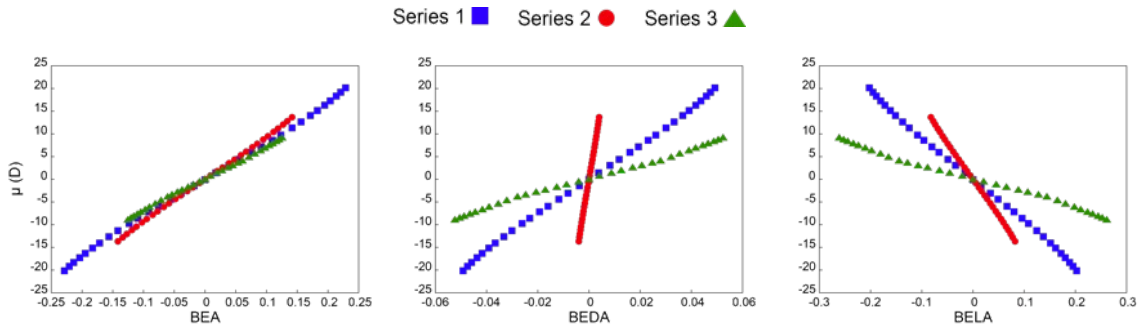

Figure 4.12: Parallel of correlation of μ_x with BEA (left), BEDA (middle) and BELA (right) in series 1, 2, and 3, as obtained at the ωB97XD/6-31++G(d,p) level of theory.

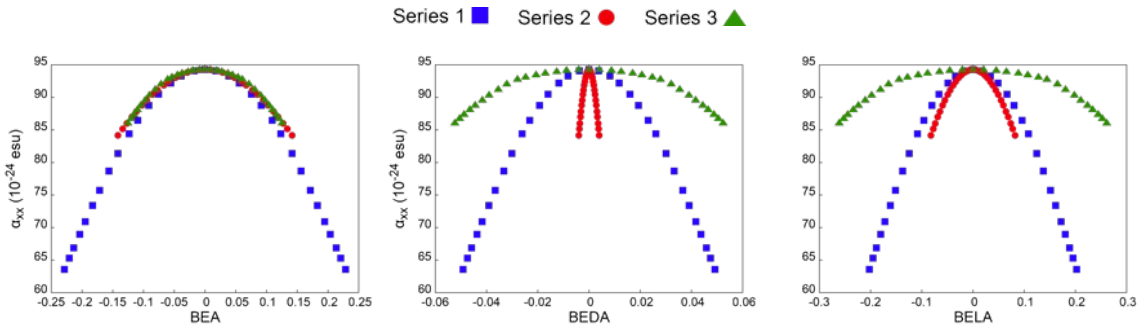

Figure 4.13: Parallel of correlation of α_{xx} with BEA (left), BEDA (middle) and BELA (right) in series 1, 2, and 3, as obtained at the ωB97XD/6-31++G(d,p) level of theory.

Looking at Figures 4.12 to 4.15 becames evident that the only parameter that presented the expected correlation with μ_x, α_{xx} and γ_{xxxx} was the BEA. The other parameters presented very different behaviors among the different molecular conditions. As for β_{xxx}, the behavior found was about the same for BOA-Mayer, already described in Section 4.2, reiterating the observation that β_{xxx} was the descriptor that most differentiates between the three series.

Although there was no good correlation between the BEA and β_{xxx}, it presented an excellent overlap of the curves for the other NLO properties. Since β_{xxx} does not show an overlap in any of the Bond Alternation descriptors, the BEA was deemed as show the QTAIM descriptor with the best-expected performance. Hence, only BEA will

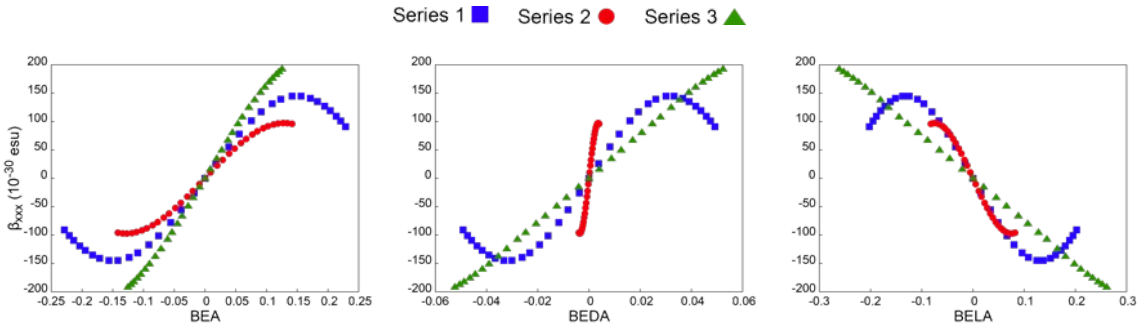

Figure 4.14: Parallel of correlation of β_{xxx} with BEA (left), BEDA (middle) and BELA (right) in series 1, 2, and 3, as obtained at the ωB97XD/6-31++G(d,p) level of theory.

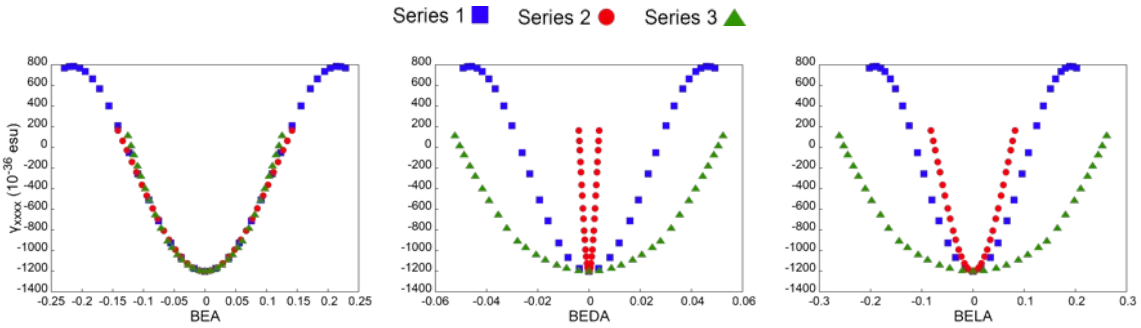

Figure 4.15: Parallel of correlation of γ_{xxxx} with BEA (left), BEDA (middle) and BELA (right) in series 1, 2, and 3, as obtained at the ωB97XD/6-31++G(d,p) level of theory.

be maintained in the following sections, while the other descriptors being restricted Appendices A.1 and A.2.

4.4.1 The Bond Ellipticity Alternation

With the BEA chosen to remain in the discussion of results, it is necessary to evaluate, in the same spirit of Section 4.2, it is dependent on the level of theory used. With this intent the Figures 4.16, 4.17, 4.18 and 4.19 depict the relationship between BEA and the NLO quantities.

In Figure 4.16 the plots between BEA and μ_x are arranged between the 4 different calculation levels. It is quite remarkable how little change in the μ_x and BEA relationship, the plots maintains the same expected pattern, with small changes in the NLO quantities, but the BEA remains constant. The same observation can be made for the α_{xx} (Figure 4.17), the β_{xxx} Figure 4.18) and the γ_{xxxx} (Figure 4.19). The plots maintain the overlap between the series, even with the change of base types from Dunning

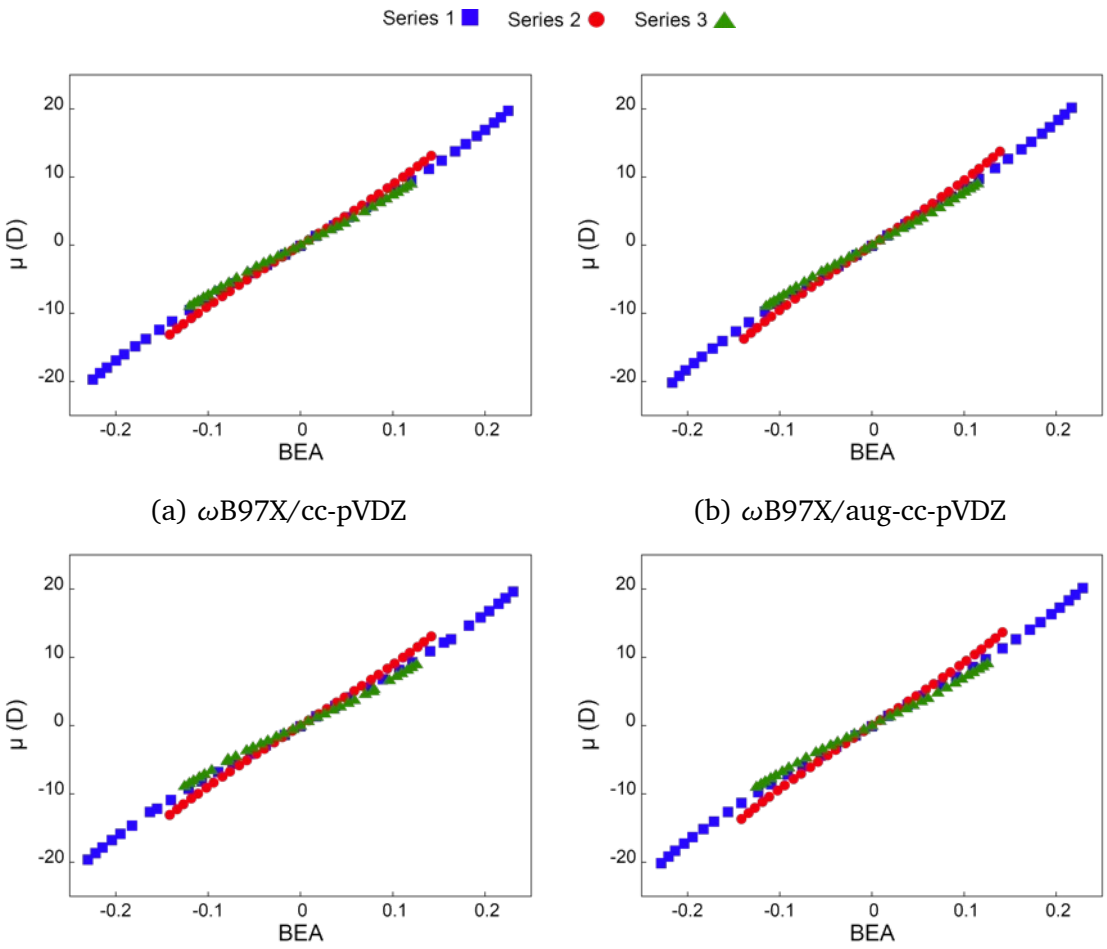

(a) ωB97X/cc-pVDZ

(b) ωB97X/aug-cc-pVDZ

(c) ωB97X/6-31G(d,p)

(d) ωB97X/6-31++G(d,p)

Figure 4.16: Correlation of μ_x with BEA for 9-Carbons Streptocyanine in series 1, 2, and 3 for 4 level of theory, Level 1 (a), Level 2 (b), Level 3 (c), Level 4 (d).

(Level 1 and 2) to Pople (Level 3 and 4), as a basis function without (Level 1 and 3) and with the presence of diffuse functions (Level 2 and Level 4).

Specifically for the β_{xxx}, although it does not demonstrate any overlap of the plots of the three series at any level of theory, it maintains exactly the same pattern, as observed in the Sections 4.2 and 4.3. Even though it does not carry an exceptional result, the BEA relation with β_{xxxx} does not downgrade BEA as an alternative to the descriptor, since none of the descriptors of the literature (BOA and BLA, see Sections 4.2 and 4.3) can not describe acceptably the β_{xxxx} simultaneously for all three series. Therefore, the BEA stands out as the most logical choice for the new descriptor, with its nuances against BOA-Mayer (the classical descriptor chosen for the final comparison) will be discussed in the next section.

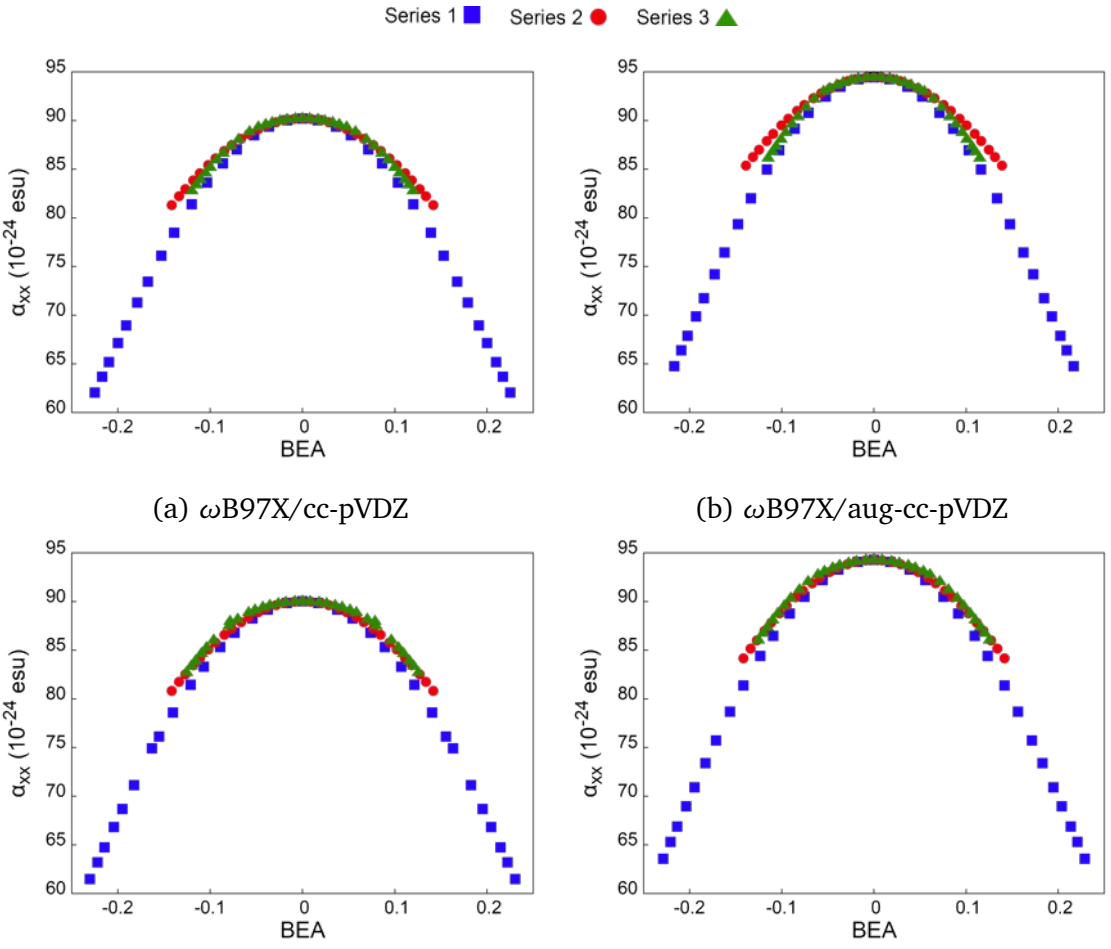

(a) ωB97X/cc-pVDZ

(b) ωB97X/aug-cc-pVDZ

(c) ωB97X/6-31G(d,p)

(d) ωB97X/6-31++G(d,p)

Figure 4.17: Correlation of α_{xx} with BEA for 9-Carbons Streptocyanine in series 1, 2, and 3 for 4 level of theory, Level 1 (a), Level 2 (b), Level 3 (c), Level 4 (d).

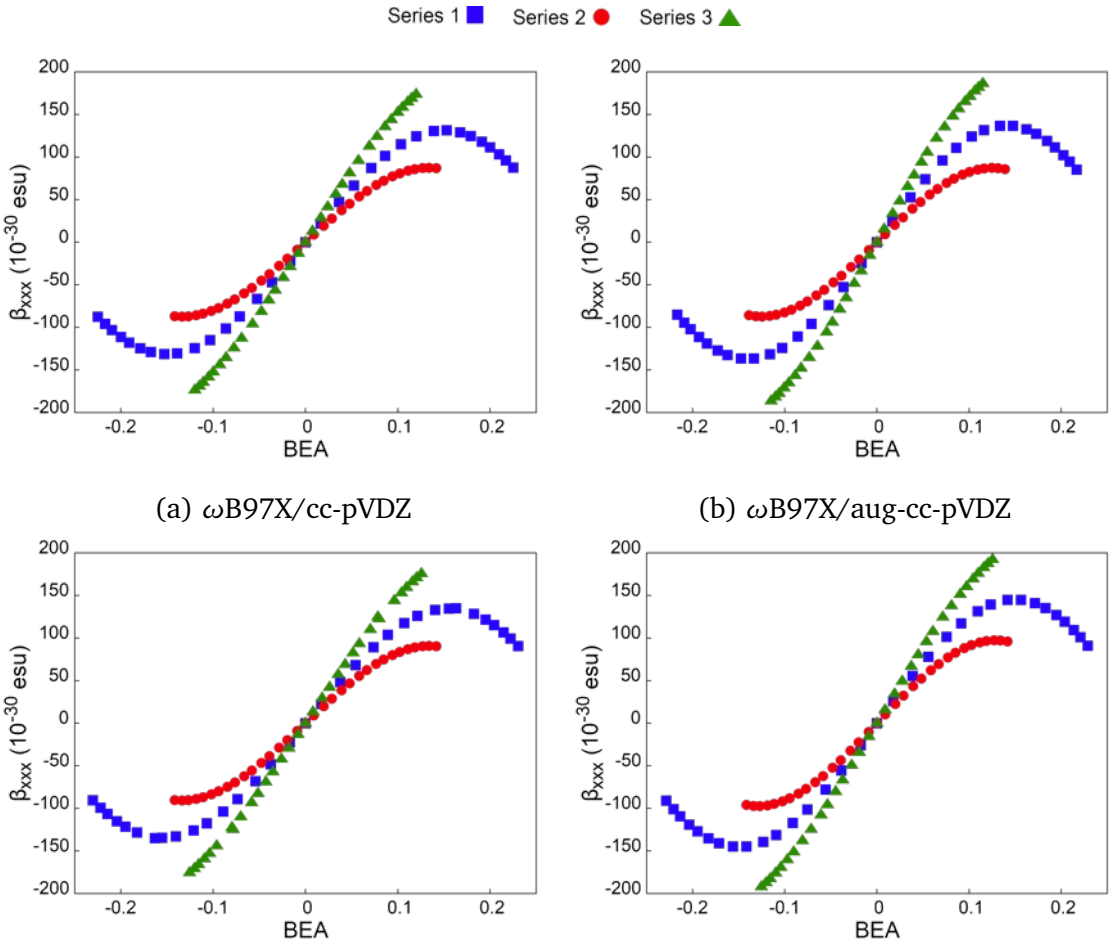

(a) ωB97X/cc-pVDZ

(b) ωB97X/aug-cc-pVDZ

(c) ωB97X/6-31G(d,p)

(d) ωB97X/6-31++G(d,p)

Figure 4.18: Correlation of β_{xxx} with BEA for 9-Carbons Streptocyanine in series 1, 2, and 3 for 4 level of theory, Level 1 (a), Level 2 (b), Level 3 (c), Level 4 (d).

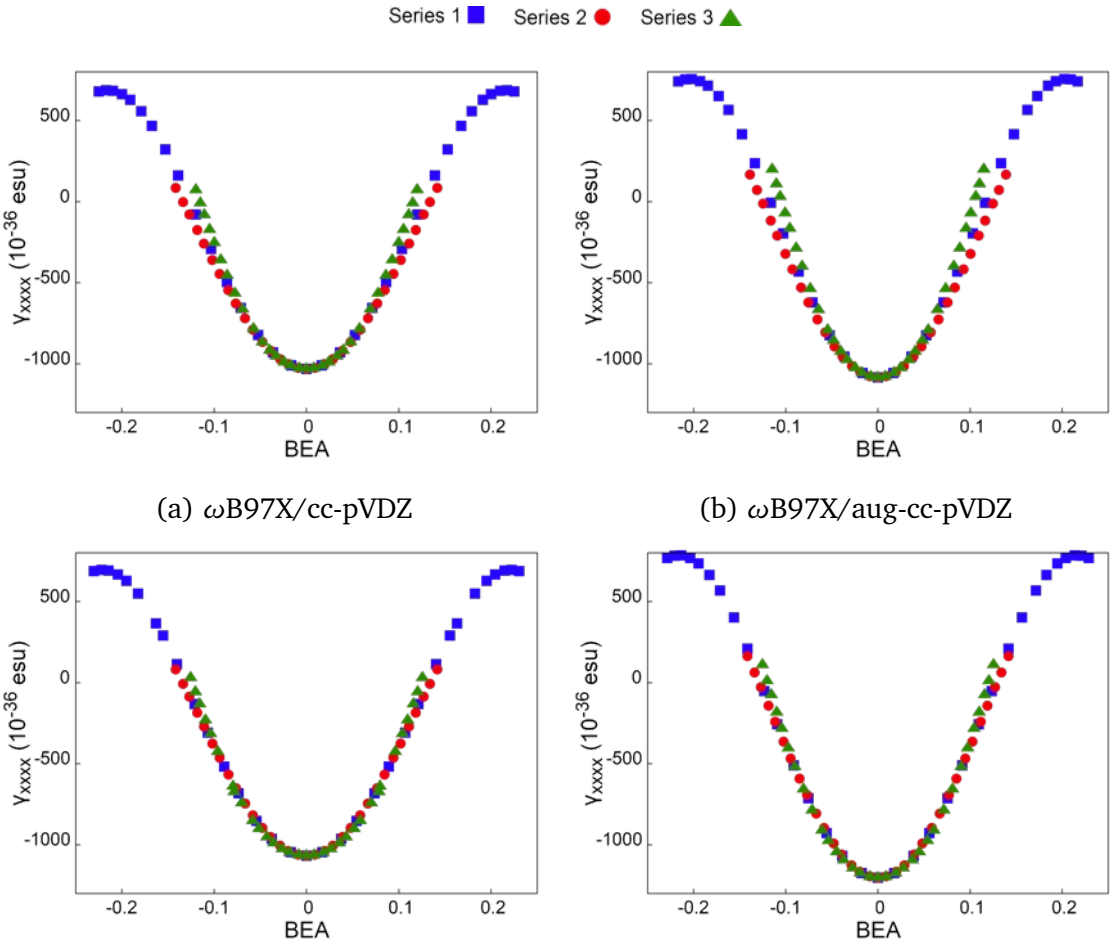

(a) ωB97X/cc-pVDZ

(b) ωB97X/aug-cc-pVDZ

(c) ωB97X/6-31G(d,p)

(d) ωB97X/6-31++G(d,p)

Figure 4.19: Correlation of γ_{xxxx} with BEA for 9-Carbons Streptocyanine in series 1, 2, and 3 for 4 level of theory, Level 1 (a), Level 2 (b), Level 3 (c), Level 4 (d).

4.5 Bond Order Alternation (BOA) versus to Bond Ellipticity Alternation (BEA)

Lastly, our discussion will be focused on the relationships of the two selected alternation parameters, BEA and BOA-Mayer between the NLO properties in 9C- streptocyanines. Once the extreme dependence of the basis set of functions is defined, and the fragility of the bond order definitions with respect to the presence of diffuse functions (Section 4.2), the main body of thesis carry on only the Pople's basis set including diffuse functions (Level 4).

First, let's look at the results of the longitudinal component of dipole moment (μ_x) (Figure 4.20, see also Figures in Appendices A.3 and A.6). BEA is notably in fine tune with the evolution of μ_x, underpinning its usefulness to correlate with μ_x and it was a general trend irrespective of the level of theory considered, as seen in Section 4.4. As addressed before in reference 12, an electronic parameter over a geometric one is a much more reliable tool for NLO materials regardless the molecular structure. Since BEA (recall that ε measures the anisotropy of the electron density) incorporates such demands, hence it can be consistently used for such analyses.

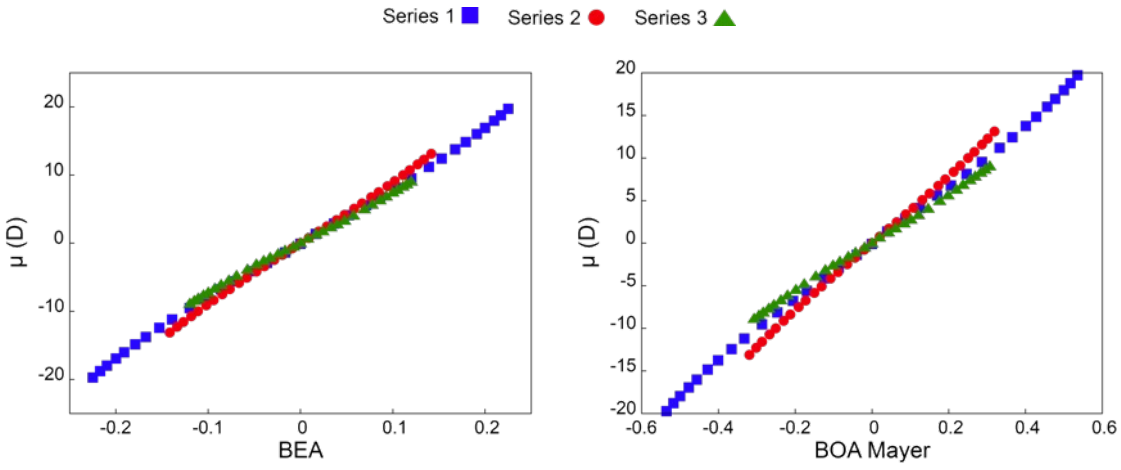

Figure 4.20: Correlation of μ_x with BEA (left) and BOA Mayer (right) for 9-Carbons Streptocyanine in series 1, 2, and 3, as obtained at the ωB97XD/6-31++G(d,p) level of theory.

Concerning the linear polarizability (α_{xx}) relationship with BEA, we find the same pattern often observed for α_{xx} versus BOA: a simple evolution with a peak at the cyanine limit and decreasing parabolic nature when the electric field causes the molecule to reach the polyene limit (Figure 4.21). As observed for μ_x, BEA corresponds well with BOA Mayer, predicting the same behavior of α_{xx} with increasing electric field

magnitude. It is important to note that, up to this point, that BEA predicts well α_{xx} (and all the other molecular properties) for each level of calculation considered (see Section 4.4 and A.3). The second-order and third-order molecular polarizabilities also correlate very well with BEA and BOA Mayer for each level of theory (Figure 4.22). BEA follows the same characteristic β_{xxx} sigmoidal evolution with BOA Mayer.[58] Further, the evolution of γ_{xxxx} (Figure 4.23) is symmetrical around the cyanine limit (BEA=0) showing that there are regions of BEA values that increasing β_{xxx} is accompanied by an increase in γ_{xxxx}. These results uphold BEA as reliable and simple parameter applicable in the rational design of NLO materials providing the same capabilities displayed in BOA Mayer definition, but superseding it in specific levels of theory.

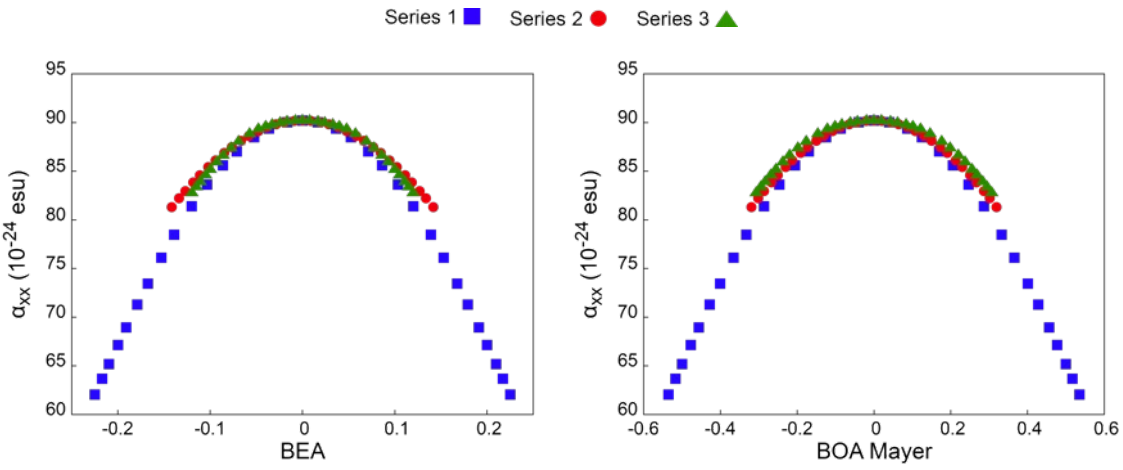

Figure 4.21: Correlation of α_{xx} with BEA (left) and BOA Mayer (right) for 9-Carbons Streptocyanine in series 1, 2, and 3, as obtained at the ωB97XD/6-31++G(d,p) level of theory.

The Correlation of Linear Polaribility and Second HyperPolarizability between BEA outperformed BOA Mulliken and BOA Wiberg (see the full results in Appendices A.5, A.7 and A.3) and slightly surpassed BOA Mayer, as depicted in Figures 4.21 and 4.23. For BEA, these properties superimpose each one of the three series for the larger magnitude of electric field. This observation poses BEA as a good predictor of molecular properties outperforming BOA.

Our findings show that BEA and BOA (according to Mayer) are well correlated in different molecular scenarios, including when larger (diffuse) basis set are implemented or increasing molecular lengths. Moreover, it will become clear that despite the good correlation of BOA with NLO quantities, the bond order values for each bond along the C-C chain loses its physical intuition when the chromophore is subjected to

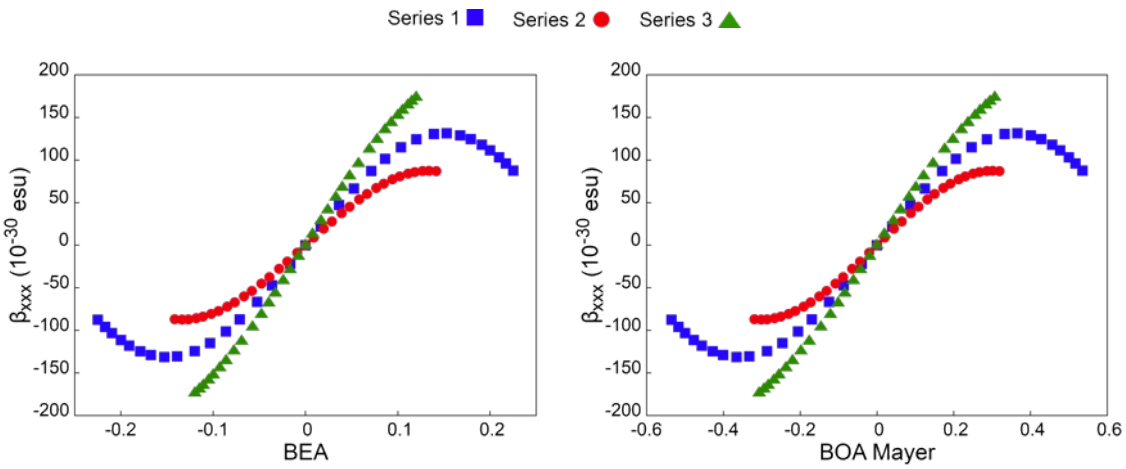

Figure 4.22: Correlation of β_{xxx} with BEA (left) and BOA Mayer (right) for 9-Carbons Streptocyanine in series 1, 2, and 3, as obtained at the ωB97XD/6-31++G(d,p) level of theory.

increasingly larger magnitude electric fields. For BEA, however, the individual ε values portray the expected behavior of the single-double bond pattern when departing from the cyanine-like structure.

Another important fact is that the three BOA definitions considered here, alternated amongst themselves as to which one was the best parameter to correlate with NLO properties of the two streptocyanines. For example, BOA Mayer, Wiberg, and Mulliken (Section 4.2) correlate better in each level of theory for a given property, but does not necessarily maintain accuracy in another set of theory/property. BEA, importantly, shows a transferable performance among different level of calculations thus proving its utility (See the Subsection 4.4.1). Jabłoński and Palusiak demonstrated that critical point QTAIM parameters aimed at describing hydrogen bond interactions are weakly dependent of both method (HF and DFT) and the basis set.[62]

To highlight how the bond properties ε and bond order (Mayer definition) is accounted on every bond of the main chain we present these properties schematically for every chemical bond across the entire 9C-streptocyanine for Level 3 and 4, Figure 4.24. In the upper part, when no electric field is present, both bond order and ε show values that corroborate the ideal polymethine state, which is obtained when two identical donor end-groups are associated with a polymethine chain.[63,64]

In the cyanine limit (no electric field) both resonance structures contribute equally so that the positive charge is primarily localized on the central carbon atom thus decreasing the central bond orders (d, e); the ending C-C bonds (a, h) have therefore the largest π-character showing large bond order and ε. Still looking at the upper part

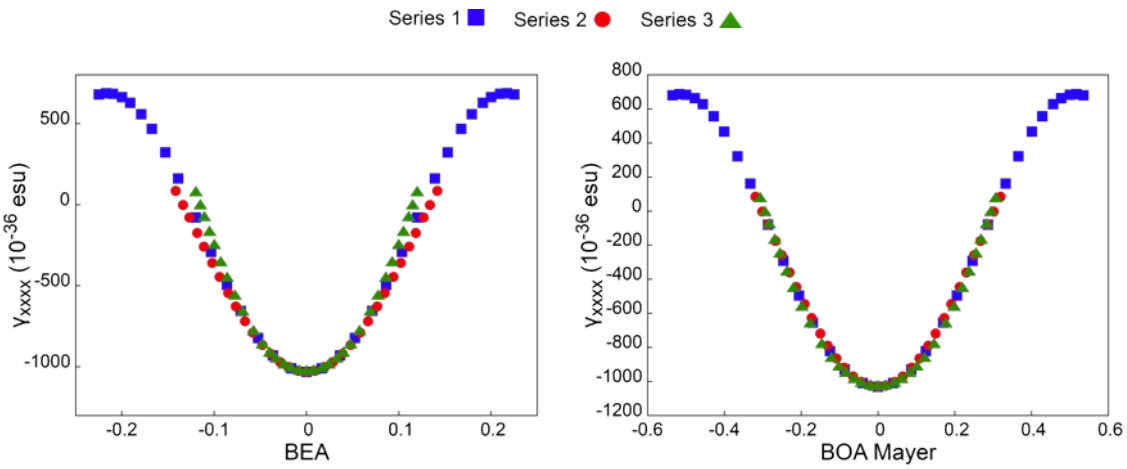

Figure 4.23: Correlation of γ_{xxxx} with BEA (left) and BOA Mayer (right) for 9-Carbons Streptocyanine in series 1, 2, and 3, as obtained at the ωB97XD/6-31++G(d,p) level of theory.

of Figure 4.24, it becomes evident how Mayer bond orders individually are strongly affected by the inclusion of diffuse functions alternating the magnitude of bond order when going from the ending C-C bonds (a, h) to the central part of the molecule (b, c, d, e, f), with are larger bond order values in Level 3. On the contrary, all the individual ε values are slightly larger in Level 3 than in Level 4 by a fixed difference whichever bond one might consider, showing its independence from the level of approximation. When the molecule is subjected to large magnitudes of electric fields, the situation becomes more chaotic for BOA Mayer: In Level 3, the bond order hierarchy is likewise found in ε; when diffuse functions are added, the largest π-character is found in the central d bond. Clearly ε values found in the maximum electric field supports the left resonance structure where the π-character is preferentially found in the bonds labeled b, d, f and h bond regardless what basis set was employed.

Since BOA and BEA were computed from average differences on adjacent bonds (Scheme 1), the BOA overall performance seems to be a result of error cancelation, whereas for BEA such serendipity was not responsible for the good correlation with NLO properties, even when considering non-equilibrium geometries.

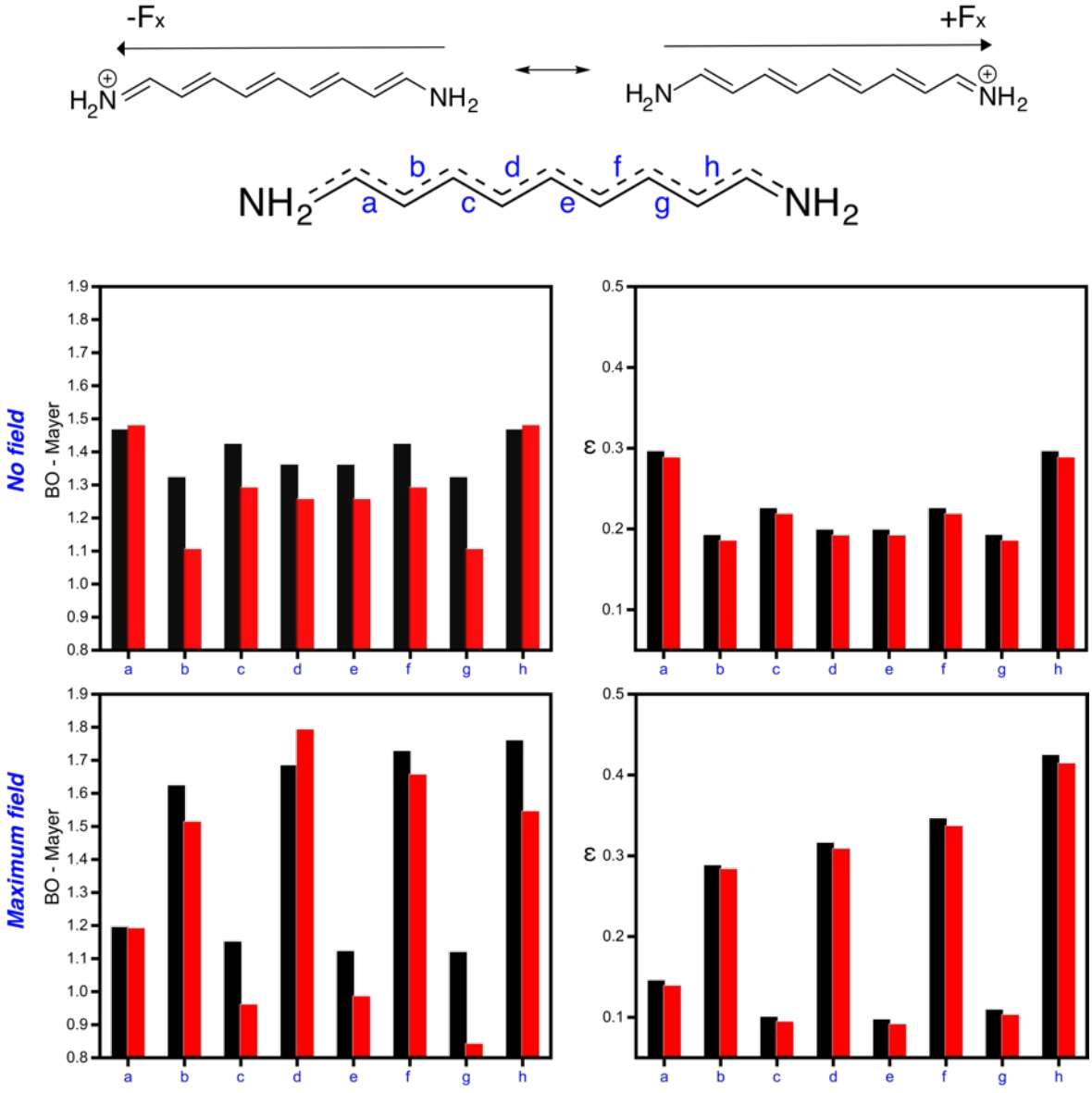

Figure 4.24: Dominant resonance structures in the 9C streptocyanine in the absence of electric field (top). The CC bonds are labeled a through h. Absolute bond orders (left) and bond ellipticities (right) with no electric field (top), and upon application (bottom) of an electric field of $4.5 \times 10^{7} V.cm^{-1}$ oriented in such a way that the positive charge locates to the left side of the molecule (left resonance structure). Results obtained at the ωB97XD/6-31G(d,p) (black bars) and ωB97XD/6-31++G(d,p) (red bars) levels. [1]

Chapter 5

Conclusions and Perspectives

In this thesis, we have shown how the BEA parameter can be an invaluable tool for the theoretical understanding of NLO organic chromophores since its predictability of molecular properties are comparable to BOA Mayer and superior to BOA Mulliken and Wiberg when different flavors of basis set are considered.

Additionally, BEA contains information about the symmetry of the electron density, an observable, and does not pertain to any arbitrary definition of electron population in between two atoms in a molecule. The feature of being based on a physical observable lends to the bond ellipticity (and consequently to BEA) the possibility to be determined from experimental electron density, which is not attainable if one considers BOA instead.

Mayer bond order, which accounts only for pairwise orbital contributions on the two atoms of a chemical bond, will have its Atomic Orbitals affected when solvent effects are considered, for instance. In a solvent medium, the electron density will be reorganized in response to the neighboring molecules thus being accompanied by changes in its distribution along the bond path. Hence, we expect BEA to become a novel parameter, akin to BOA and BLA, in the development of new generations of organic NLO materials.

Being a novel parameter, we will naturally extend it to several other systems not only differing in the length of the carbon chain. This analysis is on current progress and intend to show that BEA is also advantageous to use on a more general chemical basis. When it comes to level of theory employed herein, we will benchmark whatever BEA outperforms BOA for other exchange-correlation functionals, and possibly, some *ab initio* results (CCSD or better).

Moreover, the future perspectives of thin thesis are outlined as follows:

- carry out new studies to assess BEA's performance in an explicit solvation treatment of NLO properties, as recently confirmed that the first hyperpolarizability relationship with BLA holds for organic dyes based on atomistic approaches.[61]

This will assess the validity of BEA in more complex environments than just appling external electric fields.

- to change the terminal groups of the streptocyanines to verify the performance of the BEA for different donor-acceptor groups;
- use machine learning algorithms and data science in order to find a descriptor that is binding switcher that works with β and use the QTAIM parameters combined or not with geometric parameters.

Bibliography

[1] Lopes, T. O.; Machado, D. F. S.; Risko, C.; Brédas, J.-L.; de Oliveira, H. C. B. Bond Ellipticity Alternation: An Accurate Descriptor of the Nonlinear Optical Properties of π-Conjugated Chromophores. *J. Phys. Chem. Lett.* **2018**, *9*, p. 1377 – 1383.

[2] Levine, I. *Physical Chemistry*, 6th ed.; McGraw-Hill: New York, 2008; p 1008.

[3] Marder, S. R.; Gorman, C. B.; Meyers, F.; Perry, J. W.; Bourhill, G.; Brédas, J.-L.; Pierce, B. M. A Unified Description of Linear and Nonlinear Polarization in Organic Polymethine Dyes. *Science* **1994**, *265*, p. 632 – 635.

[4] Rustagi, K.; Ducuing, J. Third-Order Optical Polarizability of Conjugated Organic Molecules. *Optics Communications* **1974**, *10*, p. 258 – 261.

[5] Oudar, J. L.; Chemla, D. S. Hyperpolarizabilities of the Nitroanilines and their Relations to the Excited State Dipole Moment. *The J. of Chem. Phys.* **1977**, *66*, p. 2664 – 2668.

[6] Kuzyk, M. G.; Dirk, C. W. Effects of Centrosymmetry on the Nonresonant Electronic Third-Order Nonlinear Optical Susceptibility. *Phys. Rev. A* **1990**, *41*, p. 5098 – 5109.

[7] Theoretical Analysis of the Third-Order Nonlinear Optical Properties of Linear Cyanines and Polyenes. 1991; p p. 1560.

[8] Gorman, C. B.; Marder, S. R. An Investigation of the Interrelationships Between Linear and Nonlinear Polarizabilities and Bond-Length Alternation in Conjugated Organic Molecules. *Proc. Natl. Acad. Sci. U. S. A.* **1993**, *90*, p. 11297 – 11301.

[9] Brédas, J.-L. Relationship Between Band Gap and Bond Length Alternation in Organic Conjugated Polymers. *The J. of Chem. Phys.* **1985**, *82*, p. 3808 – 3811.

[10] Drobizhev, M.; Hughes, T. E.; Stepanenko, Y.; Wnuk, P.; O'Donnell, K.; Scott, J. N.; Callis, P. R.; Mikhaylov, A.; Dokken, L.; Rebane, A. Primary Role

of the Chromophore Bond Length Alternation in Reversible Photoconversion of Red Fluorescence Proteins. *Sci. Rep.* **2012**, *2*, p. 668.

[11] Murugan, N. A.; Kongsted, J.; Rinkevicius, Z.; Ågren, H. Breakdown of the First Hyperpolarizability/Bond-Length Alternation Parameter Relationship. *Proc. Natl. Acad. Sci. U. S. A.* **2010**, *107*, p. 16453 – 16458.

[12] Gieseking, R. L.; Risko, C.; Brédas, J.-L. Distinguishing the Effects of Bond-Length Alternation versus Bond-Order Alternation on the Nonlinear Optical Properties of π-Conjugated Chromophores. *J. Phys. Chem. Lett.* **2015**, *6*, p. 2158 – 2162.

[13] Mulliken, R. S. Electronic Population Analysis on LCAO-MO Molecular Wave Functions. IV. Bonding and Antibonding in LCAO and Valence-Bond Theories. *The J. of Chem. Phys.* **1955**, *23*, p. 2343 – 2346.

[14] Wiberg, K. B. Application of the Pople-Santry-Segal CNDO Method to the Cyclopropylcarbinyl and Cyclobutyl Cation and to Bicyclobutane. *Tetrahedron* **1968**, *24*, p. 1083 – 1096.

[15] Mayer, I. Charge, Bond Order and Valence in the Ab Initio SCF Theory. *Chem. Phys. Lett.* **1983**, *97*, p. 270 – 274.

[16] Bridgeman, A. J.; Cavigliasso, G.; Ireland, L. R.; Rothery, J. The Mayer Bond order as a Tool in Inorganic Chemistry. *J. Chem. Soc. Dalt. Trans.* **2001**, p. 2095 – 2108.

[17] Mayer, I. Bond Order and Valence Indices: A Personal Account. *J. of Comput. Chem.* **2007**, *28*, p. 204 – 221.

[18] Bader, R. F. W. *Atoms in Molecules A Quantum Theory (International Series of Monographs on Chemistry)*; Clarendon Press, 1994; p 438.

[19] Macchi, P. The Future of Topological Analysis in Experimental Charge-Density Research. *Acta Crystallogr., Sect. B: Struct. Sci., Cryst. Eng. Mater.* **2017**, *73*, p. 330 – 336.

[20] López, C. S.; Faza, O. N.; Cossío, F. P.; York, D. M.; de Lera, A. R. Ellipticity: A Convenient Tool to Characterize Electrocyclic Reactions. *Chem. - Eur. J.* **2005**, *11*, p. 1734 – 1738.

[21] Mota, A. A. R.; Gatto, C. C.; Machado, G.; de Oliveira, H. C. B.; Fasciotti, M.; Bianchi, O.; Eberlin, M. N.; Neto, B. A. D. Structural Organization and Supramolecular Interactions of the Task-Specific Ionic Liquid 1-Methyl-3-carboxymethylimidazolium Chloride: Solid, Solution, and Gas Phase Structures. *J. Phys. Chem. C* **2014**, *118*, p. 17878 – 17889.

[22] Neto, B. A. D.; Mota, A. A. R.; Gatto, C. C.; Machado, G.; Fasciotti, M. A.-r.; Oliveira, H. C. B. d.; Ferreira, D. A. C.; Bianchi, O.; Eberlin, M. N. Solid, Solution and Gas Phase Interactions of an Imidazolium-Based Task-Specific Ionic Liquid Derived from Natural Kojic Acid. *J. Braz. Chem. Soc.* **2014**, *25*, p. 2280 – 2294.

[23] Bader, R. F. W.; Slee, T. S.; Cremer, D.; Kraka, E. Description of Conjugation and Hyperconjugation in Terms of Electron Distributions. *J. Am. Chem. Soc.* **1983**, *105*, p. 5061 – 5068.

[24] Levine, I. *Quantum chemistry*, 6th ed.; Pearson Prentice Hall: Upper Saddle River, New Jersey, 2008; p 768.

[25] Lykos, P.; Pratt, G. W. Discussion on The Hartree-Fock Approximation. *Rev. Mod. Phys.* **1963**, *35*, p. 496 – 501.

[26] Atkins, P. W.; Friedman, R. S. *Molecular Quantum Mechanics*, 5th ed.; OUP Oxford: Oxford, 2010; p 592.

[27] Szabo, A.; Ostlund, N. *Modern Quantum Chemistry: Introduction to Advanced Electronic Structure Theory*; Dover Publications: New York, 1996; p 480.

[28] Mueller, M. P. *Fundamentals of Quantum Chemistry: Molecular Spectroscopy and Modern Electronic Structure Computations*; Kluwer Academic Publishers: Boston, 2001.

[29] Sherrill, D. An Introduction to Hartree-Fock Molecular Orbital Theory - Notes on Quantum Chemistry of The Sherrill Group. Avaliable at http://vergil.chemistry.gatech.edu.

[30] Young, D. C. *Chemistry Computational Chemistry: A Practical Guide for Applying Techniques to Real-World Problems*; John Wiley & Sons Inc.: New York, 2001; Vol. 9; p 381.

[31] Alcácer, L. *Introdução à Química Quântica Computacional*; IST Press: Lisboa, 2007.

[32] Koch, W.; Holthausen, M. C. *A Chemist's Guide to Density Functional Theory*, 6th ed.; WILEY-VCH Verlag GmbH: Weinheim, 2001; p 293.

[33] Cohen, A. J.; Mori-Sánchez, P.; Yang, W. **??**Challenges for Density Functional Theory. *Chemical Reviews* **2012**, *112*, p. 289 – 320.

[34] Frisch, M. J. et al. Gaussian 09, Revision D.01. 2009.

[35] Chattaraj, P. K. *Chemical Reactivity Theory: A Density Functional View*; CRC Press: Boca Raton, 2009; p 610.

[36] Raab, R. E.; De Lange, O. L. *Multipole Theory in Electromagnetism: Classical, Quantum, and Symmetry Aspects, with Applications*; International Series of Monographs on Physics; OUP Oxford, 2005.

[37] Heesink, G. J. T.; Ruiter, A. G. T.; van Hulst, N. F.; Bölger, B. Determination of Hyperpolarizability Tensor Components by Depolarized Hyper Rayleigh Scattering. *Physical Review Letters* **1993**, *71*, p. 999 – 1002.

[38] Calaminici, P.; Jug, K.; Köster, A. M. Density Functional Calculations of Molecular Polarizabilities and Hyperpolarizabilitie. *The J. of Chem. Phys.* **1998**, *109*.

[39] Rice, J. E.; Handy, N. C. The Calculation of Frequency-Dependent Polarizabilities as Pseudo-Energy Derivatives. *The J. of Chem. Phys.* **1991**, *94*.

[40] Johnson, L. E.; Dalton, L. R.; Robinson, B. H. Optimizing Calculations of Electronic Excitations and Relative Hyperpolarizabilities of Electrooptic Chromophores. *Accounts of Chemical Research* **2014**, *47*, p. 3258 – 3265.

[41] Bader, R. F. W. Dr. Bader's Lecture on ‘ There are no Bonds - only Bonding!’ Delivered in the ‘ Frontiers in Chemistry Series’ at Case Western Reserve University. 2008; Avalaible at https://www.chemistry.mcmaster.ca.

[42] Pauling, L.; University, C. *The Nature of the Chemical Bond and the Structure of Molecules and Crystals: An Introduction to Modern Structural Chemistry*; G - Reference,Information and Interdisciplinary Subjects Series; Cornell University Press, 1960.

[43] Teschl, G. *Mathematical Methods in Quantum Mechanics: With Applications to Schrödinger Operators*; Graduate studies in mathematics; American Mathematical Society, 2009.

[44] Oliveira, B. G.; Araújo, R. C. M. U.; Ramos, M. N. A Topologia Molecular QTAIM e a Descrição Mecânico-Quântica de Ligações de Hidrogênio e Ligações de di-Hidrogênio. *Química Nova* **2010**, *33*, p. 1155 – 1162.

[45] Popelier, P. On the Full Topology of the Laplacian of the Electron Density. *Coord. Chem. Rev.* **2000**, *197*, 169 – 189.

[46] Matta, C. F.; Boyd, R. J. *The Quantum Theory of Atoms in Molecules*; Wiley-Blackwell, 2007; Chapter 1, pp 1–34.

[47] Keith, T. A. *The Quantum Theory of Atoms in Molecules*; Wiley-Blackwell, 2007; Chapter 3, pp p. 61 – 94.

[48] Bader, R. F. W. *Encyclopedia of Computational Chemistry*; John Wiley & Sons, Ltd, 2002.

[49] Bader, R. F. W.; Bayles, D. Properties of Atoms in Molecules: Group Additivity. *J. Phys. Chem. A* **2000**, *104*, p. 5579 – 5589.

[50] Scherer, W.; Sirsch, P.; Shorokhov, D.; Tafipolsky, M.; McGrady, G. S.; Gullo, E. Valence Charge Concentrations, Electron Delocalization and β-Agostic Bonding in d0 Metal Alkyl Complexes. *Chem. - Eur. J.* **2003**, *9*, p. 6057 – 6070.

[51] Keith, T. A. AIMAll (Version 17.11.14). 2017.

[52] Lu, T.; Chen, F. Multiwfn: A multifunctional wavefunction analyzer. *J. of Comput. Chem.* **2011**, *33*, p. 580 – 592.

[53] van Rossum, G. Python Language Reference, version 3.6. 2015; Available at http://www.python.org.

[54] Williams, T.; Kelley, C.; many others, Gnuplot 5.2.2: an Interactive Plotting Program. 2017; Available at http://www.gnuplot.info.

[55] Bourhill, G.; Bredas, J.-L.; Cheng, L.-T.; Marder, S. R.; Meyers, F.; Perry, J. W.; Tiemann, B. G. Experimental Demonstration of the Dependence of the First Hyperpolarizability of Donor-Acceptor-Substituted Polyenes on the Ground-State Polarization and Bond Length Alternation. *J. Am. Chem. Soc.* **1994**, *116*, p. 2619 – 2620.

[56] Kushmerick, J. G.; Holt, D. B.; Pollack, S. K.; Ratner, M. A.; Yang, J. C.; Schull, T. L.; Naciri, J.; Moore, M. H.; Shashidhar, R. Effect of Bond-Length Alternation in Molecular Wires. *J. Am. Chem. Soc.* **2002**, *124*, p. 10654 – 10655.

[57] Blanchard-Desce, M.; Alain, V.; Bedworth, P. V.; Marder, S. R.; Fort, A.; Runser, C.; Barzoukas, M.; Lebus, S.; Wortmann, R. Large Quadratic Hyperpolarizabilities with Donor-Acceptor Polyenes Exhibiting Optimum Bond Length Alternation: Correlation Between Structure and Hyperpolarizability. *Chem. - Eur. J.* **2006**, *3*, p. 1091 – 1104.

[58] Meyers, F.; Marder, S. R.; Pierce, B. M.; Bredas, J. L. Electric Field Modulated Nonlinear Optical Properties of Donor-Acceptor Polyenes: Sum-Over-States Investigation of the Relationship between Molecular Polarizabilities (.alpha., .beta., and .gamma.) and Bond Length Alternation. *J. Am. Chem. Soc.* **1994**, *116*, p. 10703 – 10714.

[59] Kippelen, B.; Meyers, F.; Peyghambarian, N.; Marder, S. R. Chromophore Design for Photorefractive Applications. *J. Am. Chem. Soc.* **1997**, *119*, p. 4559 – 4560.

[60] Türker, L. Unusual Alternation of HMO Bond Orders in Cyclacenes. *Polycyclic Aromatic Compounds* **1996**, *8*, p. 67 – 71.

[61] Brandão, I.; Franco, L. R.; Fonseca, T. L.; Castro, M. A.; Georg, H. C. Confirming the Relationship Between First Hyperpolarizability and the Bond Length Alternation Coordinate for Merocyanine Dyes. *The J. of Chem. Phys.* **2017**, *146*, p. 224505.

[62] Jabłoński, M.; Palusiak, M. Basis Set and Method Dependence in Atoms in Molecules Calculations. *J. Phys. Chem. A* **2010**, *114*, p. 2240 – 2244.

[63] Bouit, P.-A.; Aronica, C.; Toupet, L.; Le Guennic, B.; Andraud, C.; Maury, O. Continuous Symmetry Breaking Induced by Ion Pairing Effect in Heptamethine Cyanine Dyes: Beyond the Cyanine Limit. *J. Am. Chem. Soc.* **2010**, *132*, p. 4328 – 4335.

[64] Gieseking, R. L.; Risko, C.; Marder, S. R.; Brédas, J.-L. *Understanding the Relationships Among Molecular Structure, Excited-State Properties, and Polarizabilities of π-Conjugated Chromophores*; WORLD SCIENTIFIC, 2016; Chapter 11, pp 393 – 419.

Appendix A

Appendix: Additional Results

As discussed in the main text, we tested two QTAIM quantities in addition to the bond ellipticity to compute bond property alternations. The first was the magnitude of the electron density at the BCP (ρ_c):[23] The bond electron density alternation (BEDA) at the BCP would allow one to exploit any correspondence between ρ_c and bond order.

The second QTAIM density-based function was the Laplacian of the one-electron density ($\nabla^2\rho$), which has been used as an electronic localization quantity.[18] It has been demonstrated that electronic charge is locally concentrated within a molecular system in regions where $\nabla^2\rho < 0$. Hence, the Laplacian of the electron density is another parameter whose magnitude provides chemical infor themation in terms of charge concentrated and charge depleted areas.

We therefore determined the bond Laplacian of electron density, denoted BELA in this work. As shown in the SI, both BEDA and BELA were not as successful as BEA in predicting NLO properties of the streptocyanines at any level of theory considered.

A.1 Appendix A: Bond Electronic Density Alternation

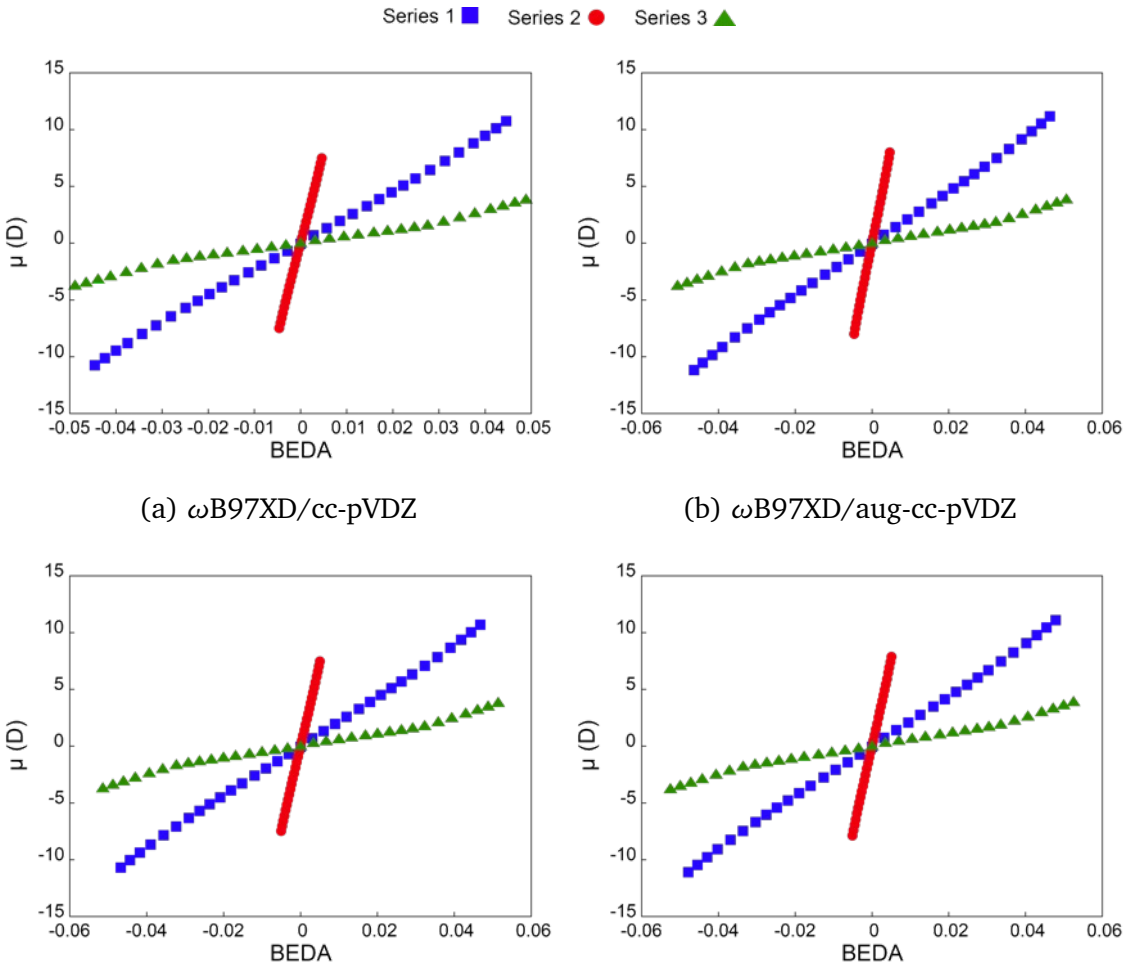

(a) ωB97XD/cc-pVDZ

(b) ωB97XD/aug-cc-pVDZ

(c) ωB97XD/6-31G(d,p)

(d) ωB97XD/ 6-31++G(d,p)

Figure A.1: Correlation of μ_x with BEDA for the the 5C-streptocyanine in Series 1, 2, 3, as obtained in the 4 studied levels of theory: Level 1 (a), Level 2 (a), Level 3 (a), Level 4 (a).

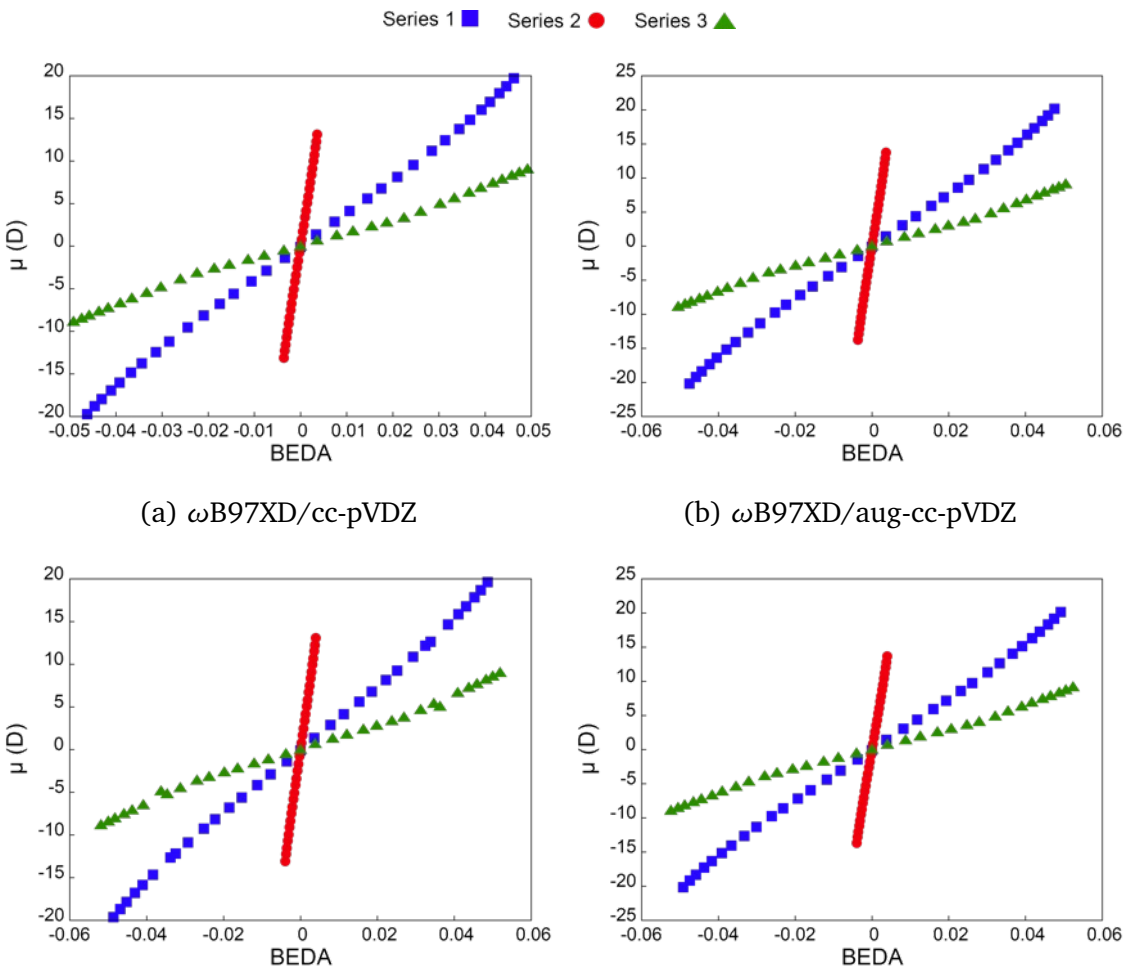

(a) ωB97XD/cc-pVDZ

(b) ωB97XD/aug-cc-pVDZ

(c) ωB97XD/6-31G(d,p)

(d) ωB97XD/ 6-31++G(d,p)

Figure A.2: Correlation of μ_x with BEDA for the the 9C-streptocyanine in Series 1, 2, 3, as obtained in the 4 studied levels of theory: Level 1 (a), Level 2 (a), Level 3 (a), Level 4 (a).

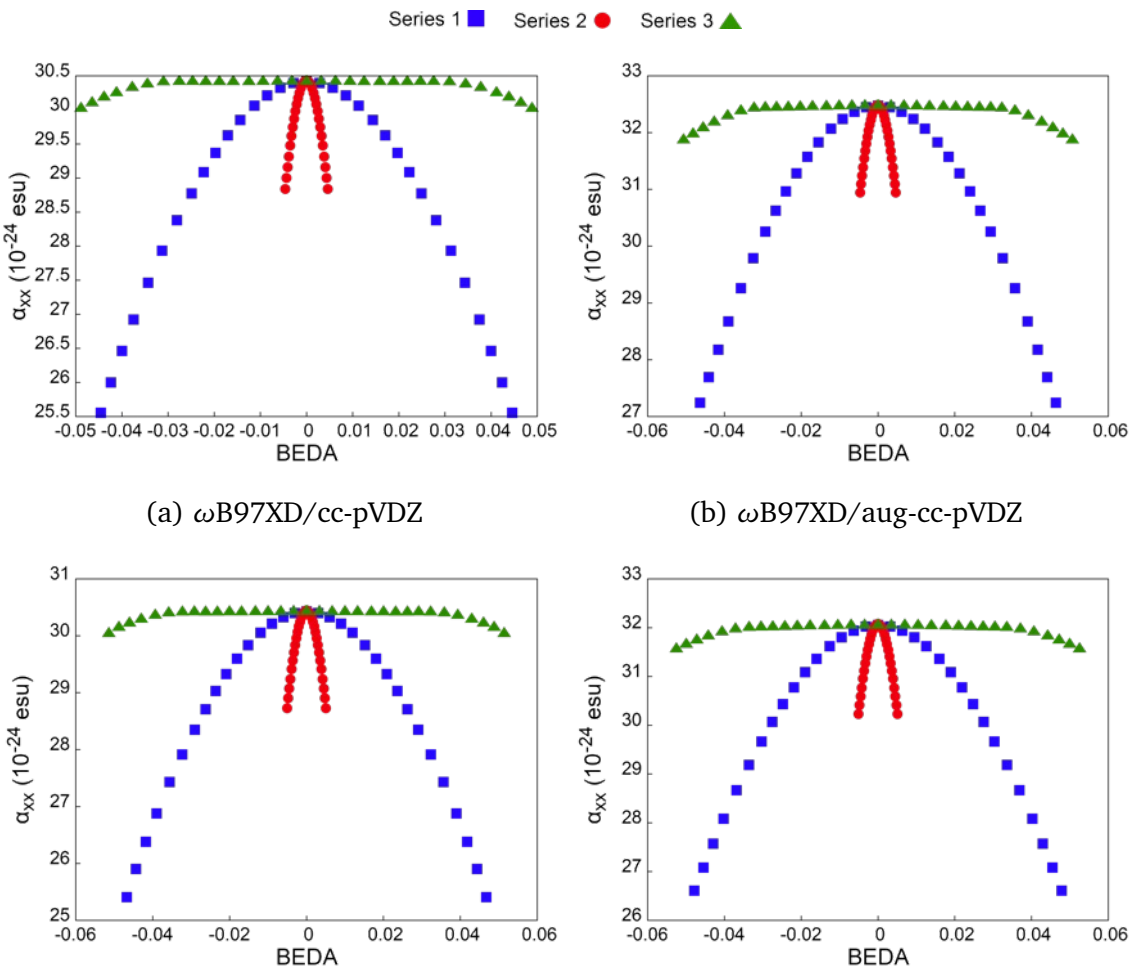

(a) ωB97XD/cc-pVDZ

(b) ωB97XD/aug-cc-pVDZ

(c) ωB97XD/6-31G(d,p)

(d) ωB97XD/ 6-31++G(d,p)

Figure A.3: Correlation of α_{xx} with BEDA for the the 5C-streptocyanine in Series 1, 2, 3, as obtained in the 4 studied levels of theory: Level 1 (a), Level 2 (a), Level 3 (a), Level 4 (a).

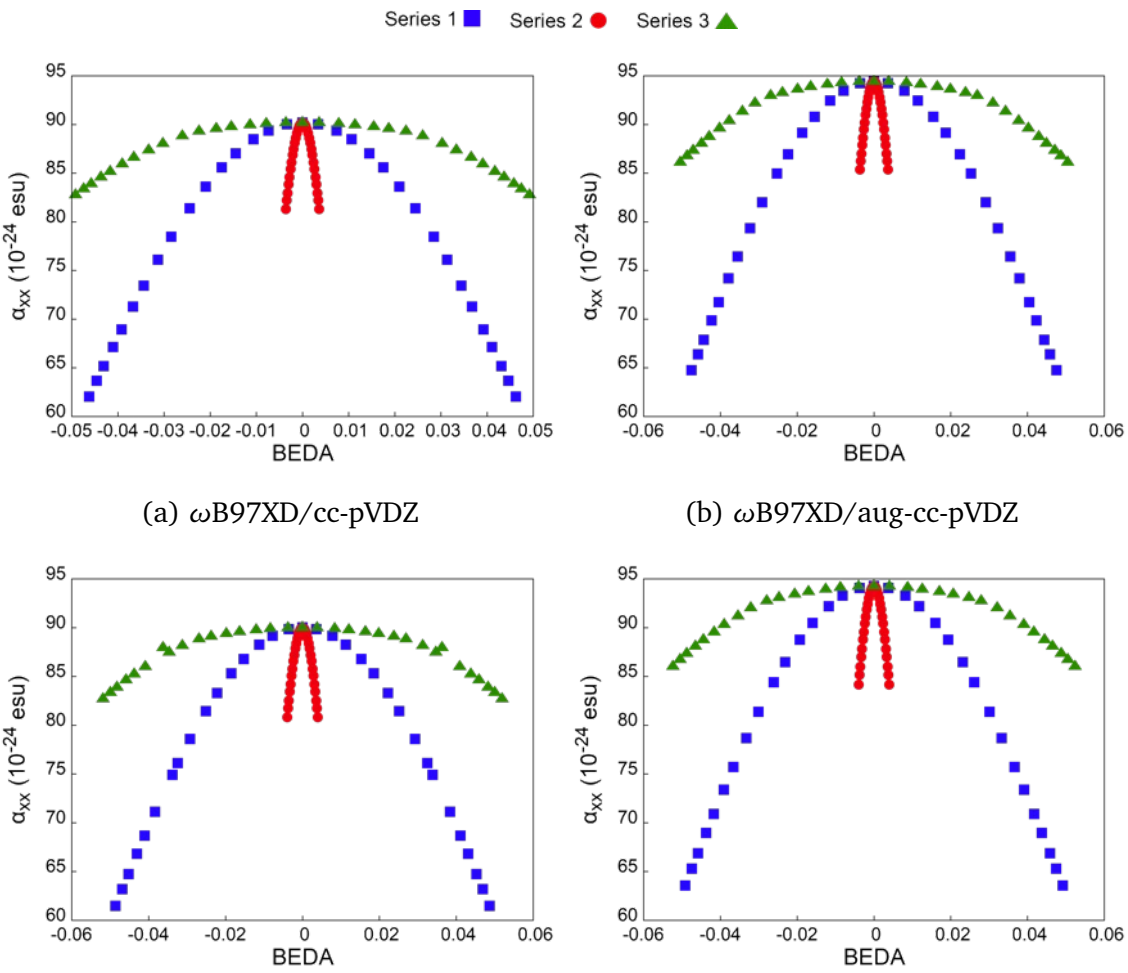

(a) ωB97XD/cc-pVDZ

(b) ωB97XD/aug-cc-pVDZ

(c) ωB97XD/6-31G(d,p)

(d) ωB97XD/ 6-31++G(d,p)

Figure A.4: Correlation of α_{xx} with BEDA for the the 9C-streptocyanine in Series 1, 2, 3, as obtained in the 4 studied levels of theory: Level 1 (a), Level 2 (a), Level 3 (a), Level 4 (a).

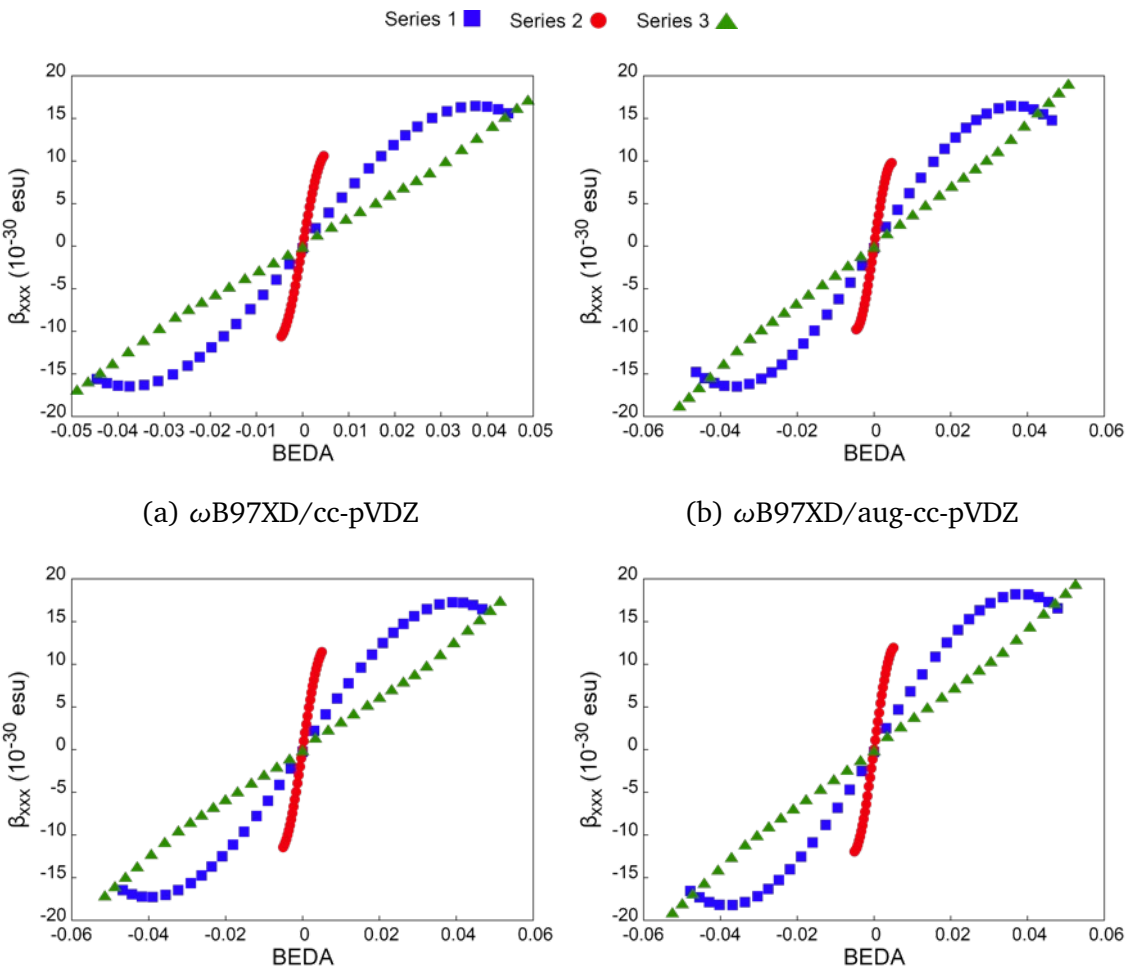

(a) ωB97XD/cc-pVDZ

(b) ωB97XD/aug-cc-pVDZ

(c) ωB97XD/6-31G(d,p)

(d) ωB97XD/ 6-31++G(d,p)

Figure A.5: Correlation of β_{xxx} with BEDA for the the 5C-streptocyanine in Series 1, 2, 3, as obtained in the 4 studied levels of theory: Level 1 (a), Level 2 (a), Level 3 (a), Level 4 (a).

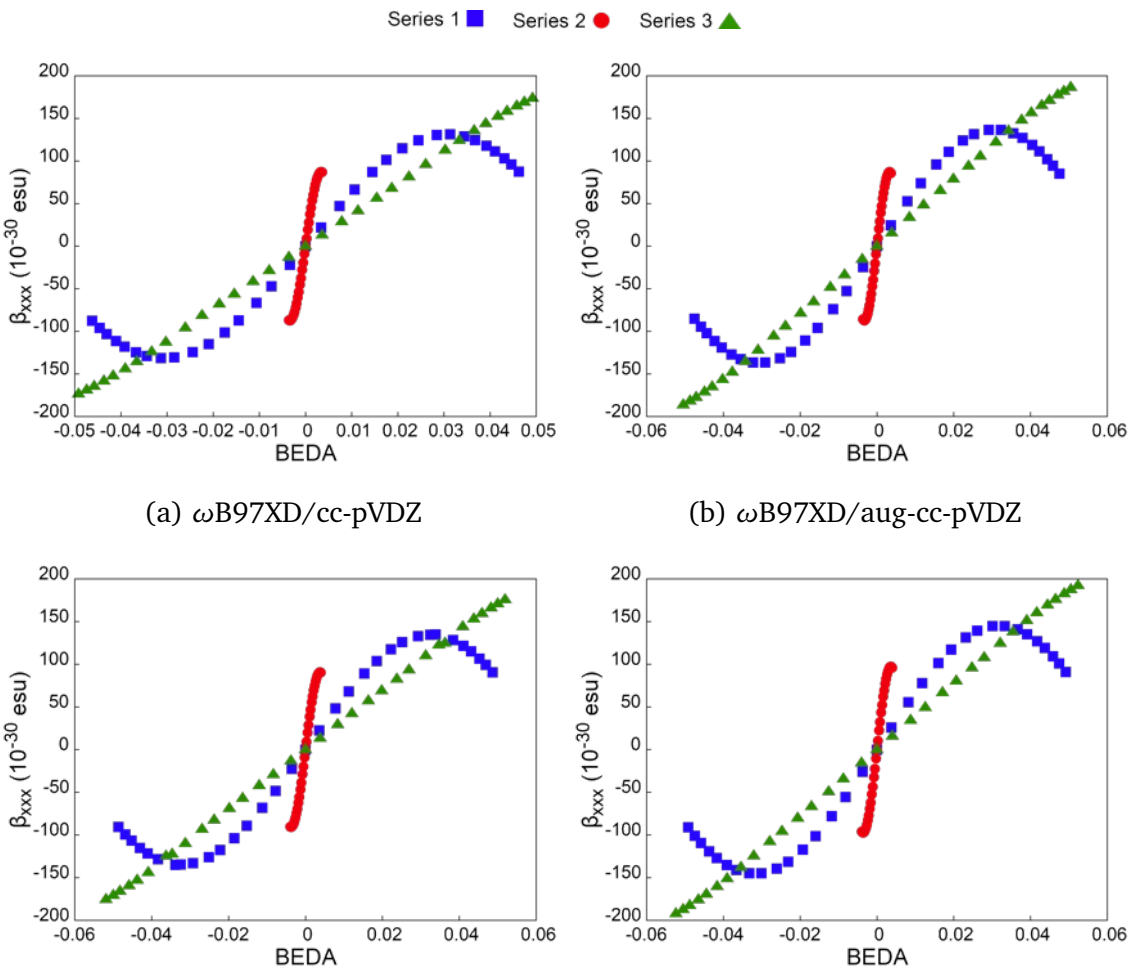

(a) ωB97XD/cc-pVDZ

(b) ωB97XD/aug-cc-pVDZ

(c) ωB97XD/6-31G(d,p)

(d) ωB97XD/ 6-31++G(d,p)

Figure A.6: Correlation of β_{xxx} with BEDA for the the 9C-streptocyanine in Series 1, 2, 3, as obtained in the 4 studied levels of theory: Level 1 (a), Level 2 (a), Level 3 (a), Level 4 (a).

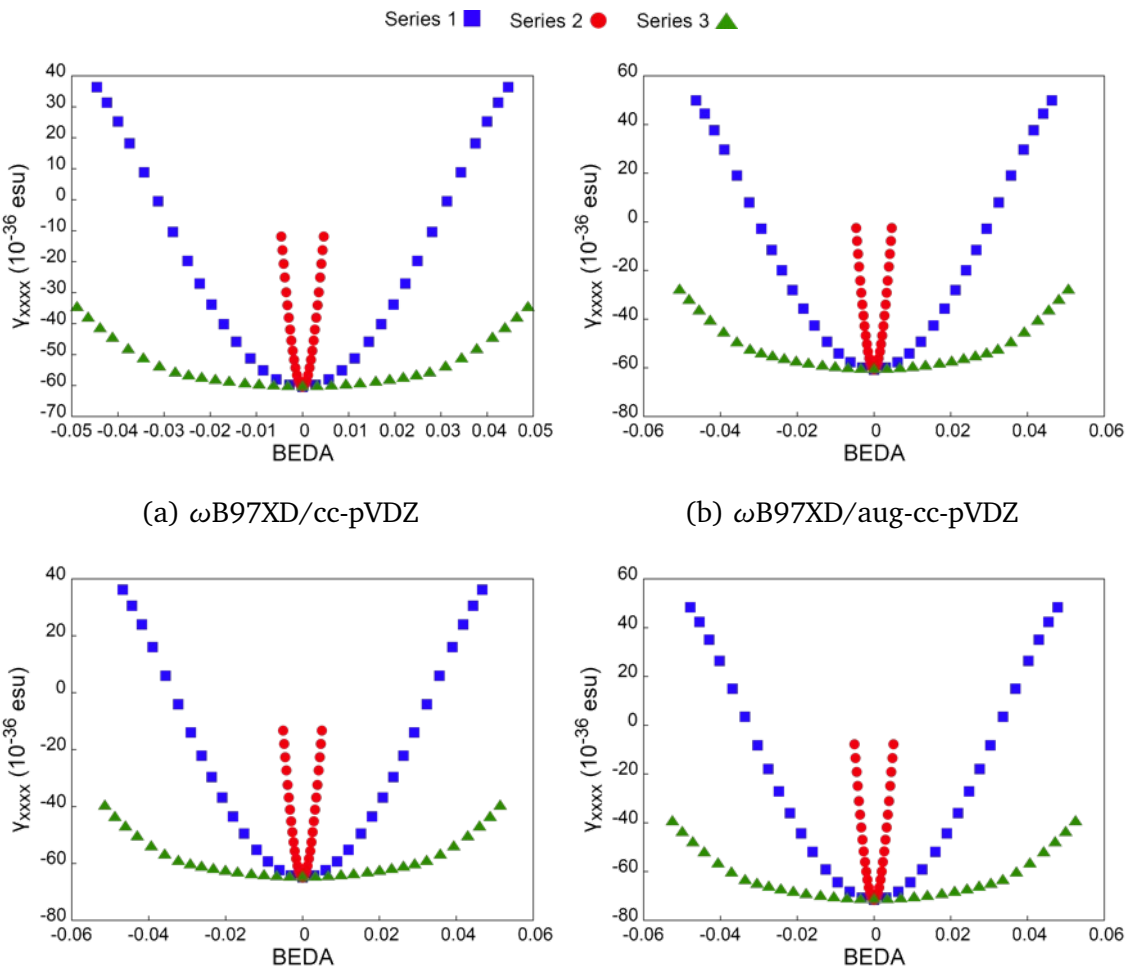

(a) ωB97XD/cc-pVDZ

(b) ωB97XD/aug-cc-pVDZ

(c) ωB97XD/6-31G(d,p)

(d) ωB97XD/ 6-31++G(d,p)

Figure A.7: Correlation of γ_{xxxx} with BEDA for the the 5C-streptocyanine in Series 1, 2, 3, as obtained in the 4 studied levels of theory: Level 1 (a), Level 2 (a), Level 3 (a), Level 4 (a).

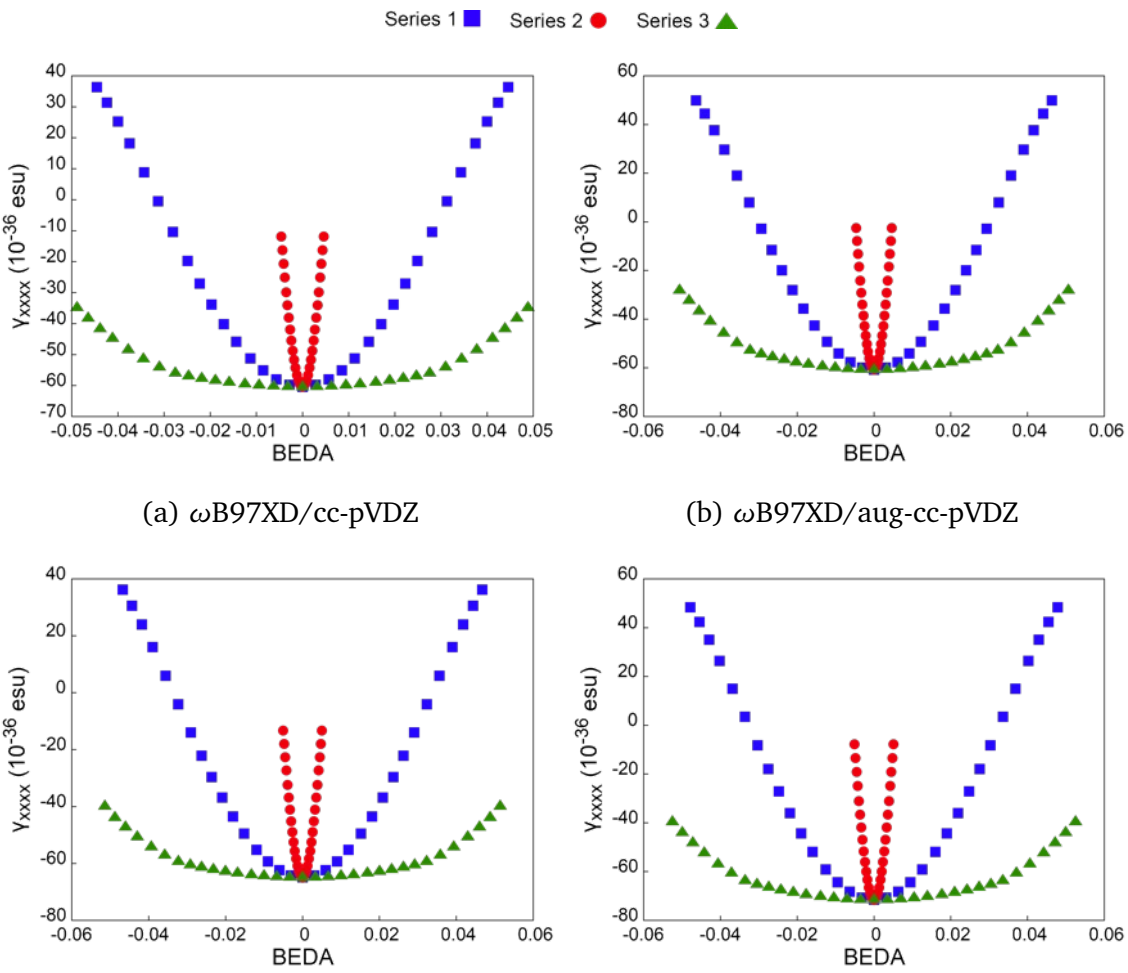

(a) ωB97XD/cc-pVDZ

(b) ωB97XD/aug-cc-pVDZ

(c) ωB97XD/6-31G(d,p)

(d) ωB97XD/ 6-31++G(d,p)

Figure A.8: Correlation of γ_{xxxx} with BEDA for the the 9C-streptocyanine in Series 1, 2, 3, as obtained in the 4 studied levels of theory: Level 1 (a), Level 2 (a), Level 3 (a), Level 4 (a).

A.2 Appendix A: Bond Laplacian of Electronic Density Alternation

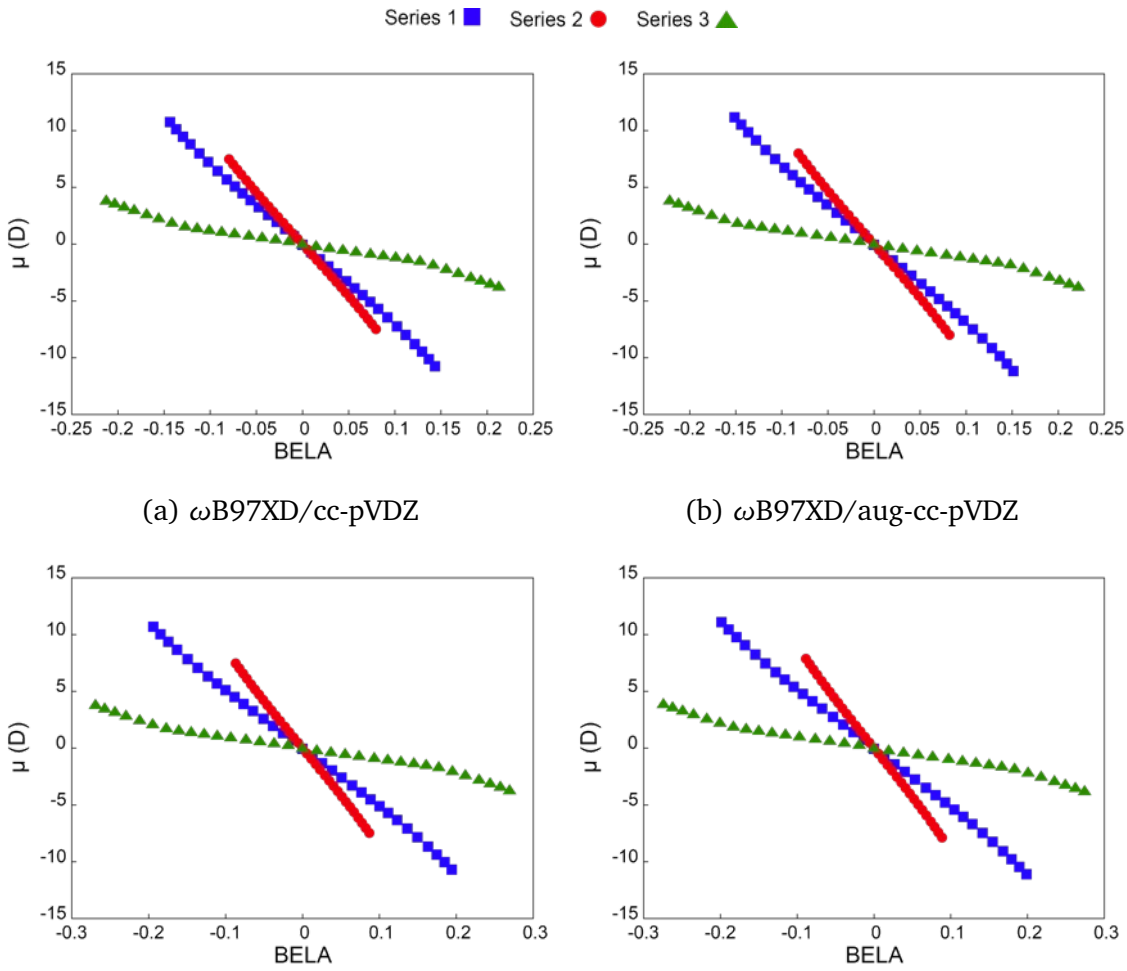

(a) ωB97XD/cc-pVDZ

(b) ωB97XD/aug-cc-pVDZ

(c) ωB97XD/6-31G(d,p)

(d) ωB97XD/ 6-31++G(d,p)

Figure A.9: Correlation of μ_x with BEDA for the the 5C-streptocyanine in Series 1, 2, 3, as obtained in the 4 studied levels of theory: Level 1 (a), Level 2 (a), Level 3 (a), Level 4 (a).

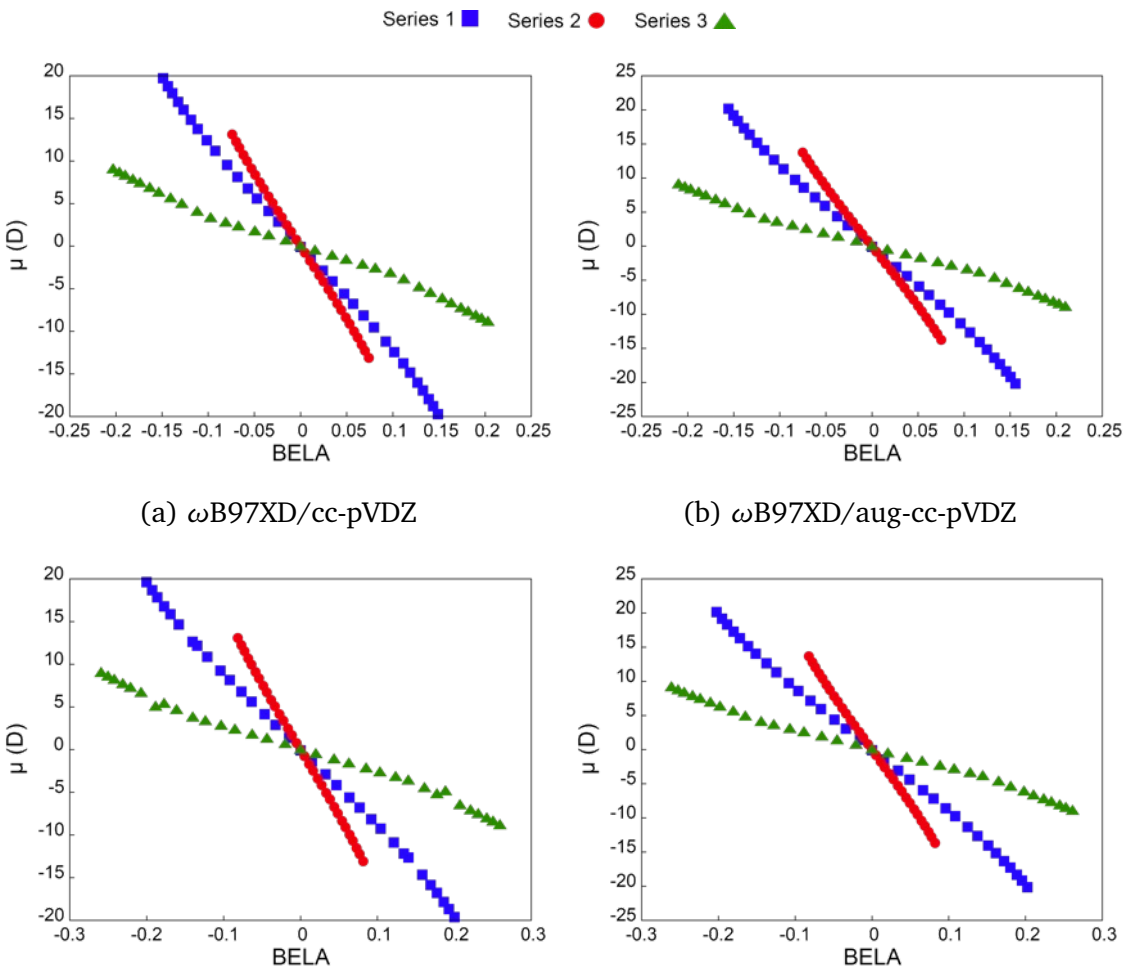

(a) ωB97XD/cc-pVDZ

(b) ωB97XD/aug-cc-pVDZ

(c) ωB97XD/6-31G(d,p)

(d) ωB97XD/ 6-31++G(d,p)

Figure A.10: Correlation of μ_x with BEDA for the the 9C-streptocyanine in Series 1, 2, 3, as obtained in the 4 studied levels of theory: Level 1 (a), Level 2 (a), Level 3 (a), Level 4 (a).

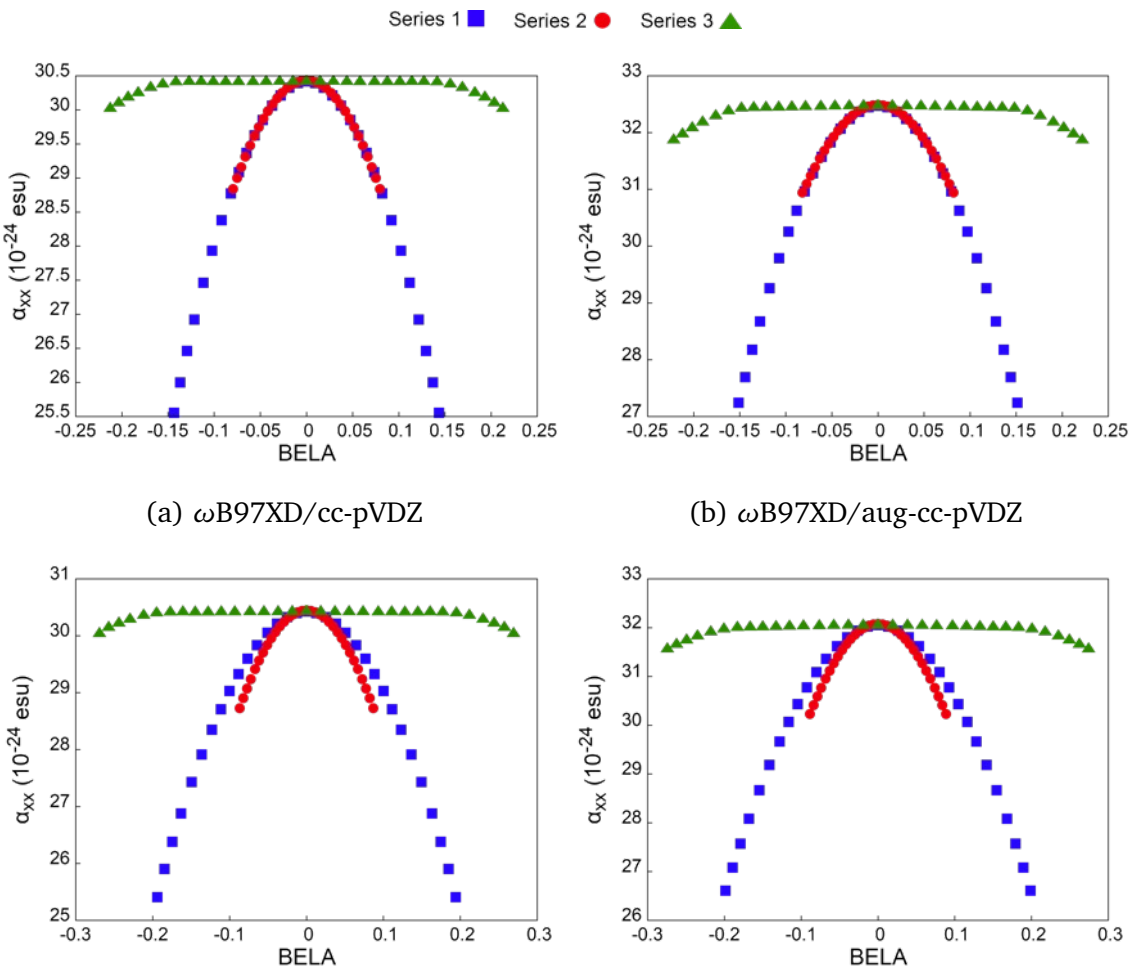

(a) ωB97XD/cc-pVDZ

(b) ωB97XD/aug-cc-pVDZ

(c) ωB97XD/6-31G(d,p)

(d) ωB97XD/ 6-31++G(d,p)

Figure A.11: Correlation of α_{xx} with BEDA for the the 5C-streptocyanine in Series 1, 2, 3, as obtained in the 4 studied levels of theory: Level 1 (a), Level 2 (a), Level 3 (a), Level 4 (a).

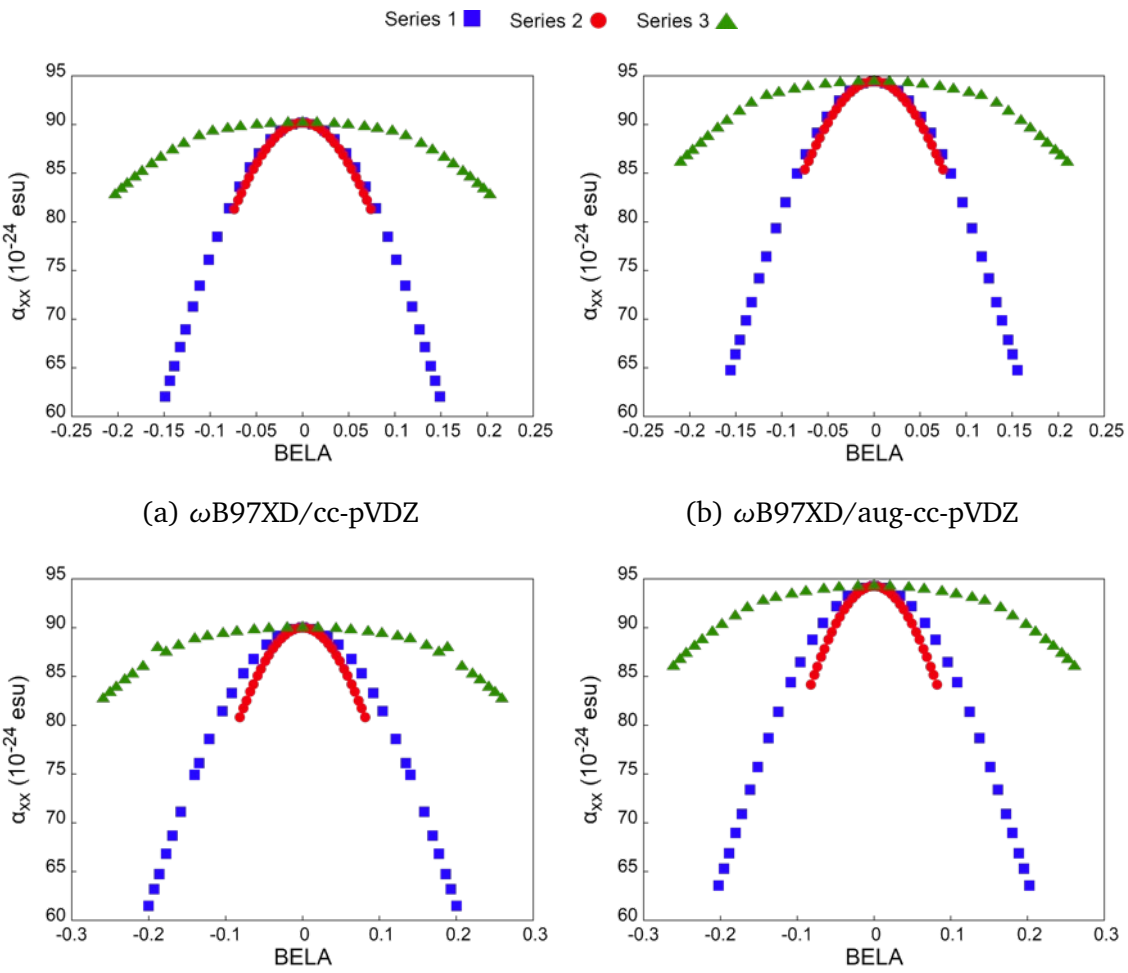

(a) ωB97XD/cc-pVDZ

(b) ωB97XD/aug-cc-pVDZ

(c) ωB97XD/6-31G(d,p)

(d) ωB97XD/ 6-31++G(d,p)

Figure A.12: Correlation of α_{xx} with BEDA for the the 9C-streptocyanine in Series 1, 2, 3, as obtained in the 4 studied levels of theory: Level 1 (a), Level 2 (a), Level 3 (a), Level 4 (a).

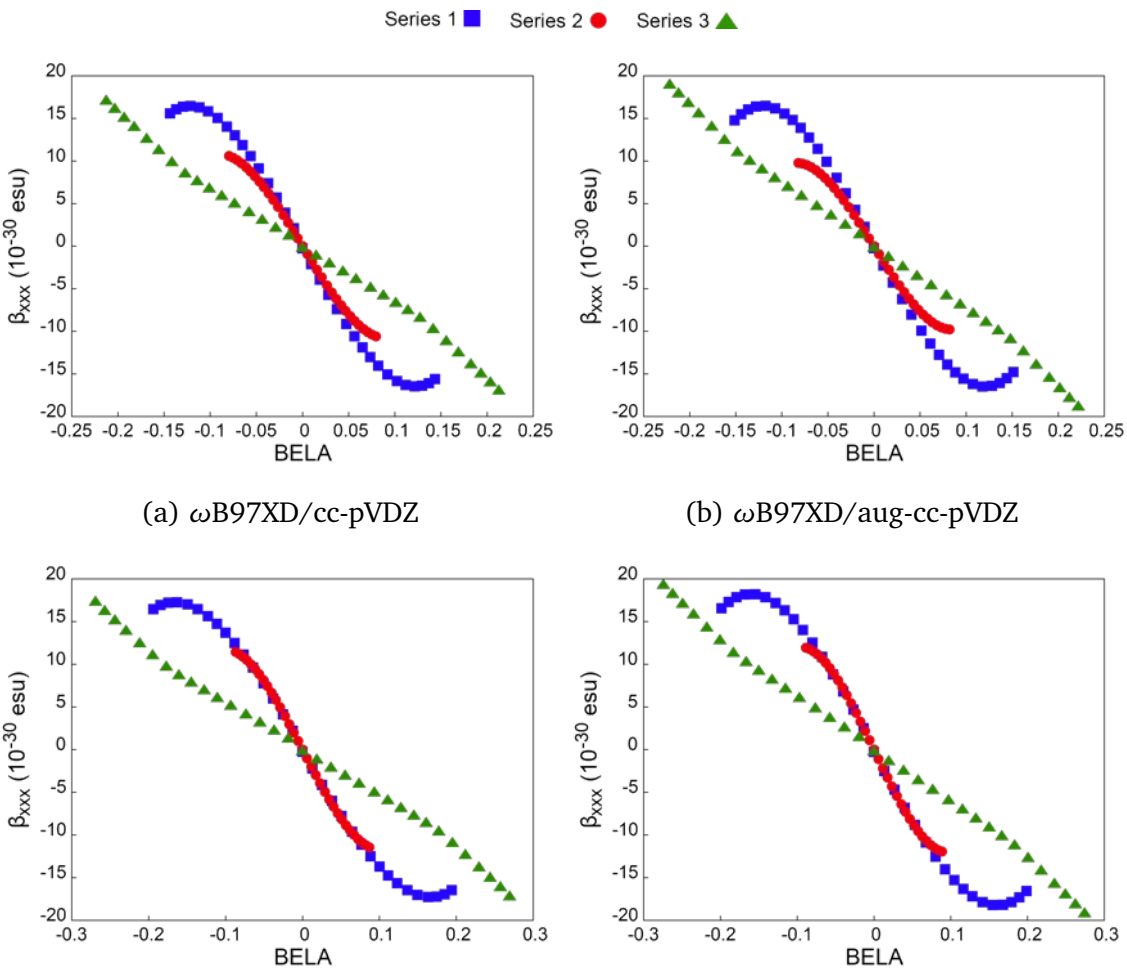

(a) ωB97XD/cc-pVDZ

(b) ωB97XD/aug-cc-pVDZ

(c) ωB97XD/6-31G(d,p)

(d) ωB97XD/ 6-31++G(d,p)

Figure A.13: Correlation of β_{xxx} with BEDA for the the 5C-streptocyanine in Series 1, 2, 3, as obtained in the 4 studied levels of theory: Level 1 (a), Level 2 (a), Level 3 (a), Level 4 (a).

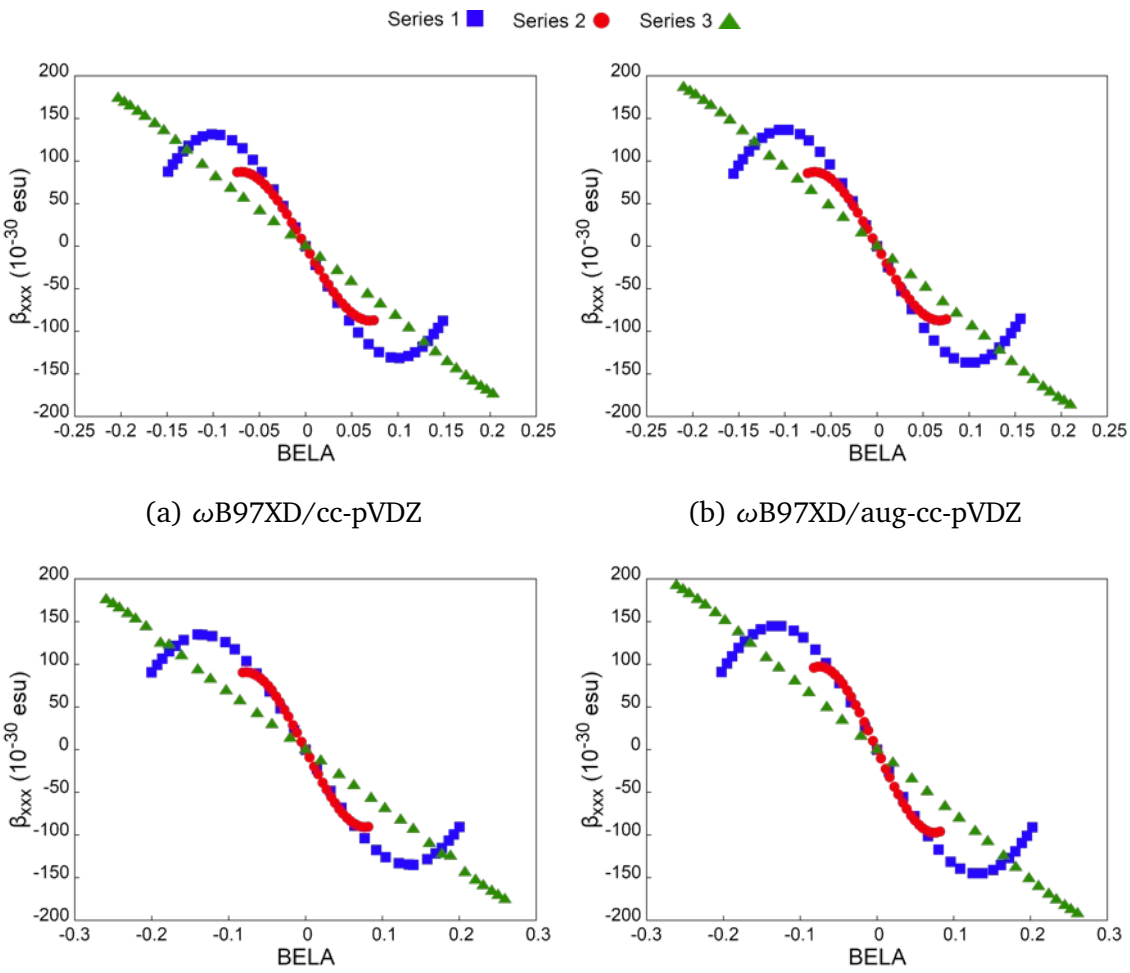

(a) ωB97XD/cc-pVDZ (b) ωB97XD/aug-cc-pVDZ

(c) ωB97XD/6-31G(d,p) (d) ωB97XD/ 6-31++G(d,p)

Figure A.14: Correlation of β_{xxx} with BEDA for the the 9C-streptocyanine in Series 1, 2, 3, as obtained in the 4 studied levels of theory: Level 1 (a), Level 2 (a), Level 3 (a), Level 4 (a).

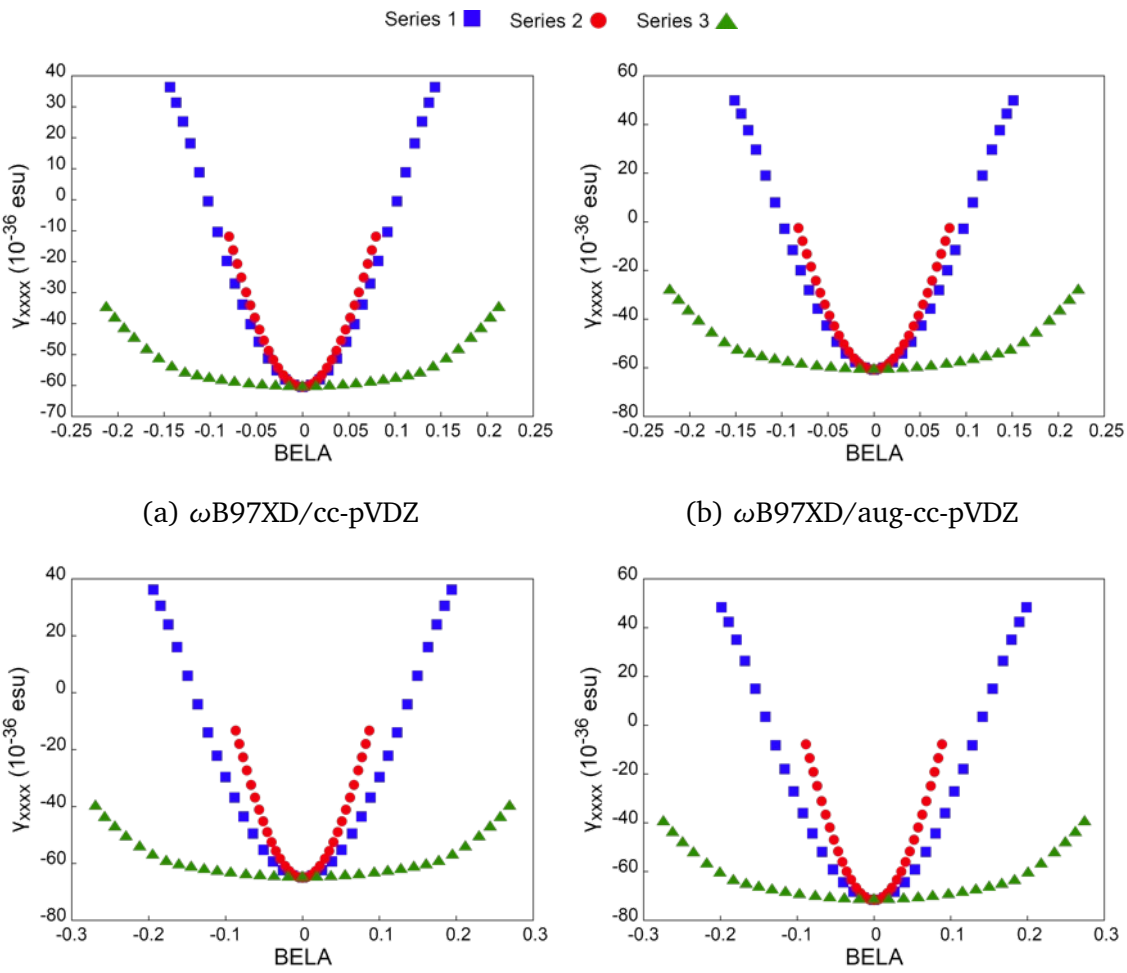

(a) ωB97XD/cc-pVDZ

(b) ωB97XD/aug-cc-pVDZ

(c) ωB97XD/6-31G(d,p)

(d) ωB97XD/ 6-31++G(d,p)

Figure A.15: Correlation of γ_{xxxx} with BEDA for the the 5C-streptocyanine in Series 1, 2, 3, as obtained in the 4 studied levels of theory: Level 1 (a), Level 2 (a), Level 3 (a), Level 4 (a).

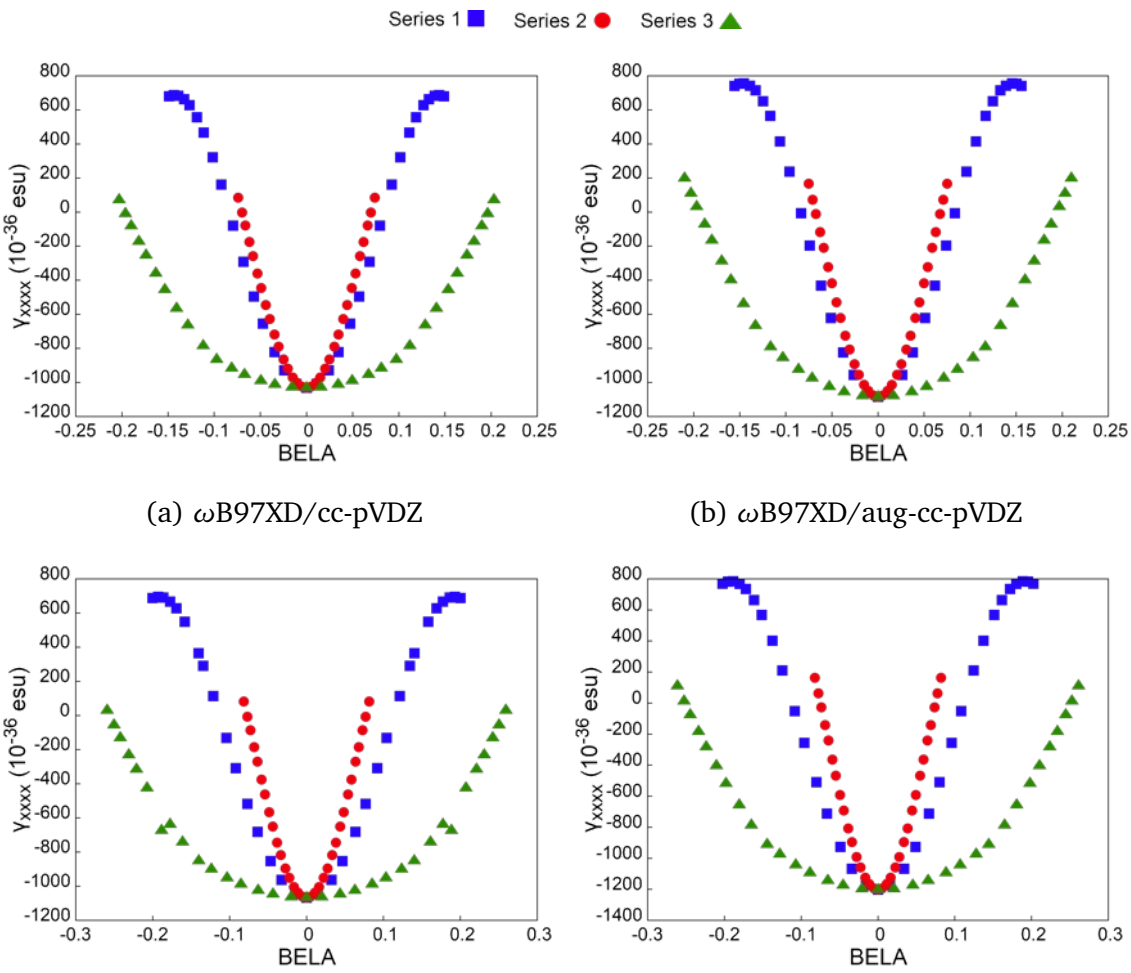

(a) ωB97XD/cc-pVDZ

(b) ωB97XD/aug-cc-pVDZ

(c) ωB97XD/6-31G(d,p)

(d) ωB97XD/ 6-31++G(d,p)

Figure A.16: Correlation of γ_{xxxx} with BEDA for the the 9C-streptocyanine in Series 1, 2, 3, as obtained in the 4 studied levels of theory: Level 1 (a), Level 2 (a), Level 3 (a), Level 4 (a).

A.3 Appendix A: Bond Ellipticity Alternation

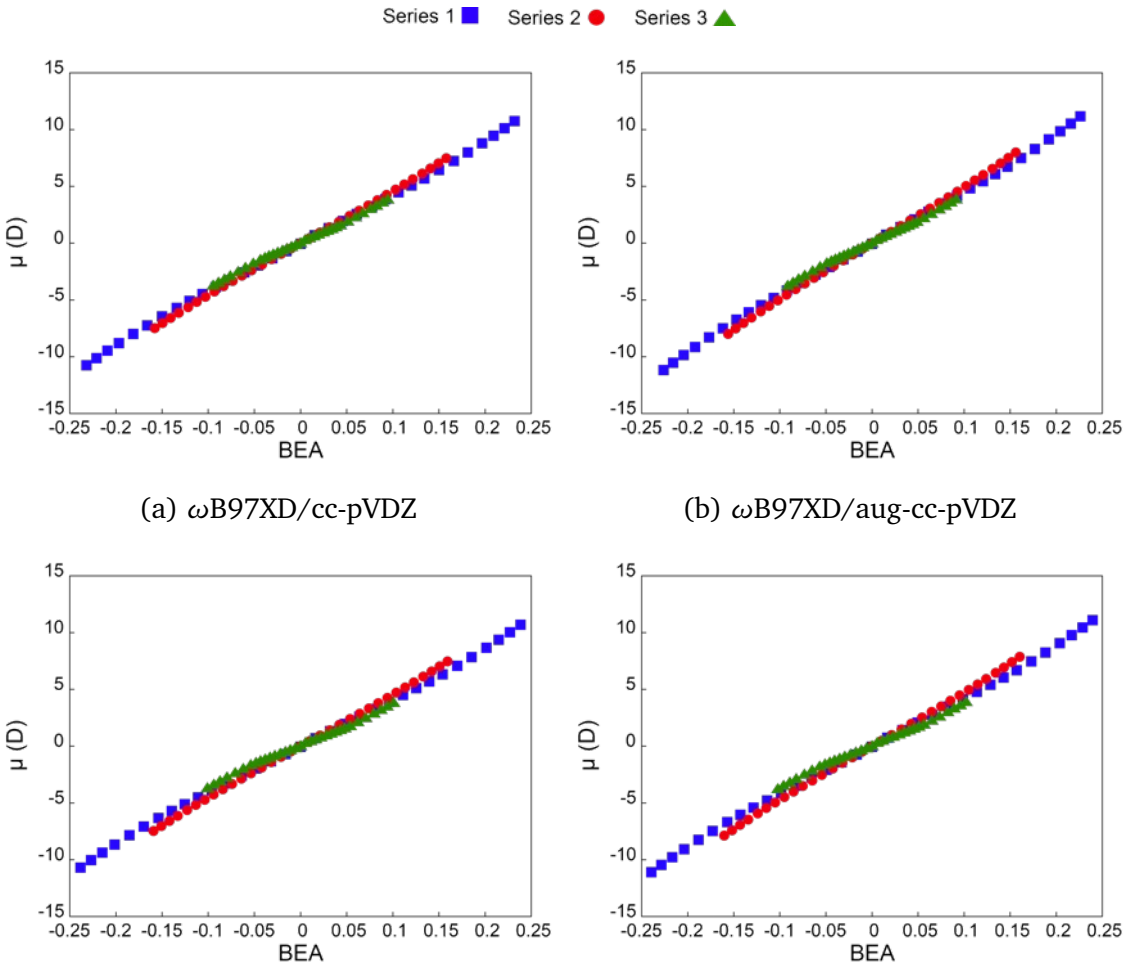

(a) ωB97XD/cc-pVDZ

(b) ωB97XD/aug-cc-pVDZ

(c) ωB97XD/6-31G(d,p)

(d) ωB97XD/ 6-31++G(d,p)

Figure A.17: Correlation of μ_x with BEA for the the 5C-streptocyanine in Series 1, 2, 3, as obtained in the 4 studied levels of theory: Level 1 (a), Level 2 (a), Level 3 (a), Level 4 (a).

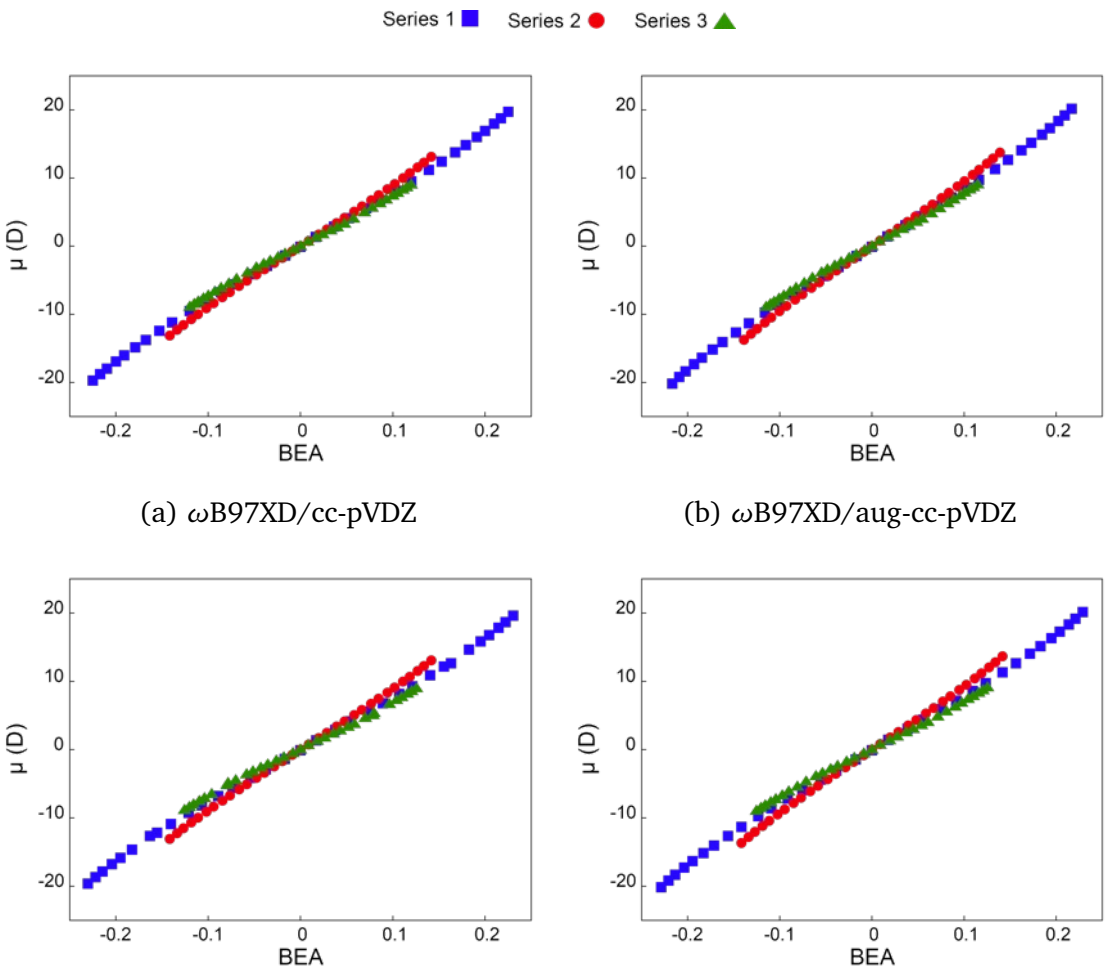

(a) ωB97XD/cc-pVDZ

(b) ωB97XD/aug-cc-pVDZ

(c) ωB97XD/6-31G(d,p)

(d) ωB97XD/ 6-31++G(d,p)

Figure A.18: Correlation of μ_x with BEA for the the 9C-streptocyanine in Series 1, 2, 3, as obtained in the 4 studied levels of theory: Level 1 (a), Level 2 (a), Level 3 (a), Level 4 (a).

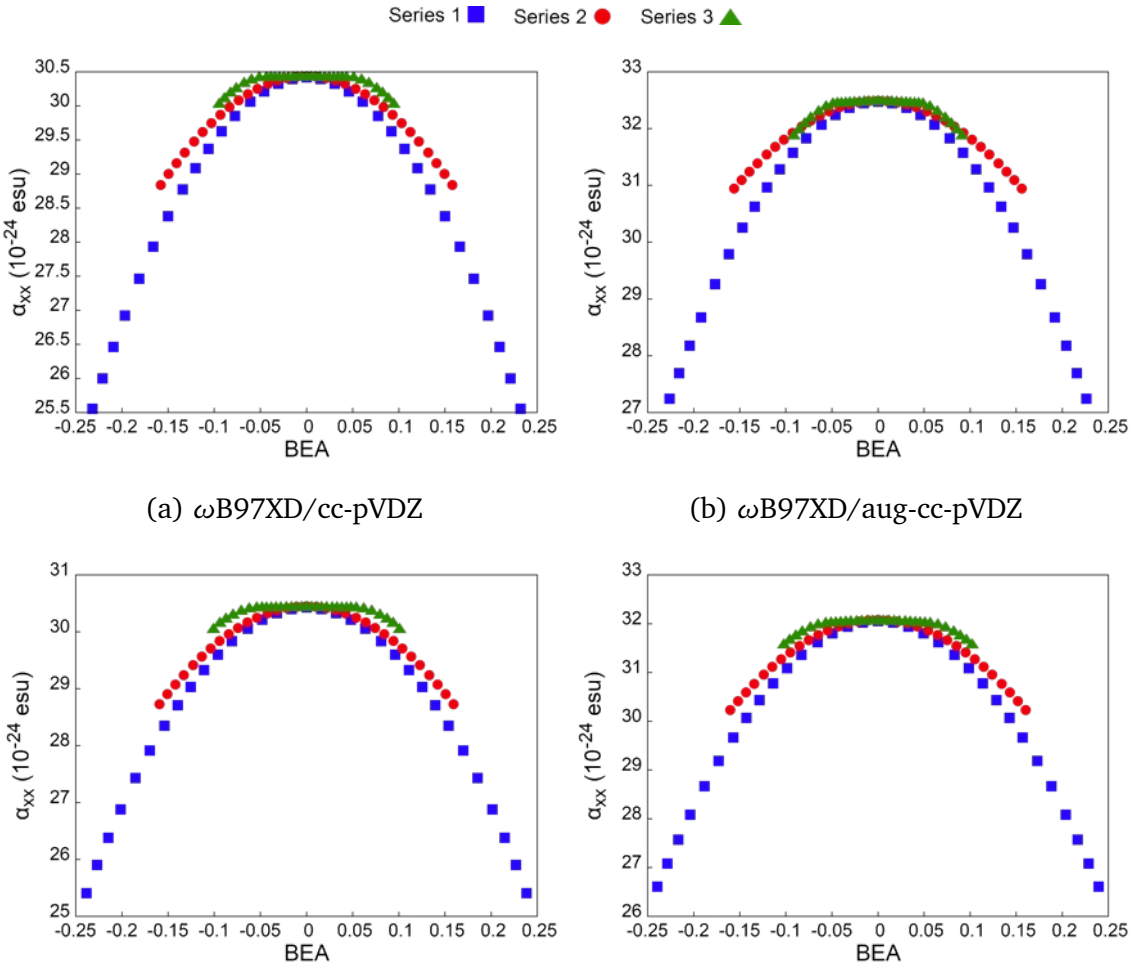

(a) ωB97XD/cc-pVDZ

(b) ωB97XD/aug-cc-pVDZ

(c) ωB97XD/6-31G(d,p)

(d) ωB97XD/ 6-31++G(d,p)

Figure A.19: Correlation of α_{xx} with BEA for the the 5C-streptocyanine in Series 1, 2, 3, as obtained in the 4 studied levels of theory: Level 1 (a), Level 2 (a), Level 3 (a), Level 4 (a).

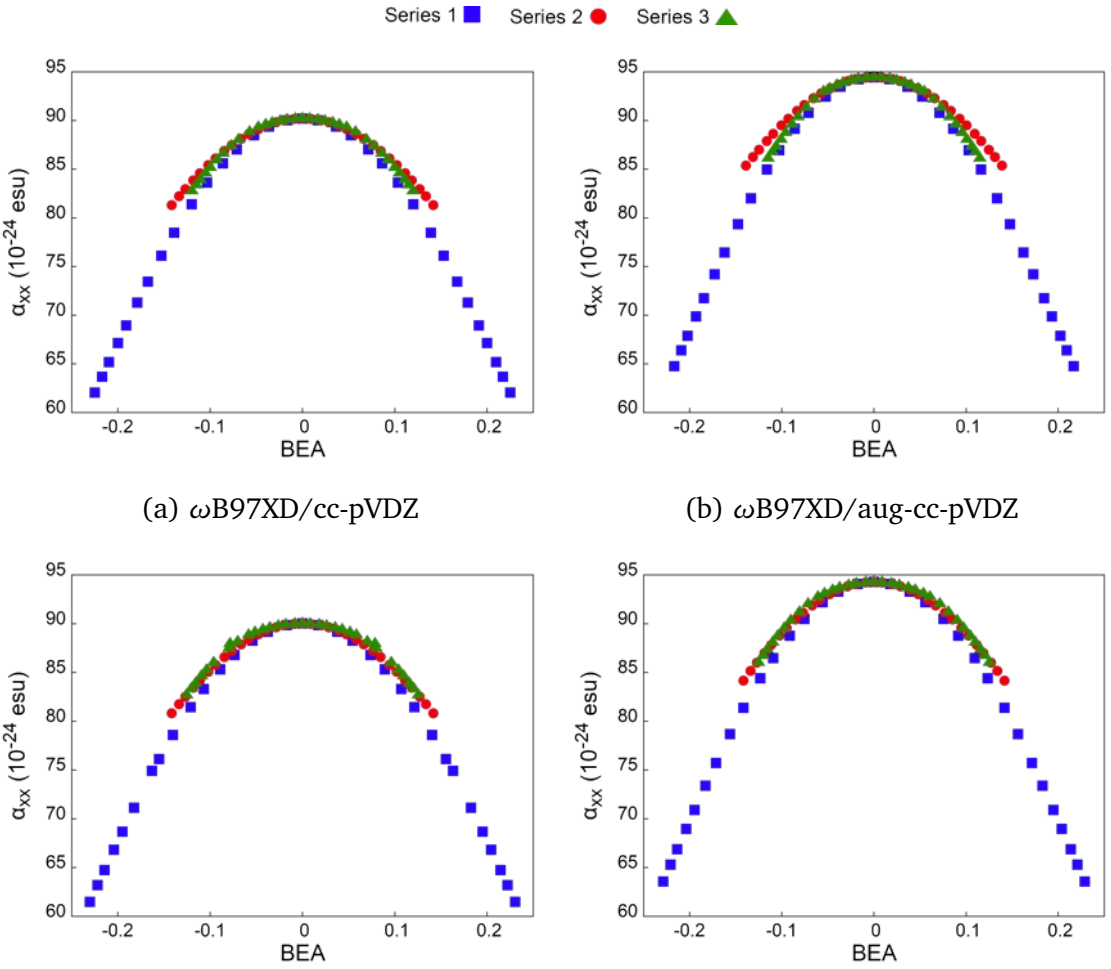

(a) ωB97XD/cc-pVDZ

(b) ωB97XD/aug-cc-pVDZ

(c) ωB97XD/6-31G(d,p)

(d) ωB97XD/ 6-31++G(d,p)

Figure A.20: Correlation of α_{xx} with BEA for the the 9C-streptocyanine in Series 1, 2, 3, as obtained in the 4 studied levels of theory: Level 1 (a), Level 2 (a), Level 3 (a), Level 4 (a).

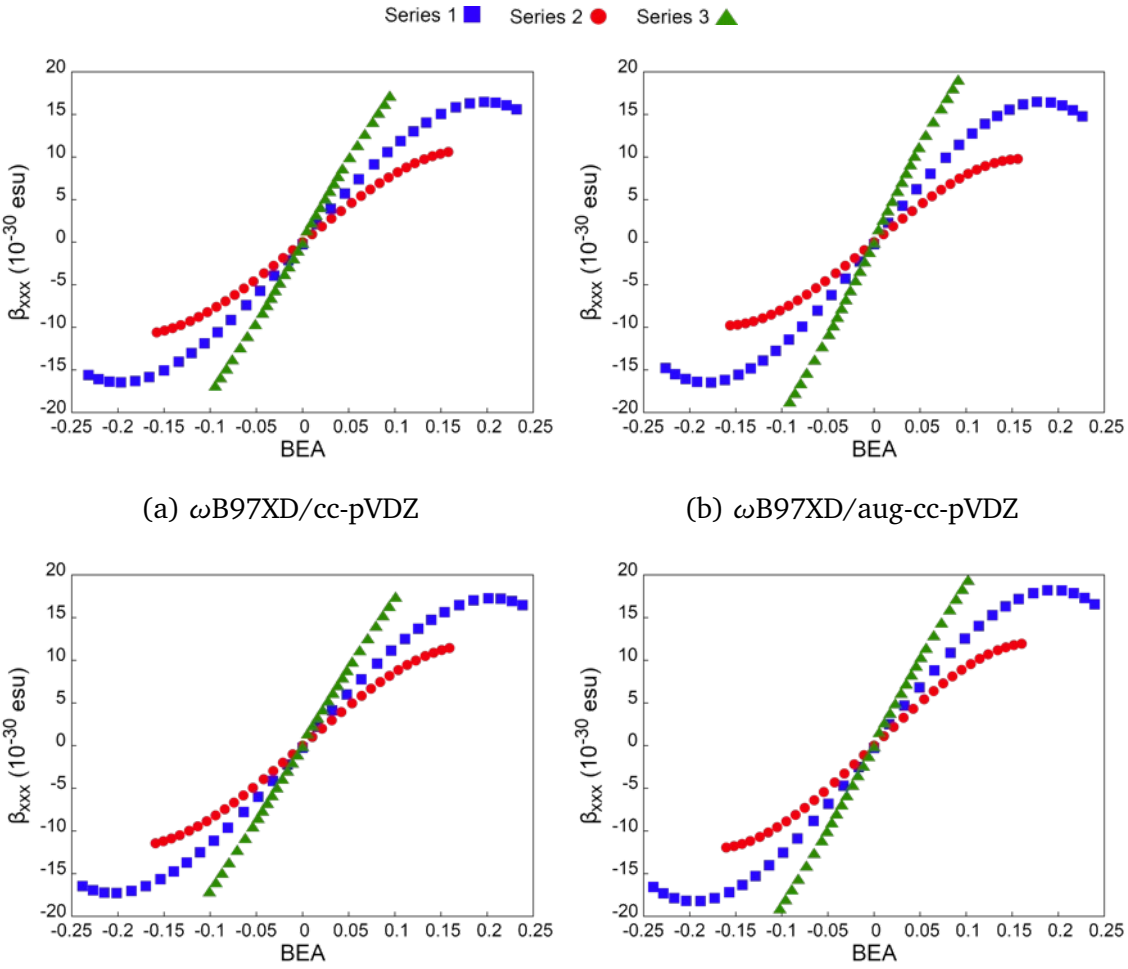

(a) ωB97XD/cc-pVDZ

(b) ωB97XD/aug-cc-pVDZ

(c) ωB97XD/6-31G(d,p)

(d) ωB97XD/ 6-31++G(d,p)

Figure A.21: Correlation of β_{xxx} with BEA for the the 5C-streptocyanine in Series 1, 2, 3, as obtained in the 4 studied levels of theory: Level 1 (a), Level 2 (a), Level 3 (a), Level 4 (a).

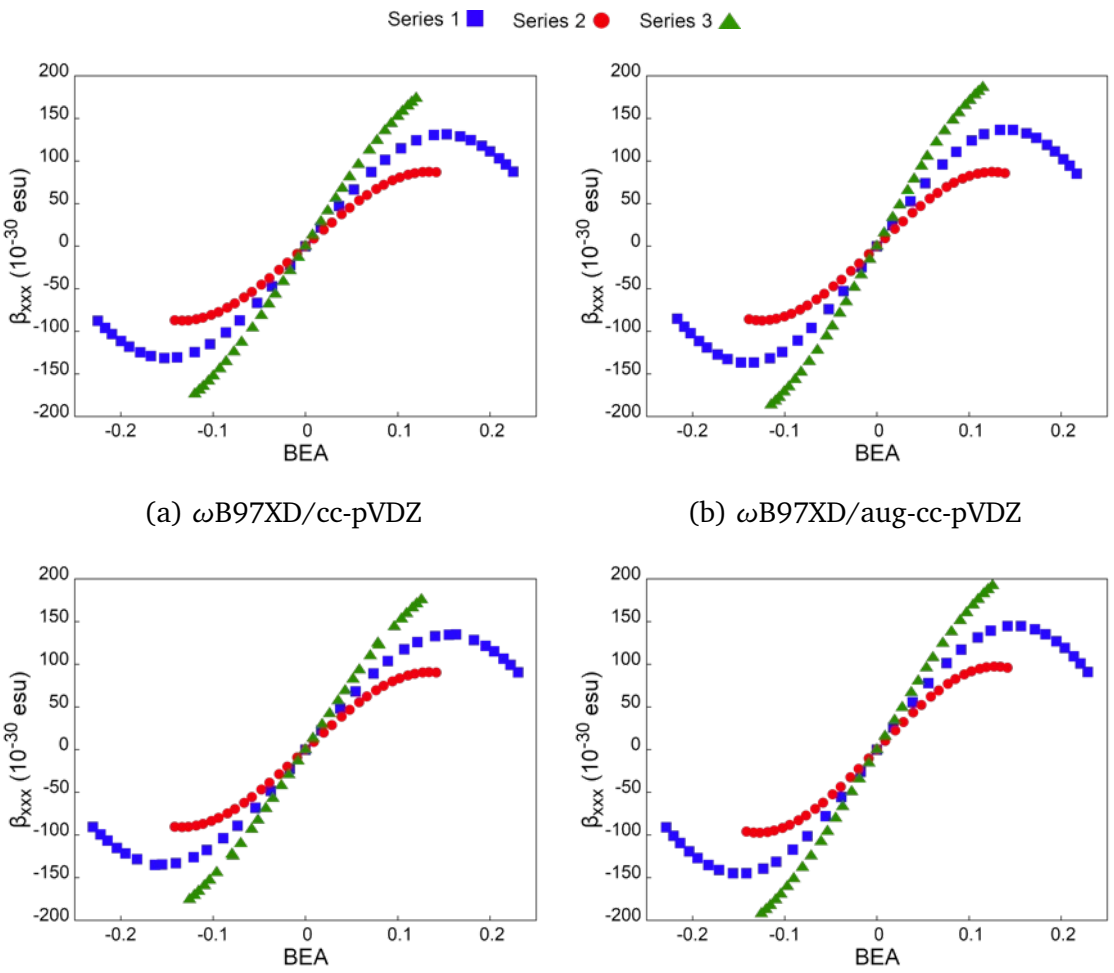

(a) ωB97XD/cc-pVDZ

(b) ωB97XD/aug-cc-pVDZ

(c) ωB97XD/6-31G(d,p)

(d) ωB97XD/ 6-31++G(d,p)

Figure A.22: Correlation of β_{xxx} with BEA for the the 9C-streptocyanine in Series 1, 2, 3, as obtained in the 4 studied levels of theory: Level 1 (a), Level 2 (a), Level 3 (a), Level 4 (a).

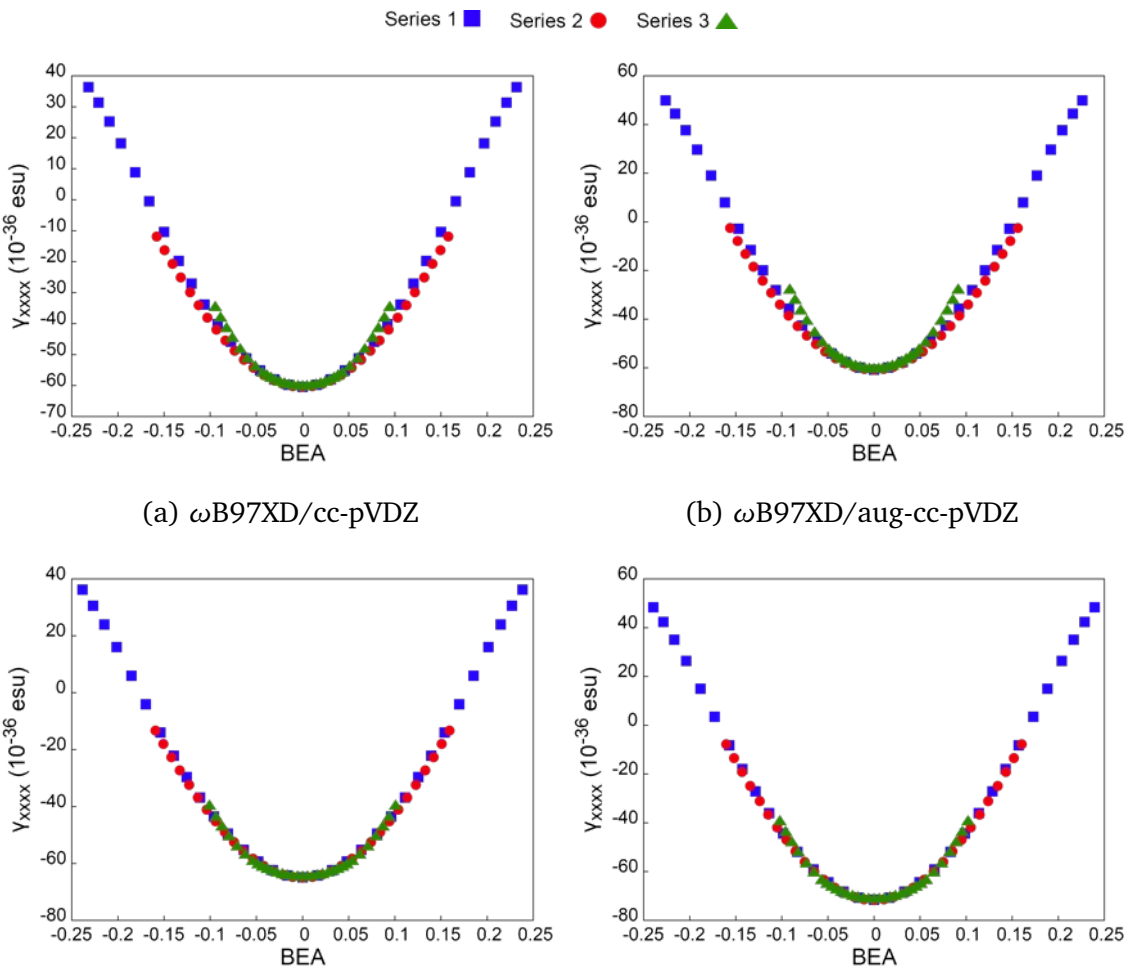

(a) ωB97XD/cc-pVDZ

(b) ωB97XD/aug-cc-pVDZ

(c) ωB97XD/6-31G(d,p)

(d) ωB97XD/ 6-31++G(d,p)

Figure A.23: Correlation of γ_{xxxx} with BEA for the the 5C-streptocyanine in Series 1, 2, 3, as obtained in the 4 studied levels of theory: Level 1 (a), Level 2 (a), Level 3 (a), Level 4 (a).

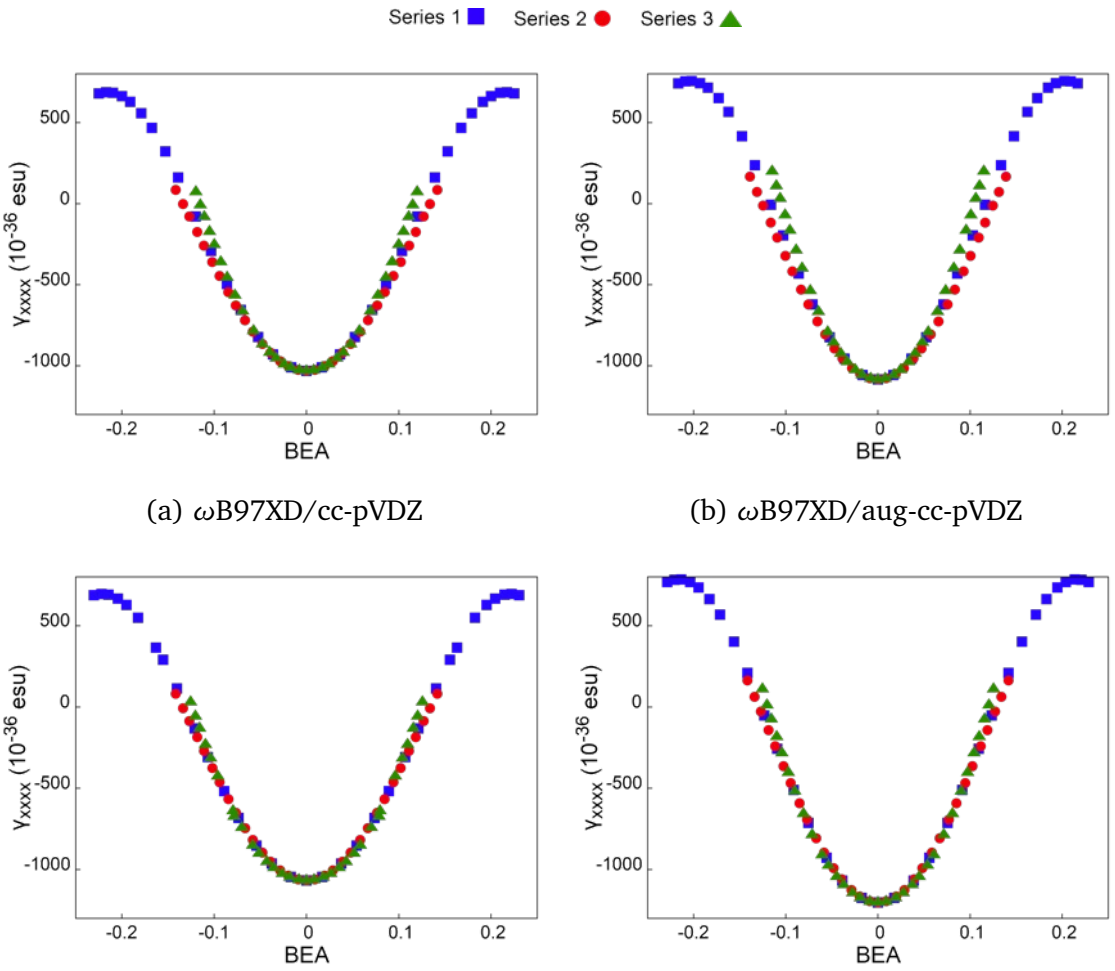

(a) ωB97XD/cc-pVDZ

(b) ωB97XD/aug-cc-pVDZ

(c) ωB97XD/6-31G(d,p)

(d) ωB97XD/ 6-31++G(d,p)

Figure A.24: Correlation of γ_{xxxx} with BEA for the the 9C-streptocyanine in Series 1, 2, 3, as obtained in the 4 studied levels of theory: Level 1 (a), Level 2 (a), Level 3 (a), Level 4 (a).

A.4 Appendix A: Bond Length Alternation

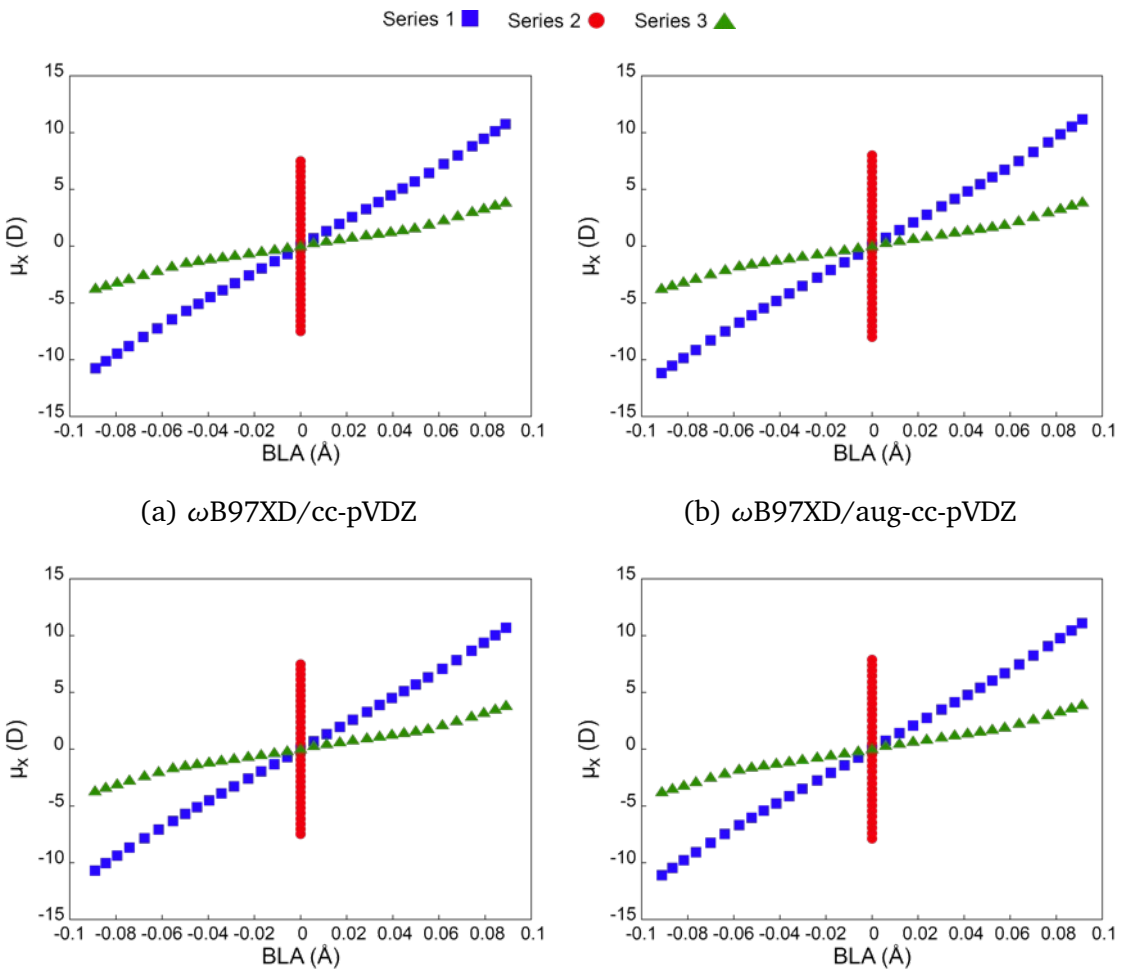

(a) ωB97XD/cc-pVDZ

(b) ωB97XD/aug-cc-pVDZ

(c) ωB97XD/6-31G(d,p)

(d) ωB97XD/ 6-31++G(d,p)

Figure A.25: Correlation of μ_x with BLA for the the 5C-streptocyanine in Series 1, 2, 3, as obtained in the 4 studied levels of theory: Level 1 (a), Level 2 (a), Level 3 (a), Level 4 (a).

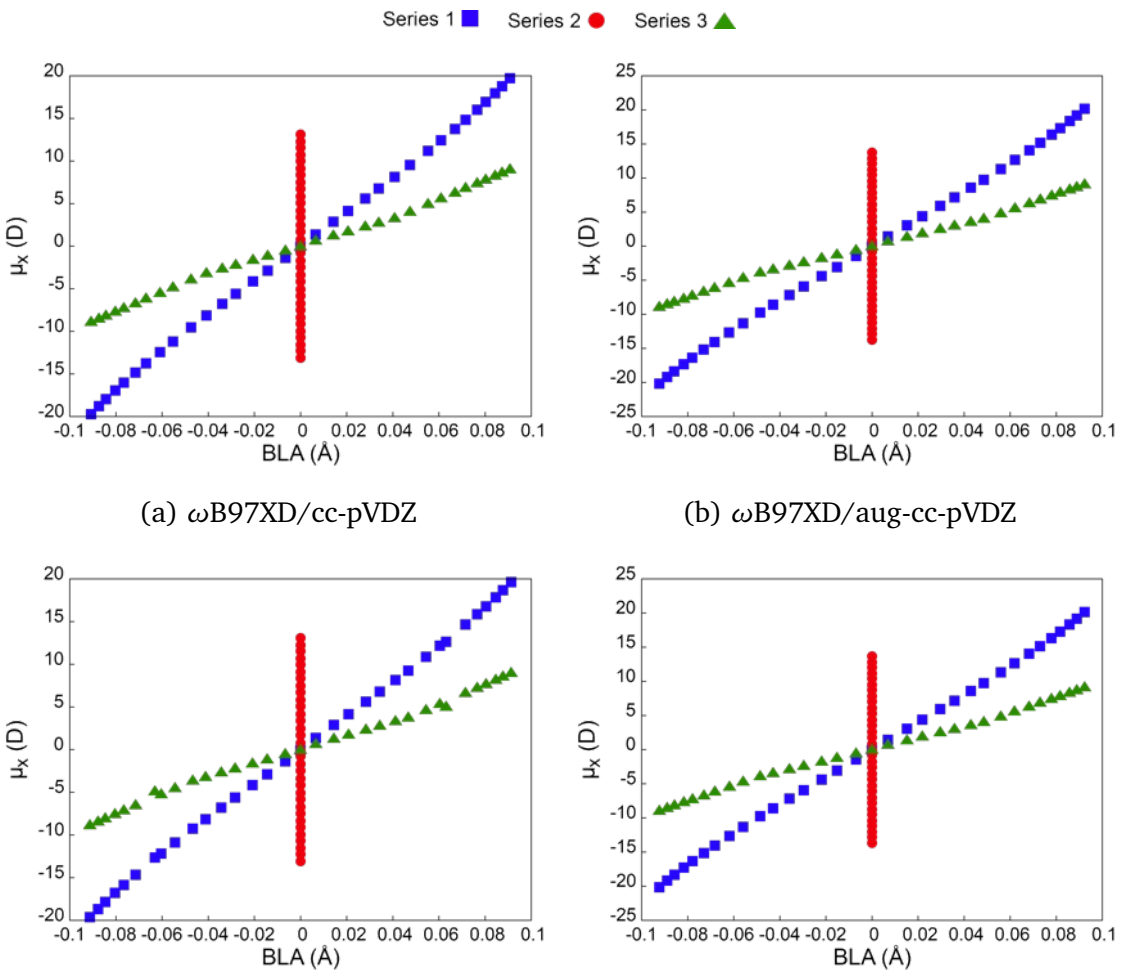

(a) ωB97XD/cc-pVDZ

(b) ωB97XD/aug-cc-pVDZ

(c) ωB97XD/6-31G(d,p)

(d) ωB97XD/ 6-31++G(d,p)

Figure A.26: Correlation of μ_x with BLA for the the 9C-streptocyanine in Series 1, 2, 3, as obtained in the 4 studied levels of theory: Level 1 (a), Level 2 (a), Level 3 (a), Level 4 (a).

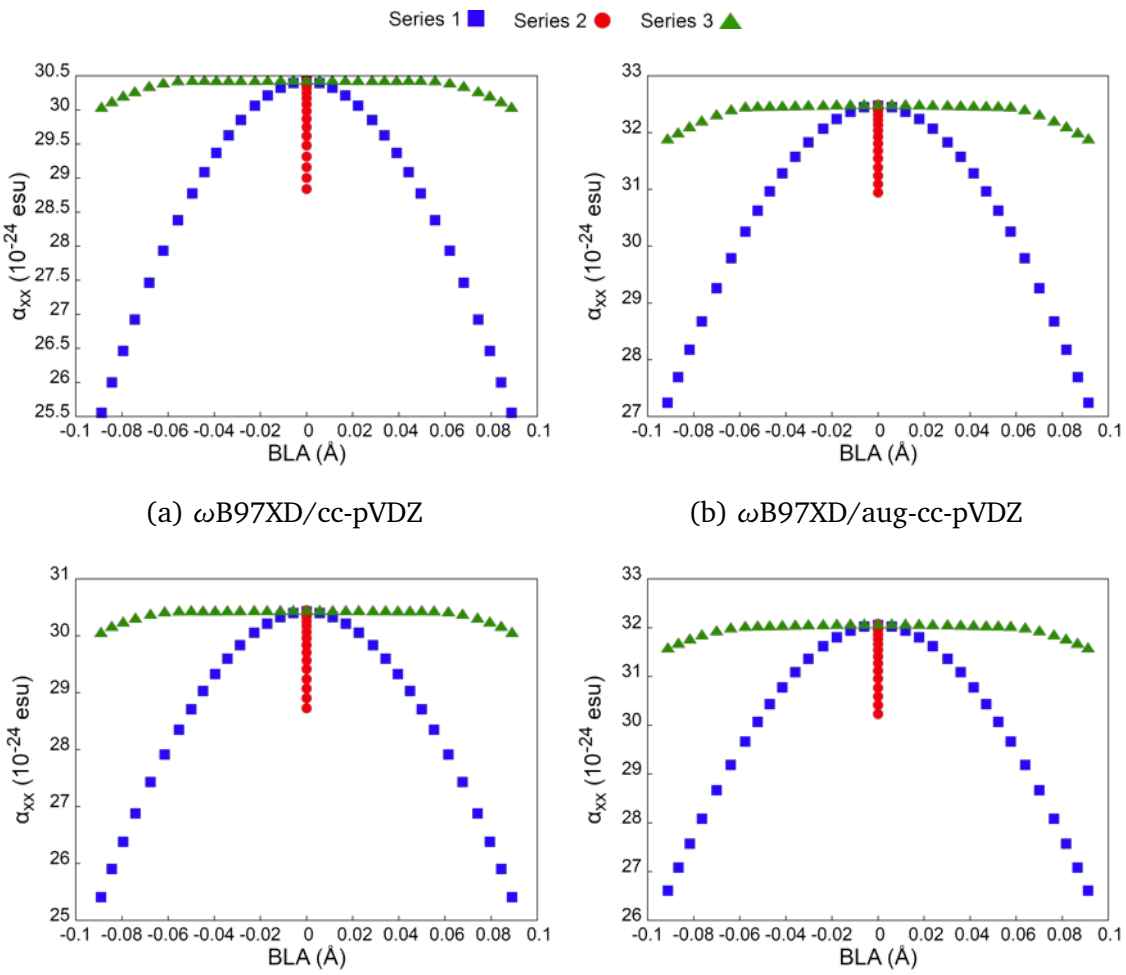

(a) ωB97XD/cc-pVDZ

(b) ωB97XD/aug-cc-pVDZ

(c) ωB97XD/6-31G(d,p)

(d) ωB97XD/ 6-31++G(d,p)

Figure A.27: Correlation of α_{xx} with BLA for the the 5C-streptocyanine in Series 1, 2, 3, as obtained in the 4 studied levels of theory: Level 1 (a), Level 2 (a), Level 3 (a), Level 4 (a).

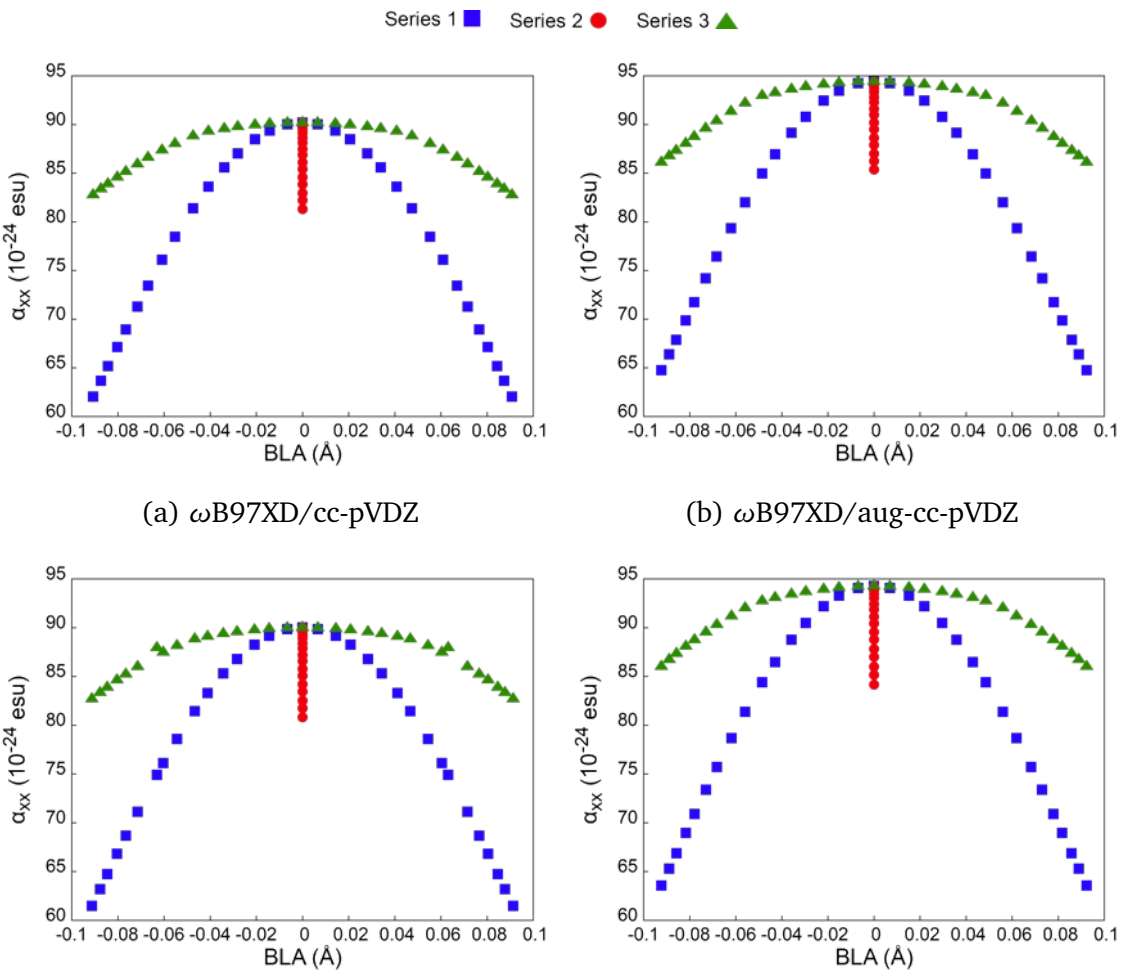

(a) ωB97XD/cc-pVDZ

(b) ωB97XD/aug-cc-pVDZ

(c) ωB97XD/6-31G(d,p)

(d) ωB97XD/ 6-31++G(d,p)

Figure A.28: Correlation of α_{xx} with BLA for the the 9C-streptocyanine in Series 1, 2, 3, as obtained in the 4 studied levels of theory: Level 1 (a), Level 2 (a), Level 3 (a), Level 4 (a).

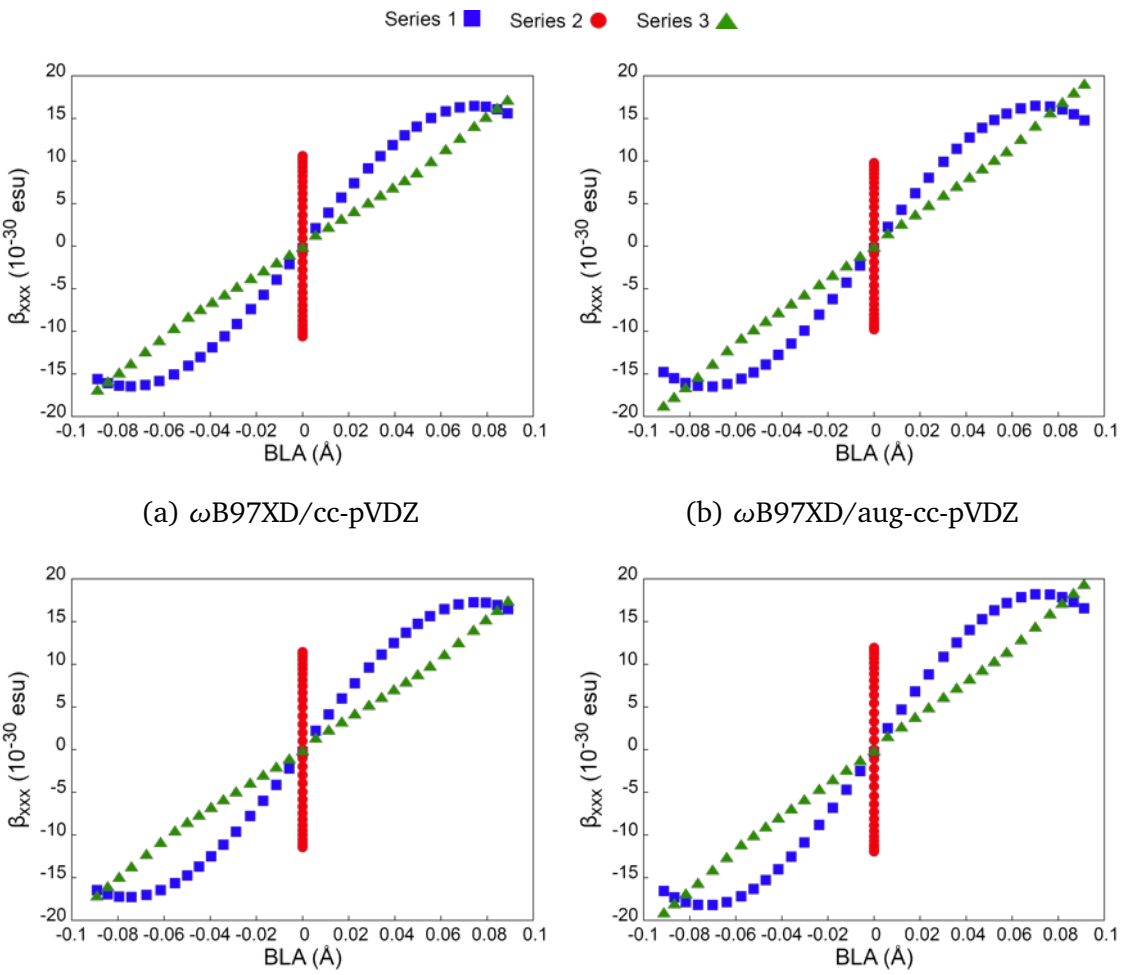

(a) ωB97XD/cc-pVDZ

(b) ωB97XD/aug-cc-pVDZ

(c) ωB97XD/6-31G(d,p)

(d) ωB97XD/ 6-31++G(d,p)

Figure A.29: Correlation of β_{xxx} with BLA for the the 5C-streptocyanine in Series 1, 2, 3, as obtained in the 4 studied levels of theory: Level 1 (a), Level 2 (a), Level 3 (a), Level 4 (a).

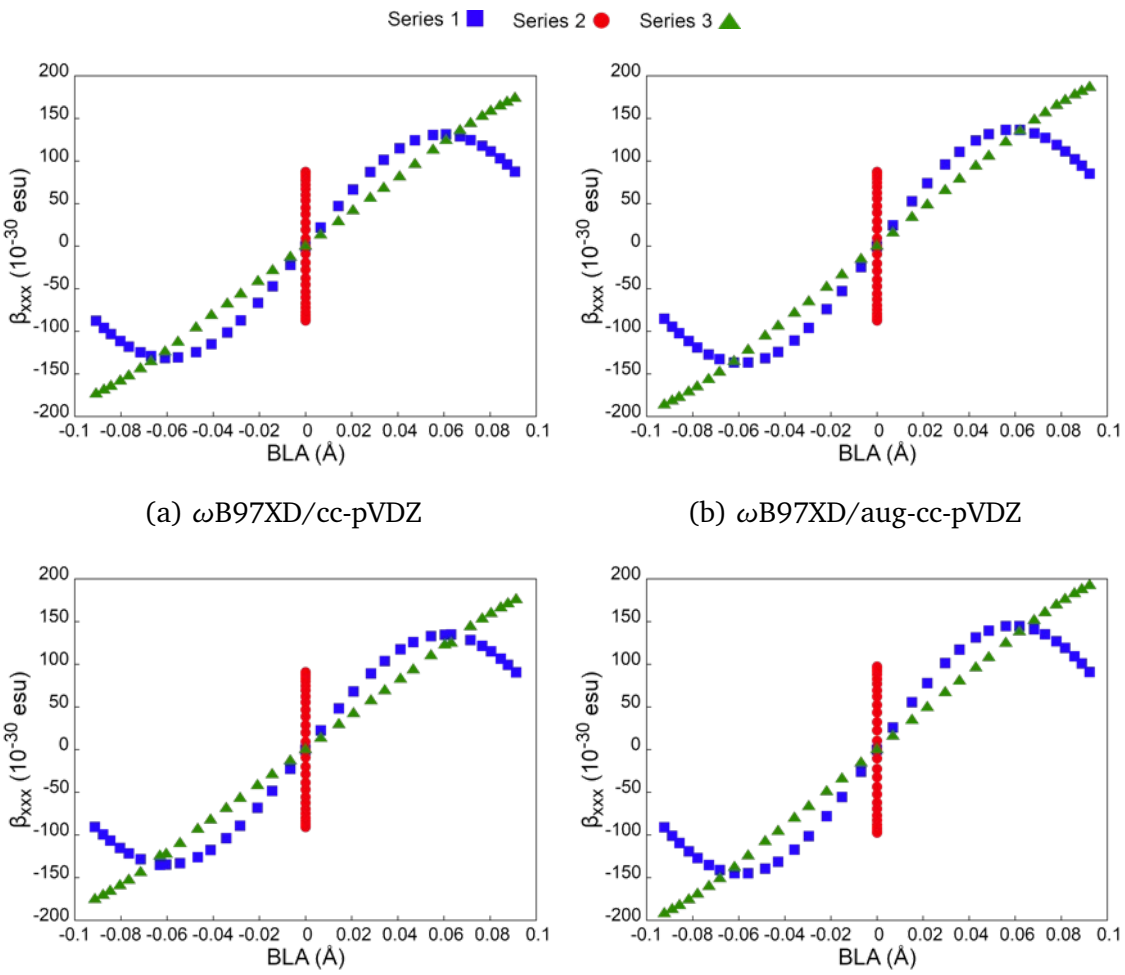

(a) ωB97XD/cc-pVDZ

(b) ωB97XD/aug-cc-pVDZ

(c) ωB97XD/6-31G(d,p)

(d) ωB97XD/ 6-31++G(d,p)

Figure A.30: Correlation of β_{xxx} with BLA for the the 9C-streptocyanine in Series 1, 2, 3, as obtained in the 4 studied levels of theory: Level 1 (a), Level 2 (a), Level 3 (a), Level 4 (a).

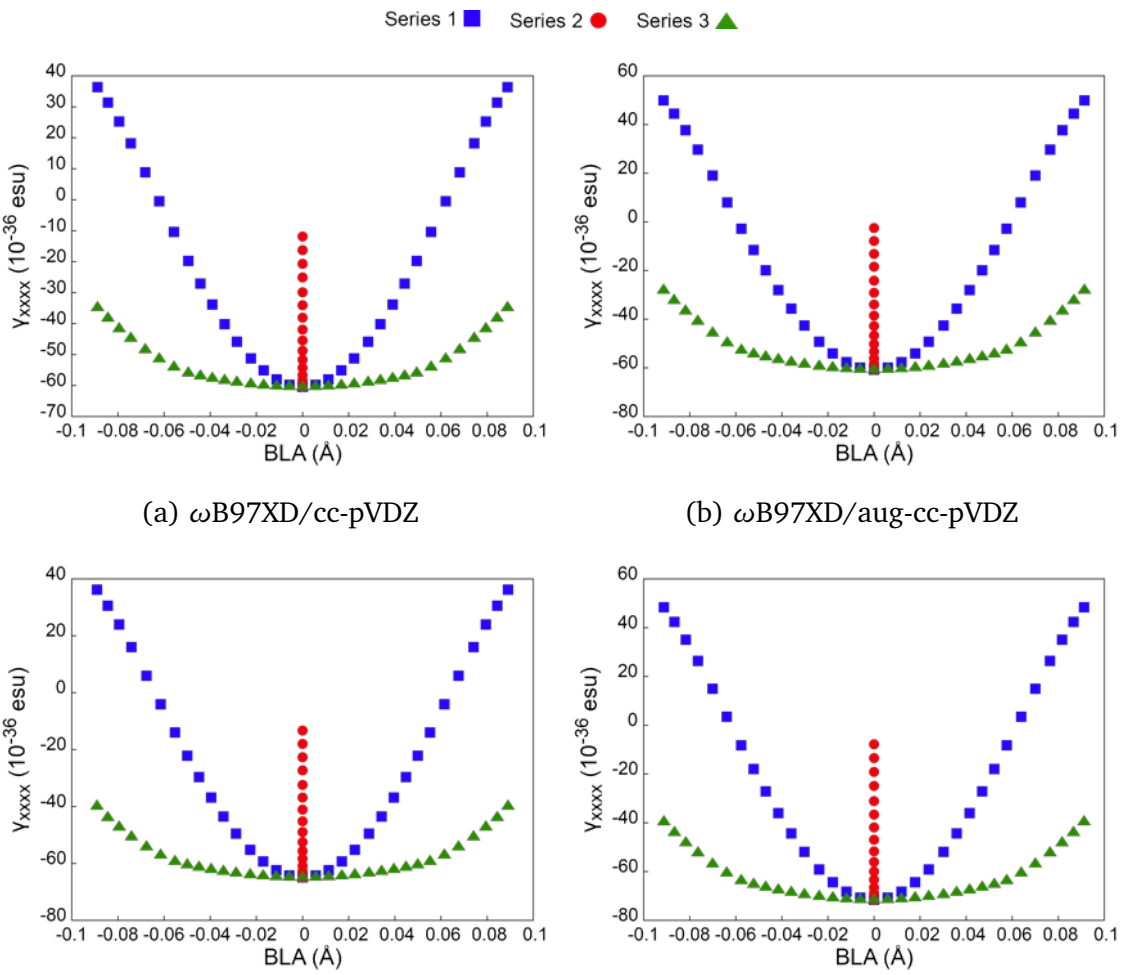

(a) ωB97XD/cc-pVDZ

(b) ωB97XD/aug-cc-pVDZ

(c) ωB97XD/6-31G(d,p)

(d) ωB97XD/ 6-31++G(d,p)

Figure A.31: Correlation of γ_{xxxx} with BLA for the the 5C-streptocyanine in Series 1, 2, 3, as obtained in the 4 studied levels of theory: Level 1 (a), Level 2 (a), Level 3 (a), Level 4 (a).

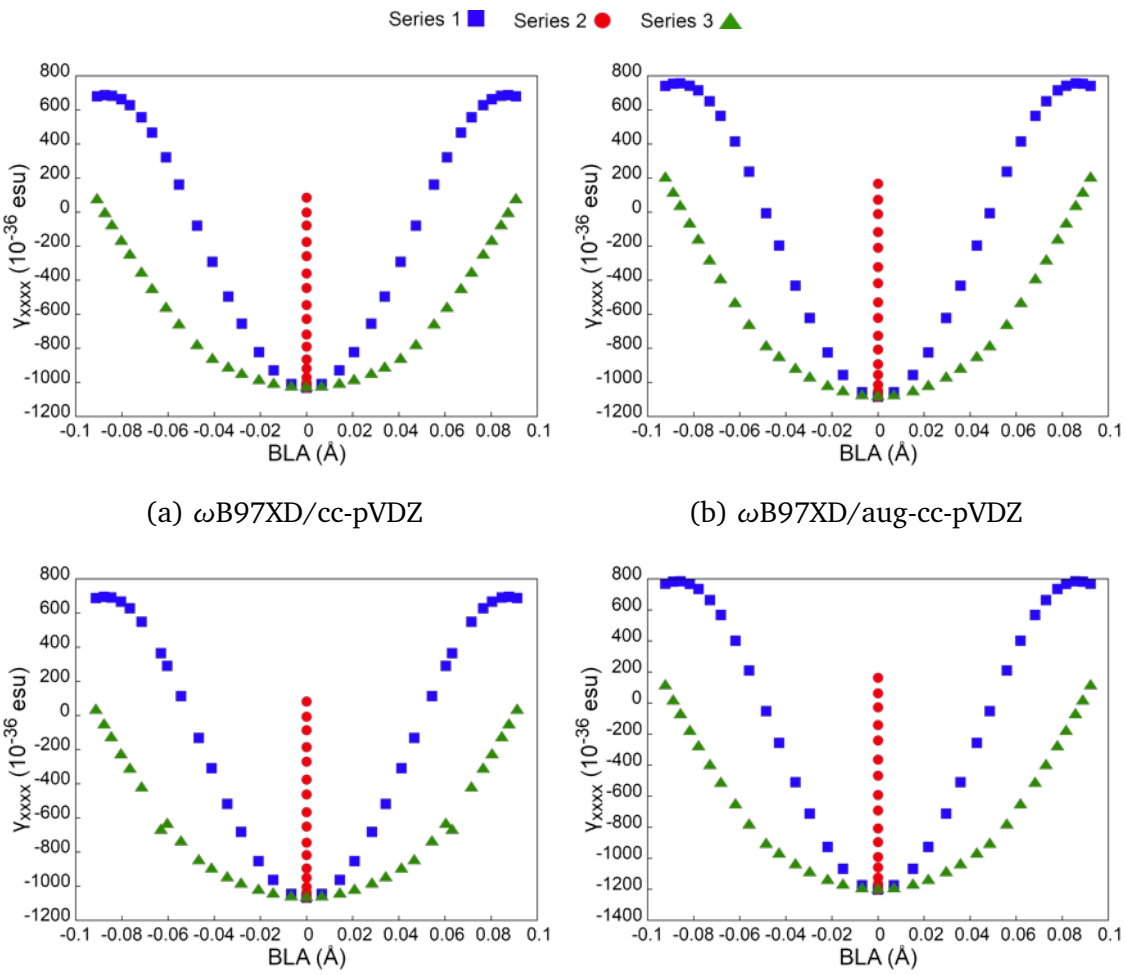

(a) ωB97XD/cc-pVDZ

(b) ωB97XD/aug-cc-pVDZ

(c) ωB97XD/6-31G(d,p)

(d) ωB97XD/ 6-31++G(d,p)

Figure A.32: Correlation of γ_{xxxx} with BLA for the the 9C-streptocyanine in Series 1, 2, 3, as obtained in the 4 studied levels of theory: Level 1 (a), Level 2 (a), Level 3 (a), Level 4 (a).

A.5 Appendix A: Mulliken Bond Order Alternation

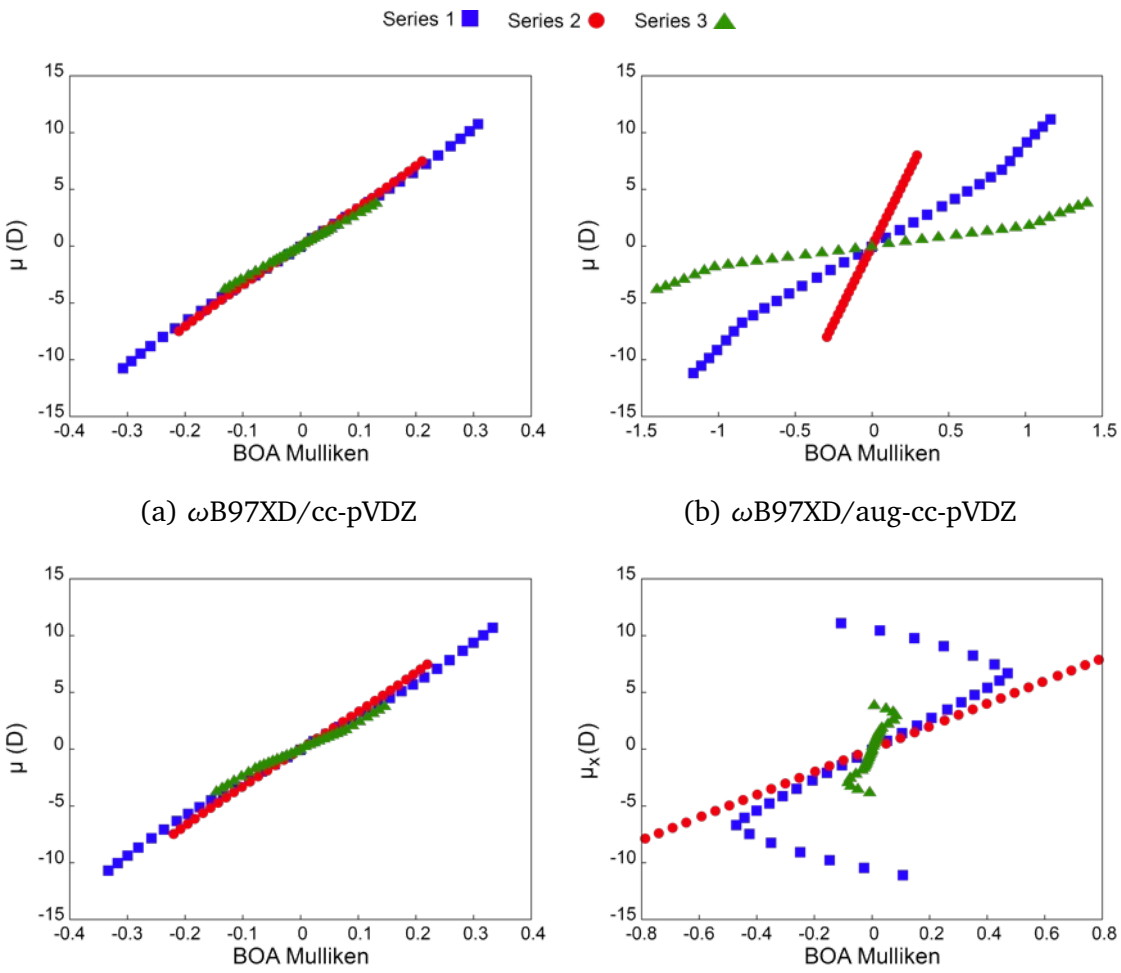

(a) ωB97XD/cc-pVDZ

(b) ωB97XD/aug-cc-pVDZ

(c) ωB97XD/6-31G(d,p)

(d) ωB97XD/ 6-31++G(d,p)

Figure A.33: Correlation of μ_x with BOA Mulliken for the the 5C-streptocyanine in Series 1, 2, 3, as obtained in the 4 studied levels of theory: Level 1 (a), Level 2 (a), Level 3 (a), Level 4 (a).

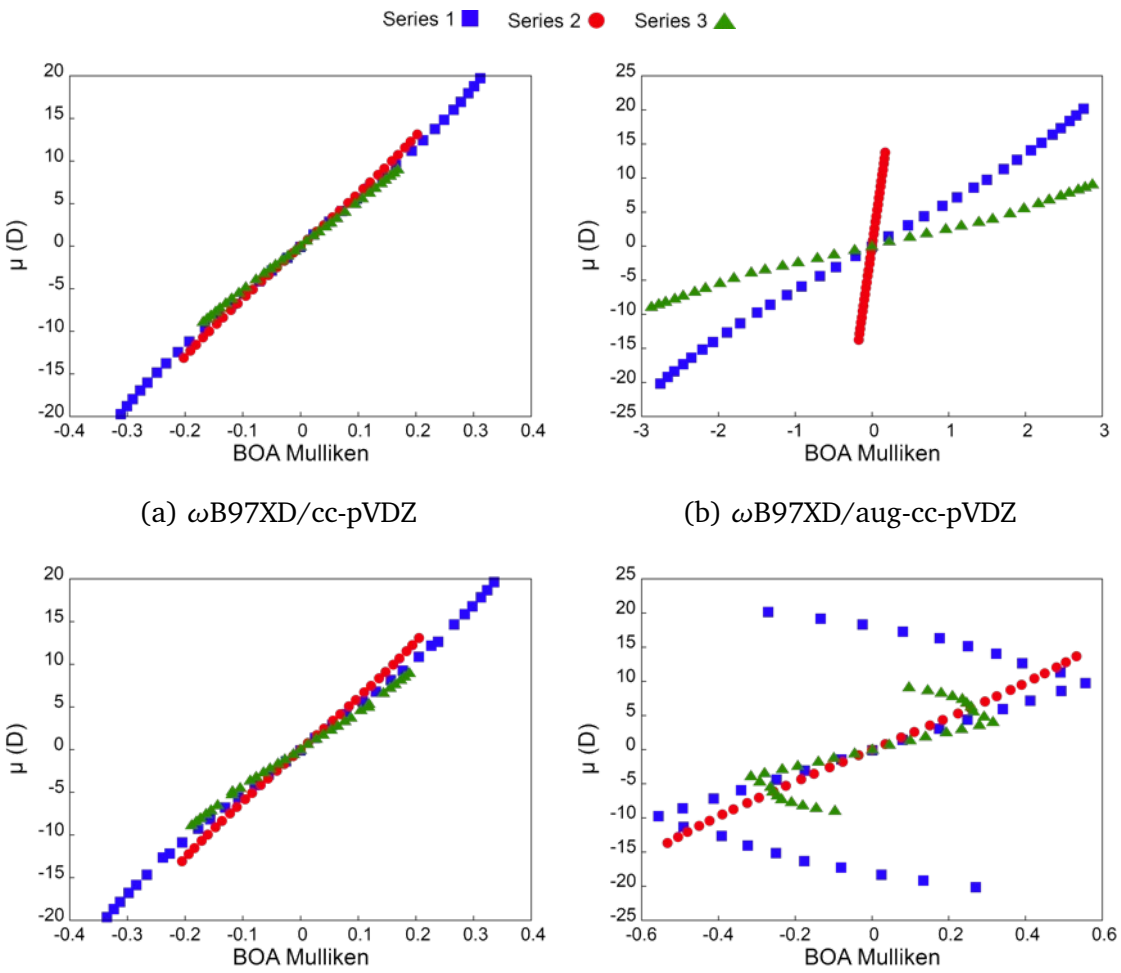

(a) ωB97XD/cc-pVDZ

(b) ωB97XD/aug-cc-pVDZ

(c) ωB97XD/6-31G(d,p)

(d) ωB97XD/ 6-31++G(d,p)

Figure A.34: Correlation of μ_x with BOA Mulliken for the the 9C-streptocyanine in Series 1, 2, 3, as obtained in the 4 studied levels of theory: Level 1 (a), Level 2 (a), Level 3 (a), Level 4 (a).

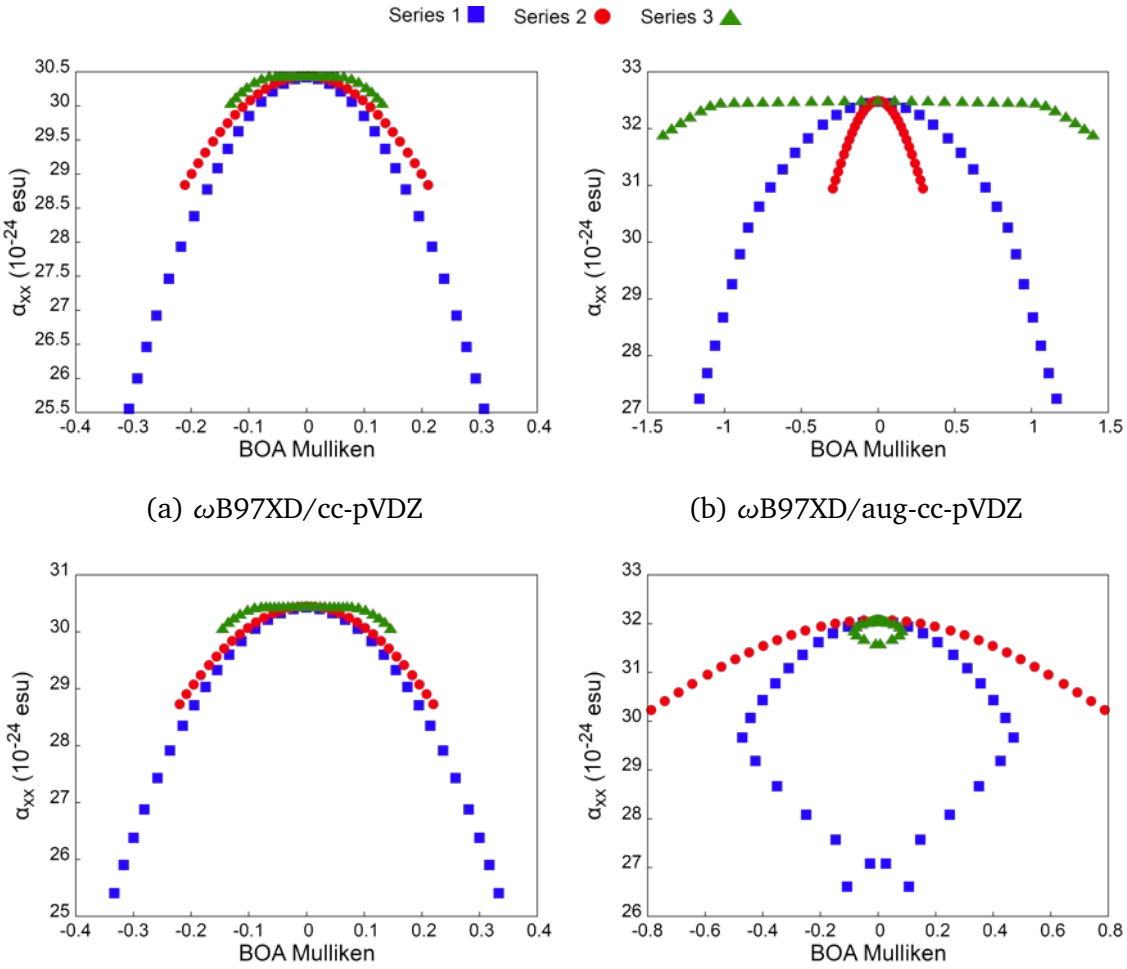

(a) ωB97XD/cc-pVDZ

(b) ωB97XD/aug-cc-pVDZ

(c) ωB97XD/6-31G(d,p)

(d) ωB97XD/ 6-31++G(d,p)

Figure A.35: Correlation of α_{xx} with BOA Mulliken for the the 5C-streptocyanine in Series 1, 2, 3, as obtained in the 4 studied levels of theory: Level 1 (a), Level 2 (a), Level 3 (a), Level 4 (a).

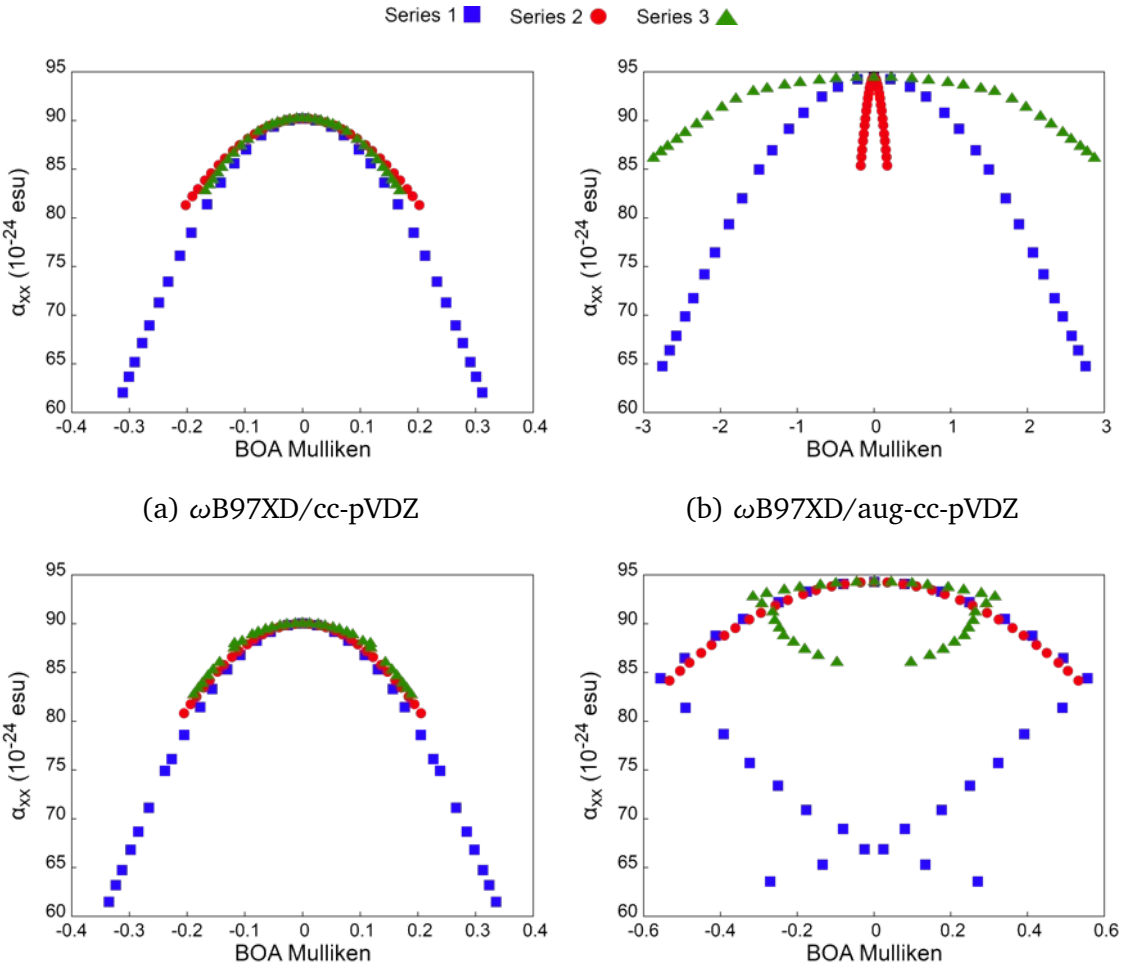

(a) ωB97XD/cc-pVDZ

(b) ωB97XD/aug-cc-pVDZ

(c) ωB97XD/6-31G(d,p)

(d) ωB97XD/ 6-31++G(d,p)

Figure A.36: Correlation of α_{xx} with BOA Mulliken for the the 9C-streptocyanine in Series 1, 2, 3, as obtained in the 4 studied levels of theory: Level 1 (a), Level 2 (a), Level 3 (a), Level 4 (a).

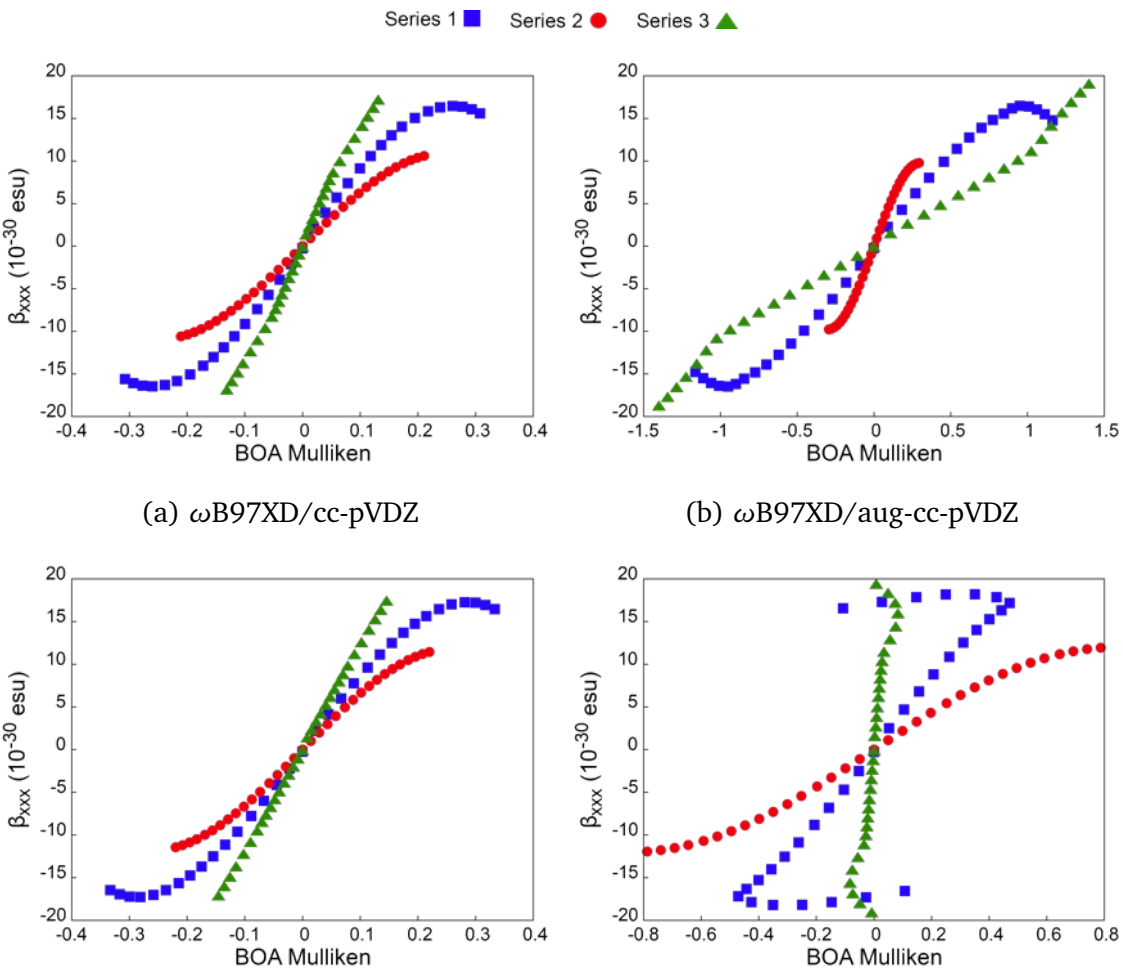

(a) ωB97XD/cc-pVDZ

(b) ωB97XD/aug-cc-pVDZ

(c) ωB97XD/6-31G(d,p)

(d) ωB97XD/ 6-31++G(d,p)

Figure A.37: Correlation of β_{xxx} with BOA Mulliken for the the 5C-streptocyanine in Series 1, 2, 3, as obtained in the 4 studied levels of theory: Level 1 (a), Level 2 (a), Level 3 (a), Level 4 (a).

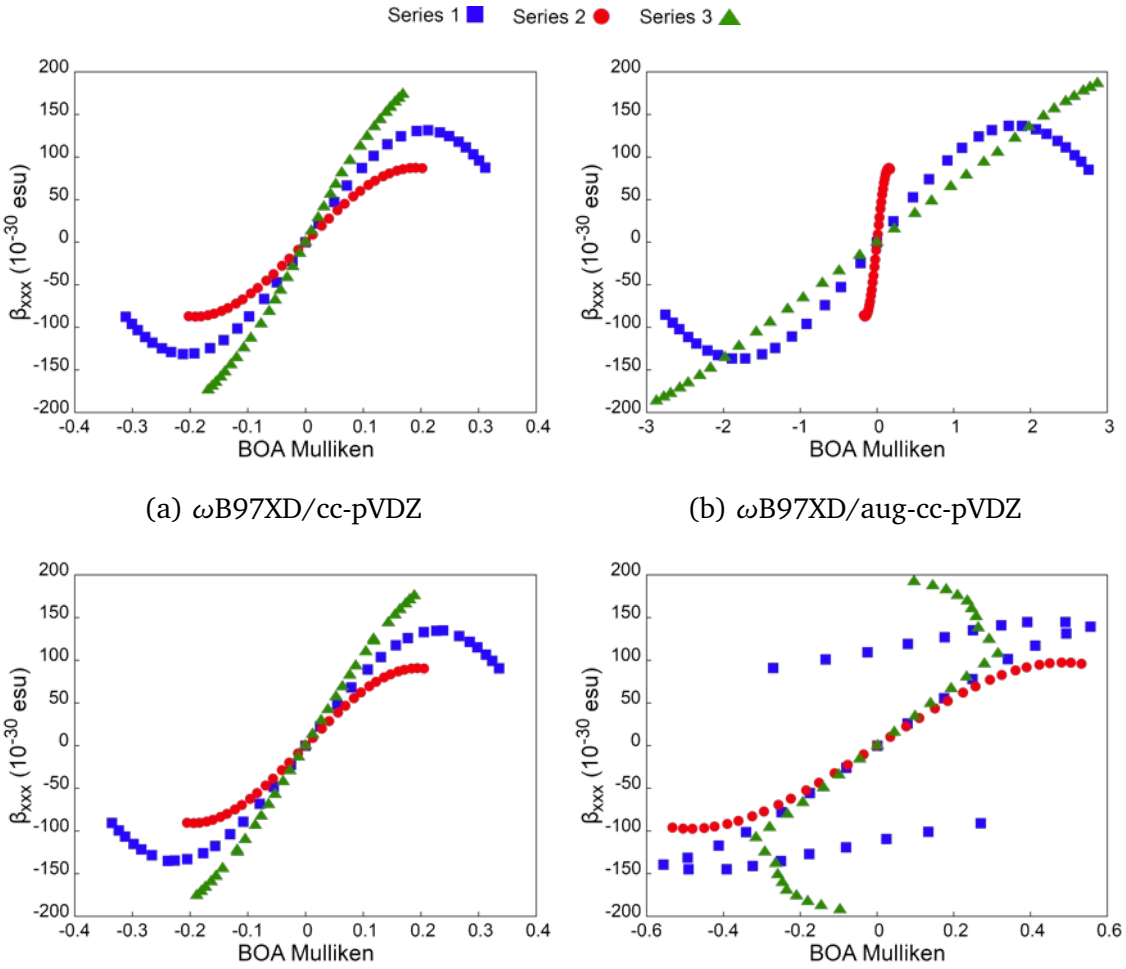

(a) ωB97XD/cc-pVDZ

(b) ωB97XD/aug-cc-pVDZ

(c) ωB97XD/6-31G(d,p)

(d) ωB97XD/ 6-31++G(d,p)

Figure A.38: Correlation of β_{xxx} with BOA Mulliken for the the 9C-streptocyanine in Series 1, 2, 3, as obtained in the 4 studied levels of theory: Level 1 (a), Level 2 (a), Level 3 (a), Level 4 (a).

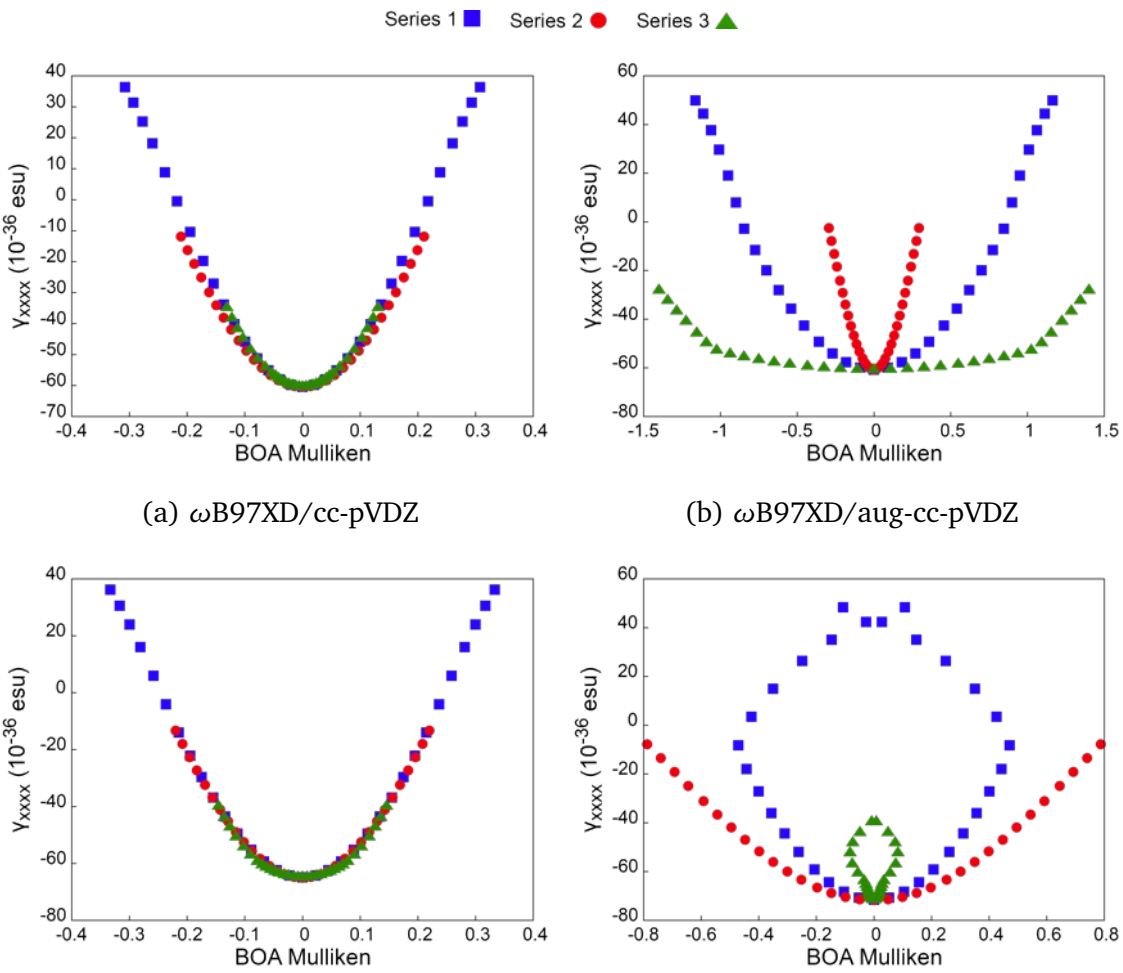

(a) ωB97XD/cc-pVDZ

(b) ωB97XD/aug-cc-pVDZ

(c) ωB97XD/6-31G(d,p)

(d) ωB97XD/ 6-31++G(d,p)

Figure A.39: Correlation of γ_{xxxx} with BOA Mulliken for the the 5C-streptocyanine in Series 1, 2, 3, as obtained in the 4 studied levels of theory: Level 1 (a), Level 2 (a), Level 3 (a), Level 4 (a).

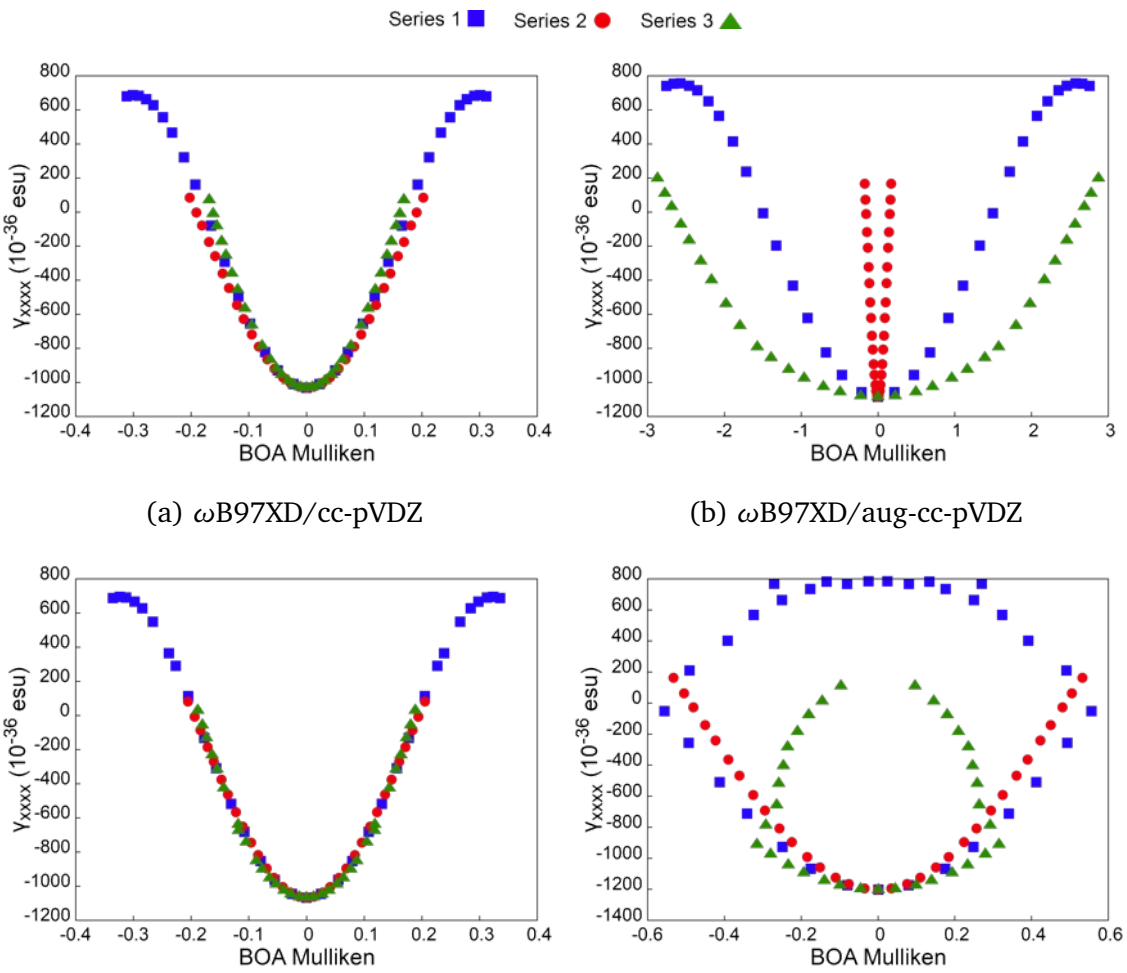

(a) ωB97XD/cc-pVDZ

(b) ωB97XD/aug-cc-pVDZ

(c) ωB97XD/6-31G(d,p)

(d) ωB97XD/ 6-31++G(d,p)

Figure A.40: Correlation of γ_{xxxx} with BOA Mulliken for the the 9C-streptocyanine in Series 1, 2, 3, as obtained in the 4 studied levels of theory: Level 1 (a), Level 2 (a), Level 3 (a), Level 4 (a).

A.6 Appendix A: Mayer Bond Order Alternation

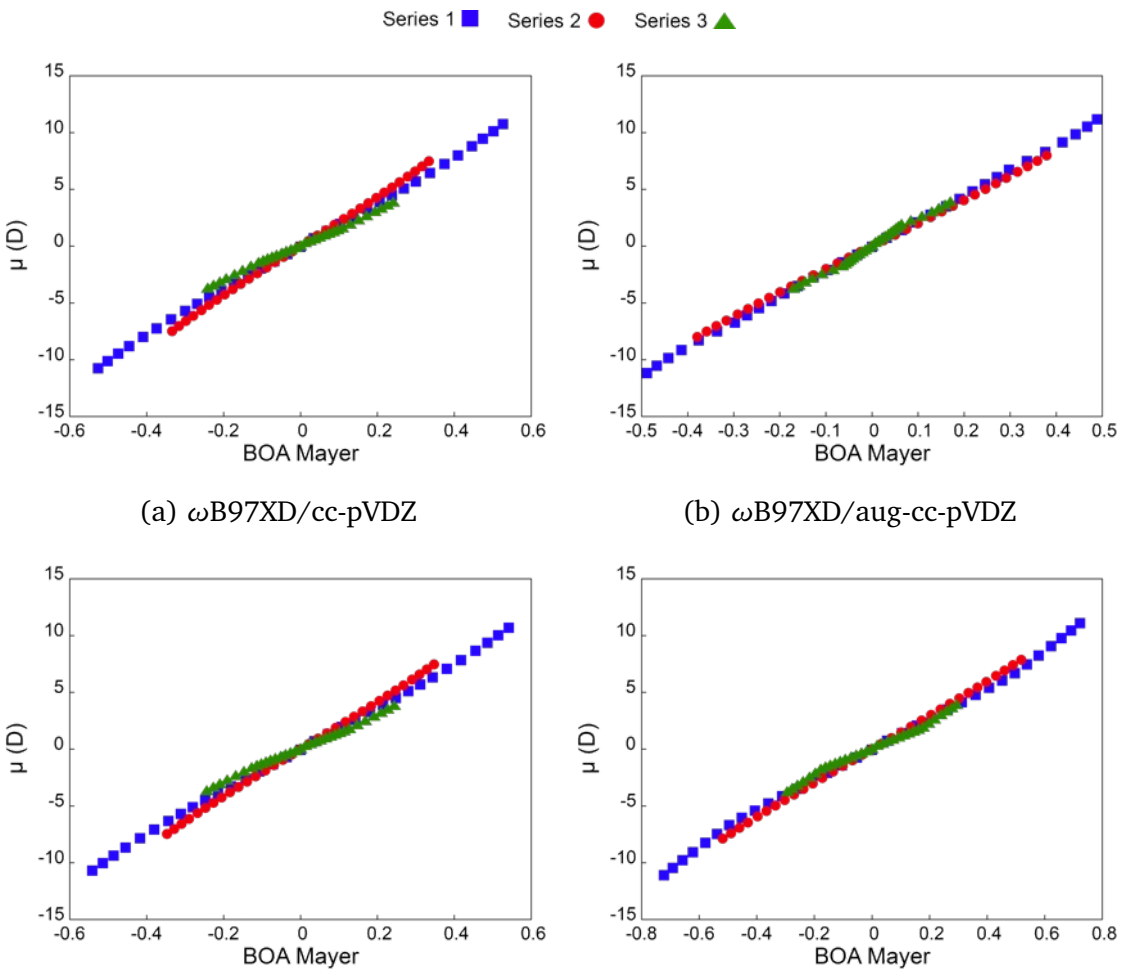

(a) ωB97XD/cc-pVDZ

(b) ωB97XD/aug-cc-pVDZ

(c) ωB97XD/6-31G(d,p)

(d) ωB97XD/ 6-31++G(d,p)

Figure A.41: Correlation of μ_x with BOA Mayer for the the 5C-streptocyanine in Series 1, 2, 3, as obtained in the 4 studied levels of theory: Level 1 (a), Level 2 (a), Level 3 (a), Level 4 (a).

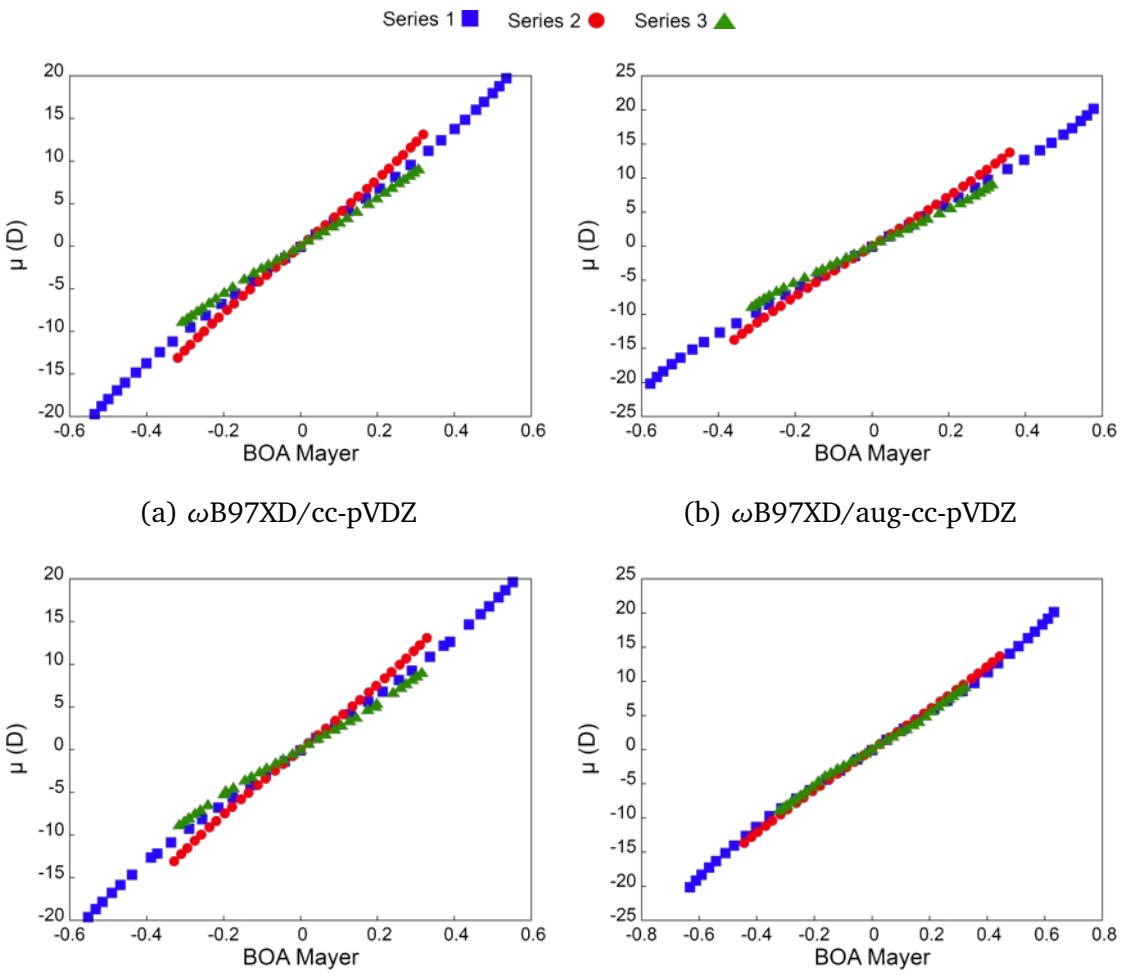

(a) ωB97XD/cc-pVDZ

(b) ωB97XD/aug-cc-pVDZ

(c) ωB97XD/6-31G(d,p)

(d) ωB97XD/ 6-31++G(d,p)

Figure A.42: Correlation of μ_x with BOA Mayer for the the 9C-streptocyanine in Series 1, 2, 3, as obtained in the 4 studied levels of theory: Level 1 (a), Level 2 (a), Level 3 (a), Level 4 (a).

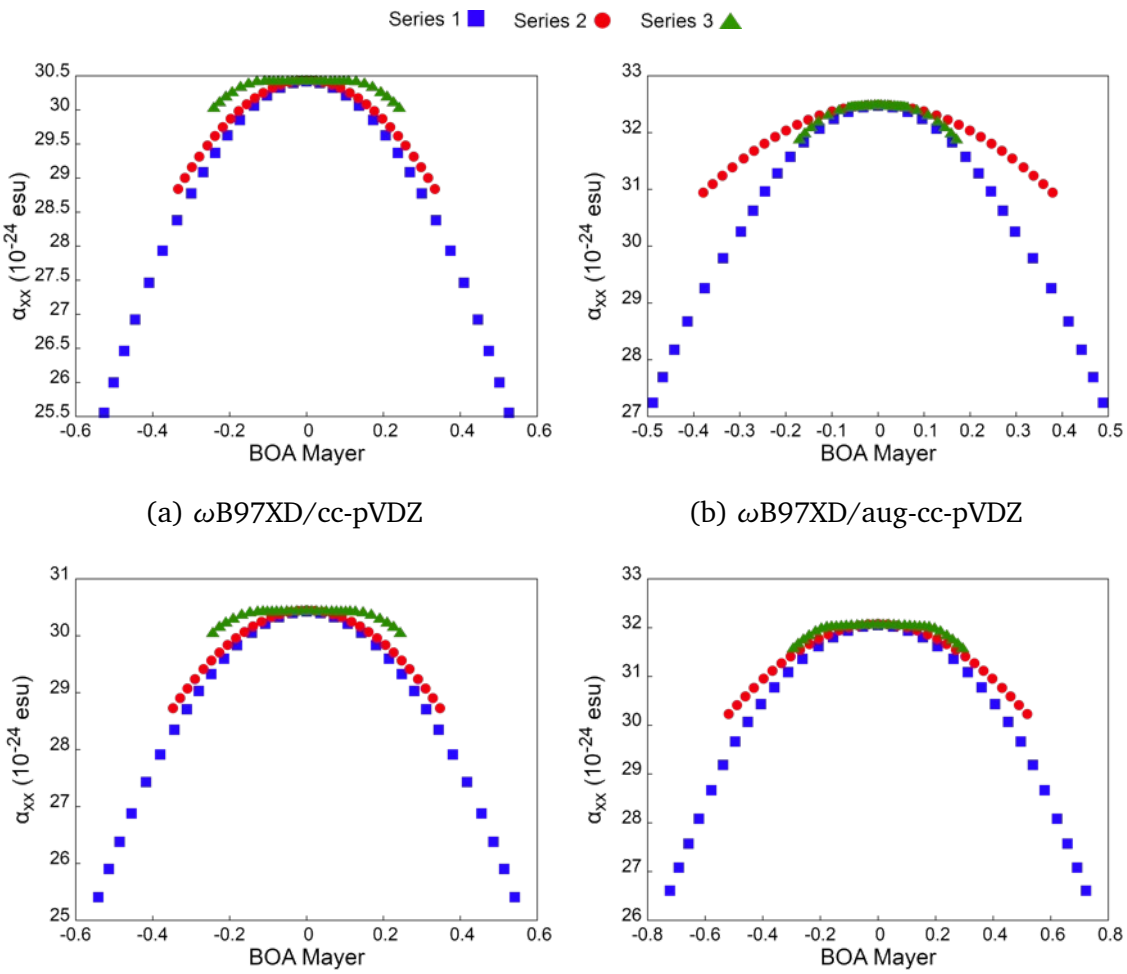

(a) ωB97XD/cc-pVDZ

(b) ωB97XD/aug-cc-pVDZ

(c) ωB97XD/6-31G(d,p)

(d) ωB97XD/ 6-31++G(d,p)

Figure A.43: Correlation of α_{xx} with BOA Mayer for the the 5C-streptocyanine in Series 1, 2, 3, as obtained in the 4 studied levels of theory: Level 1 (a), Level 2 (a), Level 3 (a), Level 4 (a).

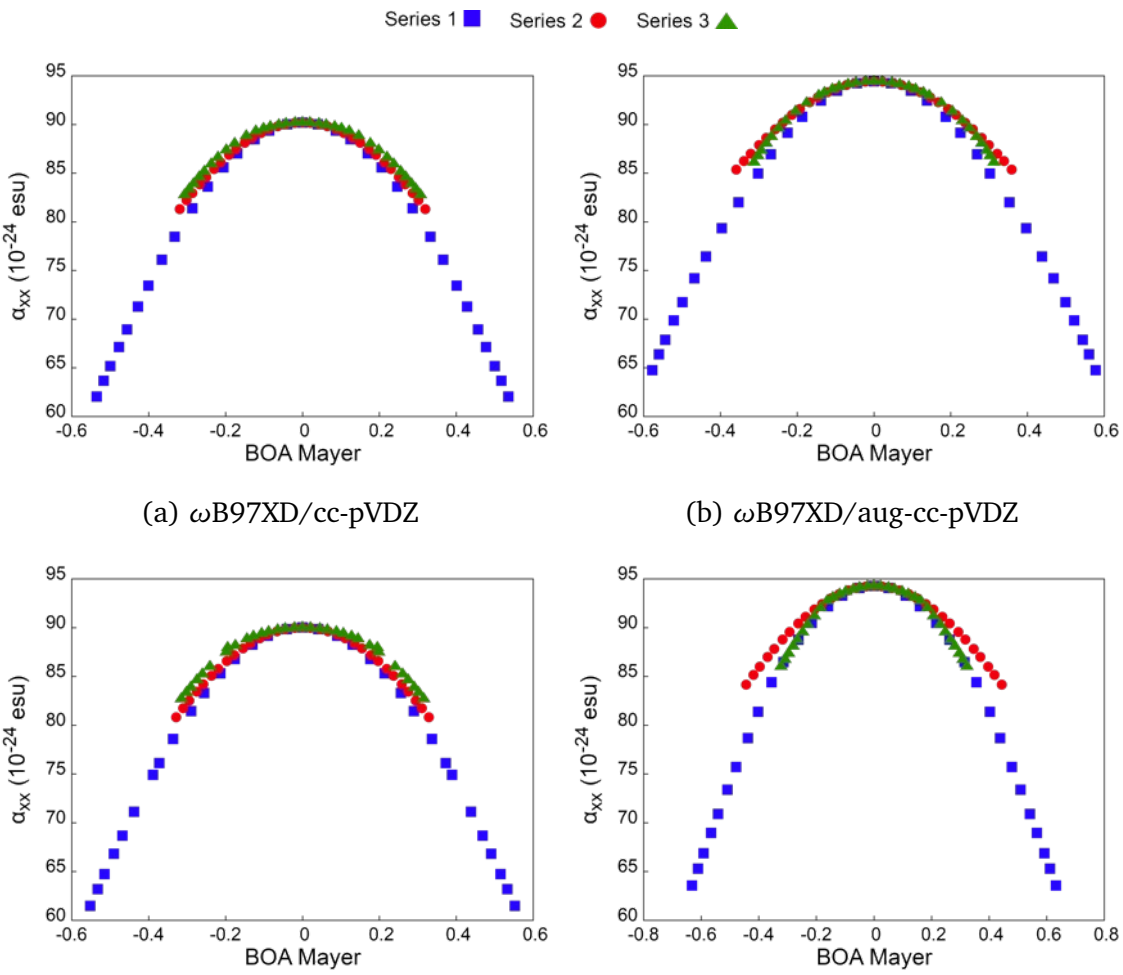

(a) ωB97XD/cc-pVDZ

(b) ωB97XD/aug-cc-pVDZ

(c) ωB97XD/6-31G(d,p)

(d) ωB97XD/ 6-31++G(d,p)

Figure A.44: Correlation of α_{xx} with BOA Mayer for the the 9C-streptocyanine in Series 1, 2, 3, as obtained in the 4 studied levels of theory: Level 1 (a), Level 2 (a), Level 3 (a), Level 4 (a).

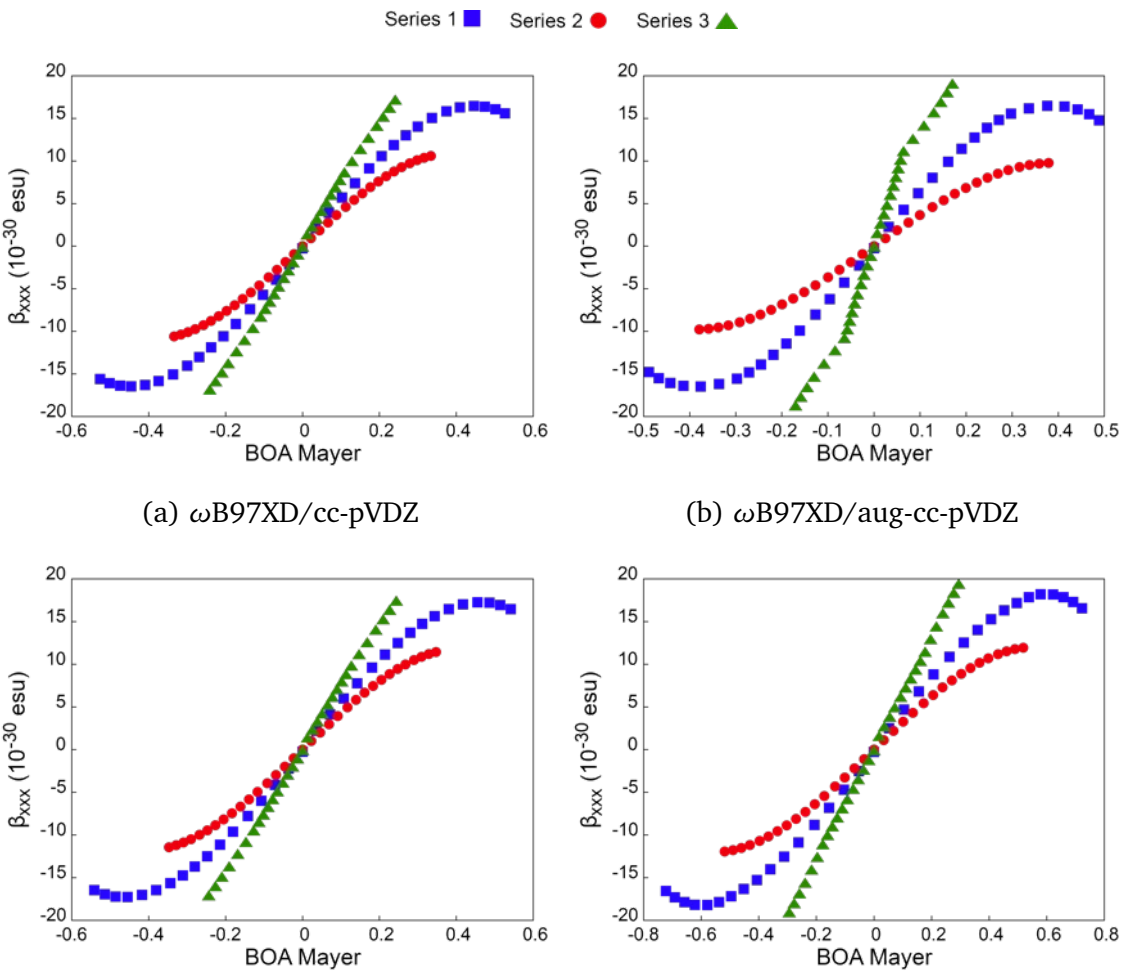

(a) ωB97XD/cc-pVDZ

(b) ωB97XD/aug-cc-pVDZ

(c) ωB97XD/6-31G(d,p)

(d) ωB97XD/ 6-31++G(d,p)

Figure A.45: Correlation of β_{xxx} with BOA Mayer for the the 5C-streptocyanine in Series 1, 2, 3, as obtained in the 4 studied levels of theory: Level 1 (a), Level 2 (a), Level 3 (a), Level 4 (a).

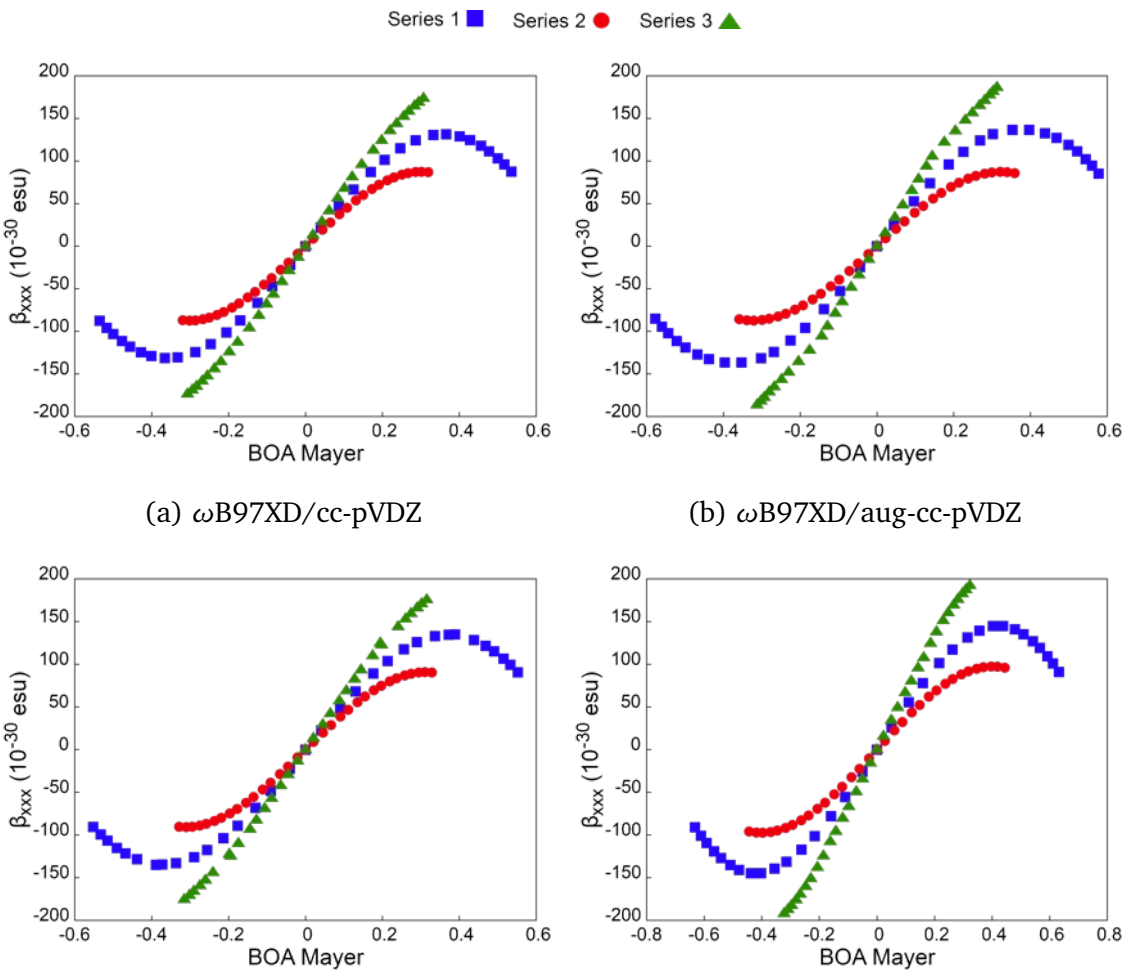

(a) ωB97XD/cc-pVDZ

(b) ωB97XD/aug-cc-pVDZ

(c) ωB97XD/6-31G(d,p)

(d) ωB97XD/ 6-31++G(d,p)

Figure A.46: Correlation of β_{xxx} with BOA Mayer for the the 9C-streptocyanine in Series 1, 2, 3, as obtained in the 4 studied levels of theory: Level 1 (a), Level 2 (a), Level 3 (a), Level 4 (a).

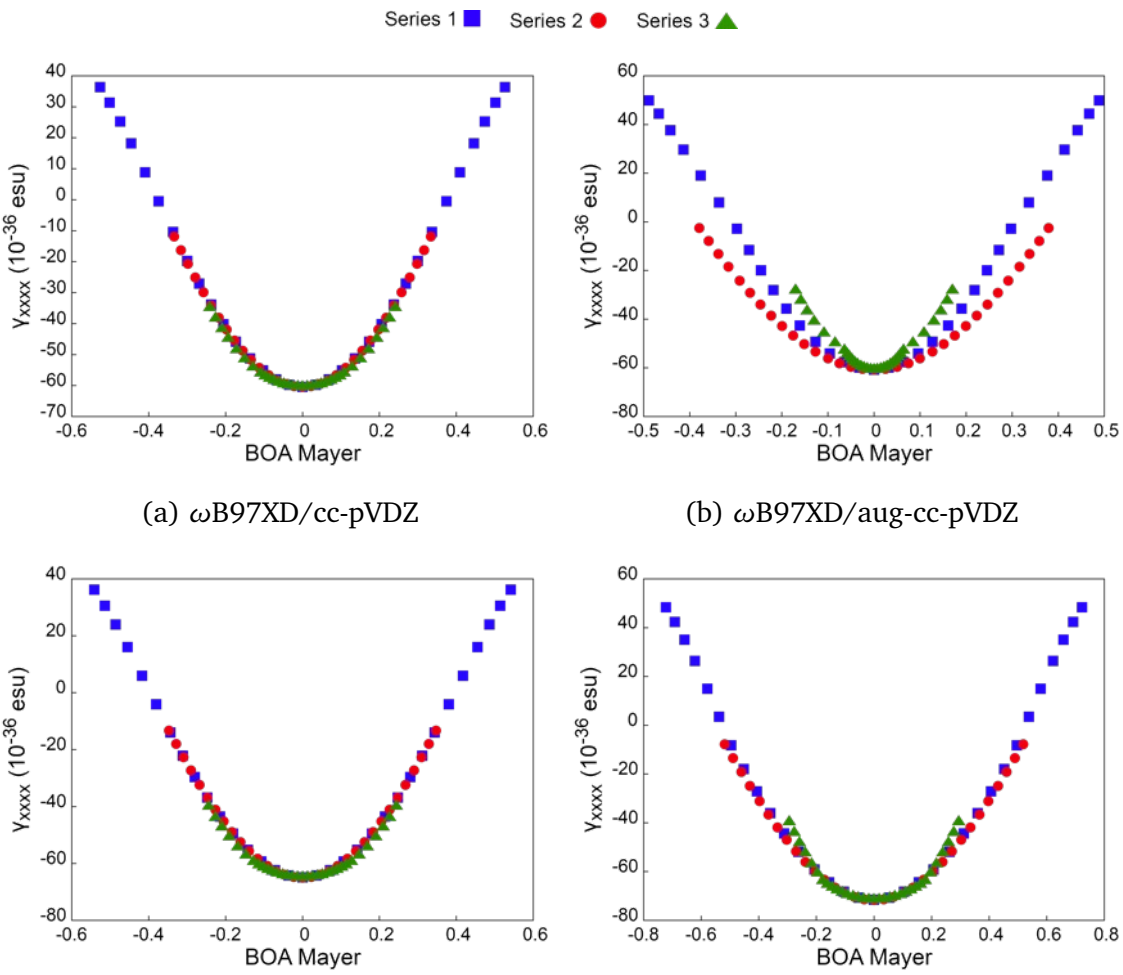

(a) ωB97XD/cc-pVDZ

(b) ωB97XD/aug-cc-pVDZ

(c) ωB97XD/6-31G(d,p)

(d) ωB97XD/ 6-31++G(d,p)

Figure A.47: Correlation of γ_{xxxx} with BOA Mayer for the the 5C-streptocyanine in Series 1, 2, 3, as obtained in the 4 studied levels of theory: Level 1 (a), Level 2 (a), Level 3 (a), Level 4 (a).

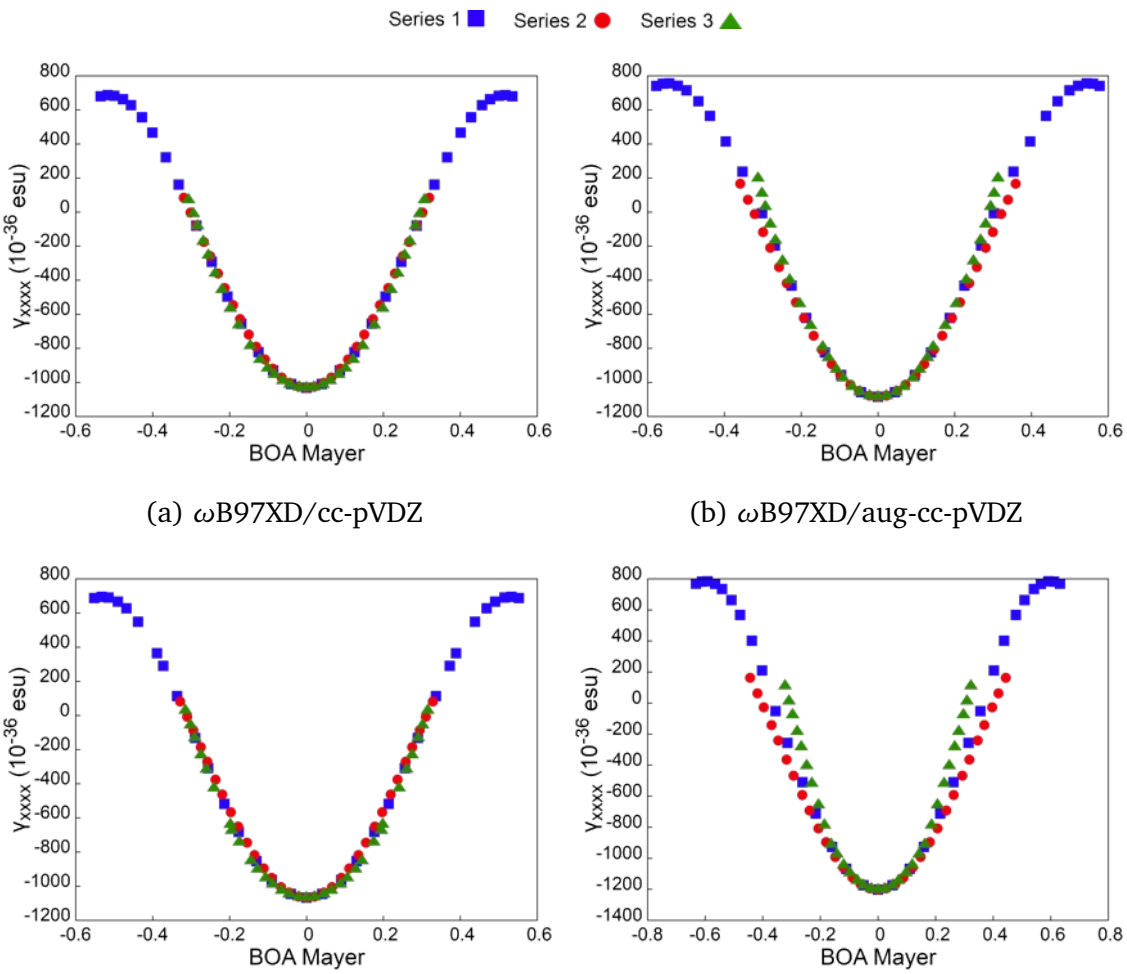

(a) ωB97XD/cc-pVDZ

(b) ωB97XD/aug-cc-pVDZ

(c) ωB97XD/6-31G(d,p)

(d) ωB97XD/ 6-31++G(d,p)

Figure A.48: Correlation of γ_{xxxx} with BOA Mayer for the the 9C-streptocyanine in Series 1, 2, 3, as obtained in the 4 studied levels of theory: Level 1 (a), Level 2 (a), Level 3 (a), Level 4 (a).

A.7 Appendix A: Wiberg Bond Order Alternation

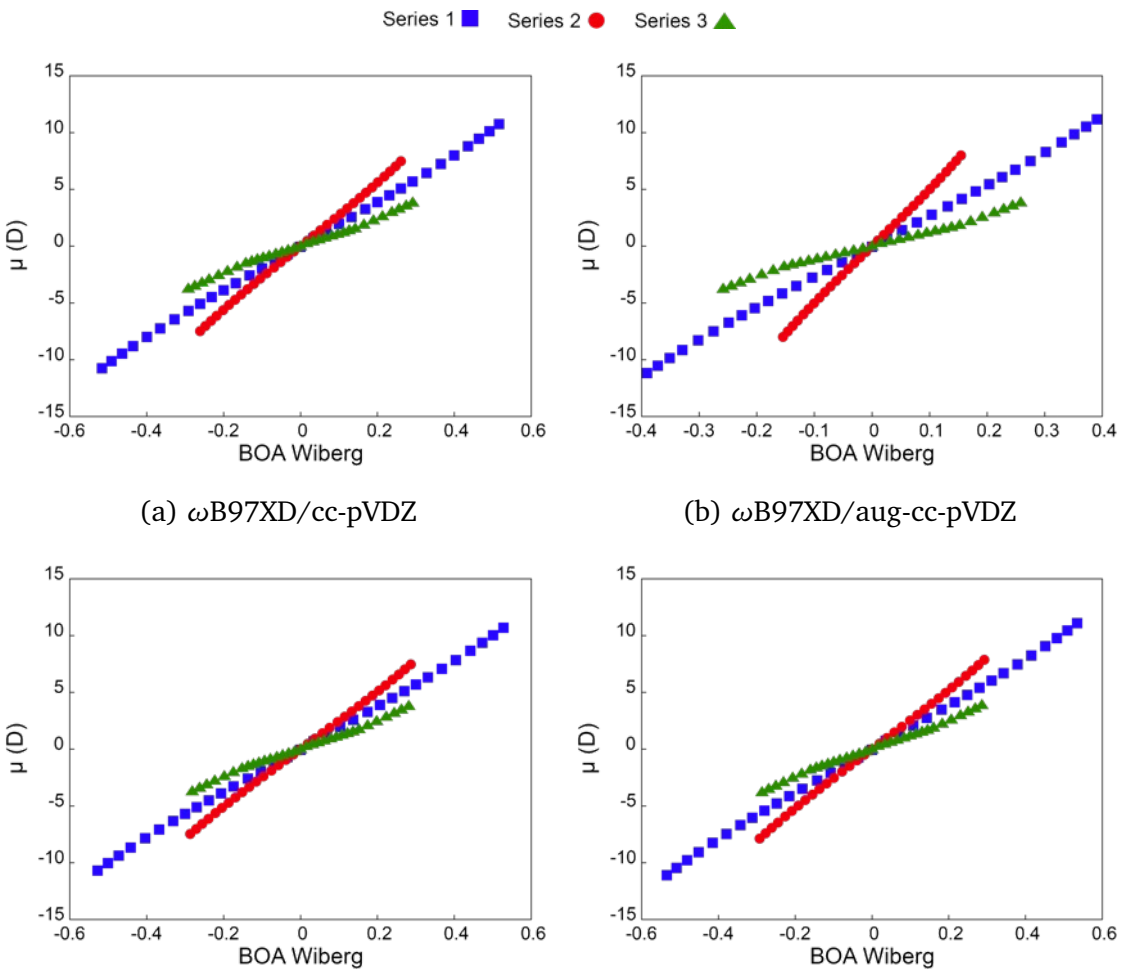

(a) ωB97XD/cc-pVDZ

(b) ωB97XD/aug-cc-pVDZ

(c) ωB97XD/6-31G(d,p)

(d) ωB97XD/ 6-31++G(d,p)

Figure A.49: Correlation of μ_x with BOA Wiberg for the the 5C-streptocyanine in Series 1, 2, 3, as obtained in the 4 studied levels of theory: Level 1 (a), Level 2 (a), Level 3 (a), Level 4 (a).

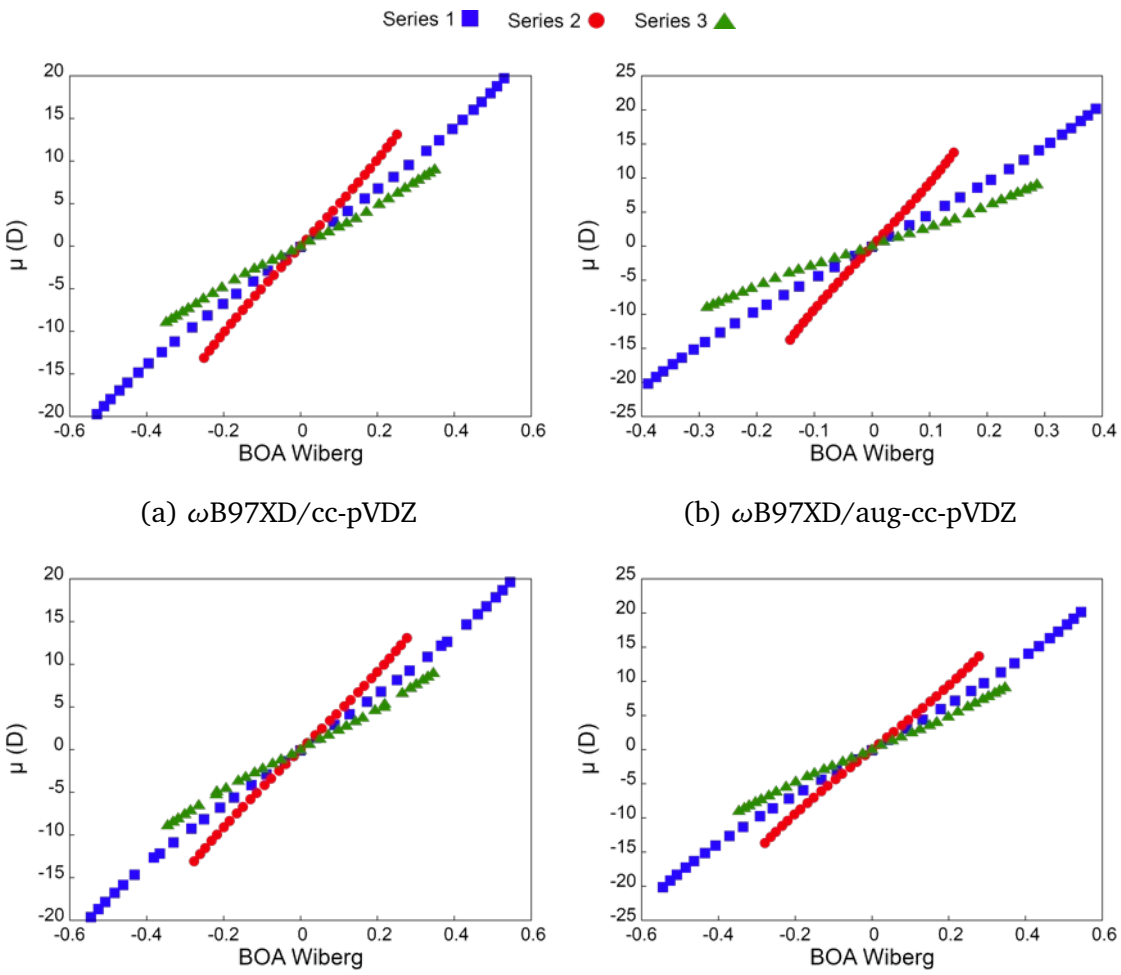

(a) ωB97XD/cc-pVDZ

(b) ωB97XD/aug-cc-pVDZ

(c) ωB97XD/6-31G(d,p)

(d) ωB97XD/ 6-31++G(d,p)

Figure A.50: Correlation of μ_x with BOA Wiberg for the the 9C-streptocyanine in Series 1, 2, 3, as obtained in the 4 studied levels of theory: Level 1 (a), Level 2 (a), Level 3 (a), Level 4 (a).

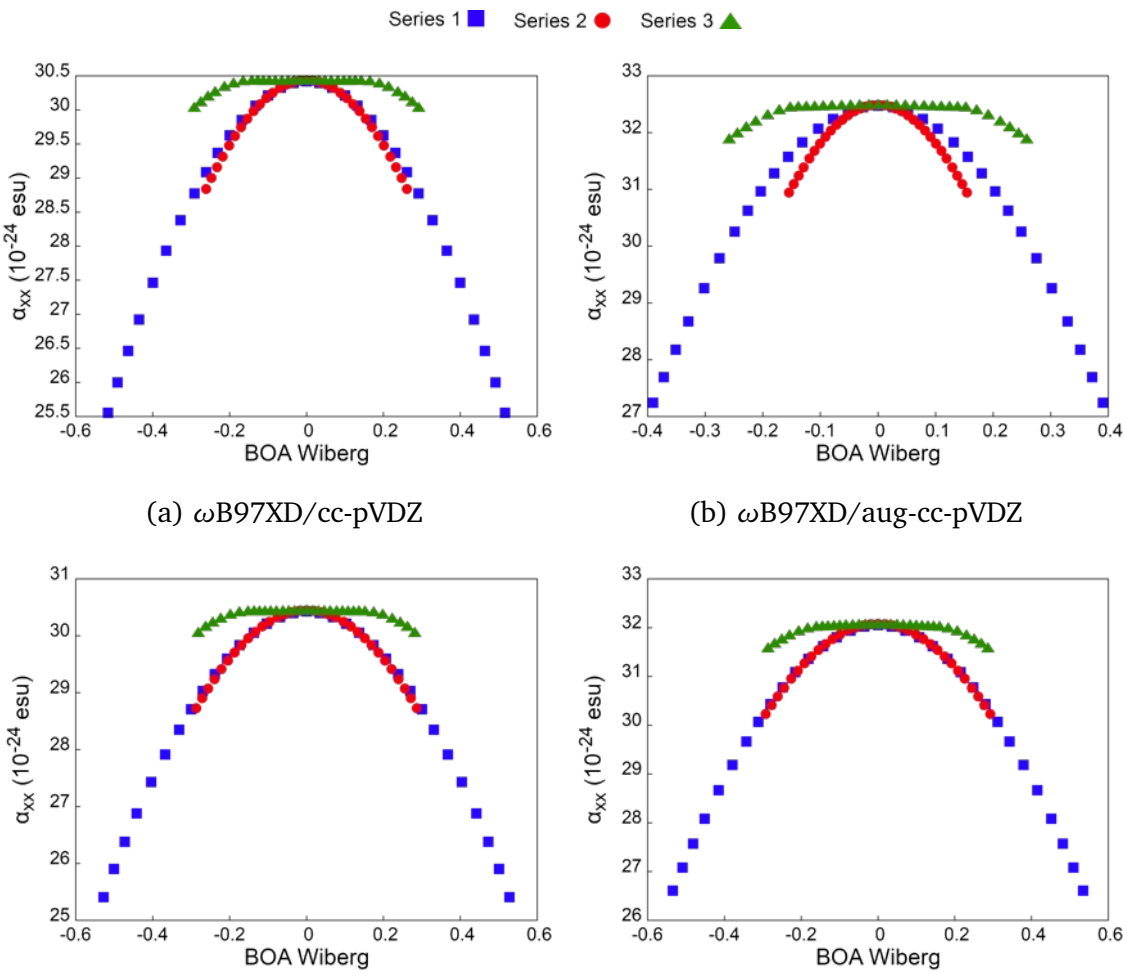

(a) ωB97XD/cc-pVDZ

(b) ωB97XD/aug-cc-pVDZ

(c) ωB97XD/6-31G(d,p)

(d) ωB97XD/ 6-31++G(d,p)

Figure A.51: Correlation of α_{xx} with BOA Wiberg for the the 5C-streptocyanine in Series 1, 2, 3, as obtained in the 4 studied levels of theory: Level 1 (a), Level 2 (a), Level 3 (a), Level 4 (a).

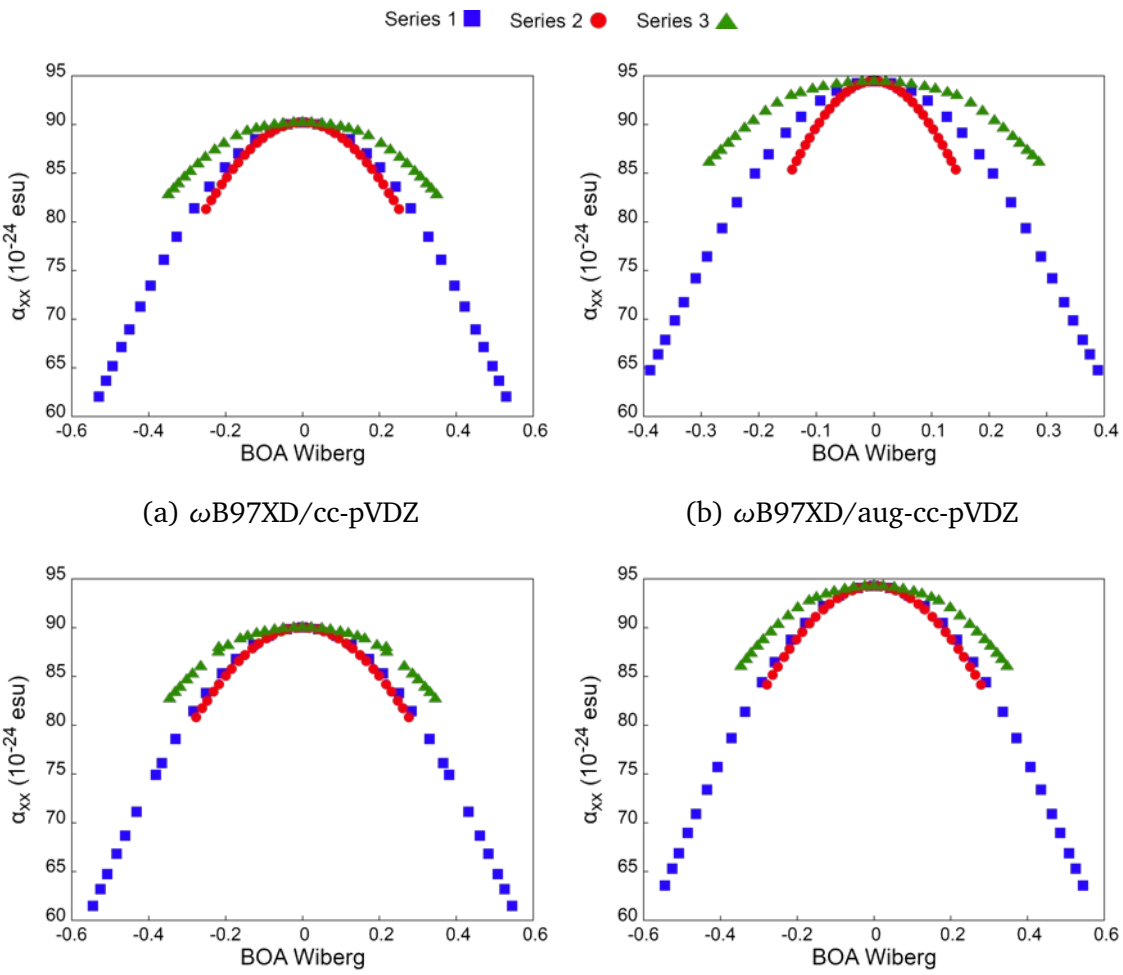

(a) ωB97XD/cc-pVDZ

(b) ωB97XD/aug-cc-pVDZ

(c) ωB97XD/6-31G(d,p)

(d) ωB97XD/ 6-31++G(d,p)

Figure A.52: Correlation of α_{xx} with BOA Wiberg for the the 9C-streptocyanine in Series 1, 2, 3, as obtained in the 4 studied levels of theory: Level 1 (a), Level 2 (a), Level 3 (a), Level 4 (a).

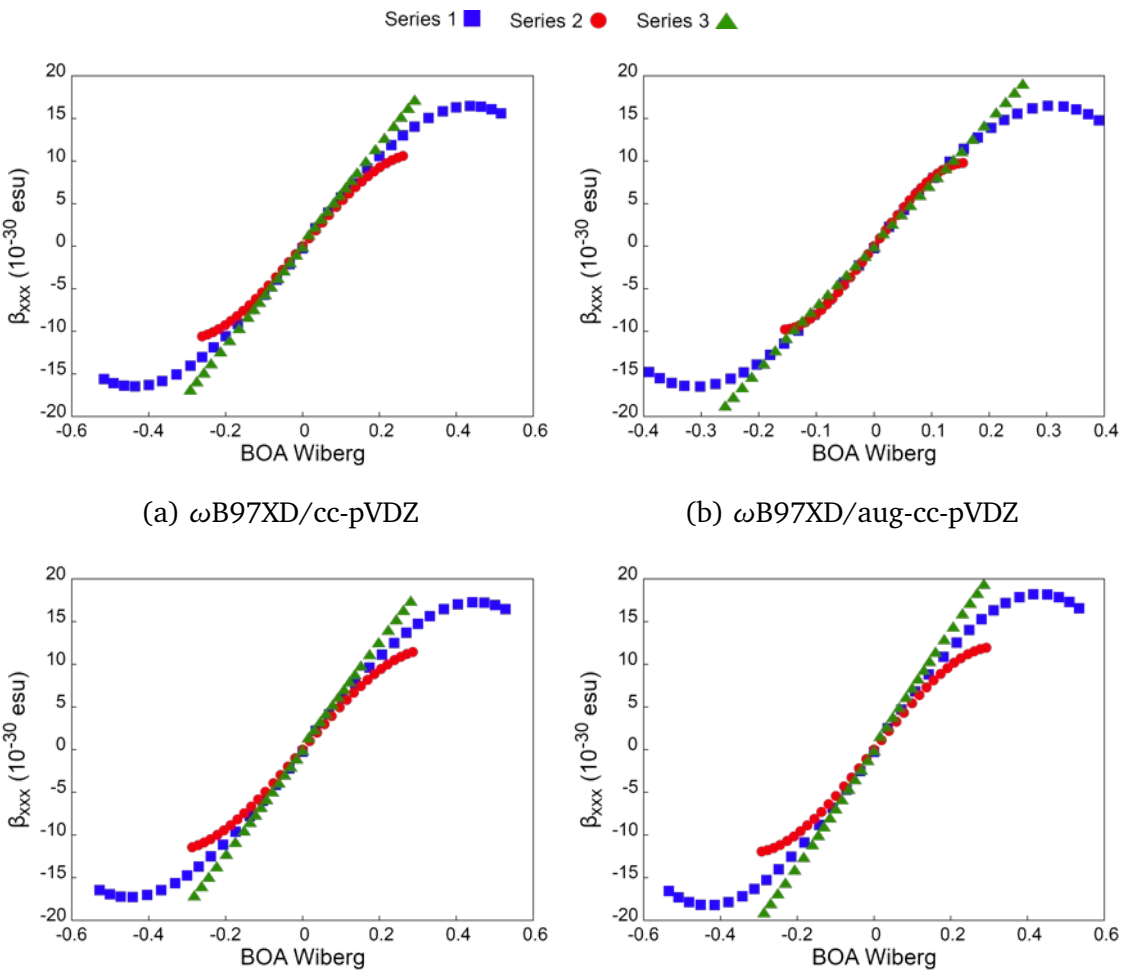

(a) ωB97XD/cc-pVDZ

(b) ωB97XD/aug-cc-pVDZ

(c) ωB97XD/6-31G(d,p)

(d) ωB97XD/ 6-31++G(d,p)

Figure A.53: Correlation of β_{xxx} with BOA Wiberg for the the 5C-streptocyanine in Series 1, 2, 3, as obtained in the 4 studied levels of theory: Level 1 (a), Level 2 (a), Level 3 (a), Level 4 (a).

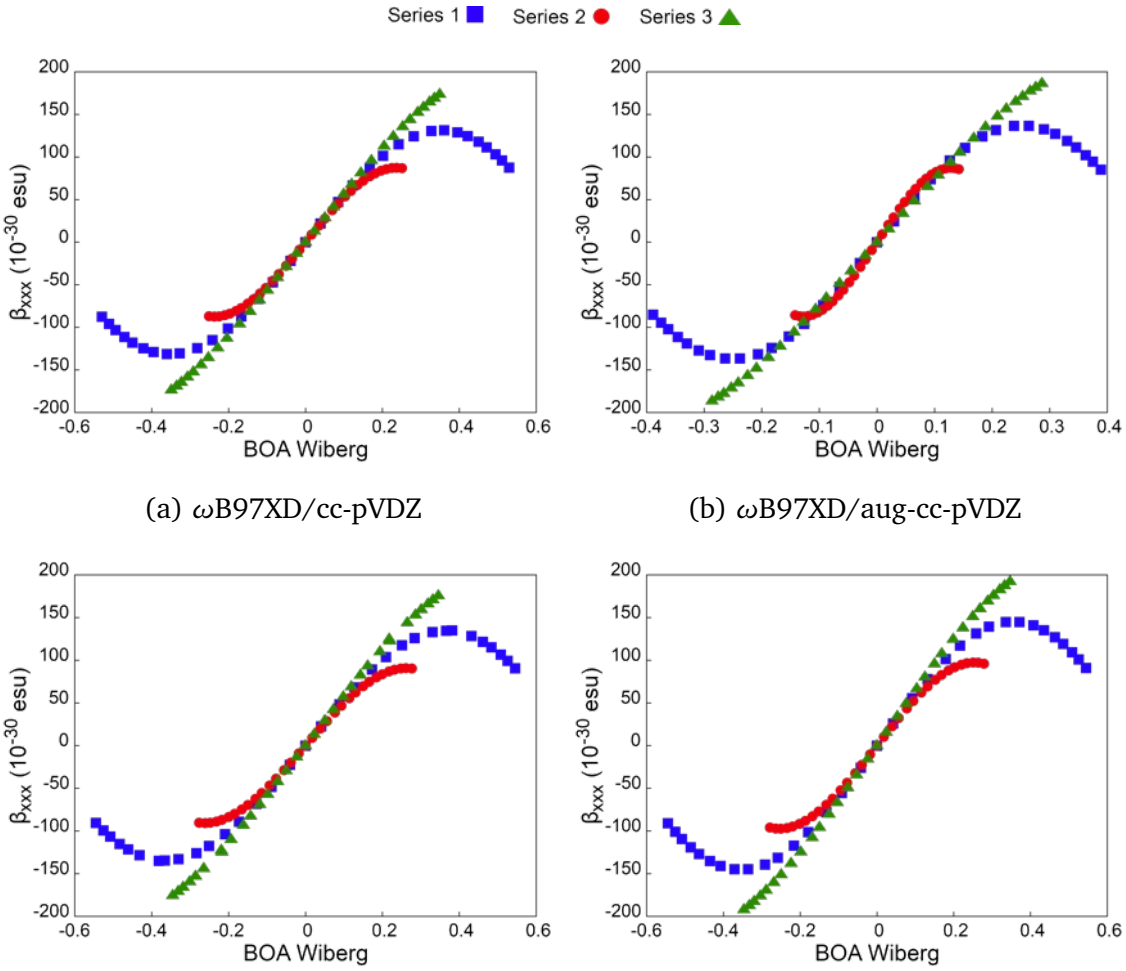

(a) ωB97XD/cc-pVDZ

(b) ωB97XD/aug-cc-pVDZ

(c) ωB97XD/6-31G(d,p)

(d) ωB97XD/ 6-31++G(d,p)

Figure A.54: Correlation of β_{xxx} with BOA Wiberg for the the 9C-streptocyanine in Series 1, 2, 3, as obtained in the 4 studied levels of theory: Level 1 (a), Level 2 (a), Level 3 (a), Level 4 (a).

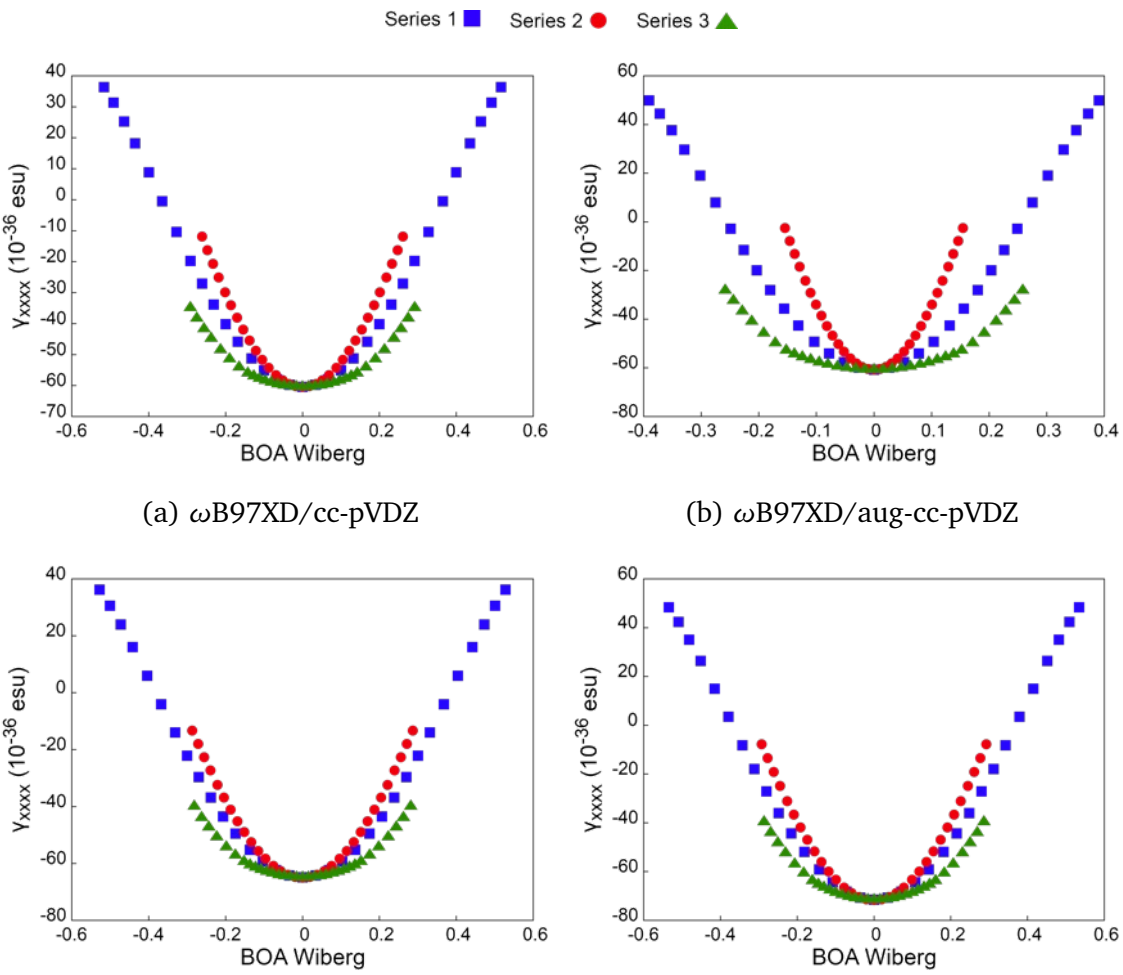

(a) ωB97XD/cc-pVDZ

(b) ωB97XD/aug-cc-pVDZ

(c) ωB97XD/6-31G(d,p)

(d) ωB97XD/ 6-31++G(d,p)

Figure A.55: Correlation of γ_{xxxx} with BOA Wiberg for the the 5C-streptocyanine in Series 1, 2, 3, as obtained in the 4 studied levels of theory: Level 1 (a), Level 2 (a), Level 3 (a), Level 4 (a).

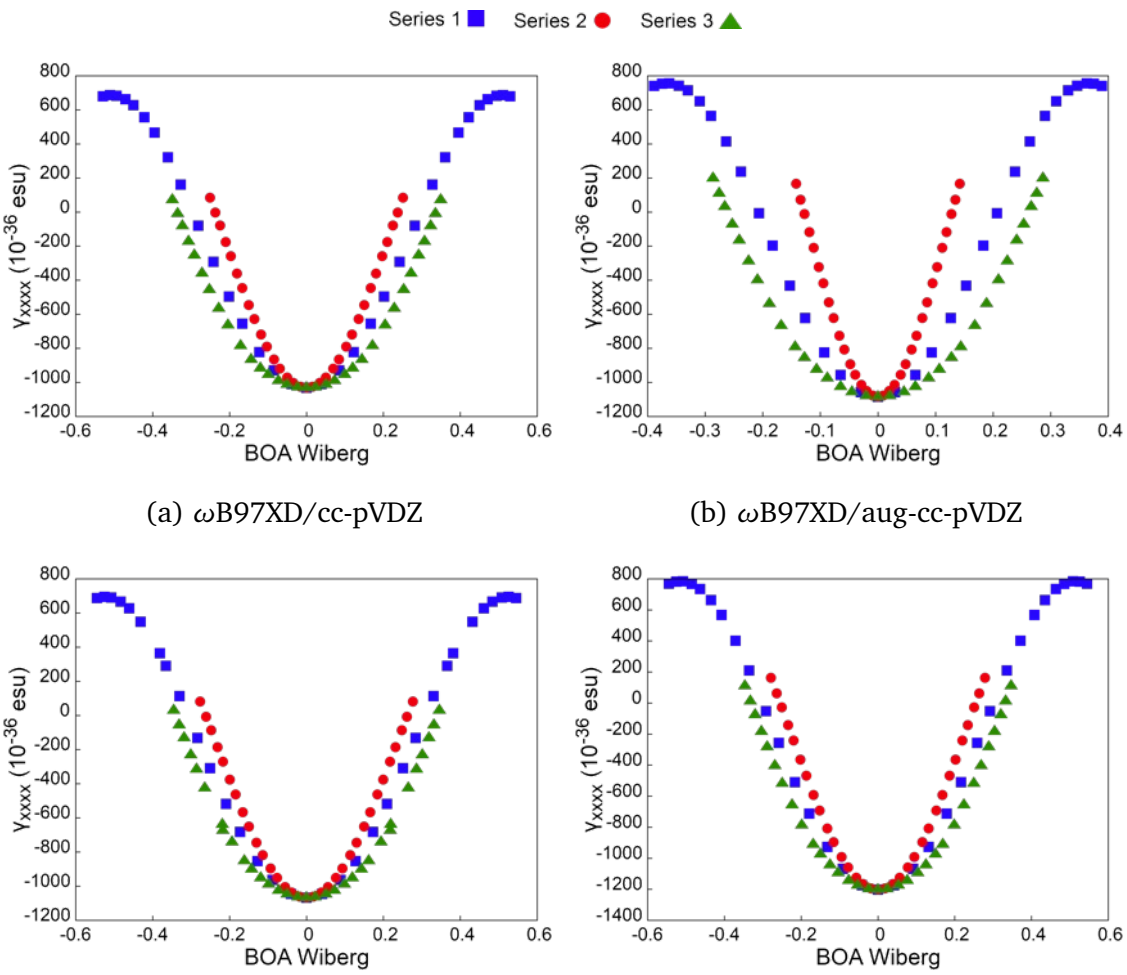

(a) ωB97XD/cc-pVDZ

(b) ωB97XD/aug-cc-pVDZ

(c) ωB97XD/6-31G(d,p)

(d) ωB97XD/ 6-31++G(d,p)

Figure A.56: Correlation of γ_{xxxx} with BOA Wiberg for the the 9C-streptocyanine in Series 1, 2, 3, as obtained in the 4 studied levels of theory: Level 1 (a), Level 2 (a), Level 3 (a), Level 4 (a).

Appendix B

Appendix: Publications and Scientific Events

B.1 Related to Thesis

Invited Speaker Critical Point Electron Density Alternation: A New Descriptor of Nonlinear Optical Properties of π-Conjugated Chromophores
II Symposium on Theoretical and Structural Chemistry (SQTEA)
2017

Published Paper Bond Ellipticity Alternation: An Accurate Descriptor of the Nonlinear Optical Properties of π-Conjugated Chromophores
The Journal of Physical Chemistry Letters
DOI: 10.1021/acs.jpclett.8b00478.
2018
Attached in this Appendix

B.2 Unrelated to Thesis

Congress Abstract Rational Synthesis and Photophysical Analysis of Fluorescents Chalcones: A Combined Theoretical and Experimental Study
V Simpósio de Estrutura Eletrônica e Dinâmica Molecular
2014

Congress Abstract DFT Study of Four New 2,1,3-Benzothiadiazole Derivatives Compounds
V Simpósio de Estrutura Eletrônica e Dinâmica Molecular
2014

Congress Abstract Síntese Racional, Estudo Teórico (DFT) e Avaliação Bioquímica de Chalconas Fluorescentes como Inibidores de *Cruzaina-Trypanosoma cruzi*
XXXVII Reunião Anual da Sociedade Brasileira de Química (SBQ)
2014

Published Paper Fotofísica Teórica (DFT) de Sondas Fluorescentes Benzotiadiazólicas
Revista Virtual de Química
DOI: 10.5935/1984-6835.20150018
2014

Congress Abstract TD-DFT Study of Chalcones with Potential Pharmacological Activity against Alzheimer's Disease
XVIII Simpoósio Brasileiro de Química Teórica (SBQT)
2015

Congress Abstract Substituent Effect in the Mesoionic Ring on Optical and Electric Properties of Mesoionics Compounds
XVIII Simpoósio Brasileiro de Química Teórica (SBQT)
2015

Published Paper Strong Solvent Effects on the Nonlinear Optical Properties of Z and E Isomers from Azo-Enaminone Derivatives
The Journal of Physical Chemistry C
DOI: 10.1021/acs.jpcc.6b01567
2016

THE JOURNAL OF PHYSICAL CHEMISTRY Letters
Letter
Cite This: J. Phys. Chem. Lett. 2018, 9, 1377−1383
pubs.acs.org/JPCL

Bond Ellipticity Alternation: An Accurate Descriptor of the Nonlinear Optical Properties of π-Conjugated Chromophores

Thiago O. Lopes,[†] Daniel F. Scalabrini Machado,[†] Chad Risko,[§] Jean-Luc Brédas,[*,‡] and Heibbe C. B. de Oliveira[*,†]

[†]Laboratório de Estrutura Eletrônica e Dinâmica Molecular (LEEDMOL), Institute of Chemistry, University of Brasília, Campus Darcy Ribeiro, Brasília, Brazil

[§]Department of Chemistry and Center for Applied Energy Research, University of Kentucky, Lexington, Kentucky 40506-0055, United States

[‡]School of Chemistry and Biochemistry and Center for Organic Photonics and Electronics, Georgia Institute of Technology, Atlanta, Georgia 30332-0400, United States

Supporting Information

ABSTRACT: Well-defined structure−property relationships offer a conceptual basis to afford a priori design principles to develop novel π-conjugated molecular and polymer materials for nonlinear optical (NLO) applications. Here, we introduce the bond ellipticity alternation (BEA) as a robust parameter to assess the NLO characteristics of organic chromophores and illustrate its effectiveness in the case of streptocyanines. BEA is based on the symmetry of the electron density, a physical observable that can be determined from experimental X-ray electron densities or from quantum-chemical calculations. Through comparisons to the well-established bond-length alternation and π-bond order alternation parameters, we demonstrate the generality of BEA to foreshadow NLO characteristics and underline that, in the case of large electric fields, BEA is a more reliable descriptor. Hence, this study introduces BEA as a prominent descriptor of organic chromophores of interest for NLO applications.

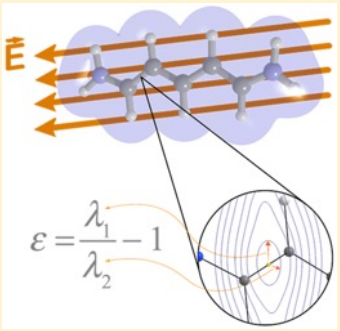

To design novel nonlinear optical (NLO) chromophores from first-principles, it is advantageous to rely on simple, yet robust, structure−function relationships. Marder and co-workers, for instance, described two important parameters, i.e., the bond length alternation (BLA) and bond order alternation (BOA) patterns,[1,2] to rationalize the molecular NLO response and guide the synthesis of efficient NLO chromophores. These authors established both experimentally and theoretically that, because a direct relationship can be found between BLA or BOA and the electric field applied to the molecule, (i) the electric field evolution of the molecular dipole moment μ can be expressed as a function of BLA or BOA and (ii) the first-order (α), second-order (β), and third-order (γ) polarizabilities can be described as derivatives at successive orders of μ versus BLA or BOA.[1,3]

While in many instances BLA correlates well with the electronic[4] and photonic properties,[5] it has been recently reported that this correlation breaks down when the molecular structures are simulated in a dielectric medium.[6] This issue was further investigated and rationalized by highlighting the limitations of BLA when considering molecular geometries away from equilibrium.[7] On the other hand, even when the molecular structure is studied in complex environments (e.g., implicit and explicit solvents, strong electric fields, etc.), BOA is found to be a more reliable parameter to analyze changes in NLO properties.[7]

The concept of bond order is a fundamental chemical concept that can be intuitively related to covalent chemical bonds and associated with structure−property relationships. Several orbital-based population analyses, such as those advanced by Mulliken,[8] Wiberg,[9] and Mayer,[10] have been proposed to estimate BOA. The Mulliken bond order may be understood as a measure of the population overlap between two atoms; however, a major drawback is that it is strongly basis-set dependent.[11] The Wiberg bond order is based on the squared density matrix, which is useful when the atomic orbital basis forms an orthonormal set, such as in the case of semiempirical methods. The Mayer bond order is an extension of the Wiberg definition in the context of ab initio molecular orbital theories.[11] Notably, these orbital-based population analyses are founded on somewhat arbitrary partitioning of density matrixes and are intimately associated with basis set orthonormalization;[12] when dealing with situations for which the use of diffuse orbitals is required, these methods can become inadequate.

Our objective is to find a robust yet simple bond descriptor that overcomes these problems. To this end, we have exploited the quantum theory of atoms in molecules (QTAIM). QTAIM

Received: February 13, 2018
Accepted: March 2, 2018
Published: March 2, 2018

DOI: 10.1021/acs.jpclett.8b00478
J. Phys. Chem. Lett. 2018, 9, 1377−1383

The Journal of Physical Chemistry Letters Letter

relies on the electron density, $\rho(\mathbf{r})$, as a fundamental physical observable.[13] On the basis of the density gradient zero-flux condition, the real space is partitioned into nonoverlapping atomic domains or atomic basins. QTAIM properties are computed from a topological analysis, provided that the electron density is known either from experimental (e.g., X-ray diffraction) measurements or from quantum-mechanical calculations [based either on wave function approximations or on density functional theory (DFT)].[14] It is useful to note that, in the QTAIM approach, every topological peculiarity of $\rho(\mathbf{r})$ (maximum, minimum, saddle point) is associated with a particular point in space, referred to as a critical point, where the gradient of $\rho(\mathbf{r})$ vanishes.[13] These critical points of the electron density define points in space related to nuclei, bonds, rings, and cages based on the rank (number of nonzero curvatures, or eigenvalues of $\rho(\mathbf{r})$ at the critical point) and the signature (the algebraic sum of the of the curvatures) of the Hessian matrix.[15] For instance, between any pair of nuclei deemed to be chemically bonded, i.e., the bond critical point (BCP), there occurs a saddle point, where two curvatures are negative and one is positive, giving rise to a critical point of rank 3 and signature −1.

Within QTAIM, the ellipticity of the electron density has been employed to characterize electrocyclic reactions, owing to its ability to capture the changes in the anisotropy of the electron density at the BCP,[15] or to clarify the nature of intermolecular interactions.[16,17] The bond ellipticity (ε) is defined in terms of the cylindricity of the electron density at the BCP, accounting for its principal curvatures (eigenvalues of the Hessian matrix, λ_1, λ_2, and λ_3, such that λ_1 and λ_2 are the negative eigenvalues) and is written as $\varepsilon = \lambda_1/\lambda_2 - 1$. The negative eigenvalues of the Hessian of the electron density ($\nabla^2\rho(\mathbf{r})$) at the BCP are degenerate when the axes associated with the respective curvatures are symmetrically equivalent, as in the single CC bond of ethane (i.e., $\lambda_1 = \lambda_2$ and $\varepsilon = 0$) (Figure 1). The ellipticity, therefore, provides a quantitative generalization of the concept of σ and π bond character, i.e., ε measures the extent to which the electron density is preferentially distributed in a particular plane containing the bond axis.[18] Illustrations in the case of the ethane and ethene hydrocarbons are given in Figure 1. The electron density distribution at the BCP can be isotropic (the curvatures perpendicular to the internuclear axis are the same, $\lambda_1 = \lambda_2$) or anisotropic ($\lambda_1 \neq \lambda_2$). For the CC bond in ethane (σ-character), the cylindric distribution of $\rho(\mathbf{r})$ around the internuclear axis has the same curvature, so the ellipticity vanishes. For CC bonds with π-character, such as in ethene, the curvature λ_2 associated with the π-direction is larger than λ_1 and ε is greater than zero.[18] As noted by Scherer and co-workers,[19] positive values of ε indicate π character in a bond; also, these authors showed that ε provides an experimentally observable criterion to assess the extent of delocalization, with a close agreement between experiment and theory.

Both geometric and electronic changes are of great importance when correlating BLA or BOA with the NLO response in the presence of strong electric fields.[7] The QTAIM bond ellipticity, hence, can potentially serve as a useful approach to analyze the effects of variations in π-bond localization−delocalization in unsaturated carbon chains, because $\rho(\mathbf{r})$ is the only quantity required to define the topological analysis. Here, we demonstrate that a general bond descriptor based on the ellipticity at the BCP can be used to predict the evolution of the electric dipole moment (μ), linear

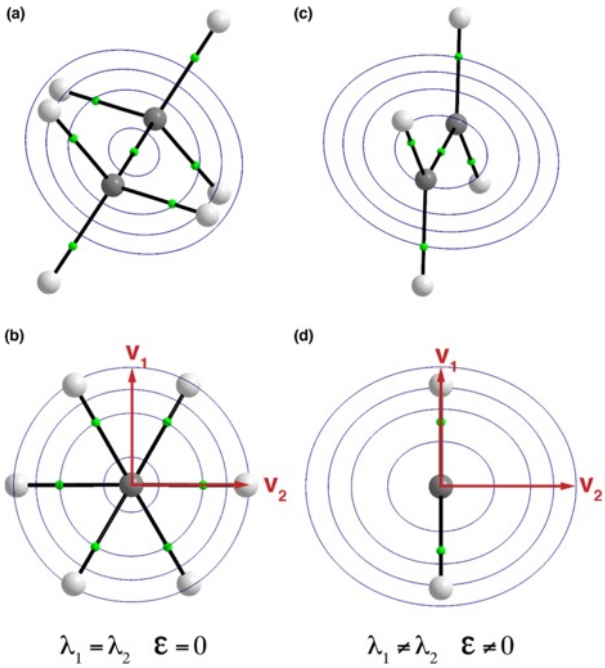

Figure 1. Qualitative contour lines of $\rho(\mathbf{r})$ in the plane that contains the bond critical point (BCP) along the CC bond for ethane (a and b) and ethene (c and d) along the eigenvectors $\mathbf{V}_1$ and $\mathbf{V}_2$ (the major axes) of the Hessian matrix $\nabla^2\rho(\mathbf{r})$, whose eigenvalues, λ_1 and λ_2, respectively, are used to calculate the ellipticity at the BCP. The CC single bond in ethane is cylindrically symmetric resulting in $\varepsilon = 0$, while for the CC double bond in ethene, the ε value is positive.

polarizability (α), and second- (β) and third-order (γ) polarizabilities with applied electric field. We refer to this parameter as the bond ellipticity alternation (BEA); it is defined in Scheme 1, along with the conventional NLO descriptors

Scheme 1. Chemical Structures of the Five-Carbon (5C) and Nine-Carbon (9C) Streptocyanines and Definition of the Bond Alternation Parameters

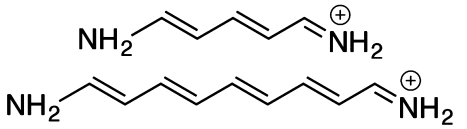

Bond Property Alternation (BPA)

$$BPA = \left\langle \text{Mean of single-bond property} \right\rangle - \left\langle \text{Mean of double-bond property} \right\rangle$$

where P = E, O, L, stands for Ellipticity, Order and Length, respectively

BLA and BOA. We find that the bond ellipticities along the molecular backbone when large electric fields are applied describe the chemically intuitive distribution of charge, especially when a diffuse basis set is employed, to a much better extent than BOA.

In the spirit of ref 7, we evaluate the performance of BEA versus BOA as a descriptor of electronic and NLO properties of two representative NLO chromophores, the 5- and 9-carbon streptocyanines (Scheme 1), by carrying out the following three series of calculations: In series 1, an electric field is applied along the longitudinal axis, and the molecular geometry is fully

DOI: 10.1021/acs.jpclett.8b00478
J. Phys. Chem. Lett. 2018, 9, 1377−1383

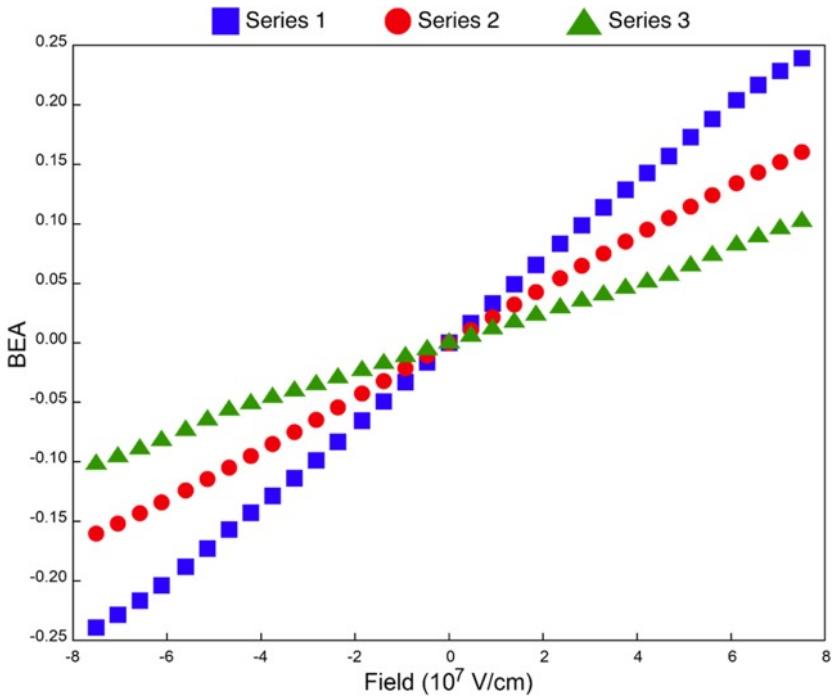

Figure 2. Evolution of bond-ellipticity alternation (BEA) as a function of applied electric field along the molecular axis for the 5C streptocyanine in series 1, 2, and 3, as obtained at the ωB97XD/6-31++G(d,p) level of theory.

optimized for each value of the electric field; this series accounts for both electronic and geometric effects on the streptocyanine NLO properties. In series 2, an electric field is applied along the longitudinal direction as in series 1, but the molecular structure is constrained to the C_{2v} point group; in this instance, only the electronic contributions to the NLO properties emerge. In series 3, based on the geometries obtained in series 1, single-point calculations are performed in the absence of any external electric field; here, only the geometric contributions are taken into account. The robustness and reliability of the alternation parameters can be assessed by examining whether the evolutions of μ, α, β, and γ versus the bond property alternation (BPA; P = E [ellipticity], O [order], L [length]) parameters (Scheme 1) are consistent across the three series of calculations. Note that we do not include BLA in the remainder of our discussion because, as we pointed out above, BLA is appropriate only when optimized geometries are considered,[7] which is not the case in series 2 and 3.

All DFT calculations were performed using the long-range corrected hybrid functional ωB97XD. To assess the impact of diffuse functions (which are generally needed in the case of large external electric fields), we used both 6-31G(d,p) and 6-31++G(d,p) basis sets. For the 5-carbon streptocyanine, the applied electric fields ranged from −7.5 to +7.5 × 10^7V/cm, and for the 9-carbon streptocyanine from −4.5 to +4.5 × 10^7V/cm (i.e., similar to those in ref 7). The NLO properties were computed by means of the coupled perturbed Kohn−Sham (CPKS) method.[20] The bond ellipticities at the critical point were computed with the "AIMAll" software package.[21] Different bond order definitions were considered to evaluate BOA and compare it with BEA: Mulliken[8] (BOA Mulliken), Wiberg[9] (BOA Wiberg), and Mayer[10] (BOA Mayer). These bond orders were calculated using the "Multiwfn" software package.[22]

The results in ref 7 highlighted that an electronic parameter is preferable over a geometric parameter when the molecular structure is driven away from equilibrium. It is important to bear in mind that because BEA originates from the electronic density, it adapts to the environment where the chromophore is embedded, even when the molecular geometry is fixed (series 3); on the other hand, bond order definitions consider the local atomic orbital coefficients between the two atoms involved in the chemical bonds. Consequently, the environmental effects are treated explicitly in BEA and only implicitly in BOA.

We first determine the evolution of BEA with the applied external electric field across the three series, using a diffuse basis set, for the 5-carbon streptocyanine. The evolution, see Figure 2, fully confirms what has been shown in refs 1 and 2: In the absence of field, there is no BEA along the backbone (BEA = 0), which is the expression of the cyanine limit (where the charge distribution is identical around the two end groups).[23−25] Upon applying an electric field, the molecular structure tends toward the polyene limit and BEA increases accordingly. At the polyene limit, for series 1 (blue squares in Figure 2), BEA reaches ±0.24. For the sake of comparison, at the same limit, BLA reaches ±0.1 Å and BOA reaches ± 0.65.[7,25] In series 2 (red circles in Figure 2), where the geometric structure remains fixed (C_{2v}), BEA at each electric-field strength is ∼67% of the corresponding value in series 1. In series 3 (green triangles in Figure 2), BEA reaches ∼43% of the value when the electric field is present. The relative percentages observed for series 2 and 3 are similar to those obtained with BOA (Mulliken) in ref 7, pointing to the ability of BEA to distinguish the geometric and electronic effects on the NLO response.

Having established the correlation of BEA with the applied electric field in the 5C-streptocyanine, we now turn to the relationships between the longitudinal component of dipole

DOI: 10.1021/acs.jpclett.8b00478
J. Phys. Chem. Lett. 2018, 9, 1377−1383

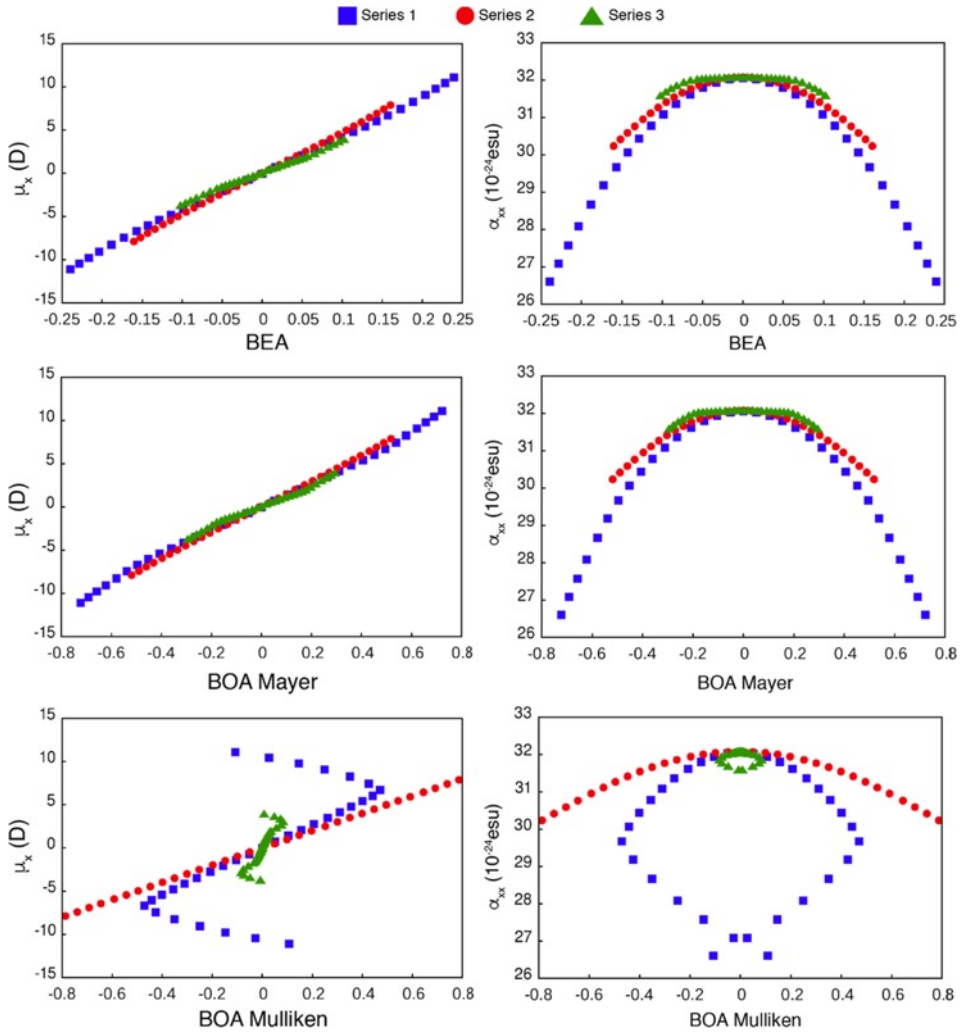

Figure 3. Correlation of μ_x and α_{xx} with BEA, BOA Mayer, and BOA Mulliken for the 5C streptocyanine in series 1, 2, and 3, as obtained at the ωB97XD/6-31++G(d,p) level of theory.

moment (μ_x) and BEA, BOA Mayer, BOA Wiberg, or BOA Mulliken (Figure 3, see also Figures S1–S5). The dipole moment evolves nearly linearly with BEA,[26] with the evolution becoming stronger toward the polyene limit. The behavior is similar to BOA Mayer but becomes erratic with BOA Wiberg when the molecular structure is not in equilibrium (see Figure S5). Figure 3 also illustrates how poorly BOA Mulliken performs when diffuse basis functions are included (while it works well in their absence, see Figure S3).

The ability to describe the μ_x evolution in the presence of an electric field through the BEA or BOA Mayer parameters translates into reliable evolutions of the polarizabilities at various orders (see Figure 3 for α_{xx} and Figure 4 for β_{xxx} and γ_{xxxx}). The α_{xx} value versus BEA peaks at the cyanine limit and decreases toward the polyene limit while (as expected from the derivative relationships) β_{xxx} goes through zero and γ_{xxxx} peaks at negative values at the cyanine limit. The evolution versus BOA Mulliken when using a diffuse basis set breaks down as soon as the molecular structure can change in series 1 and 3.

We also considered a longer molecular chain, the 9-carbon streptocyanine (Scheme 1). The evolutions of α_{xx} and γ_{xxxx} with BEA and BOA Mayer are illustrated in Figure 5. The behavior versus BEA is observed to be more consistent across the three series than versus BOA Mayer.

The preceding discussion demonstrates that BEA provides a very good correlation with a variety of NLO properties for the streptocyanines and is generally superior to BOA and BLA. To gain a deeper understanding, we compare directly in Figure 6 the bond orders and bond ellipticities (ε) for 9C as a function of (i) basis set and (ii) applied electric field.

Starting with no electric field, the bond orders and ellipticities follow a similar (cyanine-like) pattern for both basis sets considered, either without [6-31G(d,p)] or with [6-31++G(d,p)] diffuse functions. We do note that, when comparing the results as a function of the basis sets in this scenario, the bond orders overall show more variation than the ellipticities.

The situation becomes more problematic for the bond orders when a strong electric field (4.5×10^7 V/cm) is applied. Here, the electric field is directed such that the field vector points right-to-left with respect to the representations of 9C depicted in Figure 6; hence, one would expect the charge to localize on the left-most amine group and the single-bond–double-bond pattern to become less pronounced as one moves along the

DOI: 10.1021/acs.jpclett.8b00478
J. Phys. Chem. Lett. 2018, 9, 1377–1383

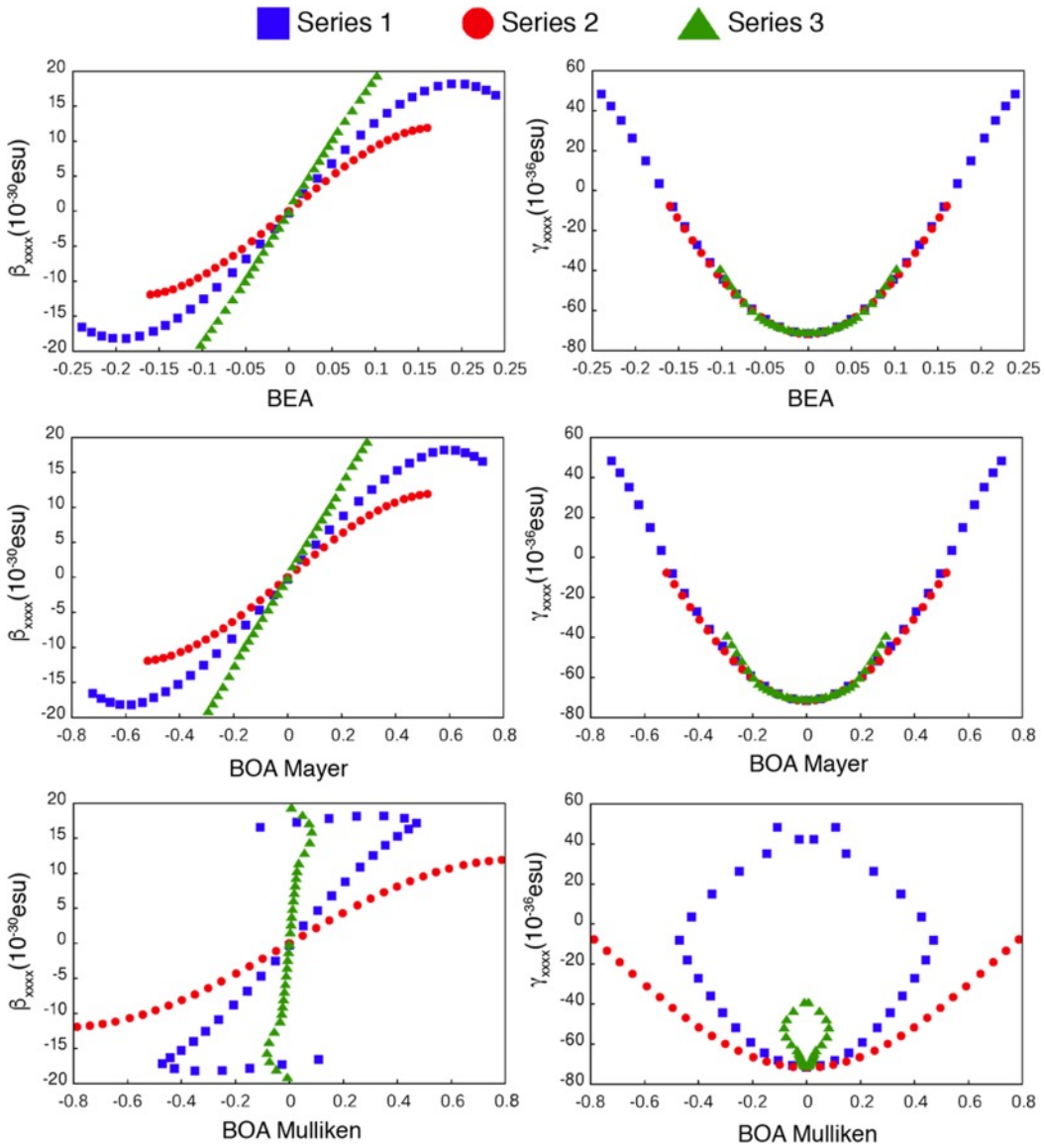

Figure 4. Correlation of β_{xxx} and γ_{xxxx} with BEA, BOA Mayer, and BOA Mulliken for the 5C streptocyanine in series 1, 2, and 3, as obtained at the ωB97XD/6-31++G(d,p) level of theory.

chain in the same direction. The ellipticities show this pattern exactly, regardless of the basis set used. The bond orders, on the other hand, show an inconsistent representation and wide variation as a function of the basis set. As BOA and BEA are both computed from average differences on adjacent bonds (Scheme 1), the generally good performance of BOA in the preceding analysis of the NLO properties appears to be a fortunate result of error cancelation, whereas for BEA the good correlation with the NLO properties does not rely on such serendipity. These results demonstrate that BEA is a reliable and simple parameter applicable to the rational design of NLO materials. We are currently carrying out additional studies to assess BEA performance in explicit solvation treatments for NLO properties and extending the set of molecules and levels of calculations.

Here, we have introduced a new structure−property parameter, based on bond ellipticity alternation, BEA, to describe the evolutions of the electric dipole moment (μ_x), linear polarizability (α_{xx}), and higher-order polarizabilities (β_{xxx} and γ_{xxxx}) as a function of an applied external field. We applied the methodology to the 5-carbon and 9-carbon streptocyanines and assessed the ability of BEA to predict the NLO properties when considering molecular geometries away from equilibrium. From our results, we can draw the following conclusions:

(i) BEA performs much better than BOA Mulliken and BOA Wiberg, especially when a diffuse basis set is employed (6-31++G(d,p); BOA Mayer performs as well as BEA in describing the evolution of μ_x and α_{xx}, but the results slightly deteriorated for β_{xxx} and γ_{xxxx} when using larger basis functions.

(ii) For larger polymethine chains such as 9C-streptocyanine, BEA is more consistent than BOA Mayer for the molecular polarizabilities α_{xx}, β_{xxx}, and γ_{xxxx} across the three series. These results underline that BEA is a more reliable structure−function

DOI: 10.1021/acs.jpclett.8b00478
J. Phys. Chem. Lett. 2018, 9, 1377−1383

The Journal of Physical Chemistry Letters Letter

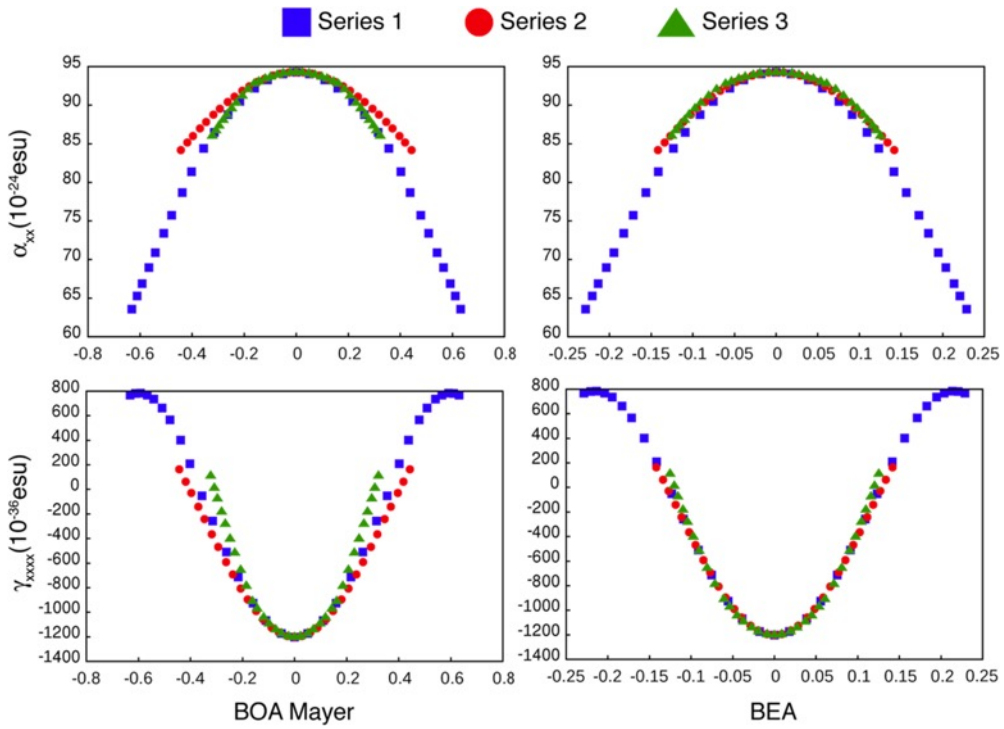

Figure 5. Correlation of α_{xx} (upper panel) and γ_{xxxx} (lower panel) with BEA and BOA Mayer for the 9C streptocyanines in series 1, 2, and 3, as obtained at the ωB97XD/6-31++G(d,p) level of theory.

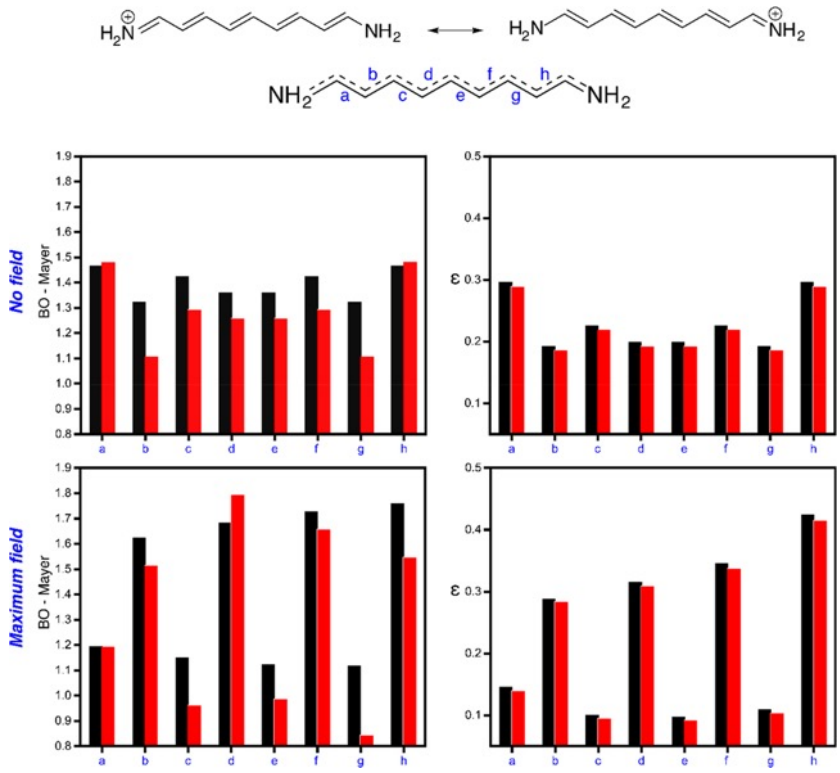

Figure 6. Dominant resonance structures in the 9C streptocyanine in the absence of electric field (top). The CC bonds are labeled *a* through *h*. Absolute bond orders (left) and bond ellipticities (right) with no electric field (top), and upon application (bottom) of an electric field of 4.5×10^7 V/cm oriented in such a way that the positive charge locates to the left side of the molecule (left resonance structure). Results obtained at the ωB97XD/6-31G(d,p) (black bars) and ωB97XD/6-31++G(d,p) (red bars) levels.

DOI: 10.1021/acs.jpclett.8b00478
J. Phys. Chem. Lett. 2018, 9, 1377−1383

The Journal of Physical Chemistry Letters Letter

parameter especially in the cases when diffuse basis sets become important.

(iii) Bond ellipticities across the molecular structure provide a good description of the chemically intuitive resonance forms when large external electric fields are applied along the longitudinal axis. Bond orders, on the other hand, display a more elusive pattern in the same conditions, suggesting that BOA's performance results from error cancelation whereas BEA portrays a consistent behavior regardless of the specific conditions of the system.

■ ASSOCIATED CONTENT

Supporting Information

The Supporting Information is available free of charge on the ACS Publications website at DOI: 10.1021/acs.jpclett.8b00478.

Additional calculations for 5C streptocyanine as obtained at the ωB97XD/6-31G(d,p) level of theory and NLO properties evolution with BOA Mayer (PDF)

■ AUTHOR INFORMATION

Corresponding Authors

*E-mail: jean-luc.bredas@chemistry.gatech.edu.
*E-mail: heibbe@unb.br.

ORCID

Chad Risko: 0000-0001-9838-5233
Jean-Luc Brédas: 0000-0001-7278-4471

Notes

The authors declare no competing financial interest.

■ ACKNOWLEDGMENTS

The work at University of Brasília was funded by Conselho Nacional de Desenvolvimento Científico e Tecnológico (CNPq) and Coordenação de Aperfeiçoamento Pessoal de Nível Superior (CAPES). The work at the University of Kentucky was supported in part by start-up funds provided to C.R. by University of Kentucky Vice President for Research. The work at Georgia Tech was supported by the Georgia Research Alliance. We are grateful to Dr. Veaceslav Coropceanu, Dr. Rebecca Gieseking, and Dr. Valter Henrique Carvalho-Silva for stimulating discussions.

■ REFERENCES

(1) Marder, S. R.; Gorman, C. B.; Meyers, F.; Perry, J. W.; Bourhill, G.; Brédas, J.-L.; Pierce, B. M. A Unified Description of Linear and Nonlinear Polarization in Organic Polymethine Dyes. *Science (Washington, DC, U. S.)* **1994**, *265* (5172), 632−635.

(2) Gorman, C. B.; Marder, S. R. An Investigation of the Interrelationships between Linear and Nonlinear Polarizabilities and Bond-Length Alternation in Conjugated Organic Molecules. *Proc. Natl. Acad. Sci. U. S. A.* **1993**, *90* (23), 11297−11301.

(3) Bourhill, G.; Bredas, J.-L.; Cheng, L.-T.; Marder, S. R.; Meyers, F.; Perry, J. W.; Tiemann, B. G. Experimental Demonstration of the Dependence of the First Hyperpolarizability of Donor-Acceptor-Substituted Polyenes on the Ground-State Polarization and Bond Length Alternation. *J. Am. Chem. Soc.* **1994**, *116* (6), 2619−2620.

(4) Brédas, J. L. Relationship between Band Gap and Bond Length Alternation in Organic Conjugated Polymers. *J. Chem. Phys.* **1985**, *82* (8), 3808−3811.

(5) Drobizhev, M.; Hughes, T. E.; Stepanenko, Y.; Wnuk, P.; O'Donnell, K.; Scott, J. N.; Callis, P. R.; Mikhaylov, A.; Dokken, L.; Rebane, A. Primary Role of the Chromophore Bond Length Alternation in Reversible Photoconversion of Red Fluorescence Proteins. *Sci. Rep.* **2012**, *2*, 688.

(6) Murugan, N. A.; Kongsted, J.; Rinkevicius; Agren, H. Breakdown of the First Hyperpolarizability/bond-Length Alternation Parameter Relationship. *Proc. Natl. Acad. Sci. U. S. A.* **2010**, *107* (38), 16453−16458.

(7) Gieseking, R. L.; Risko, C.; Brédas, J.-L. Distinguishing the Effects of Bond-Length Alternation versus Bond-Order Alternation on the Nonlinear Optical Properties of π-Conjugated Chromophores. *J. Phys. Chem. Lett.* **2015**, *6* (12), 2158−2162.

(8) Mulliken, R. S. Electronic Population Analysis on LCAO-MO Molecular Wave Functions. IV. Bonding and Antibonding in LCAO and Valence-Bond Theories. *J. Chem. Phys.* **1955**, *23* (12), 2343−2346.

(9) Wiberg, K. B. Application of the Pople-Santry-Segal CNDO Method to the Cyclopropylcarbinyl and Cyclobutyl Cation and to Bicyclobutane. *Tetrahedron* **1968**, *24* (3), 1083−1096.

(10) Mayer, I. Charge, Bond Order and Valence in the AB Initio SCF Theory. *Chem. Phys. Lett.* **1983**, *97* (3), 270−274.

(11) Bridgeman, A. J.; Cavigliasso, G.; Ireland, L. R.; Rothery, J. The Mayer Bond Order as a Tool in Inorganic Chemistry. *J. Chem. Soc. Dalt. Trans.* **2001**, No. 14, 2095−2108.

(12) Mayer, I. Bond Order and Valence Indices: A Personal Account. *J. Comput. Chem.* **2007**, *28* (1), 204−221.

(13) Bader, R. F. W. *Atoms in Molecules: A Quantum Theory*; Clarendon Press: Oxford, 1990.

(14) Macchi, P. The Future of Topological Analysis in Experimental Charge-Density Research. *Acta Crystallogr., Sect. B: Struct. Sci., Cryst. Eng. Mater.* **2017**, *73* (3), 330−336.

(15) López, C. S.; Faza, O. N.; Cossío, F. P.; York, D. M.; de Lera, A. R. Ellipticity: A Convenient Tool To Characterize Electrocyclic Reactions. *Chem. - Eur. J.* **2005**, *11* (6), 1734−1738.

(16) Mota, A. A. R.; Gatto, C. C.; Machado, G.; de Oliveira, H. C. B.; Fasciotti, M.; Bianchi, O.; Eberlin, M. N.; Neto, B. A. D. Structural Organization and Supramolecular Interactions of the Task-Specific Ionic Liquid 1-Methyl-3-Carboxymethylimidazolium Chloride: Solid, Solution, and Gas Phase Structures. *J. Phys. Chem. C* **2014**, *118* (31), 17878−17889.

(17) Neto, B. A. D.; Mota, A. A. R.; Gatto, C. C.; Machado, G.; Fasciotti, M.; de Oliveira, H. C. B.; Ferreira, D. A. C.; Bianchi, O.; Eberlin, M. N. Solid, Solution and Gas Phase Interactions of an Imidazolium-Based Task-Specific Ionic Liquid Derived from Natural Kojic Acid. *J. Braz. Chem. Soc.* **2014**, *25* (12), 2280−2294.

(18) Bader, R. F. W.; Slee, T. S.; Cremer, D.; Kraka, E. Description of Conjugation and Hyperconjugation in Terms of Electron Distributions. *J. Am. Chem. Soc.* **1983**, *105* (15), 5061−5068.

(19) Scherer, W.; Sirsch, P.; Shorokhov, D.; Tafipolsky, M.; McGrady, G. S.; Gullo, E. Valence Charge Concentrations, Electron Delocalization And β-Agostic Bonding in d0Metal Alkyl Complexes. *Chem. - Eur. J.* **2003**, *9* (24), 6057−6070.

(20) Ferrero, M.; Rérat, M.; Orlando, R.; Dovesi, R.; Bush, I. J. Coupled Perturbed Kohn-Sham Calculation of Static Polarizabilities of Periodic Compounds. *J. Phys. Conf. Ser.* **2008**, *117*, 012016.

(21) Keith, T. A. *AIMAll* (Version 17.11.14); TK Gristmill Software: Overland Park, KS, USA, 2015.

(22) Lu, T.; Chen, F. Multiwfn: A Multifunctional Wavefunction Analyzer. *J. Comput. Chem.* **2012**, *33* (5), 580−592.

(23) Ohira, S.; Hales, J. M.; Thorley, K. J.; Anderson, H. L.; Perry, J. W.; Brédas, J.-L. A New Class of Cyanine-like Dyes with Large Bond-Length Alternation. *J. Am. Chem. Soc.* **2009**, *131* (17), 6099−6101.

(24) Jacquemin, D. New Cyanine Dyes or Not? Theoretical Insights for Model Chains. *J. Phys. Chem. A* **2011**, *115* (11), 2442−2445.

(25) Meyers, F.; Marder, S. R.; Pierce, B. M.; Bredas, J. L. Electric Field Modulated Nonlinear Optical Properties of Donor-Acceptor Polyenes: Sum-Over-States Investigation of the Relationship between Molecular Polarizabilities (.alpha., .beta., and .gamma.) and Bond Length Alternation. *J. Am. Chem. Soc.* **1994**, *116* (23), 10703−10714.

(26) We have selected the molecular center of mass as the origin to compute the dipole moment.

DOI: 10.1021/acs.jpclett.8b00478
J. Phys. Chem. Lett. 2018, 9, 1377−1383

Appendix C

Appendix: Home-made Codes used to Process de Results

C.0.1 File: processResults.py

```
#################################################################
# Python file header
__author__ = "Thiago Lopes"
__GitHubPage__ = "https://github.com/lopesth"
__email__ = "lopes.th.o@gmail.com"
__date__ = "Friday, 12 January 2018"

'''Description: Script to process streptocyanins results
                (B.X.A and polarizabilities)'''
#################################################################
# Impoted Modules
import os, numpy
from createMoleculeFromG09Opt import CreateMolecule
from bondLength import BondLength
from bondOrderMultiwfn import BondOrder
from aimallQTAIM import QTAIMaimall
from processPolarizabities import PolarG09Process
#################################################################

# Function Description: Calculate Bond Length
def bdLength(fileName, bondGroup):
    moleculeBondLength = BondLength(fileName)
    bonds = []
    for bond in bondGroup:
        atoms = [int(x) for x in bond.split("-")]
        bondlgt = moleculeBondLength.returnBondLength(atoms[0]-1, atoms[1]-1)
        bonds.append(bondlgt)
    return (bonds)

# Function Description: Calculate Bond Order
def bdOrder(fileName, basis, bondGroup):
    moleculeBondOrder = BondOrder(fileName, basis)
    bonds = []
    for bond in bondGroup:
        atoms = [int(x) for x in bond.split("-")]
        bondOd = moleculeBondOrder.filter_BO_interest([atoms[0], atoms[1]])
```

```
37          bonds.append(bondOd)
38      return bonds
39
40  # Function Description: Isolates the bond pattern
41  def bonds(dictionary):
42      bonds = []
43      for element in list(dictionary.values()):
44          x = [element[0][1], element[1][1]]
45          bonds.append(x)
46      return bonds
47
48  # Function Description: Function for processing QTAIM data
49  def aimallElipt(fileName, bondGroup):
50      bondElpt = []
51      for bond in bondGroup:
52          atoms = [int(x) for x in bond.split("-")]
53          molecule = QTAIMaimall(fileName)
54          x = molecule.searchCPbetweenAtoms(atoms)
55          bondElpt.append(float(molecule.returnBondElip(x)))
56      return bondElpt
57
58  # Function Description: Function for processing QTAIM data
59  def aimallLapl(fileName, bondGroup):
60      bondElpt = []
61      for bond in bondGroup:
62          atoms = [int(x) for x in bond.split("-")]
63          molecule = QTAIMaimall(fileName)
64          x = molecule.searchCPbetweenAtoms(atoms)
65          bondElpt.append(float(molecule.returnLaplacian(x)))
66      return bondElpt
67
68  # Function Description: Function for processing QTAIM data
69  def aimallRho(fileName, bondGroup):
70      bondElpt = []
71      for bond in bondGroup:
72          atoms = [int(x) for x in bond.split("-")]
73          molecule = QTAIMaimall(fileName)
74          x = molecule.searchCPbetweenAtoms(atoms)
75          bondElpt.append(float(molecule.returnRho(x)))
76      return bondElpt
77
78  # Function Description: Function to find polarizability data
79  def findPolarizabilities(fileName, components):
80      molecule = PolarG09Process(fileName, 0)
81      dipole = list(molecule.returnDipole(components[0]).values())[0]
82      alpha = list(molecule.returnAlpha(components[1]).values())[0]
83      beta = list(molecule.returnBeta(components[2]).values())[0]
84      gamma = list(molecule.returnGamma(components[3]).values())[0]
85      return [dipole, alpha, beta, gamma]
86
87  # Function Description: Calculating the Bond Alternation pattern
88  def BondAlternance(bonds1, bonds2):
89      return abs(sum(bonds1) - sum(bonds2))/2
90
91  # Function Description: Symmetrize a list
92  def symmetry_list(list_input, type):
```

```
93      list_temp = []
94      range_num = range(0,len(list_input))
95      list_len = 2*len(list_input)-1
96      for num in range_num:
97          if num == 0:
98              pass
99          else:
100             if type == "inverse":
101                 list_temp.append((-1)*float(list_input[-num]))
102             elif type == "mirror":
103                 list_temp.append(float(list_input[-num]))
104             else:
105                 text = "The list symmetrization function is not working properly, the type
    ("+type+") is not recognized"
106                 raise Exception(text)
107     for num in range_num:
108         list_temp.append(float(list_input[num]))
109     return list_temp
110
111 # Description: main function of the script
112 if (__name__ == "__main__"):
113     dir = "/Users/thiagolopes/Downloads/strepto/level1"
114     streptocyanines = {"5C": [16,["1-3", "5-7"],["3-5", "9-7"]], "9C": [24,["15-12", "1-3",
     "5-7", "9-11"],["12-1", "3-5", "7-9", "11-13"]]}
115     categories = [streptocyanines]
116     for molecules in categories:
117         for moleculeType in list(molecules.keys()):
118             bonds1 = molecules[moleculeType][1]
119             bonds2 = molecules[moleculeType][2]
120             if moleculeType == "5C":
121                 field_temp = numpy.arange(0,146,9.12)
122             elif moleculeType == "9C":
123                 field_temp = numpy.arange(0,88,5.48)
124             for case in ["case1", "case2","case3"]:
125                 fileToWName1 = "BondAlternationFile_"+moleculeType+"_"+case+".dat"
126                 filetoWrite1 = open(dir+"/"+fileToWName1, "w")
127                 filetoWrite1.write("{:>15} {:>15} {:>15} {:>15} {:>15} {:>15} {:>15} {:>15}
     {:>15} {:>15} {:>15} {:>15}\n" .format("Field (10^7)V/cm", "BLA", "BOA-Wiberg", "BOA-
    Mulliken", "BOA-Mayer", "BEA", "BELA", "BEDA", "Dipole",   "Alpha", "Beta", "Gamma"))
128                 BLA_list = []
129                 BOAMayer_list = []
130                 BOAMulliken_list = []
131                 BOAWiberg_list = []
132                 BEA_list = []
133                 BELA_list = []
134                 BEDA_list = []
135                 dipole_list = []
136                 alpha_list = []
137                 beta_list = []
138                 gamma_list = []
139                 field_list = []
140                 for fieldValue in field_temp:
141                     field = str(round(fieldValue, 0)).split('.')[0]
142                     field_list.append(field)
```

```
143                     molecule = CreateMolecule(dir+"/polarizabilidades/"+case+"/"+
    moleculeType+"/Output/polar_"+case+"_"+moleculeType+"_"+field+".log", molecules[
    moleculeType][0]).returnMolecule()
144                     bondL1 = bdLength(molecule, bonds1)
145                     bondL2 = bdLength(molecule, bonds2)
146                     bondO1Mayer = bdOrder(dir+"/BOA/"+case+"/"+moleculeType+"/BO_files/"+"
    boa_"+case+"_"+moleculeType+"_"+field+"_bndmat_mayer.txt", molecules[moleculeType][0],
    bonds1)
147                     bondO2Mayer = bdOrder(dir+"/BOA/"+case+"/"+moleculeType+"/BO_files/"+"
    boa_"+case+"_"+moleculeType+"_"+field+"_bndmat_mayer.txt", molecules[moleculeType][0],
    bonds2)
148                     bondO1Mulliken = bdOrder(dir+"/BOA/"+case+"/"+moleculeType+"/BO_files/"
    +"boa_"+case+"_"+moleculeType+"_"+field+"_bndmat_mulliken.txt", molecules[moleculeType
    ][0], bonds1)
149                     bondO2Mulliken = bdOrder(dir+"/BOA/"+case+"/"+moleculeType+"/BO_files/"
    +"boa_"+case+"_"+moleculeType+"_"+field+"_bndmat_mulliken.txt", molecules[moleculeType
    ][0], bonds2)
150                     bondO1Wiberg = bdOrder(dir+"/BOA/"+case+"/"+moleculeType+"/BO_files/"+"
    boa_"+case+"_"+moleculeType+"_"+field+"_bndmat_wiberg.txt", molecules[moleculeType][0],
     bonds1)
151                     bondO2Wiberg = bdOrder(dir+"/BOA/"+case+"/"+moleculeType+"/BO_files/"+"
    boa_"+case+"_"+moleculeType+"_"+field+"_bndmat_wiberg.txt", molecules[moleculeType][0],
     bonds2)
152                     bondE1 = aimallElipt(dir+"/BOA/"+case+"/"+moleculeType+"/BO_files/"+"
    boa_"+case+"_"+moleculeType+"_"+field+".mgp", bonds1)
153                     bondE2 = aimallElipt(dir+"/BOA/"+case+"/"+moleculeType+"/BO_files/"+"
    boa_"+case+"_"+moleculeType+"_"+field+".mgp", bonds2)
154                     bondLapl1 = aimallLapl(dir+"/BOA/"+case+"/"+moleculeType+"/BO_files/"+"
    boa_"+case+"_"+moleculeType+"_"+field+".mgp", bonds1)
155                     bondLapl2 = aimallLapl(dir+"/BOA/"+case+"/"+moleculeType+"/BO_files/"+"
    boa_"+case+"_"+moleculeType+"_"+field+".mgp", bonds2)
156                     bondRho1 = aimallRho(dir+"/BOA/"+case+"/"+moleculeType+"/BO_files/"+"
    boa_"+case+"_"+moleculeType+"_"+field+".mgp", bonds1)
157                     bondRho2 = aimallRho(dir+"/BOA/"+case+"/"+moleculeType+"/BO_files/"+"
    boa_"+case+"_"+moleculeType+"_"+field+".mgp", bonds2)
158                     BLA_list.append(BondAlternance(bondL1, bondL2))
159                     BOAMayer_list.append(BondAlternance(bondO1Mayer, bondO2Mayer))
160                     BOAMulliken_list.append(BondAlternance(bondO1Mulliken, bondO2Mulliken))
161                     BOAWiberg_list.append(BondAlternance(bondO1Wiberg, bondO2Wiberg))
162                     BEA_list.append(BondAlternance(bondE1, bondE2))
163                     BELA_list.append(BondAlternance(bondLapl1, bondLapl2))
164                     BEDA_list.append(BondAlternance(bondRho1, bondRho2))
165                     polarizabilities = findPolarizabilities(dir+"/polarizabilidades/"+case+
    "/"+moleculeType+"/Output/polar_"+case+"_"+moleculeType+"_"+field+".log", ['x', 'xx', '
    xxx', 'xxxx'])
166                     dipole_list.append(polarizabilities[0])
167                     alpha_list.append(polarizabilities[1])
168                     beta_list.append(polarizabilities[2])
169                     gamma_list.append(polarizabilities[3])
170                 field_list = symmetry_list(field_list, "inverse")
171                 BLA_list = symmetry_list(BLA_list, "inverse")
172                 BOAMayer_list = symmetry_list(BOAMayer_list, "inverse")
173                 BOAMulliken_list = symmetry_list(BOAMulliken_list, "inverse")
174                 BOAWiberg_list = symmetry_list(BOAWiberg_list, "inverse")
175                 BEA_list = symmetry_list(BEA_list, "inverse")
176                 BELA_list = symmetry_list(BELA_list, "inverse")
```

```
177                 BEDA_list = symmetry_list(BEDA_list, "inverse")
178                 dipole_list = symmetry_list(dipole_list, "inverse")
179                 alpha_list = symmetry_list(alpha_list, "mirror")
180                 beta_list = symmetry_list(beta_list, "inverse")
181                 gamma_list = symmetry_list(gamma_list, "mirror")
182 
183                 for i in range(0, len(dipole_list)):
184                     filetoWrite1.write("{:>15.7f} {:>15.7f} {:>15.7f} {:>15.7f} {:>15.7f}
    {:>15.7f} {:>15.7f} {:>15.7f} {:>15.7f} {:>15.7f} {:>15.7f}\n" .format(
185                         field_list[i], BLA_list[i], BOAWiberg_list[i], BOAMulliken_list[i],
     BOAMayer_list[i], BEA_list[i], BELA_list[i], BEDA_list[i], dipole_list[i], alpha_list[
    i], beta_list[i], gamma_list[i]
186                     ))
187                     filetoWrite1.close
```

C.0.2 File: createMoleculeFromG09Opt.py

```
1  ################################################################
2  # Python file header
3  __author__ = "Thiago Lopes"
4  __GitHubPage__ = "https://github.com/lopesth"
5  __email__ = "lopes.th.o@gmail.com"
6  __date__ = "Friday, 12 January 2018"
7 
8  '''Description: Creates a molecule of an optimization output of G09'''
9  ################################################################
10 # Impoted Modules
11 from find_xyz_from_a_log import Find_XYZ
12 from atonsNmolecule import Atom, Molecule
13 ################################################################
14 
15 class CreateMolecule(object):
16     def __init__(self, targetFile, base):
17         self.targetFile = targetFile
18         self.base = base
19         self.molecule = Molecule()
20 
21     def returnMolecule(self):
22         lisPos = Find_XYZ(self.targetFile, self.base).gaussian_style()
23         for elementPos in lisPos:
24             rawAtom = elementPos.split()
25             atomType = rawAtom[0]
26             atomX = float(rawAtom[1])
27             atomY = float(rawAtom[2])
28             atomZ = float(rawAtom[3])
29             self.molecule.addAtom(Atom(atomType, atomX, atomY, atomZ))
30         return self.molecule
```

C.0.3 File: bondLength.py

```
1  ################################################################
2  # Python file header
3  __author__ = "Thiago Lopes"
4  __GitHubPage__ = "https://github.com/lopesth"
```

```
__email__ = "lopes.th.o@gmail.com"
__date__ = "Friday, 12 January 2018"

''' Description: Calculate the bond length '''
#####################################################################
# Impoted Modules
from twoPoints import TwoPoints
#####################################################################

class BondLength(object):
    def __init__(self, molecule):
        self.molecule = molecule

    def returnBondLength(self, atomNumber1, atomNumber2):
        atom1 = self.molecule.returnAtom(atomNumber1)
        atom2 = self.molecule.returnAtom(atomNumber2)
        bondLength = self.calculeBondLenght(atom1, atom2)
        return bondLength

    def calculeBondLenght(self, atom1, atom2):
        x1 = atom1.returnXPos()
        x2 = atom2.returnXPos()
        y1 = atom1.returnYPos()
        y2 = atom2.returnYPos()
        z1 = atom1.returnZPos()
        z2 = atom2.returnZPos()
        bondLength = TwoPoints([x1, y1, z1], [x2, y2, z2]).distanceBetween()
        return bondLength
```

C.0.4 File: bondOrderMultiwfn.py

```
#####################################################################
# Python file header
__author__ = "Thiago Lopes"
__GitHubPage__ = "https://github.com/lopesth"
__email__ = "lopes.th.o@gmail.com"
__date__ = "Saturday, 13 January 2018"

''' Description: Multiwfn Output Bond Orders '''
#####################################################################

class BondOrder(object):
    def __init__(self, fileName, basis):
        self.basis = basis
        self.fileName = fileName
        self.bondOrders = self.takeBondOrders()

    def takeBondOrders(self):
        bondOrdersMAP = {}
        fileString = []
        with open(self.fileName) as myFile:
            for num, line in enumerate(myFile):
                fileString.append(line.split())
            numberBlock = int(num / self.basis)
            initRange = 3
```

```
            endRange = 3+self.basis
            startPoint = 1
            endPoint = 6
            for block in range(0, numberBlock):
                el1 = 1
                for element in range(initRange, endRange):
                    count = 1
                    for el2 in range(startPoint, endPoint):
                        bondOrdersMAP.update({ str(el1) + " - " + str(el2) : float(
    fileString[element][count])})
                        count += 1
                    el1 +=1
                initRange = endRange +1
                endRange = initRange + self.basis
                startPoint = endPoint
                endPoint = startPoint +5
                if endPoint < self.basis+1:
                    pass
                else:
                    endPoint = self.basis+1
            return bondOrdersMAP

    def filter_BO_interest(self, bond):
        bondName = str(bond[0]) + " - " + str(bond[1])
        return self.bondOrders[bondName]
```

C.0.5 File: aimallQTAIM.py

```
#####################################################################
# Python file header
__author__ = "Thiago Lopes"
__GitHubPage__ = "https://github.com/lopesth"
__email__ = "lopes.th.o@gmail.com"
__date__ = "Sunday, 14 January 2018"

'''Description: Class to bundle QTAIM data from AIMALL outputs'''
#####################################################################
# Impoted Modules
from find_a_string_in_file import Find_a_String
from re import sub
#####################################################################

class QTAIMaimall(object):

    def __init__(self, fileName):
        self.fileName = fileName
        self.CPs = self.__catCPs()
        self.CPtypes = self.__catCPtype()
        self.Rhos = self.__catRho()
        self.HessMAt = self.__catHessMat()
        self.Laplacian = self.__catLaplacian()
        self.BondElip = self.__catBondElip()

    def __catCPs(self):
        linesCPs = Find_a_String(self.fileName, "CP#").return_numbers_of_line()
```

```
28          fileString = []
29          with open(self.fileName) as myFile:
30              for line in myFile:
31                  fileString.append(line.split())
32          resultList = []
33          for origCP in linesCPs:
34              startNumber = origCP - 1
35              endNumber = startNumber + 35
36              x = []
37              for i in range(startNumber, endNumber):
38                  x.append(fileString[i])
39              resultList.append(x)
40          return resultList
41
42      def __catCPtype(self):
43          lines = [0, 1]
44          bcpType = "(3,-1)"
45          ccpType = "(3,+3)"
46          rcpType = "(3,+1)"
47          acpType = "(3,-3)"
48          result = []
49          for cp in self.CPs:
50              v1 = "{} {}".format(cp[0][0], cp[0][1])
51              v2 = "{:11.7f}, {:11.7f}, {:11.7f}" .format(float(cp[0][4]), float(cp[0][5]),
    float(cp[0][6]))
52              posCP = "Positioning between atoms {} and {}" .format(", ".join(cp[1][4:-1]),
    cp[1][-1])
53              if (cp[1][2] == bcpType):
54                  cptype = "{}: Bond Critical Point (BCP)".format(cp[1][2])
55                  posCP = "Positioning between atoms {}" .format(" and ".join(cp[1][4:]))
56                  atonsB = "" .format()
57              elif (cp[1][2] == ccpType):
58                  cptype = "{}: Cage Critical Point (CCP)" .format(cp[1][2])
59              elif (cp[1][2] == rcpType):
60                  cptype = "{}: Ring Critical Point (RCP)" .format(cp[1][2])
61              elif (cp[1][2] == acpType):
62                  cptype = "{}: Non-Nuclear Attractor Critical Point (NNACP)" .format(cp
    [1][2])
63                  posCP = "Position of Atom {}" .format(cp[1][4])
64              else:
65                  cptype = "{}: Critical point not found" .format(cp[1][2])
66              result.append([v1, v2, cptype, posCP])
67          return result
68
69      def __catRho(self):
70          result = []
71          for cp in self.CPs:
72              x = "{:.7f}" .format(float(cp[2][2]))
73              result.append(x)
74          return result
75
76      def __catGradient(self):
77          result = []
78          for cp in self.CPs:
79              x = "{:16.7e} {:16.7e} {:16.7e}" .format(float(cp[3][2]), float(cp[3][3]),
    float(cp[3][4]))
```

```
80              result.append(x)
81          return result
82
83      def __catHessMat(self, type = 'vector'):
84          result = []
85          if type == "vector":
86              for cp in self.CPs:
87                  x = "{:16.7e} {:16.7e} {:16.7e}" .format(float(cp[5][2]), float(cp[5][3]),
    float(cp[5][4]))
88                  y = "{:16.7e} {:16.7e} {:16.7e}" .format(float(cp[6][2]), float(cp[6][3]),
    float(cp[6][4]))
89                  z = "{:16.7e} {:16.7e} {:16.7e}" .format(float(cp[7][2]), float(cp[7][3]),
    float(cp[7][4]))
90                  result.append([x, y, z])
91          else:
92              for cp in self.CPs:
93                  x = "{:16.7e} {:16.7e} {:16.7e}" .format(float(cp[4][2]), float(cp[4][3]),
    float(cp[4][4]))
94                  result.append(x)
95          return result
96
97      def __catLaplacian(self):
98          result = []
99          for cp in self.CPs:
100             x = "{:.7f}" .format(float(cp[8][2]))
101             result.append(x)
102         return result
103
104     def __catBondElip(self):
105         result = []
106         for cp in self.CPs:
107             try:
108                 x = "{:.7f}" .format(float(cp[9][3]))
109             except:
110                 x = "{}" .format(cp[9][3])
111             result.append(x)
112         return result
113
114     def returnBondElip(self, cpNumber):
115         return self.BondElip[cpNumber-1]
116
117     def returnLaplacian(self, cpNumber):
118         return self.Laplacian[cpNumber-1]
119
120     def returnRho(self, cpNumber):
121         return self.Rhos[cpNumber-1]
122
123     def searchCPbetweenAtoms(self, atomsToLook):
124         for cp in self.CPtypes:
125             atoms = [int(s) for s in sub("\D", " ", cp[3]).split()]
126             if len(atoms) == len(atomsToLook):
127                 number = 0
128                 continueWhile = True
129                 while continueWhile:
130                     try:
131                         if atomsToLook[number] in atoms:
```

```
                            number+=1
                        else:
                            break
                    except:
                        return int(cp[0].split()[1])

    def searchAtomicCP(self, atom1):
        return self.CPtypes[cpNumber-1]

    def returnCPcoord(self, cpNumber):
        return self.CPtypes[cpNumber-1][1]

    def returnCPS(self, cpNumber):
        return self.CPtypes[cpNumber-1]
```

C.0.6 File: processPolarizabities.py

```
#####################################################################
# Python file header
__author__ = "Thiago Lopes"
__GitHubPage__ = "https://github.com/lopesth"
__email__ = "lopes.th.o@gmail.com"
__date__ = "Sunday, 14 January 2018"

''' Description: Class to process the polarization results in an output of G09'''
#####################################################################
# Impoted Modules
from find_a_string_in_file import Find_a_String
#####################################################################

class PolarG09Process(object):

    def __init__(self, fileName, numberOfFreqs):
        self.fileName = fileName
        self.numberOfFreqs = numberOfFreqs
        self.__catPolar()

    def __catPolar(self):
        fileString = []
        self.dipoles = {}
        self.alphas = [{}]
        self.betas = [{}]
        self.gammas = [{}]
        with open(self.fileName) as myFile:
            for line in myFile:
                fileString.append(line.split())
        singleAnchor = [0]
        dualAnchor = []
        for freqNumber in range(0, self.numberOfFreqs):
            dualAnchor.append(freqNumber)
        dipoleLines = self.__findLines("Electric dipole moment", singleAnchor, 2, 4)
        self.dipoleRaw = self.__toSeparate(fileString, dipoleLines)
        for i in range(0, len(self.dipoleRaw[0])):
            self.dipoles.update({self.dipoleRaw[0][i][0]:float(self.dipoleRaw[0][i][2].
    replace("D", "E"))})
```

```
38          alpha1Lines = self.__findLines("Alpha(0;0)", singleAnchor, 1, 8)
39          self.alpha1Raw = self.__toSeparate(fileString, alpha1Lines)
40          for i in range(0, len(self.alpha1Raw[0])):
41              self.alphas[0].update({self.alpha1Raw[0][i][0]:float(self.alpha1Raw[0][i][2].
    replace("D", "E"))})
42          beta1Lines = self.__findLines("Beta(0;0,0)", singleAnchor, 1, 16)
43          self.beta1Raw = self.__toSeparate(fileString, beta1Lines)
44          for i in range(0, len(self.beta1Raw[0])):
45              self.betas[0].update({self.beta1Raw[0][i][0]:float(self.beta1Raw[0][i][2].
    replace("D", "E"))})
46          gamma1Lines = self.__findLines("Gamma(0;0,0,0)", singleAnchor, 1, 17)
47          self.gamma1Raw = self.__toSeparate(fileString, gamma1Lines)
48          for i in range(0, len(self.gamma1Raw[0])):
49              self.gammas[0].update({self.gamma1Raw[0][i][0]:float(self.gamma1Raw[0][i][2].
    replace("D", "E"))})
50          if self.numberOfFreqs > 0:
51              alpha2Lines = self.__findLines("Alpha(-w;w)", dualAnchor, 1, 8)
52              self.alpha2Raw = self.__toSeparate(fileString, alpha2Lines)
53              self.alphas.append({})
54              self.alphas.append({})
55              for i in range(0, len(self.alpha2Raw[0])):
56                  self.alphas[1].update({self.alpha2Raw[0][i][0]:float(self.alpha2Raw[0][i
    ][2].replace("D", "E"))})
57                  self.alphas[2].update({self.alpha2Raw[1][i][0]:float(self.alpha2Raw[1][i
    ][2].replace("D", "E"))})
58              beta2Lines = self.__findLines("Beta(-w;w,0)", dualAnchor, 1, 24)
59              self.beta2Raw = self.__toSeparate(fileString, beta2Lines)
60              self.betas.append({})
61              self.betas.append({})
62              for i in range(0, len(self.beta2Raw[0])):
63                  self.betas[1].update({self.beta2Raw[0][i][0]:float(self.beta2Raw[0][i][2].
    replace("D", "E"))})
64                  self.betas[2].update({self.beta2Raw[1][i][0]:float(self.beta2Raw[1][i][2].
    replace("D", "E"))})
65              gamma2Lines = self.__findLines("Gamma(-w;w,0,0)", dualAnchor, 1, 38)
66              self.gamma2Raw = self.__toSeparate(fileString, gamma2Lines)
67              self.gammas.append({})
68              self.gammas.append({})
69              for i in range(0, len(self.gamma2Raw[0])):
70                  self.gammas[1].update({self.gamma2Raw[0][i][0]:float(self.gamma2Raw[0][i
    ][2].replace("D", "E"))})
71                  self.gammas[2].update({self.gamma2Raw[1][i][0]:float(self.gamma2Raw[1][i
    ][2].replace("D", "E"))})
72              if self.numberOfFreqs > 1:
73                  self.betas.append({})
74                  self.betas.append({})
75                  self.gammas.append({})
76                  self.gammas.append({})
77                  beta3Lines = self.__findLines("Beta(-2w;w,w)", dualAnchor, 1, 24)
78                  self.beta3Raw = self.__toSeparate(fileString, beta3Lines)
79                  for i in range(0, len(self.beta3Raw[0])):
80                      self.betas[3].update({self.beta3Raw[0][i][0]:float(self.beta3Raw[0][i
    ][2].replace("D", "E"))})
81                      self.betas[4].update({self.beta3Raw[1][i][0]:float(self.beta3Raw[1][i
    ][2].replace("D", "E"))})
82                  gamma3Lines = self.__findLines("Gamma(-2w;w,w,0)", dualAnchor, 1, 56)
```

```
83                  self.gamma3Raw = self.__toSeparate(fileString, gamma3Lines)
84                  for i in range(0, len(self.gamma3Raw[0])):
85                      self.gammas[3].update({self.gamma3Raw[0][i][0]:float(self.gamma3Raw[0][
    i][2].replace("D", "E"))})
86                      self.gammas[4].update({self.gamma3Raw[1][i][0]:float(self.gamma3Raw[1][
    i][2].replace("D", "E"))})
87
88      def __toSeparate(self, listT, rangePos):
89          listF = []
90          for x in rangePos:
91              listX = []
92              for i in range(x[0], x[1]):
93                  listX.append(listT[i])
94              listF.append(listX)
95          return listF
96
97      def __findLines(self, lookup, posList, addLines, finished):
98          numberListTemp = Find_a_String(self.fileName, lookup).return_numbers_of_line()
99          numberListFinal = []
100         for number in posList:
101             x = numberListTemp[number]+addLines
102             listT = [x, x + finished]
103             numberListFinal.append(listT)
104         return numberListFinal
105
106     def returnDipole(self, component):
107         dipoles = {}
108         dipoles.update({"Dipole Moment" : self.dipoles[component]})
109         return dipoles
110
111     def returnAlpha(self, component):
112         alpha = {}
113         text = ["Alpha(0;0)", "Alpha(-w;w) w= 1906.4nm", "Alpha(-w;w) w= 1064.1nm"]
114         for i in range(0,len(self.alphas)):
115             alpha.update({text[i] : self.alphas[i][component]})
116         return alpha
117
118     def returnBeta(self, component):
119         beta = {}
120         text = [
121             "Beta(0;0,0)", "Beta(-w;w,0) w= 1906.4nm", "Beta(-w;w,0) w= 1064.1nm",
122             "Beta(-2w;w,w) w= 1906.4nm", "Beta(-2w;w,w) w= 1064.1nm"
123         ]
124         for i in range(0,len(self.betas)):
125             beta.update({text[i] : self.betas[i][component]})
126         return beta
127
128     def returnGamma(self, component):
129         gamma = {}
130         text = [
131             "Gamma(0;0,0,0)", "Gamma(-w;w,0,0) w= 1906.4nm", "Gamma(-w;w,0,0) w= 1064.1nm",
132             "Gamma(-2w;w,w,0) w= 1906.4nm", "Gamma(-2w;w,w,0) w= 1064.1nm"
133         ]
134         for i in range(0,len(self.gammas)):
135             gamma.update({text[i] : self.gammas[i][component]})
136         return gamma
```

C.0.7 File: find_a_string_in_file.py

```
#####################################################################
# Python file header
__author__ = "Thiago Lopes"
__GitHubPage__ = "https://github.com/lopesth"
__email__ = "lopes.th.o@gmail.com"
__date__ = "Friday, 12 January 2018"

''' Description: Find a specific string in a file '''
#####################################################################

class Find_a_String(object):

    def __init__(self, file, lookup):
        self.file = file
        self.lookup = lookup

    def return_numbers_of_line(self):
        numbers = []
        myFileString = []
        with open(self.file) as myFile:
            for num, line in enumerate(myFile):
                if (self.lookup in line):
                    numbers.append(num+1)
        return numbers

    def return_the_line(self):
        lines = []
        with open(self.file) as myFile:
            for num, line in enumerate(myFile):
                if (self.lookup in line):
                    lines.append(line.split('\n')[0])
        return lines
```

C.0.8 File: atomsNmolecule.py

```
#####################################################################
# Python file header
__author__ = "Thiago Lopes"
__GitHubPage__ = "https://github.com/lopesth"
__email__ = "lopes.th.o@gmail.com"
__date__ = "Friday, 12 January 2018"

''' Description: Creates a molecule as an object '''
#####################################################################

class Atom(object):
    def __init__(self, atomType, xPos, yPos, ZPos):
        self.atomType =atomType
        self.xPos = xPos
        self.yPos = yPos
        self.zPos = ZPos

    def returnAtomType(self):
```

```
19          return self.atomType
20
21      def returnXPos(self):
22          return self.xPos
23
24      def returnYPos(self):
25          return self.yPos
26
27      def returnZPos(self):
28          return self.zPos
29
30      def returnPos(self):
31          return [self.xPos, self.yPos, self.zPos]
32
33      def returnAtom(self):
34          return [self.atomType, self.xPos, self.yPos, self.zPos]
35
36      def moveAtom(self, newX, newY, newZ):
37          self.xPos = newX
38          self.yPos = newY
39          self.zPos = newZ
40
41  class Molecule(object):
42      def __init__(self):
43          self.atons = []
44
45      def addAtom(self, atom):
46          self.atons.append(atom)
47
48      def returnAtom(self, number):
49          return self.atons[number]
50
51      def moveAtom(self, numer, newPOS):
52          newX = newPOS[0]
53          newY = newPOS[1]
54          newZ = newPOS[2]
55          self.atons[number].moveAtom(newX, newY, newZ)
56
57      def returnAllAtons(self):
58          return self.atons
```

C.0.9 File: find_xyz_from_a_log.py

```
1  ################################################################
2  # Python file header
3  __author__ = "Thiago Lopes"
4  __GitHubPage__ = "https://github.com/lopesth"
5  __email__ = "lopes.th.o@gmail.com"
6  __date__ = "Friday, 12 January 2018"
7
8  ''' Description: Find the position of atoms in an output of G09'''
9  ################################################################
10 # Impoted Modules
11 from find_a_string_in_file import Find_a_String
12 from periodic_table import Convert_Period_Table
```

```
#################################################################

class Find_XYZ(object):

    def __init__(self, file, base):
        self.file = file
        self.base = base

    def stop_the_pigeon(self):
        self.temp_list = []
        pos_start = Find_a_String(self.file, "Input orientation").return_numbers_of_line()[-1] + 5
        pos = range(pos_start, pos_start + self.base)
        with open(self.file) as myFile:
            for num, line in enumerate(myFile, 1):
                if (num in pos):
                    self.temp_list.append(line.split())
        return self.temp_list

    def gaussian_style(self):
        self.stop_the_pigeon()
        final_list = []
        for line in self.temp_list:
            atomic_symbol = Convert_Period_Table([int(line[1])], []).number_to_symbol()
            final_list.append("{:>2s} {:>13.7f} {:>13.7f} {:>13.7f}".format(atomic_symbol[0], float(line[3]), float(line[4]), float(line[5])))
        return final_list
```

C.0.10 File: periodic_table.py

```
#################################################################
# Python file header
__author__ = "Thiago Lopes"
__GitHubPage__ = "https://github.com/lopesth"
__email__ = "lopes.th.o@gmail.com"
__date__ = "Friday, 12 January 2018"

''' Description: Converts atomic number to atomic symbol and vice versa '''
#################################################################

PERIODIC_TABLE = {1: "H", 2: "He", 3: "Li", 4: "Be", 5: "B", 6: "C", 7: "N", 8: "O", 9: "F", 10: "Ne", 11: "Na", 12: "Mg", 13: "Al", 14: "Si", 15: "P", 16: "S", 17: "Cl", 18: "Ar", 19: "K", 20: "Ca",
                  21: "Sc", 22: "Ti", 23: "V", 24: "Cr", 25: "Mn", 26: "Fe", 27: "Co", 28: "Ni", 29: "Cu", 30: "Zn", 31: "Ga", 32: "Ge", 33: "As", 34: "Se", 35: "Br", 36: "Kr", 37: "Rb", 38: "Sr", 39: "Y",
                  40: "Zr", 41: "Nb", 42: "Mo", 43: "Tc", 44: "Ru", 45: "Rh", 46: "Pd", 47: "Ag", 48: "Cd", 49: "In", 50: "Sn", 51: "Sb", 52: "Te", 53: "I", 54: "Xe", 55: "Cs", 56: "Ba", 57: "La", 58: "Ce", 59: "Pr",
                  60: "Nd", 61: "Pm", 62: "Sm", 63: "Eu", 64: "Gd", 65: "Tb", 66: "Dy", 67: "Ho", 68: "Er", 69: "Tm", 70: "Yb", 71: "Lu", 72: "Hf", 73: "Ta", 74: "W", 75: "Re", 76: "Os", 77: "Ir", 78: "Pt", 79: "Au",
                  80: "Hg", 81: "Tl", 82: "Pb", 83: "Bi", 84: "Po", 85: "At", 86: "Rn", 87: "Fr", 88: "Ra", 89: "Ac", 90: "Th", 91: "Pa", 92: "U", 93: "Np", 94: "Pu", 95: "Am", 96: "Cm", 97: "Bk", 98: "Cf", 99: "Es",
```

```
                  100: "Fm", 101: "Md", 102: "No", 103: "Lr", 104: "Rf", 105: "Db", 106: "
    Sg", 107: "Bh", 108: "Hs", 109: "Mt", 110: "Ds", 111: "Rg", 112: "Cn", 113: "Uut", 114:
     "Fl", 115: "Uup", 116: "Lv", 117: "Uus", 118: "Uuo", 119: "Uue", 120: "Ubn"}

class Convert_Period_Table(object):

    def __init__(self, atomic_number = [], atomic_symbol = []):
        self.atomic_number = atomic_number
        self.atomic_symbol = atomic_symbol

    def symbol_to_number(self):
        temp = list(PERIODIC_TABLE.values())
        result = []
        for symbol in self.atomic_symbol:
            nao_contem = True
            contador = 0
            for element in temp:
                if (symbol == element):
                    pos = 0
                    for number in list(PERIODIC_TABLE.keys()):
                        if (pos == contador):
                            result.append(number)
                        pos +=1
                        nao_contem = False
                    break
                contador +=1
            if (nao_contem):
                result.append(0)
        return result

    def number_to_symbol(self):
        result = []
        for number in self.atomic_number:
            try:
                result.append(PERIODIC_TABLE[number])
            except:
                result.append("???")
        return result
```

C.0.11 File: twoPoints.py

```
#####################################################################
# Python file header
__author__ = "Thiago Lopes"
__GitHubPage__ = "https://github.com/lopesth"
__email__ = "lopes.th.o@gmail.com"
__date__ = "Friday, 12 January 2018"

''' Description: Calculate the distance between two points '''
#####################################################################
# Impoted Modules
from math import sqrt
from math import pow
#####################################################################

```

```
15 class TwoPoints(object):
16     def __init__(self, point1, point2):
17         self.x1 = point1[0]
18         self.x2 = point2[0]
19         self.y1 = point1[1]
20         self.y2 = point2[1]
21         self.z1 = point1[2]
22         self.z2 = point2[2]
23 
24     def distanceBetween(self):
25         xDif = pow((self.x1 - self.x2), 2)
26         yDif = pow((self.y1 - self.y2), 2)
27         zDif = pow((self.z1 - self.z2), 2)
28         return sqrt(xDif + yDif + zDif)
```